1975

ELASTO-PLASTIC ANALYSIS OF ORTHOTROPIC SKEW PLATES.

PIJUSH K. CHOWDHURY
University of Windsor

ELASTO-PLASTIC ANALYSIS OF ORTHOTROPIC SKEW PLATES

A DISSERTATION

Submitted to the Faculty of Graduate Studies

through the Department of Civil Engineering

in Partial Fullfilment of the Requirements

for the Degree of

Doctor of Philosophy at the

University of Windsor

by

Pijush K. Chowdhury
B.Sc. Engg., Bangladesh University of Engg. and Technology, 1963.
M.A.Sc., University of Windsor, 1970.

Windsor, Ontario, Canada

1975

Dedicated to

My Parents

ABSTRACT

The objective of this investigation is to develop a step by step solution procedure to find the structural response of orthotropic (orthogonally anisotropic) skew plates undergoing large deflections into the elasto-plastic range. A numerical method of analysis is presented on the basis of finite difference approximations of the two coupled fourth order differential equations of equilibrium and compatibility with variable coefficients, describing the behaviour of orthotropic skew plates.

The solution of the resulting sets of simultaneous equations for the stress function and transverse deflections of the plate is obtained by a successive approximation technique. Beyond the initiation of first yield at sections of maximum stressed ribs, an iterative incremental procedure has been adopted to take into account the reduction of stiffnesses with the corresponding increment of loading, thus converting the non-linear problem into a series of incrementally linear problems in the elastic-plastic range. The step by step solution procedure is continued until the ribs at the sections of maximum stress intensity have fully yielded.

Comparisons are made with existing results for skewed plates with small deflections as well as with results of rectangular plates with large deflection behaviour; good agreement is shown.

Experiments, on one rectangular and two skew model plates stiffened by longitudinal and transverse ribs, simulating bridge decks, were conducted both in the elastic and elastic-plastic stress region. Initially, the plates were tested in the elastic domain under concentrated lateral loading applied symmetrically and asymmetrically with the two boundary conditions:

(i) simply supported on all sides and

(ii) simply supported on two sides and free at the other two. Finally, the plate models were tested in the elasto-plastic stress region under uniformly distributed load with the boundary condition of simple support on all sides. The experimental results verify and substantiate the theoretical solution.

ACKNOWLEDGEMENTS

I wish to express my sincere gratitude to Dr. J.B. Kennedy for his many valuable suggestions and constant encouragement during the course of this investigation. The constructive criticism of other members of my doctoral committee at the time of the comprehensive examination is also gratefully acknowledged.

Many thanks are expressed to the laboratory technicians of the Department of Civil Engineering and the Central Research Workshop for their generous help in fabricating the bridge models and setting up of the experiments. Thanks are also due to the Computer Centre staff for their many helpful suggestions during the numerical solution of the problem.

Deepest appreciation is also expressed to my wife Sipra, for her patience, understanding and encouragement during the last four years which made this dissertation possible.

The financial assistance for this investigation by the National Research Council of Canada is also gratefully acknowledged.

TABLE OF CONTENTS

	Page
ABSTRACT	iv
ACKNOWLEDGEMENTS	vi
TABLE OF CONTENTS	vii
CHAPTER	
1. INTRODUCTION	1
2. REVIEW OF LITERATURE	6
2.1 Linear Analysis of Skew Plates	6
2.2 Non-Linear Analysis of Plate Problems	9
2.3 Elastic-Plastic Analysis	14
3. MATHEMATICAL FORMULATION	19
3.1 General Concept	19
3.2 Behaviour of Elastic-Perfectly Plastic Material	21
3.3 Yield Criterion	22
3.4 Basic Assumptions	25
3.5 Differential Equation of Equilibrium Due to Bending and Membrane Effects	27
3.6 Compatibility Equation Due to Membrane Forces	32
3.7 The Oblique Co-ordinate System	36
3.8 Computation of Plate Rigidities	38

Page

4. APPLICATION OF FINITE DIFFERENCE TECHNIQUE TO THE SOLUTION OF THE COUPLED NON-LINEAR DIFFERENTIAL EQUATIONS 43

4.1 Introduction 43

4.2 Finite Difference Approximation 43

4.3 Boundary Conditions 57

4.3.1 Bending Boundary Conditions 58

4.3.2 Membrane Boundary Conditions 58

4.3.3 Two Opposite Edges Simply Supported and the Other Two Edges Free (Small-Deflection Elastic Analysis) 60

4.4 Formulation of the Simultaneous Equations for Large-Deflection Plate Behaviour 62

5. MATHEMATICAL SOLUTION 64

5.1 Procedure of Iterative Solutions for the Initial Stages of Loading 65

5.2 Search for Initiation of First Yield 68

5.3 Determination of the Remaining Elastic Cross-Section and the Step by Step Solution Procedure 68

5.4 The Computer Program and the Flow Diagram . 74

5.5 Accuracy of the Numerical Solutions 76

6. EXPERIMENTAL INVESTIGATION 81

6.1 Model Plates and Material Properties 82

6.2 Abutment Frames 83

6.3 Loading Device and Instrumentation 83

Page

7. DISCUSSIONS OF THEORETICAL SOLUTIONS AND EXPERIMENTAL RESULTS 87

7.1 Rectangular Orthotropic Test Panel (Model Plate No. 1) 87

7.2 Orthotropic Skew Plate with Ribs in the x-Direction Only (Model Plate No. 2) 91

7.3 Orthotropic Skew Plate with Stiffening Ribs in both Directions (Model Plate No. 3) 95

7.4 Errors in the Experimental Investigation and Limitations of the Theoretical Assumptions 98

7.5 Study of the Effect of Skew in the Elasto-Plastic Analysis of Orthotropic Plate Structures 99

7.6 Discussions of Small-Deflection Theoretical Solutions and the Experimental Results within the Elastic Stress Region. 102

8. SUMMARY AND CONCLUSIONS 105

NOMENCLATURE 108

BIBLIOGRAPHY 111

9. APPENDICES 119

APPENDIX A - Transformation of the Orthotropic Plate Equations into Skew Co-ordinates 120

APPENDIX B - Finite Difference Equations for Large Deflection Behaviour of Orthotropic Skew Plates 124

APPENDIX C - Finite Difference Equations for Small Deflection Behaviour of Orthotropic Skew Plates 156

10. FINITE DIFFERENCE MOLECULES FOR COMPATIBILITY AND EQUILIBRIUM EQUATIONS: Non-Linear (Large-Deflection) Theory 167

11. FINITE DIFFERENCE MOLECULES FOR EQUILIBRIUM EQUATION : Linear (Small-Deflection) Theory 180

Page

12. TABLES 190

13. FIGURES 205

14. COMPUTER PROGRAM 259

VITA AUCTORIS 287

CHAPTER 1

INTRODUCTION

Orthotropic skew plates are found in many structures, such as, skew bridges, building floor systems, decks of welded ships and swept wings. In modern design, particularly with the advent of jet age followed closely by space age, the load carrying elements of air craft, missiles and space vehicles are, in general, used to the limit of their capacity. This requires that the design be based on an inelastic analysis. If inelastic action is permitted to occur only within a small region of a structural element, the resulting deformations will not be excessive and an elasto-plastic analysis can be used in design for proper evaluation of strength or deformation (1),(2),(3)*.

During the past twenty years, the introduction of the concept of orthotropic bridge theory has achieved considerable material economy by the use of steel decks in highway bridges which possess not only aesthetic beauty but also excellent structural characteristics. Lincoln design manual of orthotropic bridges (4) and the A.I.S.C. design manual (5) are the two comprehensive references on

*Numbers in parenthesis refer to the references in the Bibliography.

orthotropic deck bridges, which summarize much of the past experience and research. Although elastic analysis dominates the field of bridge engineering, it is now generally accepted that the understanding of any structure is incomplete unless its structural response beyond the elastic range is investigated.

The use of increasingly heavy vehicular loading on highways has given a stimulus to the study of orthotropic skew bridges spanning over waterways, railways and other obstacles. Available analytical methods of analysis are in conformance with the small-deflection theory of orthotropic plates. However, in order to ascertain their inherent overload-carrying capacity due to ductility and redistribution of stresses with yield, a large deflection elasto-plastic analysis is required. Thus, a precise evaluation of the ultimate strength of orthotropic skew plates will invariably enable the designer to achieve further improvements in design efficiency. No such theoretical analysis was found in the literature.

The work presented herein stems from such a need to predict the structural responses of eccentrically stiffened skew plate structures in the inelastic range to assess the effects of overloading and to compute their ultimate load-carrying capacity. Other widespread use of such reinforced panels are found in air craft, space craft, hull and bulkhead panels in ship structures whose

orthotropic properties arise from geometry of the reinforced section rather than from anisotropy of the material itself. In many cases, the discrete reinforcement may be assumed to be continuously distributed giving rise to an equivalent orthotropic structure. The equivalent structure may then be analyzed to determine the displacements as well as overall stress resultants and stress couples.

The work embodied in this dissertation comprises:

(i) A theoretical non-linear (large-deflection) analysis of orthotropic skew plates simply supported on all sides and subjected to concentrated and uniformly distributed load.

(ii) An extension of the above large deflection solution of orthotropic skew plates into the elasto-plastic range to assess the ultimate load-carrying capacity for the cases of stiffened plates simply supported on all sides and subjected to uniformly distributed load.

(iii) An experimental investigation on orthotropic plate models to verify the theoretical solutions, (i) and (ii), for different skew angles, aspect and rigidity ratios.

In order to obtain the theoretical solutions for orthotropic skew plates undergoing large deflections into the elasto-plastic range, the plate behaviour is defined by the coupled sets of fourth-order differential equations

together with a set of boundary conditions. These governing equations are then approximated by their finite difference equivalents and the solution of the resulting sets of simultaneous equations is obtained by a successive approximation technique. Beyond the initiation of first yield at sections of maximum stressed ribs, an iterative incremental procedure has been adopted to take into account the reduction of stiffness with the corresponding increment of loading. Thus even though the overall behaviour of the structure is non-linear, it has been adequately expressed by a series of linearly incremental solutions. The step by step solution procedure is continued until the ribs at the sections of maximum stress intensity have fully yielded.

Finite difference equations are developed, both for the equilibrium and compatibility equations governing the large deflection orthotropic skew plate behaviour, at all the points influenced by the boundary conditions. Numerical solutions are obtained for different cases of loadings and boundary conditions in the elastic and elastic-plastic stress regions. A comparison with Levy's classical series solution as a non-linear problem for an isotropic square plate undergoing large deflections showed good agreement with the present solution.

The experimental investigation consisted of testing of three orthotropic plate models fabricated from

high strength structural steel. In order to obtain the numerical solutions, the entire step by step solution procedure of this boundary-value problem was automated on an IBM system 360/65 computer.

CHAPTER 2

REVIEW OF LITERATURE

The available large-deflection orthotropic plate theory used for the analysis of rectangular plates, may be extended to study the large-deflection behaviour of orthotropic skew plates, in spite of the mathematical complexities encountered in their analysis. These mathematical complexities are due to the selecting of a proper mathematical model capable of describing the actual physical behaviour, the absence of orthogonal relationship due to the introduction of skew in geometry and the presence of singular behaviour at obtuse corners (6). Hence the available methods of elastic analysis of orthotropic skew plates are based on classical small deflection theory of plates. Literature pertaining to this investigation at various stages of plate behaviour will be reviewed in this chapter.

2.1 Linear Analysis of Skew Plates

The linear (small-deflection) behaviour of skew plates and slabs has been investigated by various methods, e.g. finite difference, finite element, series solutions, variational technique, Ritz method, perturbation, strip and others.

One of the first investigators to use the finite difference method for the solution of skew plate problems was Vogt (7) who obtained the results for a uniformly loaded skew slab with two opposite sides simply supported and the other two edges free. Jensen (8),(9) used this method to study the behaviour of skew slab bridges with curbs. Ehasz (10) employed the finite difference method for the solution of uniformly loaded 30° skew plates with all edges simply supported as well as clamped. The finite difference technique was also used by Robinson (11),(12), Brewster (13), Yeginobali (14) and Morley (15),(16) for various skew plate problems.

Naruoka and Ohmura (17) used Marcus' finite difference approach to calculate influence coefficients for deflections and bending moments for simply supported orthotropic skew plates with the two opposite edges elastically supported. Theoretical results were substantiated by experimental results of model skew girder bridges (18),(19). Similar analysis was reported by Basar and Yuksel (20), but no numerical results were given.

Cheung, King and Zienkiewicz (21) applied the finite element method for the solution of isotropic skew plate problems. Powell and Ogden (22) used the finite element method to analyze orthotropic steel plate bridge decks in orthogonal configuration. Recently, Monforton (23) developed a finite element formulation for the small

displacement analysis of orthotropic skew plates.

In 1964, Kennedy and Huggins (24) developed a method using a single infinite Fourier series representation of the deflection of stiffened skew plates under a uniformly distributed load. Kennedy and Ng (25),(26) solved the small deflection problem of uniformly loaded skew plates by means of variational techniques and the results were verified by experiments.

Coull (27),(28) published an approximate method for the analysis of simply supported uniformly loaded orthotropic skew bridge slabs with two opposite edges free. He used the principle of least work in conjunction with the assumption that the load and stress components may be represented by a power series in the chordwise co-ordinates, the coefficients of the series being functions of the spanwise position only. Minimizing the strain energy stored, the resulting sets of ordinary differential equations were solved. He found on comparison with model tests on isotropic slabs that agreement between the theoretical and experimental results deteriorated with increasing skew.

The Rayleigh-Ritz technique was used by Dorman (29) to obtain approximate solutions of uniformly loaded clamped skew plates. Iyenger, Sundera and Srinivasan (30) used Lardy's method of series solution to solve isotropic skew plate problems. Sampath (31) presented the solution

of simply supported isotropic skew plates using polar functions and Taylor expansions.

Simply supported skew plate problems with small deflections have also been dealt with by Morley (15) using corner functions, Aggarwala (32) by conformal mapping and Argyris (33) by the matrix displacement method of finite element. Karrholm (34) used the strip technique in combination with trigometric series in the analysis of simply supported skew plates. Recently, Gupta (85) presented a series solution of single and continuous span orthotropic skew plate problems. His results were substantiated and verified by test results.

2.2 Non-linear Analysis of Plate Problems

In 1910, von Kármán (35) formulated non-linear (large-deflection) theory of thin isotropic plates. He considered the effect of both bending and membrane stresses which arise from the stretching of the middle plane of the plate. The resulting coupled set of two non-linear fourth order partial differential equations are:

$$\nabla^4 w = \frac{h}{D}\left[\frac{q}{h} + F_{,yy}\, w_{,xx} - 2F_{,xy}\, w_{,xy} + F_{,xx}\, w_{,yy}\right] \tag{2.1}$$

$$\nabla^4 F = E\left[(w_{,xy})^2 - w_{,xx}\, w_{,yy}\right] \tag{2.2}$$

where the comma notation signifies differentiation;

w is the transverse plate deflection*; and,

F is the Airy stress function defined by

$$N_x = h\,F_{,yy} \quad , \quad N_y = h\,F_{,xx} \quad , \quad N_{xy} = -h\,F_{,xy} \tag{2.3}$$

h is the uniform plate thickness, and the plate flexural rigidity is defined by $D = \frac{Eh^3}{12(1-\nu^2)}$

N_x, N_y are the resultant in-plane axial force per unit length in the x- and y-direction, respectively.

E is the modulus of elasticity and ν is Poisson's ratio.

In general, exact solution of equations (2.1) and (2.2) combined with a set of boundary conditions as a boundary value problem is extremely difficult. It is therefore necessary to apply approximate methods for the solution of these coupled sets of governing equations.

Kaiser (36) used the finite difference method to solve these equations in terms of the transverse deflection and Airy stress function for a square isotropic plate having simply supported edges without in-plane restraint. Wang (37) extended this method along with an iterative scheme to find a solution of simply supported and clamped

*Definition of all symbols used are summarized in the nomenclature.

rectangular plates, for aspect ratio = 1, 1.5 and 2.

Levy (38),(39) expressed the deflection and the Airy stress function in terms of two infinite series, the coefficients of which were subsequently obtained by substituting the series into the governing equations and solving a set of simultaneous cubic equations. He obtained a high degree of accuracy even with a limited number of non-zero terms.

Way (40) used the Ritz method to solve the deflection of uniformly loaded clamped rectangular plates. The same method was used by Bengston (41) to obtain the solution of rectangular plates with simply supported and clamped edges under combined axial and lateral loading. Recently, Yang (42) presented a finite element incremental stiffness formulation for determining the finite displacement flexural behaviour of thin elastic isotropic plates. The results included rectangular plates under lateral pressure with various edge conditions and aspect ratio. Kennedy and Ng (43) have utilized a perturbation technique to yield an approximate solution to the non-linear problem of uniformly loaded isotropic skew plates with clamped edges.

Rostovtsev (44) presented the non-linear differential equations for the large-deflection behaviour of an ideal orthotropic plate, which may be presented as follows:

$$D_x w_{,xxxx} + 2H w_{,xxyy} + D_y w_{,yyyy}$$

$$= q(x,y) + h(F_{,yy} w_{,xx} - 2F_{,xy} w_{,xy} + F_{,xx} w_{,yy}) \tag{2.4}$$

$$\frac{1}{E_y} F_{,xxxx} + \left(\frac{1}{G_{xy}} - 2\frac{\nu_x}{E_x}\right) F_{,xxyy} + \frac{1}{E_x} F_{,yyyy}$$

$$= \left[(w_{,xy})^2 - w_{,xx} w_{,yy}\right] \tag{2.5}$$

where D_x and D_y are the plate bending stiffnesses in the x- and y-directions, respectively, (2H) is the plate torsional rigidity, E_x and E_y are the moduli of elasticity in the x- and y-direction, ν_x is Poisson's ratio associated with x-direction and G_{xy} is the shear modulus.

As with the von Kármán's equations, there is no exact known solution for equations (2.4) and (2.5). However, approximate solutions have been obtained by various investigators. Some have been concerned with orthotropic plates in general, while others have considered deck plates with orthogonal stiffening ribs.

Yusuff (45) solved the case of simply supported rectangular orthotropic plate composed of fibreglass panel with initial curvature and two parallel edges subjected to compression loading. Two double cosine series were used to represent the plate deflection w and the Airy stress function F. The coefficients of each of

the series were determined by solving the resulting set of simultaneous equations.

Otto Steinhardt and G. Abdel-Sayed (46) presented a solution of a laterally loaded rectangular flanged plate with membrane action in the middle plane of the plate. A series solution combined with an iterative scheme was used to yield deflections and stresses of an edge stiffened plate which is simply supported on two opposite sides. Soper (47) solved the problem of a uniformly loaded stiffened rectangular plate with rotational edge restraint. He used double sine series to express deflections as well as loadings. A double cosine series was used to express the Airy stress function. The solution involved solving a set of simultaneous equations for the coefficients in the series.

Basu and Chapman (48) used finite difference approximation to solve the problem of transversely loaded orthotropic rectangular plate undergoing large deflection, having elastic, flexural, extensional and shearing edge restraint. A similar procedure has been adopted by Adotte (49) to obtain bending and membrane stresses of rectangular orthotropic plates with large deflections.

Vogel (50) used a combination procedure based on the Ritz energy method to solve for the large deflections of reinforced plates. He modified Rostovtsev compatibility equation (2.5) to take into account that part of the

membrane stresses is carried by the reinforcing ribs. He assumed that part of the load is carried by the bending and shearing stresses calculated by the first order linear theory and other part of the load is carried by the membrane stresses. The linear solution may be obtained from one of several solutions of Huber's orthotropic plate equations (52). Vogel used Mader's (51) solution in his computations. The membrane solution was obtained by the Ritz energy method.

It is to be noted that in all the foregoing literature reviewed, only elastic behaviour was assumed. In what follows contributions which considered either plastic or elastic-plastic behaviour or both are reviewed.

2.3 Elastic-Plastic Analysis

Ilyushin (53) appears to be the first to apply the method of successive elastic solutions with an iterative procedure to the solution of the problem of a thin shell with plastic deformation. Each iteration involved essentially the solution of an elastic problem. In the variational method proposed by Ilyushin (53), expressions for deflections are first assumed in terms of some unknown parameters. These expressions are then substituted into the variational equations of equilibrium and the unknown parameters for deflection functions are determined. The problem of plastic deformation of a thick plate was discussed as an illustrative example.

The application of limit analysis to plates was introduced by Prager (69), (54) and extensive developments in the general theory of plasticity were made by Hill (55). Hill pointed out that the principles of limit analysis are most conveniently formulated for a rigid-perfectly plastic material whenever the combined stresses are less than those which determine the yield criterion. However, a limit analysis formulated on the plastic flow concept resulting in formation of a collapse mechanism does not examine elastic deflections. Tekinalp (56) and Haythornthwaite (57) indicated that a separate and more involved elasto-plastic analysis is required to study deflections of plates on the verge of collapse.

Elastic-plastic strength analysis of infinitely long rectangular plates under lateral pressure was presented by Clarkson (59). In his analysis, Clarkson solved the von Kármán's large-deflection plate equations by a power series method in which he used two terms of the series to obtain final results. By means of direct integration of simplified plate deflection equations, Wah (60) succeeded in obtaining a closed form solution for deflections, membrane tensions, etc., for the same problem. Lee (61) used an energy approach to the elastic-plastic analysis of simply supported rectangular plates under combined axial and lateral loading. He assumed that the displacement functions in the elastic

and elastic-plastic ranges have the same form, all of them defined by a single unknown parameter; an approximate solution was then obtained by means of the principle of minimum potential energy.

Recently, small deflection elastic-plastic solutions of rectangular plates under uniform lateral pressure were given by Lin and Ho (62). They used the analogy between inelastic strains and a set of lateral load, edge forces and edge moments. Finite difference techniques have been utilized by Bhaumic and Hanley (63) for the elasto-plastic analysis of isotropic rectangular plates. A similar method was adopted by Kagan (64) for an elasto-plastic analysis of rectangular reinforced plates. Ang and Lopez (65) developed a discrete model of a plate consisting of a system of flexible nodes, rigid bars and torsional elements to represent an elasto-plastic analysis of an isotropic rectangular plate.

Circular plates of various types and loadings have been analyzed extensively with rigid-plastic and elastic-plastic properties; these problems lend themselves to closed form solutions (66,67,68). Polygonal plates have not yet been satisfactorily solved. In 1952, Prager (69) obtained the critical load of an isotropically reinforced concrete square plate simply supported on all sides by using Johansen's (70) failure criterion which corresponds to the principal stress type of failure and results in a diagonal yield pattern.

Recently, Kennedy and Jain (87) published a method for evaluating ultimate strength of reinforced concrete slabs. The method considers the behaviour of both isotropically and nonisotropically reinforced slabs from initial to collapse load with the ultimate load obtained independent of the bound theorem. The experimental results provided direct support for the yield criterion established as well as for the complete elastic-plastic solution.

Granholm and Rowe (71) have derived a yield line theory for calculating the collapse load for simply supported reinforced concrete skew slab. The derivations pertain to the condition where the reinforcing steel is placed parallel to the edges of the slab. This is the only solution known to the author for the evaluation of the ultimate strength of a skew slab. The method has all the limitations of the yield line theory; for example, it leads to an upperbound solution to the collapse load, since the assumed yield pattern is not necessarily the most critical mechanism. The solution procedure does not provide sufficient information regarding the distribution of bending and twisting moments away from the yield line and thus the distribution of reinforcement becomes difficult. Moreover, the method fails to trace the deformation path while evaluating the collapse load.

A survey of the pertinent literature related to the problem of elasto-plastic analysis of orthotropic skew plates undergoing large deflection reveals that no such theoretical solution is available in the literature. The review also explored some of the basic difficulties which should be considered to analyze the response of eccentrically stiffened skew plates on the verge of collapse.

CHAPTER 3

MATHEMATICAL FORMULATION

3.1 General Concept

If a homogeneous material has three mutually perpendicular planes of symmetry with respect to its elastic properties, it is called orthotropic, i.e. materials which are orthogonally anisotropic. Strictly speaking, two-way reinforced concrete slabs, for instance, are inherently anisotropic. Other examples of such natural anisotropy are wood, plywood and fiber-reinforced plastics. In some cases, however, structural anisotropy is introduced by means of ribs or corrugations such as decks of contemporary steel bridges, composite beam-grid works, plates reinforced with closely spaced flexible ribs, corrugated plates, to name a few. These must be analyzed using orthotropic plate theory which postulates that the orthotropy of structures may be replaced by the orthotropy of constituent material. Huber (52) was the first to apply this technique to the solution of reinforced concrete plates. Although the actual structural behaviour of a plate stiffener combination cannot be completely replaced by that of an equivalent orthotropic plate, theoretical investigations (79),(80),(81),(82),(83) and experimental data (19) indicate good agreement with this

idealization under the following conditions (4):

1. The ratio of stiffener spacing to plate boundary dimensions is small enough (C_1/L_y, $C_2/L_x << 1$) to insure approximate homogeneity of stiffness.

2. Flexural and torsional rigidities do not depend on the boundary conditions of the plate or on the distribution of vertical load.

3. The plate and stiffeners are integral, i.e. a perfect bond exists between them.

4. In the case of steel stiffened plates, it is assumed that both plates and stiffeners are fabricated from the same isotropic material.

In the absence of a horizontal plane of symmetry for a deck plate with eccentrically stiffening ribs, rigorous solution of such a structurally orthotropic plate would require the consideration of the variation of the displacement components, u, v, and w in all the three directions x, y and z; (72),(73). This treatment, although rigorous, is also the most difficult to solve because it involves a complex system of three simultaneous equations. The three dimensional problem leads to a partial differential equation of the 8th order in the variable $w = w(x,y,z)$. Bares (74) has shown from an analytical study of the problem that the shear distribution is considerably dependent on the support conditions and loading intensity. Although some of the problems are

clear in theory, the procedures are as yet not apt for use in design practice, since the solutions are still too cumbersome and time consuming.

The primary purpose of this chapter is to define the differential equations of equilibrium and compatibility, governing the large deflection behaviour of an orthotropic skew plate. However, since the coefficients of these non-linear equations will be a function of the inelastic properties of the constituent material in the post-yield range, a brief discussion of the material behaviour and the assumed yield criterion will be given before the final equations are derived. In this investigation only the cases involving elastic-perfectly plastic material are treated.

3.2 Behaviour of Elastic-Perfectly Plastic Material

In an elastic-perfectly plastic solid, indefinite strain is possible once the stress condition for yield has been reached for a large enough region for plastic flow to be geometrically possible. Figure 3.1 shows the behaviour of a specimen of such material subjected to uniaxial state of stress. In the elastic stress range Hooke's law applies and the stress-strain relationship is defined by

$$\sigma_{ij} = E\,\varepsilon_{ij} \qquad (3.1)$$

where E is the constant of proportionality, equal to the slope of the line **oa**, σ_{ij} and ϵ_{ij} are the state of stress and strain, respectively. Once the value of σ_{ij} reaches $\sigma_{p_{ij}}$, plastic action begins. As postulated by Ziegler (75), the plastic behaviour of a material can be described by specifying: (1) an initial yield condition defining the elastic limit of the material; (2) a flow rule relating the plastic strain increments; and (3) a hardening rule used to establish the conditions of subsequent yielding from a plastic state of stress. Detailed discussions of yield criteria and plastic stress-strain relations of an inelastic material can be found in any classical treatise on the theory of plasticity (55), (76).

Since a method of successive elastic solution will be developed on a basis of incremental loading for the complete elasto-plastic analysis of this boundary-value problem, the assumption of elastic-perfectly plastic material behaviour will simplify the computations of rigidity properties with reference to the remaining elastic core of the cross-section in the post-yield range. This will be based on the initial yield condition defining the elastic limit of the material.

3.3 Yield Criterion

A law defining the limit of elasticity under any possible combinations of stresses is known as a yield criterion. It is possible to express the yield condition

as a function of the stress variables in a manner that plastic action will be possible when the function reaches some critical value. The two simple and the most widely used yield criteria, which are consistent with experimental evidence are Tresca and von Mises yield criteria. For most metals, von Mises yield criterion fits the experimental values more closely than Tresca's, but in general, Tresca's is simpler to use.

In this dissertation von Mises yield criterion will be utilized. This theory, known as the Distortion Energy theory, which is also associated with Hencky, assumes that yielding begins when the elastic strain energy required to distort the metal equals the volume of the energy required to cause yielding in simple tension or compression. For a general state of plane stress and in terms of cartesian co-ordinate system, this criterion states that yielding occurs when

$$\sigma_x^2 + \sigma_y^2 - \sigma_x\sigma_y + 3\,\tau_{xy}^2 = \sigma_p^2 \qquad (3.2)$$

in which σ_x and σ_y are the stresses in the x- and y-directions, respectively, τ_{xy} is the shear stress and σ_p is the yield stress.

In the case of uniaxial state of stress, if it is desired to extend the yield condition to include direct compression as well as tension of the specimen, equation

(3.2) reduces to

$$|\sigma_x| = \sigma_p \tag{3.3}$$

assigning a negative value to σ_x to indicate compression.

Certain further assumptions and simplifications that are consistent with experimental evidence are made in arriving at this criterion. These pertinent assumptions as explained by Hill (55) are:

(a) Time dependent effects are not considered; this means, for example, that creep, thermal and viscous effects are disregarded. In the governing equations to be defined, time enters as a homogeneous factor; therefore, the equations are independent of time element.

(b) The material of the stiffened plate system is assumed to be isotropic throughout its loading history.

(c) The Bauschinger effect arising from the anisotropy of the dislocation field produced by loading and unloading is also disregarded. This assumption will hold for cases involving no reversal in stress field. Hence yield is assumed to occur in uniform compression at the same level of stress for which yielding occurs in uniform tension.

3.4 Basic Assumptions

The analytical approach to the problem of orthotropic skew plates undergoing large deflections into the elasto-plastic range has to be based on some simplifying assumptions related to the form and material of the plate and to the state of strains induced by the external loading. These assumptions are considered to be valid both in the elastic and elasto-plastic stress regions. They are:

1. The material of the plate is elastic-perfectly plastic. The yielded material does not carry any additional load and may be neglected in computing elastic section properties for load increments in the post-yield range.

2. The thickness of the plate is small compared to its other dimensions.

3. Points in the plate and stiffener system lying initially on the normal to the neutral surface before bending remain on the normal to the neutral surface of the plate-stiffener system after bending. This is equivalent to Bernoulli's hypothesis which neglects the effects of shear on deformation, i.e. $\gamma_{xz} = \gamma_{yz} = 0$. (35).

4. Normal stresses in the direction transverse to the plane of the plate are negligible compared with the in-plane stresses. The problem is then one of plane stress.

5. The deflections of the plate may be large enough to induce strains in the middle plane of the plate.

6. The plate is perfectly plane before loading.

7. No unloading, i.e. no reversal of stress intensity in the plastic region takes place.

8. Structurally orthotropic plate dimensions are such that there will be no local buckling or other instability conditions.

9. The plates and ribs are free of residual stresses.

10. The plate geometry is such that the centroidal axes of the system lie close to the deck plate. This postulates that first yield is initiated in the ribs and subsequently propagates up to the deck plate which remains elastic during the entire loading history.

Assumption (1) is commonly used for structural steel which exhibits a definite yield point and undergoes a fairly large amount of deformation before strain hardening sets in.

Residual stresses due to cooling, cold bending or welding may be present in actual fabricated structures, but beyond the elastic range they do not have any effect on the ultimate strength of the structural system whose load capacity is not limited by instability (78,58).

Assumption (5) leads to the large deflection plate equations considering the deformation of the middle

plane of the plate which is caused by bending and membrane effects.

3.5 Differential Equation of Equilibrium due to Bending and Membrane Effects

Figure 3.2 shows a typical element cut from a plate structure which is stiffened by integral ribs where the principal directions of orthotropy coincide with the x- and y- co-ordinate axes. Neglecting body forces, the external forces and moments acting on the element satisfy the following equilibrium conditions:

$$\Sigma M_z = 0 \quad N_{xy} = N_{yx} \tag{3.4a}$$

$$\Sigma F_x = 0 \quad N_{x,x} + N_{yx,y} = 0 \tag{3.4b}$$

$$\Sigma F_y = 0 \quad N_{xy,x} + N_{y,y} = 0 \tag{3.4c}$$

(3.4)

$$\Sigma M_x = 0 \quad M_{xy,x} - M_{y,y} + Q_y = 0 \tag{3.4d}$$

$$\Sigma M_y = 0 \quad -M_{yx,y} - M_{x,x} + Q_x = 0 \tag{3.4e}$$

$$\Sigma F_z = 0 \quad Q_{x,x} + Q_{y,y} + q(x,y) + N_x w_{,xx} + N_y w_{,yy} + 2 N_{xy} w_{,xy} = 0 \tag{3.4f}$$

observing that $M_{yx} = -M_{xy}$ by virtue of $\tau_{xy} = \tau_{yx}$, the last three equations can be combined into the following

expression, by eliminating Q_x and Q_y:

$$M_{x,xx} - 2 M_{xy,xy} + M_{y,yy} + q(x,y) + N_x w_{,xx}$$

$$+ N_y w_{,yy} + 2 N_{xy} w_{,xy} = 0 \qquad (3.5)$$

The detailed derivations of the above equations are shown elsewhere (35).

Integrating over the sectional areas of the element of an ideal orthotropic plate, the forces and moments are related to the stresses in the following manner:

$$N_x = \int_{-h/2}^{h/2} \sigma_x \, dz \qquad (3.6a)$$

$$N_y = \int_{-h/2}^{h/2} \sigma_y \, dz \qquad (3.6b) \qquad (3.6)$$

$$N_{xy} = \int_{-h/2}^{h/2} \tau_{xy} \, dz \qquad (3.6c)$$

and

$$M_x = \int_{-h/2}^{h/2} \sigma_x \, z dz \qquad (3.7a)$$

$$M_y = \int_{-h/2}^{h/2} \sigma_y \, z dz \qquad (3.7b) \qquad (3.7)$$

$$M_{xy} = -M_{yx} = -\int_{-h/2}^{h/2} \tau_{xy}\, z\,dz \qquad (3.7c)$$

Considering only the bending stresses, it becomes evident that four elastic constants (E_x, E_y, ν_x, ν_y) are required for the description of orthotropic stress-strain relations:

$$\varepsilon_x = \frac{\sigma_x}{E_x} - \nu_y \frac{\sigma_y}{E_y}$$

$$\varepsilon_y = \frac{\sigma_y}{E_y} - \nu_x \frac{\sigma_x}{E_x} \qquad (3.8)$$

$$\gamma_{xy} = \frac{\tau_{xy}}{G_{xy}}$$

where the shear modulus G_{xy} of the orthotropic material can be expressed in terms of E_x and E_y as follows (86):

$$G_{xy} \approx \frac{\sqrt{E_x E_y}}{2(1 + \sqrt{\nu_x \nu_y})} \approx \frac{E}{2(1 + \sqrt{\nu_x \nu_y})} \qquad (3.9)$$

Expressing the strains in terms of lateral deflections, the following stress-displacement relations are obtained :

$$\sigma_x = -z \frac{E_x}{1 - \nu_x \nu_y} (w_{,xx} + \nu_y w_{,yy})$$

$$\sigma_y = -z \frac{E_y}{1 - \nu_x \nu_y} (w_{,yy} + \nu_x w_{,xx}) \qquad (3.10)$$

$$\tau_{xy} = -2 z G_{xy} w_{,xy}$$

Substitution of these relations into equation (3.7) gives

$$M_x = -(D_x w_{,xx} + D_1 w_{,yy})$$

$$M_y = -(D_y w_{,yy} + D_2 w_{,xx}) \qquad (3.11)$$

$$M_{xy} = 2 D_t w_{,xy}$$

where D_x and D_y are the flexural rigidities of the plate-stiffener system per unit width in x- and y-directions, respectively. $2 D_t$ is known as the torsional rigidity coefficient defined as the reciprocal value of the angle of twist of a plate element with the side length $dx = dy = 1$ due to the action of twisting moment $M_{yx} = -M_{xy} = 1$; and $D_1 = \nu_y D_x$; $D_2 = \nu_x D_y$; $4 D_t = D_{xy} + D_{yx}$. D_1 and D_2 are the contributions of bending to the torsional rigidity and D_{xy}, D_{yx} are the longitudinal and transverse torsional rigidities of the plate-stiffener system (74).

In order to express the governing differential equation of an orthotropic plate in terms of the transverse displacement w of the plate neutral surface, expressions (3.11) are substituted into equation (3.5) and the following equation is obtained:

$$D_x w_{,xxxx} + 2H w_{,xxyy} + D_y w_{,yyyy}$$

$$= q(x,y) + N_x w_{,xx} + N_y w_{,yy} + 2N_{xy} w_{,xy} \qquad (3.12)$$

where H is the effective torsional rigidity defined by (74), $H = (D_1 + D_2 + D_{xy} + D_{yx})/2$; this characterizes the resistance of the orthotropic plate element to twisting.

In accordance with Betti's law of reciprocity,

$$\frac{D_x}{D_y} = \frac{\nu_x}{\nu_y} \qquad (3.13)$$

it is apparent that the factors ν_x and ν_y, although representing the relationship between the stress σ and the transverse strain ϵ, are not material constants as 'Poisson's ratio' proper but are elastic constants corresponding to the geometric configuration of the structure...hence the name orthotropy of form as distinct from orthotropy of material.

3.6 Compatibility Equation Due to Membrane Forces

Considering the effect of large deflections, the strain-displacement relations for the middle plane of the plate element, Fig. 3.3, may be obtained by retaining only the first power of the derivatives of u and v_1 and the second power of the derivative of w, as follows:

$$\varepsilon_x^m = u_{,x} + \tfrac{1}{2}(w_{,x})^2$$

$$\varepsilon_y^m = v_{1,y} + \tfrac{1}{2}(w_{,y})^2 \qquad (3.13)$$

$$\gamma_{xy}^m = u_{,y} + v_{1,x} + w_{,x}\, w_{,y}$$

Combining the above equations yields the compatibility equation as follows:

$$\varepsilon_{x,yy}^m + \varepsilon_{y,xx}^m - \gamma_{xy,xy}^m = \left[(w_{,xy})^2 - w_{,xx}\, w_{,yy}\right] \qquad (3.14)$$

The relationship between the strain in the middle plane and the membrane forces can be represented by:

$$\varepsilon_x^m = \frac{N_x}{t_x E_x} - \nu_y \frac{N_y}{t_y E_y}$$

$$\varepsilon_y^m = \frac{N_y}{t_y E_y} - \nu_x \frac{N_x}{t_x E_x} \qquad (3.15)$$

$$\gamma_{xy}^m = \frac{N_{xy}}{t G_{xy}}$$

where t is the thickness of the deck plate, t_x and t_y are the weighted effective thickness referred to the x- and y-directions, respectively.

Introducing the Airy stress function F, the membrane stresses and the membrane forces may be defined as (50):

$$\sigma_x^m = \frac{t}{t_x} F,yy$$

$$\sigma_y^m = \frac{t}{t_y} F,xx \qquad (3.16)$$

$$\tau_{xy}^m = -F,xy$$

where σ_x^m, σ_y^m are the membrane stresses in the x- and y-directions and τ_{xy}^m is the shearing stress in the deck plate due to membrane action; and,

$$N_x = t_x \sigma_x^m$$

$$N_y = t_y \sigma_y^m \qquad (3.17)$$

$$N_{xy} = - t \tau_{xy}^m$$

The definitions of N_x, N_y and N_{xy} are the same as for an isotropic plate; i.e.

$$N_x = t\,F_{,yy}\ ,\ N_y = t\,F_{,xx} \text{ and } N_{xy} = -t\,F_{,xy} \tag{3.18}$$

Most of the membrane stresses are still carried by the deck plate and only a small portion is taken by the ribs.

Substituting equation (3.18) into equation (3.15), the strains in the middle plane can be expressed in terms of the Airy stress function as

$$\varepsilon_x^m = \frac{t}{t_x E_x} F_{,yy} - \nu_y \frac{t}{t_y E_y} F_{,xx}$$

$$\varepsilon_y^m = \frac{t}{t_y E_y} F_{,xx} - \nu_x \frac{t}{t_x E_x} F_{,yy} \tag{3.19}$$

$$\gamma_{xy}^m = -\frac{1}{G_{xy}} F_{,xy}$$

In order to obtain the compatibility equation in terms of the transverse displacement w and the Airy stress function F, equations (3.19) are substituted into equation (3.14) yielding the following equation:

$$\frac{t}{t_x}\frac{1}{E_x} F_{,yyyy} + \left[2\,\frac{(1+\sqrt{\nu_x \nu_y})}{\sqrt{E_x E_y}} - \frac{t}{t_y}\frac{\nu_y}{E_y} - \frac{t}{t_x}\frac{\nu_x}{E_x} \right] F_{,xxyy}$$

$$+ \frac{t}{t_y}\frac{1}{E_y} F_{,xxxx} = \left[(w_{,xy})^2 - w_{,xx}\, w_{,yy} \right] \tag{3.20}$$

Since it was assumed in section (3.3) that the material behaviour of the stiffened plate structure remains isotropic during the entire loading history, the two governing equations (3.12) and (3.20) defining the large-deflection behaviour of an orthotropic plate element may be expressed as follows:

$$D_x w_{,xxxx} + 2H w_{,xxyy} + D_y w_{,yyyy} = q(x,y) + t(w_{,xx} F_{,yy} - 2F_{,xy} w_{,xy} + w_{,yy} F_{,xx}) \qquad (3.21)$$

and,

$$B_x F_{,xxxx} + 2H' F_{,xxyy} + B_y F_{,yyyy} = E\left[(w_{,xy})^2 - w_{,xx} w_{,yy}\right] \qquad (3.22)$$

In the compatibility equation (3.22) the in-plane rigidities are defined as:

$$B_x = \frac{t}{t_y} \qquad (a)$$

$$B_y = \frac{t}{t_x} \qquad (b) \qquad (3.23)$$

$$2H' = \left[2(1 + \sqrt{\nu_x \nu_y}) - t\left(\frac{\nu_y}{t_y} + \frac{\nu_x}{t_x}\right)\right] \qquad (c)$$

where $E_x = E_y = E$; $G = \dfrac{E}{2(1 + \sqrt{\nu_x \nu_y})}$

$$t_x = \frac{A_x}{c_1}$$

$$t_y = \frac{A_y}{c_2}$$

A_x, A_y are the cross-sectional areas of the slab and beam portion of the repeating section and c_1,c_2 are the spacing of ribs in x- and y-directions, respectively.

For an isotropic plate of uniform thickness without stiffening ribs, equation (3.21) and (3.22) reduce to von Kármán's large deflection coupled sets of non-linear equations (2.1) and (2.2) as was shown in chapter 2.

3.7 The Oblique Co-ordinate System:

In investigating the problem of orthotropic skew plates undergoing large deflections into the elastic-plastic range, it is often advantageous to transform the governing equations into an oblique co-ordinate system parallel to the edges of the plate as shown in Fig. 3.4. If (x,y) are the rectangular co-ordinate of a point in the neutral surface of the equivalent orthotropic plate and ϕ is the skew angle, then the corresponding oblique co-ordinates are:

$$u = x + y \tan \phi$$

and (3.24)

$$v = y \sec \phi$$

Equations (3.21) and (3.22) may now be transformed into the following coupled sets of differential equations defining the large deflection behaviour of an orthotropic skew plate (see Appendix A).

Equilibrium equation (3.21) becomes

$$\left(D_x + 2H\frac{s^2}{c^2} + D_y\frac{s^4}{c^4}\right) w_{,uuuu} + \left(4H\frac{s}{c^2} + 4D_y\frac{s^3}{c^4}\right) w_{,uuuv}$$

$$+ \left(2H\frac{1}{c^2} + 6D_y\frac{s^2}{c^4}\right) w_{,uuvv} + 4D_y\frac{s}{c^4} w_{,uvvv} + D_y\frac{1}{c^4} w_{,vvvv}$$

$$- \frac{t}{c^2}\left[(F_{,vv})(w_{,uu}) - 2(F_{,uv})(w_{,uv}) + (F_{,uu})(w_{,vv})\right]$$

$$= q(x,y) \qquad (3.25)$$

and the compatibility equation (3.22) is transformed to:

$$\left(B_x + 2H'\frac{s^2}{c^2} + B_y\frac{s^4}{c^4}\right) F_{,uuuu} + \left(4H'\frac{s}{c^2} + 4B_y\frac{s^3}{c^4}\right) F_{,uuuv}$$

$$+ \left(2H'\frac{1}{c^2} + 6B_y\frac{s^2}{c^4}\right) F_{,uuvv} + 4B_y\frac{s}{c^4} F_{,uvvv}$$

$$+ B_y\frac{1}{c^4} F_{,vvvv} = \frac{E}{c^2}\left[(w_{,uv})^2 - (w_{,uu})(w_{,vv})\right] \qquad (3.26)$$

Equations (3.25) and (3.26) together with the proper set of boundary conditions define the boundary-value problem of an orthotropic skew plate undergoing large deflections. Solutions of these equations will yield functions w and F from which the bending and membrane stress components can be found at any point within the plate boundary. These stresses will be superimposed to determine the initiation of yield at sections of maximum stress intensity. Beyond the initiation of yield, non-linearity due to the reduction in the plate-rib rigidities also appears. As indicated by Lee (61), the expressions for intensity of strains in the post-yield region is a very complicated one. Thus equations (3.6) and (3.7) can not be readily integrated and their substitution into equation (3.5) results in integro-differential equations of very complicated form. Thus, since the problem of finding the complete elastic-plastic response of eccentrically stiffened skew plates is very complex and is not amenable to any analytic solution, a numerical solution procedure will be presented based on the finite difference technique. The choice of this method is due to its relatively simple and easy mathematical formulation.

3.8 Computation of Plate Rigidities

By applying the principle of elastic equivalence, the structurally orthotropic plate which is geometrically discontinuous, is represented by an idealized substitute

orthotropic plate, reflecting the characteristic properties of the actual system. As mentioned previously, investigators, realizing the limitations in direct application of the Huber equation to eccentrically stiffened plates have tried to overcome these restrictions by various approaches.

Giencke (79) and Massonet (80) accounts for the eccentric placement of stiffening ribs by making certain modifications of the constants in the Huber equation. Schuman (81) and Madar (51) have computed the stresses in the decks accounting in different ways for the discontinuous arrangements of the reinforcing ribs. Hoffman (82) used experimental techniques while Huffington (83) evaluated theoretically the rigidities of the Huber equation. The complexity arises from the unknown location of the neutral surfaces of the plate-stiffener system for bending and membrane stresses. Moreover, the neutral surfaces of the structure do not coincide in the x- and y-directions.

In order to circumvent this situation, certain assumptions are made to determine the location of the neutral surface by considering the neutral planes for bending and membrane stresses in both x- and y-directions to be located at the centre of gravity of the section. This is an approximation only, since it can be shown that the location of the neutral surfaces is a function of the

deflections as well as geometry of the section. Another condition which is assumed herein is that the longitudinal and transverse stiffening ribs are thin and relatively closely spaced so that effective width of the plate is equal to the centre to centre distance between ribs. Bares and Massonet (74) have shown that the errors resulting from this assumption are less than 3%.

In this investigation the foregoing published methods (74),(83) are used to determine the elastic rigidities, both in the elastic and elasto-plastic stress regions; the latter rigidities are calculated with reference to the elastic portion of the cross-section.

Referring to Fig. 3.4, the flexural rigidities can be expressed as (83):

$$D_x = \frac{E\,t^3}{12(1-\nu_x\nu_y)} + \frac{E\,t\,(e_x - \frac{t}{2})^2}{1-\nu_x\nu_y} + \frac{E\,I_{ox}}{c_1} \qquad (3.27)$$

$$D_y = \frac{E\,t^3}{12(1-\nu_x\nu_y)} + \frac{E\,t\,(e_y - \frac{t}{2})^2}{1-\nu_x\nu_y} + \frac{E\,I_{oy}}{c_2}$$

where I_{ox}, I_{oy} = moment of inertia of the longitudinal and transverse ribs about the neutral surface in the x- and y-directions, respectively.

c_1, c_2 = spacings of longitudinal and transverse ribs.

e_x, e_y = distances of the neutral surface of the repeating section from top fibre of the plate in the longitudinal and transverse directions, respectively.

The effective torsional rigidity is expressed as

$$2H = D_1 + D_2 + D_{xy} + D_{yx}$$

According to Bares and Massonet (74) the values of D_{xy} and D_{yx} are determined by means of the torsional constants corresponding to the different elements constituting the section.

In case of an open-web slab and beam section (T-beam section), Fig. 3.4, the torsional rigidities are expressed as:

$$D_{xy} = \frac{G_{xy}}{c_1}\left[\tfrac{1}{3}\, c_1\, t^3\, n_i + t_1^3 (d_1 - t)\, n_i\right]$$

$$\text{for} \quad \begin{pmatrix} t < c_1 \\ t_1 < (d_1 - t) \end{pmatrix} ; \qquad (3.28)$$

$$D_{yx} = \frac{G_{xy}}{c_2}\left[\tfrac{1}{3}\, c_2\, t^3\, n_i + t_2^3 (d_2 - t)\, n_i\right]$$

$$\text{for} \quad \begin{pmatrix} t < c_2 \\ t_2 < (d_2 - t) \end{pmatrix} .$$

where the first term of the right hand side refers to the slab portion and the second term to the beam portion of the section. The value of n_i depends on the ratio of the sides d_1/t_1 (or d_2/t_2) and is called the shape factor (74).

The various bending, torsional and membrane rigidities, appearing as coefficients of the coupled equations (3.25) and (3.26), are functions of the material properties and geometry of the elastic portion of the cross-section. Since the yielded zone will be neglected in carrying additional load increments in the post-yield range, these coefficients of the differential equation will vary from point to point within the plate boundary.

CHAPTER 4

APPLICATION OF FINITE DIFFERENCE TECHNIQUE TO THE SOLUTION OF THE COUPLED NON-LINEAR DIFFERENTIAL EQUATIONS

4.1 Introduction

The consideration and inclusion of the non-linear material behaviour of the structural system beyond the elastic range, requires a numerical solution technique since there is no available general solution. Finite difference technique is employed in this investigation to convert the differential equations into two sets of simultaneous algebric equations which are then solved by a method of successive approximations.

The solution of equations (3.25) and (3.26) is performed both for the elastic and the elastic-plastic stress regions. In the elastic stress region, the entire cross-section is effective in carrying the applied load. However, beyond the initiation of yield, an incremental iterative procedure is adopted with only the remaining elastic section being available for carrying the additional load.

4.2 Finite Difference Approximation

The method of finite difference replaces functions and their derivatives by algebraic expressions involving only the values of the functions at a finite number of

points in or near the region of interest. Adopting Marcus' method, the fourth order coupled sets of differential equations (3.21) and (3.22) are split conveniently into two second order equations. Equation (3.21) becomes:

$$\left(\frac{\partial^2}{\partial x^2} + \frac{\partial^2}{\partial y^2}\right)\left(D_x \frac{\partial^2 w}{\partial x^2} + D_y \frac{\partial^2 w}{\partial y^2}\right) + (2H - D_x - D_y) \frac{\partial^2}{\partial y^2}\left(\frac{\partial^2 w}{\partial x^2}\right)$$

$$- t\left(\frac{\partial^2 F}{\partial y^2} \frac{\partial^2 w}{\partial x^2} - 2 \frac{\partial^2 F}{\partial x \partial y} \frac{\partial^2 w}{\partial x \partial y} + \frac{\partial^2 F}{\partial x^2} \frac{\partial^2 w}{\partial y^2}\right) = q(x,y) \tag{4.1}$$

and

$$\left(\frac{\partial^2}{\partial x^2} + \frac{\partial^2}{\partial y^2}\right)\left(D_x \frac{\partial^2 w}{\partial x^2} + D_y \frac{\partial^2 w}{\partial y^2}\right) + (2H - D_x - D_y) \frac{\partial^2}{\partial x^2}\left(\frac{\partial^2 w}{\partial y^2}\right)$$

$$- t\left(\frac{\partial^2 F}{\partial y^2} \frac{\partial^2 w}{\partial x^2} - 2 \frac{\partial^2 F}{\partial x \partial y} \frac{\partial^2 w}{\partial x \partial y} + \frac{\partial^2 F}{\partial x^2} \frac{\partial^2 F}{\partial y^2}\right) = q(x,y) \tag{4.2}$$

Writing

$$U = D_x w_{,xx} + D_y w_{,yy}$$

$$D = 2H - D_x - D_y$$

$$X = w_{,xx} \; ; \; Y = w_{,yy}$$

$$F_y = F_{,yy} \text{ and } F_x = F_{,xx}$$

equations (4.1) and (4.2) reduce to

$$U_{,xx} + U_{,yy} + D\,X_{,yy} - t(F_y\,X - 2\,F_{,xy}\,w_{,xy} + F_x\,Y)$$

$$= q(x,y) \qquad (4.3a)$$

and

$$U_{,xx} - U_{,yy} + D\,Y_{,xx} - t(F_y\,X - 2\,F_{,xy}\,w_{,xy} + F_x\,Y)$$

$$= q(x,y) \qquad (4.3b)$$

Similarly, equation (3.22) may be written as:

$$V_{,xx} + V_{,yy} + Z\,F_{y,xx} = E\left[(w_{,xy})^2 - X\,Y\right] \qquad (4.4a)$$

and

$$V_{,xx} + V_{,yy} + Z\,F_{x,yy} = E\left[(w_{,xy})^2 - X\,Y\right], \qquad (4.4b)$$

where $V = B_x\,F_{,xx} + B_y\,F_{,yy}$

and $Z = 2H' - B_x - B_y$.

The deformation of the equivalent skew plate defined by the elastic surfaces $w = w(x,y)$ and $F = F(x,y)$ is also a function of $w = w(u,v)$ and $F = F(u,v)$. In this investigation central difference approximations are used in deriving the finite difference equations of equilibrium and compatibility. Recalling the finite difference approximations of the partial derivatives at a

point (x,y) or (u,v) ranging over the domain of definition of the function, derivatives can be approximated in terms of the deflections and Airy stress function at nodal points of a Favre's skew network with modified co-ordinate notation, Fig. 4.1, as follows:

$$(\bar{w}_{,uu}) = \frac{1}{\lambda_u^2}(\bar{w}_{i-1,j} - 2\,\bar{w}_{i,j} + \bar{w}_{i+1,j})$$

$$(\bar{w}_{,uv}) = \frac{1}{4\lambda_u\lambda_v}(\bar{w}_{i+1,j+1} - \bar{w}_{i-1,j+1} + \bar{w}_{i-1,j-1} - \bar{w}_{i+1,j-1}) \qquad (4.5)$$

$$(\bar{w}_{,vv}) = \frac{1}{\lambda_v^2}(\bar{w}_{i,j+1} - 2\,\bar{w}_{i,j} + \bar{w}_{i,j-1})$$

where $\bar{w}$ is a function representing both deflection w and Airy stress function F; λ_u, λ_v are the spacing of network points in u- and v-directions.

Some of the derivatives, presented in Appendix A, are now written in finite difference approximations as

$$X_{ij} = (w_{,xx})_{i,j} = \frac{\varkappa^2}{\lambda_y^2}(w_{i-1,j} - 2\,w_{i,j} + w_{i+1,j}) \qquad (4.6a)$$

$$Y_{i,j} = (w_{,yy})_{i,j} = \frac{1}{\lambda_y^2}\Big[\beta^2(w_{i-1,j} + w_{i+1,j}) - 2(1+\beta^2)w_{i,j} + \frac{\beta}{2}(w_{i+1,j+1} - w_{i-1,j+1} + w_{i-1,j-1} - w_{i+1,j-1}) + w_{i,j+1} + w_{i,j-1}\Big] \tag{4.6b}$$

$$(w_{,xy})_{i,j} = \frac{\varkappa}{\lambda_y^2}\Big[\beta(w_{i-1,j} - 2w_{i,j} + w_{i+1,j}) + \tfrac{1}{4}(w_{i+1,j+1} - w_{i-1,j+1} + w_{i-1,j-1} - w_{i+1,j-1})\Big] \tag{4.6c}$$

and

$$(w_{,xx} + w_{,yy})_{i,j} = \frac{1}{\lambda_y^2}\Big[\alpha(w_{i-1,j} + w_{i+1,j}) - 2(1+\alpha)w_{i,j} + \frac{\beta}{2}(w_{i+1,j+1} - w_{i-1,j+1} + w_{i-1,j-1} - w_{i+1,j-1}) + w_{i,j+1} + w_{i,j-1}\Big] \tag{4.6d}$$

where $\varkappa = \frac{\lambda_y}{\lambda_x}$, $\beta = \varkappa \tan\phi$ and $\alpha = \beta^2 + \varkappa^2$. λ_y and λ_x are the network spacing in the y- and x-directions, respectively.

The expression for U can be approximated in its finite difference form as

$$U_{i,j} = D_x(w_{,xx})_{i,j} + D_y(w_{,yy})_{i,j}$$

$$= \frac{1}{\lambda_y^2}\left[A(w_{i-1,j} + w_{i+1,j}) - 2(A + D_y)w_{i,j}\right.$$

$$+ \frac{\beta}{2} D_y(w_{i+1,j+1} - w_{i-1,j+1} + w_{i-1,j-1} - w_{i+1,j-1})$$

$$\left. + D_y\,(w_{i,j+1} + w_{i,j-1})\right] \qquad (4.7)$$

where $A = D_x \alpha^2 + D_y \beta^2$.

Similar expressions for the derivatives of the stress function F are also obtained as follows:

$$(F_x)_{i,j} = (F_{,xx})_{i,j} = \frac{\alpha^2}{\lambda_y^2}\,(F_{i-1,j} - 2F_{i,j} + F_{i+1,j}) \qquad (4.8a)$$

$$(F_y)_{i,j} = (F_{,yy})_{i,j} = \frac{1}{\lambda_y^2}\left[\beta^2(F_{i-1,j} + F_{i+1,j})\right.$$

$$- 2(1 + \beta^2)F_{i,j} + \frac{\beta}{2}\,(F_{i+1,j+1} - F_{i-1,j+1}$$

$$\left. + F_{i-1,j-1} - F_{i+1,j-1}) + F_{i,j+1} + F_{i,j-1}\right] \qquad (4.8b)$$

$$(F_{xy})_{i,j} = \frac{\alpha}{\lambda_y^2} \left[\beta (F_{i-1,j} - 2 F_{i,j} + F_{i+1,j}) + \tfrac{1}{4} (F_{i+1,j+1} - F_{i-1,j+1} + F_{i-1,j-1} - F_{i+1,j-1}) \right] \quad (4.8c)$$

and,

$$V_{i,j} = \frac{1}{\lambda_y^2} \left[A' (F_{i-1,j} + F_{i+1,j}) - 2 (A' + B_y) F_{i,j} + \frac{\beta}{2} B_y (F_{i+1,j+1} - F_{i-1,j+1} + F_{i-1,j-1} - F_{i+1,j-1}) + B_y (F_{i,j+1} + F_{i,j-1}) \right] \quad (4.8d)$$

where $A' = B_x \alpha^2 + B_y \beta^2$.

Following equations (4.6b) and (4.6d), the governing equation (4.3a) can be written in its finite difference equivalence as:

$$\frac{1}{\lambda_y^2} \left[\alpha (U_{i-1,j} + U_{i+1,j}) - 2(1 + \alpha) U_{i,j} + \frac{\beta}{2} (U_{i+1,j+1} - U_{i-1,j+1} + U_{i-1,j-1} - U_{i+1,j-1}) + U_{i,j+1} + U_{i,j-1} \right]$$

$$+ D \frac{1}{\lambda_y^2} \left[\beta^2 (X_{i-1,j} + X_{i+1,j}) - 2(1 + \beta^2) X_{i,j} \right.$$

$$+ \frac{\beta}{2} (X_{i+1,j+1} - X_{i-1,j+1} + X_{i-1,j-1} - X_{i+1,j-1})$$

$$\left. + X_{i,j+1} + X_{i,j-1} \right]$$

$$- \frac{t\alpha^2}{\lambda_y^2} \left[\left\{ \beta^2 (F_{i-1,j} + F_{i+1,j}) - 2(1 + \beta^2) F_{i,j} \right. \right.$$

$$+ \frac{\beta}{2} (F_{i+1,j+1} - F_{i-1,j+1} + F_{i-1,j-1} - F_{i+1,j-1})$$

$$\left. + F_{i,j+1} + F_{i,j-1} \right\} \times \left\{ w_{i-1,j} - 2w_{i,j} + w_{i+1,j} \right\}$$

$$- 2 \left\{ \beta (F_{i-1,j} - 2 F_{i,j} + F_{i+1,j}) + \tfrac{1}{4} (F_{i+1,j+1} \right.$$

$$\left. - F_{i-1,j+1} + F_{i-1,j-1} - F_{i+1,j-1}) \right\} \times$$

$$\left\{ \beta (w_{i-1,j} - 2 w_{i,j} + w_{i+1,j}) + \tfrac{1}{4} (w_{i+1,j+1} - w_{i-1,j+1} \right.$$

$$\left. + w_{i-1,j-1} - w_{i+1,j-1}) \right\} + \left\{ F_{i-1,j} - 2 F_{i,j} + F_{i+1,j} \right\} \times$$

$$\left\{ \beta^2 (w_{i-1,j} + w_{i+1,j}) - 2(1 + \beta^2) w_{i,j} \right.$$

$$\left. + \frac{\beta}{2} (w_{i+1,j+1} - w_{i-1,j+1} + w_{i-1,j-1} - w_{i+1,j-1}) \right.$$

$$+ w_{i,j+1} + w_{i,j-1} \Big\} \Big] = q(x,y) \qquad (4.9)$$

where

$$U_{i-1,j} = \frac{1}{\lambda_y^2} \Big[A(w_{i-2,j} + w_{i,j}) - 2 (A + D_y) w_{i-1,j} + \frac{\beta}{2} D_y (w_{i,j+1} - w_{i-2,j+1} + w_{i-2,j-1} - w_{i,j-1}) + D_y (w_{i-1,j+1} + w_{i-1,j-1}) \Big] \qquad (4.10a)$$

$$U_{i+1,j} = \frac{1}{\lambda_y^2} \Big[A(w_{i+2,j} + w_{i,j}) - 2 (A + D_y) w_{i+1,j} + \frac{\beta}{2} D_y (w_{i+2,j+1} - w_{i,j+1} + w_{i,j-1} - w_{i+2,j-1}) + D_y (w_{i+1,j+1} + w_{i+1,j-1}) \Big] \qquad (4.10b)$$

$$U_{i+1,j+1} = \frac{1}{\lambda_y^2} \Big[A(w_{i,j+1} + w_{i+2,j+1}) - 2 (A + D_y) w_{i+1,j+1} + \frac{\beta}{2} D_y (w_{i+2,j+2} - w_{i,j+2} + w_{i,j} - w_{i+2,j}) + D_y (w_{i+1,j+2} + w_{i+1,j}) \Big] \qquad (4.10c)$$

$$U_{i-1,j+1} = \frac{1}{\lambda_y^2}\left[A(w_{i-2,j+1} + w_{i,j+1}) - 2(A + D_y)\, w_{i-1,j+1}\right.$$

$$+ \frac{\beta}{2} D_y\,(w_{i,j+2} - w_{i-2,j+2} + w_{i-2,j} - w_{i,j})$$

$$\left. + D_y\,(w_{i-1,j+2} + w_{i-1,j})\right] \qquad (4.10d)$$

$$U_{i-1,j-1} = \frac{1}{\lambda_y^2}\left[A(w_{i-2,j-1} + w_{i,j-1}) - 2(A + D_y)\, w_{i-1,j-1}\right.$$

$$+ \frac{\beta}{2} D_y\,(w_{i,j} - w_{i-2,j} + w_{i-2,j-2} - w_{i,j-2})$$

$$\left. + D_y\,(w_{i-1,j} + w_{i-1,j-2})\right] \qquad (4.10e)$$

$$U_{i+1,j-1} = \frac{1}{\lambda_y^2}\left[A(w_{i,j-1} + w_{i+2,j-1}) - 2(A + D_y)\, w_{i+1,j-1}\right.$$

$$+ \frac{\beta}{2} D_y\,(w_{i+2,j} - w_{i,j} + w_{i,j-2} - w_{i+2,j-2})$$

$$\left. + D_y\,(w_{i+1,j} + w_{i+1,j-2})\right], \qquad (4.10f)$$

$$U_{i,j+1} = \frac{1}{\lambda_y^2}\left[A(w_{i-1,j+1} + w_{i+1,j+1}) - 2(A + D_y)\, w_{i,j+1}\right.$$

$$+ \frac{\beta}{2} D_y\,(w_{i+1,j+2} - w_{i-1,j+2} + w_{i-1,j} - w_{i+1,j})$$

$$\left. + D_y\,(w_{i,j+2} + w_{i,j})\right] \qquad (4.10g)$$

$$U_{i,j-1} = \frac{1}{\lambda_y^2}\left[A(w_{i-1,j-1} + w_{i+1;j-1}) - 2(A + D_y)\, w_{i,j-1} + \frac{\beta}{2} D_y\,(w_{i+1,j} - w_{i-1,j} + w_{i-1,j-2} - w_{i+1,j-2}) + D_y\,(w_{i,j} + w_{i,j-2})\right] \quad (4.10h)$$

and

$$X_{i-1,j} = \frac{\varkappa^2}{\lambda_y^2}\,(w_{i-2,j} - 2\, w_{i-1,j} + w_{i,j}) \quad (a)$$

$$X_{i+1,j} = \frac{\varkappa^2}{\lambda_y^2}\,(w_{i,j} - 2\, w_{i+1,j} + w_{i+2,j}) \quad (b)$$

$$X_{i+1,j+1} = \frac{\varkappa^2}{\lambda_y^2}\,(w_{i,j+1} - 2\, w_{i+1,j+1} + w_{i+2;j+1}) \quad (c)$$

$$X_{i-1,j+1} = \frac{\varkappa^2}{\lambda_y^2}\,(w_{i-2,j+1} - 2\, w_{i-1,j+1} + w_{i,j+1}) \quad (d)$$

$$X_{i-1,j-1} = \frac{\varkappa^2}{\lambda_y^2}\,(w_{i-2,j-1} - 2\, w_{i-1,j-1} + w_{i,j-1}) \quad (e) \quad (4.11)$$

$$X_{i+1,j-1} = \frac{\varkappa^2}{\lambda_y^2}\,(w_{i,j-1} - 2\, w_{i+1,j-1} + w_{i+2,j-1}) \quad (f)$$

$$X_{i,j+1} = \frac{\varkappa^2}{\lambda_y^2}\,(w_{i-1,j+1} - 2\, w_{i,j+1} + w_{i+1,j+1}) \quad (g)$$

$$X_{i,j-1} = \frac{\varkappa^2}{\lambda_y^2}\,(w_{i-1,j-1} - 2\, w_{i,j-1} + w_{i+1,j-1}) \quad (h)$$

Substituting equations (4.6a), (4.7), (4.10) through (4.11) into equation (4.9) and letting

$$(D_{11})_{i,j} = t\alpha^2 \Big[\beta^2 (F_{i-1,j} + F_{i+1,j}) - 2(1 + \beta^2) F_{i,j}$$

$$+ \frac{\beta}{2} (F_{i+1,j+1} - F_{i-1,j+1} + F_{i-1,j-1} - F_{i+1,j-1})$$

$$+ F_{i,j+1} + F_{i,j-1} \Big] \qquad (4.12a)$$

$$(D_{12})_{i,j} = -2t\alpha^2 \Big[\beta (F_{i-1,j} - 2 F_{i,j} + F_{i+1,j})$$

$$+ \tfrac{1}{4} (F_{i+1,j+1} - F_{i-1,j+1} + F_{i-1,j-1} - F_{i+1,j-1}) \Big] \qquad (4.12b)$$

$$(D_{13})_{i,j} = t\alpha^2 (F_{i-1,j} - 2 F_{i,j} + F_{i+1,j}) \qquad (4.12c)$$

and separating the coefficients associated with different nodal points, the equilibrium equation can be expressed in terms of the transverse deflections and Airy stress functions as follows:

$$\Big\{ 2A(3\alpha + 2) + D_y(\beta^2 + 4\alpha + 6) + D\alpha^2(6\beta^2 + 4)$$

$$+ 2(D_{11} + \beta D_{12}) + 2D_{13}(1 + \beta^2) \Big\}_{i,j} \times$$

$$w_{i,j} + \Big\{ -2\alpha (2A + D_y) - 2A - 2D\alpha^2(2\beta^2 + 1)$$

$$- D_{11} - \beta D_{12} - \beta^2 D_{13} \Big\}_{i,j} (w_{i+1,j} + w_{i-1,j})$$

$$+ \left\{ (1 - \beta)(\alpha D_y + A + D\mathcal{X}^2) - 2\beta D_y - D_{12}/4 - \frac{\beta}{2} D_{13} \right\}_{i,j} \times$$

$$(w_{i+1,j+1} + w_{i-1,j-1}) + \left\{ -2D_y(\alpha + 2) - 2(A + D\mathcal{X}^2) \right.$$

$$\left. - D_{13} \right\}_{i,j} (w_{i,j+1} + w_{i,j-1}) + \left\{ (1 + \beta) (\alpha D_y + A + D\mathcal{X}^2) \right.$$

$$\left. + 2\beta D_y + D_{12}/4 + \frac{\beta}{2} D_{13} \right\}_{i,j} (w_{i-1,j+1} + w_{i+1,j-1})$$

$$+ \left\{ \frac{\beta}{2} (\alpha D_y + A + D\mathcal{X}^2) \right\}_{i,j} (w_{i+2,j+1} - w_{i-2,j+1}$$

$$+ w_{i-2,j-1} - w_{i+2,j-1}) + \left\{ \beta^2 D_y/4 \right\}_{i,j} (w_{i+2,j+2}$$

$$+ w_{i-2,j+2} + w_{i-2,j-2} + w_{i+2,j-2}) + \left\{ \beta D_y \right\}_{i,j} \times$$

$$(w_{i+1,j+2} - w_{i-1,j+2} + w_{i-1,j-2} - w_{i+1,j-2})$$

$$+ \left\{ D_y(1 - \frac{\beta^2}{2}) \right\}_{i,j} (w_{i,j+2} + w_{i,j-2}) = \lambda_y^4 \, q(x,y) \qquad (4.14)$$

Equation (4.14) is presented as a finite difference molecule as Equation 10.1 in chapter 10.

Following the same procedure, the compatibility equation (4.4a) can be expressed also in its finite difference form as follows:

$$\left\{ 2A'(3\alpha + 2) + B_y(\beta^2 + 4\alpha + 6) + Z\varkappa^2(6\beta^2 + 4) \right\}_{i,j} F_{i,j}$$

$$+ \left\{ -2\alpha(2A' + B_y) - 2A' - 2Z\varkappa^2(2\beta^2 + 1) \right\}_{i,j} \times$$

$$(F_{i+1,j} + F_{i-1,j}) + \left\{ (1 - \beta)(\alpha B_y + A' + Z\varkappa^2) - 2\beta B_y \right\}_{i,j} \times$$

$$(F_{i+1,j+1} + F_{i-1,j-1}) + \left\{ -2B_y(\alpha + 2) - 2(A' + Z\varkappa^2) \right\}_{i,j} \times$$

$$(F_{i,j+1} + F_{i,j-1}) + \left\{ (1 + \beta)(\alpha B_y + A' + Z\varkappa^2) + 2\beta B_y \right\}_{i,j} \times$$

$$(F_{i-1,j+1} + F_{i+1,j-1}) + \left\{ \frac{\beta}{2} (\alpha B_y + A' + Z\varkappa^2) \right\}_{i,j} \times$$

$$(F_{i+2,j+1} - F_{i-2,j+1} + F_{i-2,j-1} - F_{i+2,j-1})$$

$$+ \left\{ \beta^2 \frac{D_y}{4} \right\}_{i,j} (F_{i+2,j+2} + F_{i-2,j+2} + F_{i-2,j-2} + F_{i+2,j-2})$$

$$+ \left\{ \beta B_y \right\}_{i,j} (F_{i+1,j+2} - F_{i-1,j+2} + F_{i-1,j-2} - F_{i+1,j-2})$$

$$+ \left\{ B_y(1 - \frac{\beta^2}{2}) \right\}_{i,j} (F_{i,j+2} + F_{i,j-2})$$

$$= \lambda_y^4 \left\{ (B_{11})_{i,j} - (B_{12})_{i,j} \right\} \qquad (4.15)$$

where $(B_{11})_{i,j} = \varkappa^2 \left\{ \beta(w_{i-1,j} - 2 w_{i,j} + w_{i+1,j}) \right.$

$$\left. + \tfrac{1}{4}(w_{i+1,j+1} - w_{i-1,j+1} + w_{i-1,j-1} - w_{i+1,j-1}) \right\}$$

and

$$(B_{12})_{i,j} = \alpha^2 (w_{i-1,j} - 2\,w_{i,j} + w_{i+1,j}) \times$$

$$\left\{ \beta^2 (w_{i-1,j} + w_{i+1,j}) - 2(1 + \beta^2)\, w_{i,j} \right.$$

$$+ \frac{\beta}{2} (w_{i+1,j+1} - w_{i-1,j+1} + w_{i-1,j-1} - w_{i+1,j-1})$$

$$\left. + w_{i,j+1} + w_{i,j-1} \right\}$$

Equation (4.15) is presented as a finite difference molecule as Equation 10,2 is chapter 10.

Equations (4.14) and (4.15) can now be applied at any discrete point to generate two sets of algebric equations. If a nodal point of a finite difference molecule falls on or outside the plate boundary, the molecule is modified with the appropriate boundary conditions as discussed in the following section.

4.3 Boundary Conditions

There are two sets of boundary conditions: the bending conditions involving the transverse displacement w, and the membrane conditions involving the Airy stress function F. For the elastic large deflection theory, the two governing equations are interrelated as indicated by the equations (4.14) and (4.15); and require the consideration of both bending and membrane effects simultaneously.

4.3.1 Bending Boundary Conditions

i. All simply supported edges - considering the edge of the plate parallel to the x- and v-axes, the geometrical conditions are:

1. $w = 0$, i.e. deflection is equal to zero at all points along the edge (4.16a)

2. $M_n = -D_n (w_{,nn} + \nu_t w_{,vv}) = 0$, i.e. moment perpendicular to the edge is equal to zero (4.16b)

Since the condition of zero slope ($w_{,v}$) along the edge parallel to the v-axis gives $w_{,vv} = 0$, the zero moment condition $M_n = 0$ implies that $w_{,nn} = 0$, leading to the following condition

$$M_n + M_v = M_x + M_y = 0 \tag{4.17}$$

along the skew support.

Along the edge parallel to the x-axis:

$$M_y = -D_y (w_{,yy} + \nu_x w_{,xx}) = 0 \tag{4.18}$$

4.3.2 Membrane Boundary Conditions

For the case of all simply supported edges (on rollers), the in-plane stresses (σ_n^m, $\tau_{\xi\eta}^m$, σ_y^m and τ_{xy}^m) are equal to zero along the edges. If the edges are pinned, the in-plane displacements u_x, v_y and v_η along x, y and η

directions are equal to zero. Since the experimental boundary conditions for simply supported plate models (Chapter 6) were somewhat in between the two edge conditions, the following membrane conditions are used for the solution of this complicated boundary-value problem:

i. Along the edge parallel to the v-axis

1. $v_\eta = 0$, therefore $\partial v_\eta / \partial \eta = \varepsilon^m_\eta = 0$, i.e. linear reference surface strains along the η-direction vanishes at all points. (4.19a)

This closely represents the experimental conditions as the corners were rigidly clamped down.

2. $\tau^m_{\xi\eta} = 0$, i.e. shearing stress along the edges in the plane of the plate is equal to zero. (4.19b)

Since the four edges were stiffened by diaphragm, shear distortion along the edge in the plane of the plate is assumed to be zero. Similar boundary condition of zero shearing stress along the simply supported edge of an isotropic rectangular plate has been assumed by previous investigators (88).

Similarly:

ii. Along the edge parallel to the x-axis:

1. $u = 0$, therefore $\partial u/\partial x = \varepsilon_x^m = 0$, i.e. linear reference surface strains along the x-direction vanishes at all points. (4.20a)

2. $\tau_{xy}^m = 0$, i.e. shearing stress along the edges in the plane of the plate is equal to zero. (4.20b)

Both bending and membrane boundary conditions were mathematically formulated and the associated finite difference equations at different network points were derived in Appendix B and are given in Chapter 10.

4.3.3 Two Opposite Edges Simply Supported and the Other Two Edges Free (Small-Deflection Elastic Analysis

Because of the various physical or mathematical restrictions in the validity of the large deflection orthotropic plate equations at the free edges, the large deflection elasto-plastic analysis is considered only for the cases of plates with all simply supported edges. The free edge can be treated by the classical theory of small deflection where it does not impose a physical problem, since the edge effects vanish rapidly and do not influence the interior stress distributions. Fung and Wittrick (84) have pointed out that in certain special cases, the membrane stresses may be confined to a 'boundary layer' along the free edge while the rest of the plate undergoes bending stress only. For large deflections, however, the presence of a free edge does not allow the direct application of the usual set of differential equations.

The clamped edge, in the treatment of bending and membrane boundary conditions has by definition zero slope and zero strain in the median fibres along the edge. Such an edge would not likely be realized in a bridge deck structure because of the requirement of considerable rotational edge restraint.

In this section the small deflection theory of orthotropic skew plates which are simply supported on two sides and free at the other two sides will be considered. In this case the equilibrium equation and hence only the

bending boundary conditions are to be evaluated to obtain numerical solutions. For the elastic small deflection theory, the stretching of the middle plane of the plate is neglected. Hence the two coupled sets of large deflection plate equations become uncoupled, and neglecting the membrane action, the governing differential equation (3.25) for an orthotropic skew plate reduces to

$$(D_x + 2H \frac{s^2}{c^2} + D_y \frac{s^4}{c^4}) w_{,uuuu}$$

$$+ (4H \frac{s}{c^2} + 4 D_y \frac{s^3}{c^4}) w_{,uuuv}$$

$$+ (2H \frac{1}{c^2} + 6 D_y \frac{s^2}{c^4}) w_{,uuvv} + 4 D_y \frac{s}{c^4} w_{,uvvv}$$

$$+ D_y \frac{1}{c^4} w_{,vvvv} = q(x,y) \qquad (4.27)$$

Numerical solutions for the small deflection plate behaviour were obtained and compared with the experimental results for the model plates tested in the elastic domain.

The bending boundary condition as discussed in section 4.3.1 will also be applicable here to the edges parallel to the v-axis. On the free edge parallel to the x-axis the boundary conditions become:

1. $(M_y)_{edge} = -D_y(w_{,yy} + \nu_x w_{,xx}) = 0$, i.e. Moment perpendicular to the edge is equal to zero (4.28a)

2. $(V_y)_{edge} = -D_y\left\{w_{,yyy} + \left(\frac{4D_t}{D_y} + \nu_x\right) w_{,xxy}\right\}$

$= 0$ (4.28b)

i.e. the vertical reaction along the free edge is equal to zero.

The latter boundary condition is obtained by making Kirchoff modification, i.e. combining the forces replaced by the twisting couples with the shear force along the free edge.

These boundary conditions have been used to formulate finite difference equations for the linear small deflection plate behaviour. The detailed mathematical derivations of these equations are presented in Appendices B and C.

4.4 Formulation of the Simultaneous Equations for the Large Deflection Plate Behaviour

Superposition of the skew network on the equivalent orthotropic plate and applying the finite difference equations at each network points yield two groups of simultaneous equations, representing equilibrium and compatibility conditions. Expressed in matrix notations these equations are:

$$[A]\{w\} = \{q\}$$

or

$$\{w\} = [A]^{-1}\{q\} \tag{4.29}$$

and

$$[B]\{F\} = \{c\}$$

or

$$\{F\} = [B]^{-1}\{c\} \tag{4.30}$$

where $a_{i,j} = f(D_{xi}, D_{yi}, H_i, \beta, , \ldots F_i, F_{i-1},$

$F_{i+1}, \ldots$etc.)

$q_i = f(q(x,y))$

and

$b_{i,j} = f(B_{xi}, B_{yi}, H_i, \ldots$etc.)

$c_i = f(w_i, w_{i-1}, w_{i+1}, \ldots$etc.)

[A] and [B] are two sets of square matrices of the order nxn where n is the number of unknown deflections and Airy stress functions.

Solutions of equations (4.29) and (4.30) have been obtained both in the elastic and elasto-plastic stress regions.

CHAPTER 5

MATHEMATICAL SOLUTIONS

In the preceding chapter, the problem of large deflection behaviour of orthotropic skew plates has been reduced to the problem of the simultaneous solutions of two groups of algebraic equations (4.29) and (4.30) for any given intensity of loading. Although, the solution is straightforward for the elastic stress region, the method of successive approximation with an iterative procedure has to be used for the solution of the two groups of equations. This method of solution is a modification of the form given the Adotte (49) for the solution of transversely loaded rectangular orthotropic plate. However, it should be mentioned that Wang (37) appears to be the first to introduce this iterative process to obtain the non-linear large deflection elastic solutions of transversely loaded isotropic rectangular plates. In the elasto-plastic range, beyond the initiation of first yield, an iterative incremental procedure has been adopted to take into account the reduction of stiffnesses with the corresponding increment of loading.

In this chapter, the basic steps involved in the iterative technique for the solutions of the two groups of simultaneous equations will be described. The

procedure of locating the first yield will be discussed. An incremental iterative approach to investigate the propagation of yield for each intensity of loading followed by the step by step solution procedure for the complete elasto-plastic analysis of orthotropic skew plates will be presented. The computer program developed through the investigation will be described in a flow diagram and the accuracy of the numerical solutions will be evaluated in comparison with existing results.

5.1 Procedure of Iterative Solutions for the Initial Stages of Loading

It is assumed that for the initial stages of loading, the plate remains entirely elastic; then the basic steps in solving these equations are as follows:

Step 1. Assume the membrane stresses to be zero, which implies that the Airy stress function (F) = 0. Find $(w)^{1,1}$ from equation (4.29). It is to be noted that $(w)^{1,1}$ represents the small deflection elastic solution.

Step 2. Assume (w) = $(w)^{1,1}$ as initial values for the successive approximations and solve $(F)^{1,1}$ from equation (4.30).

Step 3. Assume (F) = $(F)^{1,1}$. Compute $(w)^{1,2}$ from equation (4.29). Calculate

$$(w)^{1,2}_{\text{average}} = \tfrac{1}{2}\left\{(w)^{1,1} + (w)^{1,2}\right\}$$

It should be noted here that originally, the w values were used directly in equation (4.30) to evaluate the stress function F in the next cycle. However, it was found that for larger loads the results either converged very slowly or remained almost stationary in value. Wang (37) also encountered such a problem in his large deflection solution of isotropic plates. To circumvent this difficulty the above method of averaging was used herein to hasten convergence.

Step 4. Assume $(w) = (w)^{1,2}_{average}$. Compute $(F)^{1,2}$ from equation (4.30).

Step 5. Compare deflections at each node point with the corresponding deflection $(w)^{1,2}_{average}$; and test for convergency within a certain tolerable limit. A limit of 0.075% agreement between two successive deflection values was considered as reasonable tolerable limit for the desired accuracy. If the difference is nowhere greater than the specified percentage of the latter, then $(w)^{1,2}_{average}$ and $(F)^{1,2}$ represent the required large deflection elastic solution correct to the degree of the specified accuracy. If however, the degree of convergency was not satisfied at each point within the plate boundary, the calculations were repeated as follows:

Step 6. Assume $(F) = (F)^{1,2}$. Compute $(w)^{1,3}$ from equations (4.29). Calculate

$$(w)^{1,3}_{average} = \tfrac{1}{2}\left\{(w)^{1,2}_{average} + (w)^{1,3}\right\}$$

Step 7. Assume $(w) = (w)^{1,3}_{average}$. Compute $(F)^{1,3}$ from equation (4.30).

Step 8. Compare deflections at each node point with the corresponding deflections $(w)^{1,3}_{average}$ and test for convergency as described in Step 5. This procedure is repeated until the required degree of accuracy is obtained.

Step 9. The moment tensor (M_x, M_y and M_{xy}) is calculated from the equations (3.11) and the membrane stress tensor (σ^m_x, σ^m_y, τ^m_{xy}) is found from equations (3.16) at all the discrete points.

Equations (3.11) and (3.16) were expressed in their finite difference equivalence for computing the bending moments and membrane stress intensities.

Step 10. The bending stress tensor (σ^b_x, σ^b_y, τ^b_{xy}) is calculated from the moment tensor and superimposed on the membrane stress tensor to find the total stress intensity. The yield criterion is then checked for uniaxial stress condition in the rib material, i.e. equation (3.3) and von Mises yield condition in the deck plate, i.e. equation (3.2). If the yield conditions were not satisfied, guaranteeing the elastic behaviour of the stiffened plate, loading is continued. In this case, the preceding deflection surface is used as the starting value for w.

An illustration of the typical stress distributions in the elastic range is shown in Figure 5.1.

5.2 Search for Initiation of First Yield

Step 10 of the preceding section is continued until the yield stress is obtained within 0.15% of the yield point stress σ_p. If it appeared that the yield stress was exceeded for a certain intensity of loading $(q)^{j-1}$ with a corresponding deflection surface $(w)^{j-1,s}$ and stress function $(F)^{j-1,s}$, then the load increment $(\Delta q)^{j-1}$ was reduced to $(\Delta q/2)^{j}$ and the cycle was repeated until the maximum stress fell below the yield stress. The load was then incrementally proportioned until the maximum stress was within 0.15% of the yield stress. If the specified tolerable limit was not attained, the load was again decreased until the specified agreement with the yield stress was reached. The tolerable limit of 0.15% agreement was arrived at as a reasonable compromise between efficient use of computer time and desirable accuracy. The closer agreement would require excessive computer time to search and locate the initiation of first yield.

5.3 Determination of the Remaining Elastic Portion of the Cross-Section and the Step by Step Solution Procedure

After locating the initiation of first yield, a different approach was used which involved incremental loading and the reduction of stiffness. Although the governing equations in terms of transverse deflections and Airy stress functions such as expressions (3.25) and

(3.26) may be derived for the elastic state, there exists no such relationship in the elasto-plastic state. Therefore, in this investigation the complete solution of the problem is obtained as a series of linear incremental solutions which approximate the overall behaviour of elasto-plastic orthotropic skew plates. The governing equilibrium and compatibility equations are assumed to be valid in the post-yield region as well, as long as the stiffnesses related to bending, torsion and membrane rigidities of the orthotropic skew plates are related to the remaining elastic core of the cross-section to carry the proportional incremental loading. This is a method of successive elastic solutions since each iteration involves essentially a solution of the elastic problem.

For the sake of mathematical representation, if the plate is replaced by a number of discrete mesh points, at the elastic limit load, the first point at the section of maximum stress intensity yields. The elastic equations govern at all the points except the one that has yielded. Any yielding of the section material will reduce the stiffness of this mesh point. The assumption of elastic-perfectly plastic material behaviour of the orthotropic plate entails the condition that the yielded zone does not carry any further load increment and may be neglected for any computation of rigidity. For the load increments in the elastic-plastic range, the rigidities are computed

by the usual formulas based on the section that remains elastic. The extent of yielding is computed and the reduced area of the elastic material is used as the effective load carrying section. The structure acts linearly during the next load increment to cause further propagation of yield in the ribs. This iterative incremental procedure serves as a rational basis for determining the decrease of plate stiffness as yielding progresses. At a certain stage of loading, yielding may be initiated simultaneously at more than one point and if so, the effective rigidities related to bending, torsion and membrane stiffnesses must be computed based on the remaining elastic sections at all such discrete points and accordingly equations (4.29) and (4.30) will be modified.

Beyond the initiation of first yield, the load q is taken as Δq and a new set of deflections, Airy stress functions and stresses are computed through the same type of procedure as followed in the elastic range. The incremental values of deflections and stresses are then added to the existing values at every discrete point, at the end of each increment of loading, to provide a new total, i.e.

$$\{w\}_{i+1} = \{w\}_i + \{\Delta w\}_{i+1} \tag{5.1a}$$

$$\{\sigma_x^b\}_{i+1} = \{\sigma_y^b\}_i + \{\Delta\sigma_x^b\}_{i+1} \tag{5.1b}$$

$$\{\sigma_y^b\}_{i+1} = \{\sigma_y^b\}_i + \{\Delta\sigma_y^b\}_{i+1} \tag{5.1c}$$

$$\{\tau_{xy}^b\}_{i+1} = \{\tau_{xy}^b\}_i + \{\Delta\tau_{xy}^b\}_{i+1} \tag{5.1d}$$

$$\{\sigma_x^m\}_{i+1} = \{\sigma_x^m\}_i + \{\Delta\sigma_x^m\}_{i+1} \tag{5.1e}$$

$$\{\sigma_y^m\}_{i+1} = \{\sigma_y^m\}_i + \{\Delta\sigma_y^m\}_{i+1} \tag{5.1f}$$

$$\{\tau_{xy}^m\}_{i+1} = \{\tau_{xy}^m\}_i + \{\tau_{xy}^m\}_{i+1} \tag{5.1g}$$

where b and m designates bending stresses and membrane stresses, respectively; these are superimposed to determine further propagation of yield through the ribs and initiation of yield in the deck plate defined by the von Mises yield criterion. Figure 5.2 shows the stress distribution at a particular range of loading at the post-yield region. As mentioned previously, the effective section resisting any incremental loading is the elastic part of the sectional area. As a first trial, the section properties are based on Z_i, the depth of material remaining elastic for the stress distribution under q_i, i.e. state I of loading. The stress increments in stage II under the incremental loading Δq are added to the stresses at stage I according to equations (5.1). At this trial stress distribution shown in stage III, the resultant stress σ_{i+1}^{hot} will exceed σ_p as shown by the crossed area in Figure 5.2(c). The

excess stress above σ_p results from the fact that the actual depth value is less than the preceding one. A relation of reduced depth Z_{i+1} with the previously computed depth Z_i may be obtained by the simplifying assumptions that the stress distribution in the ribs is essentially uniaxial and its variation is linear within the elastic zone.

From Fig. 5.2(c) an approximate trial value for the effective depth can be found by linear interpolation, i.e.

$$Z_{i+1} = Z_i \left[1 - \frac{\sigma_{i+1}^{bot} - \sigma_p}{\sigma_{i+1}^{bot} + \sigma_{i+1}^{top}} \right] \qquad (5.2)$$

From equation (5.2) it is apparent that if the resultant stress σ_{i+1}^{bot} is equal to σ_p, then no adjustment in the trial depth is required. If σ_{i+1}^{bot} exceeds σ_p, the depth must be reduced before starting the new trial. If σ_{i+1}^{bot} is less than σ_p, then the depth must be increased. At this stage of the solution procedure an iterative incremental or decremental technique was again adopted to serve as a rational basis so that the inclusion of any yielded zone could be avoided from the elastic stiffness computations. This iteration reduced the depth to the actual elastic depth and a difference of 0.05% between depths of two successive cycles was considered to be sufficiently close to terminate the iterative cycling.

With the convergence to the specified tolerable limit of 0.05%, the new depth Z_{i+1} obtained from equation (5.2) was used for the computation of the sectional properties to solve equations (4.29) and (4.30) for the load increment $\{\Delta q\}_{i+1}$ through the same steps of iterations as described in section 5.1. Incremental stresses are added at depth Z_{i+1} to the stresses due to q_{i+1}. A new depth Z_{i+2} is then computed. Again convergency between the two depths is tested for the specified limit; otherwise the cycle is repeated with Z_{i+2} as the trial depth as shown in stage IV in Fig. 5.2. The maximum stress nowhere exceeds σ_p. The propagation of yield through the ribs is also demonstrated at this stage. This step by step solution procedure is continued until the ribs at the section of maximum stress intensity have fully yielded. Stage V of Fig. 5.2 shows the terminal stage of the solution procedure. At this stage of loading, almost all the ribs have yielded close to the deck plate thickness and only the deck plate remains to carry additional load increments by membrane action; collapse is indicated when very large deflection or singularity of matrices are noted just prior to the full yielding of all the ribs. Thus the estimated ultimate strength was considered as a sort of deflection criterion for the limit of usefulness of the structure.

Based on the above illustration, the complexity in solving the non-linear generalized equations governing the large deflection behaviour of orthotropic skew plates both in the elastic and elasto-plastic stress region can be easily realized. In addition, the iterations involved a great deal of computations. In order to obtain step by step numerical solutions, the entire computations were performed on a digital computer. These computations involved: generating the two sets of matrix equations, calculations of deflections and the Airy stress functions, computations of bending and membrane stresses, superposition of stresses to check yielding of rib materials and von Mises yield criteria for stress distributions in the deck plate and ribs, proportioning of load increments by an iteration process, adding increments to preceding values, computation of appropriate section properties to account for the reduction of stiffnesses, modifications of the equations on account of the yielded zone and yielding of discrete points up to the terminal stage of solution procedure.

5.4 The Computer Program and the Flow Diagram

The computer program was written in Fortran IV symbolic language for IBM 360/65 computer. The generation of the matrix equations for both equilibrium and compatibility conditions was performed by the two subroutines DEFLEC and MEMBRN, respectively. The matrix

equations thus generated were solved by the Gauss-Jordan elimination method or the Gaussian elimination method. The inversion of the equations was obtained by a pre-checked subroutine MINV, built into the computer, which is based on the above method. Subroutine PROP was used to compute the elastic properties of the structural system at each stage of loading. Subroutine STRESS computes the stress couples and stress resultants and checks the stress distribution in the ribs and deck plate for comparison with the von Mises' yield criterion. Subroutine RESULT was used to print out the solutions at different stages of loading conditions to trace the complete stress and deformation path of orthotropic skew plates leading to collapse as defined in section 5.3. The main body of the program is presented as a flow diagram in Fig. 5.3 to aid in understanding the solution procedure of the problem.

The computer program was written in general terms so that a variety of numerical problems may be solved. Factors which may be varied are the number of ribs in both longitudinal and transverse directions, the dimensions of the plate-rib system, mesh spacing in the x- and y-directions, Poisson's ratio, moduli of elasticity E_x and E_y, yield point stress of the constituent material and the angle of skew. Because of polar symmetry of the plate and boundary conditions for uniformly distributed

load pertaining to the present investigation, particular programs were written dividing the plate into 6 x 6 and 8 x 4 meshes in which only one half of the plate was considered. This reduced the number of equations to one half than otherwise required for the general analysis of orthotropic skew plates. Since in the case of asymmetric loading, the load vector cannot be divided into symmetric and antisymmetric components and results cannot be superimposed for elastic-plastic analysis in the post-yield range, the general computer program considers the entire plate to ensure no loss in generality of the solution to the problem. A listing of the main program for an elasto-plastic analysis of an orthotropic skew plate is included in chapter 14.

A separate computer program was written for the linear elastic solution of orthotropic skew plates with the two opposite sides simply supported and the other two sides free; in this case only the equilibrium equation (4.27) was necessary for the solution of the problem.

5.5 Accuracy of the Numerical Solution

In order to investigate the accuracy of the present method of solutions, comparisons were made between the results from this investigation and those from other sources both for the linear and non-linear cases.

For the linear (small-deflection) theory of orthotropic skew plates the results of this analysis are compared with those of Monforton (23) using the finite element method and Gupta (85) using a series solution. Table 5.1 shows a comparison of results for simply supported orthotropic skew plates. Close agreement is observed between the solutions, the maximum difference being less than 1% for deflections and 5% for moments. The linear solution is obtained by omitting the compatibility equation and other non-linear terms used in the present analysis. Table 5.2 shows the comparison of results of isotropic simply supported skew plates with those of Iyenger (30) and Gupta (85) using a series solution, Sampath (31) using polar functions and Taylor expansion, Aggarwalla (32) using conformal mapping, Argyris (33) using matrix displacement method of finite element and Morley (15) using corner functions. The results show very close agreement with all the available methods for small-deflection analysis.

For the non-linear (large-deflection) theory, the results of the present analysis are compared with those of Levy (38) who used a series solution for simply supported isotropic plates. Levy stipulated that the plate boundary must remain straight under lateral loading, e.g. there is no strain in the median fibers along the boundary. This restriction was also used for the

solution procedure developed in this investigation. However, it should be noted that the number of simultaneous equations solved in this case, were twice as many as compared to the linear case. For a theoretical lateral pressure q = 0.0525 psi, the central deflection of a 72 inch x 72 inch x 0.25 inch steel plate (ν = 0.316) with all simply supported edges was found to be 0.119 inch. A corresponding value of 0.122 inch was reported by Levy; the difference being less than 3% based on Levy's solution. Table 5.3 shows a comparison between the two solutions indicating that at higher loads the difference reaches up to 6.3%. This is a reasonably close agreement since Levy's solution involves a certain amount of approximation. He evaluated only the first six non-zero terms of the series. However, he does mention that for higher loads ten terms would be needed to obtain a solution accurate to 1%. Figure 5.4 presents the graphical comparison between the present and Levy's solutions; results from the linear small-deflection analysis are also shown.

The rate of convergence of the iterative process used for solving the two sets of simultaneous equations in the two variables w and F was found to be reasonably rapid. In most cases convergence of the solution was attained within 15 iterative cycles. However, as the intensities of applied load and/or $w_{max/h}$ increased, the

number of iterations required for convergence also increased considerably. For higher intensities of loadings about 50 cycles of iterations were required to achieve the specified convergence.

It was observed that for the isotropic plate problems relatively coarse network yielded results that are within reasonable accuracy, while the finer networks entail large numbers of equations and convergence is achieved after lengthy computations. Thus, it is recognized that coarse networks are adequate for all practical purposes as the round off errors associated with finer grids would tend to affect the accuracy achieved by increasing the number of network points.

For orthotropic skew plates, the convergence of deflection values was achieved within 4 iterative cycles at the initial stages of loading up to the initiation of first yield. This is due to the fact that bending stresses are predominant while deflections are small. Beyond the initiation of first yield, at the incremental stages of loading, the number of iterations required for convergency increased considerably as the membrane effects became predominant. At the terminal stage of full rib yielding, about 40 iterative cycles were required to achieve the specified convergence.

The accuracy of the numerical results both in the elastic and elasto-plastic stress domain will be

evaluated and compared with the experimental values in Chapter 7.

CHAPTER 6

EXPERIMENTAL INVESTIGATION

In order to verify the theoretical results, two series of tests were conducted on one rectangular and two skew orthotropic plate models fabricated from 7/8 inch thick hot rolled high strength structural steel ASTM A-441. The model plates were fabricated by the process of shearing, grinding and milling operations, respectively. Thus, the normal procedure of welding the ribs to the deck plate was avoided to eliminate the introduction of residual stresses and local warping due to welding and subsequent cooling of the plate-rib system. Tests were conducted in two distinct sequences.

(a) First the plate models were tested only in the elastic stress domain under concentrated lateral loading applied symmetrically and asymmetrically with the boundary conditions (i) simply supported on all sides, and (ii) simply supported on two sides and free at the other two;

(b) Secondly, in the elasto-plastic stress regime, the plates were tested under uniformly distributed load with the boundary conditions of simple supports on all sides.

6.1 Model Plates and Material Properties

The aspect ratio, skew angle, plate rib dimensions and thickness of the deck plates are shown in Table 6.1. Altogether, 20 tests were conducted in the elastic domain for the three test plates. In the elasto-plastic stress region, the plate models were tested to substantiate the theoretical analysis. Table 6.2 and 6.3 show the list of tests conducted on the three model panels.

The elastic properties E, σ_p and ν of the plate materials were determined by conducting tension tests according to the latest ASTM E_8-69 standard specifications. Four tension test specimens were fabricated from the plate material. Two were ½ inch x ½ inch at the reduced cross-section and two were ½ inch diameter circular specimens. The longitudinal and transverse strains were measured by electrical resistance strain gauges mounted in pair on the test specimens. All the specimens showed very close elastic-perfectly plastic material behaviour up to a strain of 1.45% elongation at which point strain hardening set in. The average value of the modulus of elasticity and yield stress were found to ~~be 30 x 10^6~~ lbs./sq. in. and 50,000 lbs./sq.in., respectively. The average value of Poisson's ratio was found to be 0.3.

6.2 Abutment Frames

Model plates were simply supported on built-up tees ½ inch x 2 inch x 3 inch deep having a smooth circular groove carrying 3/8 inch diameter rollers. The tee supports were mounted on one rectangular and two skewed frames fabricated from ½ inch x 3½ inch x 15 inch deep channels which were rigidly connected to each other by welding. To increase the rigidity of the frames, ¼ inch thick vertical stiffeners were welded to the channel. These were spaced approximately six inches apart. Clamps were provided at the corners of model plates to prevent uplift against lateral loadings. The frames were in turn supported on standard heavy structural pedastels resting on a flat steel base. This arrangement provided sufficient space underneath the plate for accurate positioning of the dial gauges.

6.3 Loading Device and Instrumentation

Point loads were simulated through a special loading arrangement consisting of a portal frame supporting a loading beam. The loading beam was pre-fabricated from a solid steel section, 3 inch wide and 6 inch deep with a 2 inch diameter hole at the centre which holds a nut welded at the bottom of the beam. A prefabricated load cell (type: strainsert, flat load cell - universal) together with a portable strain

indicator (Budd model P-350) was attached at the lower end of the loading screw that acts through the hole in the solid steel beam. The point load was transferred to the deck plate through a 3 inch diameter 2 inch thick loading block with a groove underneath to accommodate the strain gauge at the point of application of the load. For the skew orthotropic model plates, shims were placed at the bottom along the support lines so that a uniform contact is maintained between support and the model plate which are demonstrated in Figs. 6.5 and 6.6.

To simulate a uniformly distributed load, air pressure was used, the pressure being regulated and recorded by means of two pressure gauges, one located at the entrance of the test plate, the other in the vicinity of the centre of the plate. A 3/8 inch thick top plate was used to form the upper lid of the chamber fabricated from 4 inch deep channels with rubber membrane to form an airlight pressure bag. Similar experimental set-ups using air as a loading medium were used for testing the model plates beyond the elastic range into the elastic-plastic stress domain. Figure 6.1 shows the loading device for the uniformly distributed load.

Mechanical dial gauges (Mercer type, accuracy 10^{-3} inch) were used to measure the deflections at different points. To record strains, three legged stacked strain rosettes (BAB-06-125-RS-120) were mounted

on the top surface of the deck plate and linear gauges (fully annealed foil for post-yield application: BAE-06-125-BB-120) were installed at the bottom of the ribs. At the centre of the plate, linear gauges were mounted at mid-depth of the ribs. Linear strain gauges were also installed along the edge on the top surface to check the strain variation at the supported edges. Strains were measured by means of switch and balance units, a digital strain indicator and an automatic print-out unit.

Point loads were applied in increments of 100 lbs. for the orthotropic test plates and care was taken to ensure that the stresses everywhere in the plate were all within elastic limit.

For the uniformly distributed loading within the elastic limit, load was applied in increments of 1 psi. Beyond the elastic limit, incremental loading was regulated carefully to ensure that the iterative loading intensity and deflections as obtained by the step by step solution procedure could be compared directly with the experimental values at different stages of loading. These values have been documented in Tables 7.1 through 7.3. Residual deflections were measured after unloading, to record the permanent deformations of the model plates.

For the first sequence of testing of the model plates under concentrated and uniformly distributed load within the elastic domain, deflections and moments were compared with the theoretical results.

In the elastic-plastic stress domain, theoretical deflections were compared with the experimental values for all the three model plates. Experimental strains were converted into stresses to determine the initiation of first yield in the rib material.

In the following chapter, the validity of orthotropic plate theory both in the elastic and elastic-plastic analysis of orthotropic skew plates will be examined and the theoretical solutions will be presented in the form of Tables and Graphs while comparing them with experimental results.

Figures 6.2 to 6.8 are shown to clarify the description of the aforementioned apparatus and general set-up of the experiments.

CHAPTER 7

DISCUSSIONS OF THEORETICAL SOLUTIONS AND EXPERIMENTAL RESULTS

To demonstrate the application of the analytical method developed in this investigation, results from the elasto-plastic analysis of orthotropic plate models will be presented first. Although, test results were obtained in the elastic stress domain during the first sequence of testing, these results will be presented later , since it will be shown that a first order linear analysis predicts sufficiently accurate results for orthotropic plates subjected to lateral loading in the elastic stress region.

7.1 Rectangular Orthotropic Test Panel (Model Plate No. 1)

Fig. 7.1 shows the comparison between the theoretical and experimental results for deflections of orthotropic plate model subjected to uniformly distributed load with the boundary condition of simple support on all sides. At the initiation of first yield in the y-direction at nodal point 11, the theoretical load of 6.25 p.s.i. was found to be a lower bound value compared to the experimental load of 6.52 p.s.i., the difference being less than 5% based on the experimental result. At 6.25 p.s.i. lateral pressure, the theoretical deflection at the central

point was found to be 0.158 in. compared to an experimental value of 0.156 in., which shows that a very close agreement exists between them. First yield in the x-direction rib at nodal point 11 (Fig. 7.1) occurs at a load of 8.65 p.s.i. compared to the test load of 9.3 p.s.i., the difference being less than 6%. At the terminal stage of full rib yielding in the y-direction, the theoretical deflection at the central point was found to be 1.327 in. compared to an experimental value of 1.219 in.; a deviation of 9% which may be considered a reasonably close agreement considering the experimental errors involved and limitation of mathematical model. This deviation will be accounted for later in this chapter, while examining the errors involved in the experimental investigation and the limitations set by the theoretical assumptions. The experimental results and the theoretical deflection values at different points are presented in Table 7.1. A permanent deformation of about 0.75 in. was observed at the central point after removal of loading. This residual deflection could not be predicted because of the limits placed on the solution procedure by the original set of assumptions.

Figure 7.2 shows the variation of effective bending rigidities at the central and quarter points with the load increments on the model plate. It is observed that although initiation of yielding occurs at

different intensity of loading, the reduction of plate stiffness occurs in such a way that considerable re-distribution of stresses takes place in the post-yield range. At the terminal stage of full rib yielding at the section of maximum stress intensity almost all the points are exhausted of bending and hence load-carrying capacity. Only the deck plate remains to carry the additional load increments by membrane action. At this stage of loading the ratio of deflection to span-length (w/L_y) is approximately 1/20 in terms of the shorter span. This large deflection ratio was taken as an indication that the collapse load was reached.

Variation of the membrane stress intensity with increase in lateral load is shown in Fig. 7.3. It is observed that at the initial stages of loading up to the initiation of first yield, membrane stresses increase very slowly in either direction. But at the terminal stages of lateral pressure, as the bending rigidities diminish rapidly, the membrane action becomes predominant with the increasing deflection of the system. As expected, at the central point, the membrane stresses in the x-direction are larger than those in the y-direction. The membrane stress of 7100 p.s.i. at the central point is of the order of 14% of the yield point stress of 50,000 p.s.i. Hence it is mandatory to consider the non-linear theory incorporating membrane action in the

analysis of orthotropic plates undergoing large deflection into the elasto-plastic stress domain.

Figure 7.1 shows an important aspect of orthotropic plate behaviour. At the initial stages of loading, say, at 4 p.s.i. (which is well below the load level initiating first yield at the section of maximum stress), the theoretical values of deflections at centre are 0.104 in. and 0.103 in. based on the linear elastic solution and non-linear elastic solution, respectively; the difference is approximately 1%. At this load level membrane stress is small and bending action dominates the plate behaviour. This demonstrates that the solution of orthotropic plate problems in the elastic domain can be predicted by considering only the linear (small-deflection) theory of an orthotropic plate which requires only the solution of the equilibrium equation.

Figure 7.4 shows the variation of effective depth with incremental loading at centre. It is observed that although initiation of yielding in both the x- and y-directions occur at different intensity of loading, at the terminal stage of full rib yielding, the effective elastic depth reduces close to the deck plate thickness simultaneously in both directions. As in Fig. 7.2, this shows that considerable redistribution of stresses takes place with continual plastification of rib material. This is due to ductility of the constituent material

leading to its inherent overload-carrying capacity. Comparing the loading on the model plate (Table 7.1), the results seem to indicate that if collapse is assumed to occur at a load factor of say, 2.0, (Ref. 3), then first yield occurs at a load factor of 0.85. This is less than the minimum load factor of 1.0 at which first yield may occur for distributed loads and point loads. This demonstrates that an inherent overload-carrying capacity of at least 15% may be counted upon in the design of orthotropic plate structures.

Figure 7.5 shows the sequences of yielding of ribs along the y- and x-central axes of the model plate. As expected, first yield is initiated at the central point along the y-axis since the bulk of the load distribution takes place in the shorter direction. But at the terminal stage of loading, propagation of yield along the depth has taken place close to the deck plate thickness at all the ribs. This may be considered as a collapse load, as mentioned previously, since the limit of usefulness of the structural system has been reached.

7.2 Orthotropic Skew Plate with Ribs in the x-Direction Only (Model Plate No. 2)

Since one way reinforcement is sometimes used in a bridge deck design, it was considered instructive to investigate the structural response of a skew model plate stiffened with unidirectional ribs. The elastic solutions

in comparison with the experimental results will be discussed later.

In the elastic-plastic range, theoretical solutions for deflections are compared with the experimental values for the test plate under uniformly distributed load (Fig. 7.6). First yield at the central point is initiated in the x-direction at a loading pressure of 7.41 p.s.i., the corresponding test load being 7.67 p.s.i. This is a reasonably close agreement, although the theoretical solution is again a lower-bound value as in model plate No. 1. At a lateral loading of 7.41 p.s.i., the theoretical deflection was 0.129 in. at the central point, compared to the experimental result of 0.121 in., the difference being less than 7% based on the experimental value. At 18.75 p.s.i. lateral pressure, the theoretical maximum deflection at central point was found to be 0.917 in. compared to the experimental value of 0.855 in. This agreement as in model plate no. 1 is reasonably close, considering the limitations of the mathematical model and errors involved in the experimental investigation.

Fig. 7.7 shows the variation of membrane stress with loading intensity. Since the bending rigidities in the x-direction are much more than in the y-direction, the membrane stresses are of a small fraction of the total stress for the loading range considered. It appears

that bending action predominates until considerable plastification of ribs has taken place.

At a load level well below the initiation of first yield, say, 5 p.s.i., the maximum deflection at the central point was 0.0892 in. and 0.0888 in. based on the linear and non-linear elastic solutions, respectively. The differnce between the two solutions is less than 0.5%. This again justifies the use of the small-deflection theory for the analysis of skew plates within elastic range.

Figure 7.8 shows the sequence of yielding of the ribs at discrete points within the plate boundary. As expected, first yield occurs at the central point in the x-direction and subsequently propagates to mid-span of the ribs located at the two third points. Yielding occurs in the vicinity of the obtuse corners before it occurs in the region of the acute corners. This was expected, since the obtuse corner regions of skew plates are normally regions of higher stress intensity than those at the acute corners.

Figure 7.9(a) and (b) show the distribution of membrane stresses at a uniformly distributed load of 18.75 p.s.i. As demonstrated in Fig. 7.9(a), compressive membrane stresses are induced in the y-direction at the central line close to the skew support while in the x-direction, there exists only tensile membrane stresses. Along the one-third line compressive membrane stresses

are induced both in the x- and y-directions at points close to the acute corners. The regions close to the obtuse corner are always under tensile membrane action. The inducement of compressive membrane stresses at the acute corner regions and close to the skew support may be attributed to the geometrical configuration of the orthotropic skew plate structure.

Load-deflection response at different typical nodal points for the model plate are presented in Table 7.2. The ratio of maximum theoretical deflection at the point of collapse load to deflection at first yield at central point is of the order of 7.1 to 1, the corresponding experimental ratio being 6.84 to 1. Comparing the loadings on the skew plate, as in the first test panel, the results seem to indicate that, if collapse is assumed to occur at a load factor of, say, 2.0, then first yield occurs at a load factor of 0.79; this demonstrates that an inherent overload-carrying capacity of at least 21% could be counted upon in the design of an orthotropic skew plate structure. This is a slightly higher value compared to the rectangular plate model.

7.3 Orthotropic Skew Plate with Stiffening Ribs in Both Directions (Model Plate No. 3)

This orthotropic plate model was fabricated with ribs of equal spacing but different thicknesses in the longitudinal and transverse directions. The rigidity ratio and skew aspect ratio were close to those of the rectangular plate model, so that the effect of skew could be examined.

Figure 7.10 shows the comparison between the theoretical and experimental results for deflections at central point of the orthotropic skew plate model under uniformly distributed load in the elastic-plastic stress region. At the initiation of first yield in the y-direction, the theoretical value of the load was 6.91 p.s.i., which was a lower bound value when compared to the experimental result of 7.28 p.s.i., the difference being less than 5.5% based on the experimental result. At a lateral pressure of 6.91 p.s.i., the theoretical deflection at the centre was found to be 0.118 in. compared to test value of 0.111 in. At the terminal stage of full rib yielding in the y-direction, the theoretical deflection was found to be 1.001 in. compared to the experimental result of 0.915 in.

The load-deflection response of orthotropic skew plate model no. 3 in comparison to the rectangular plate model no. 1, for the same rigidity and almost the same aspect ratio, indicates that the load carrying capacity

of the 45° skew plate is about 25% more at the initiation of first yield and 18% more at collapse load than the corresponding rectangular plate.

Figure 7.11 shows the variation of the membrane stress with loading intensity, at the centre of the plate. As observed in model plates 1 and 2, membrane stresses are only a small fraction of the total stress for the loading range considered. After considerable plastification has taken place, membrane stresses become increasingly predominant as was observed in model plates 1 and 2.

At a lateral pressure of 4 p.s.i. which is well below the load level initiating first yield, the maximum deflection at the centre was found to be 0.0692 in. and 0.0691 in. based on the linear and non-linear elastic solutions, respectively; the difference is very small. Thus it is justified, as in model plates 1 and 2, that a non-linear analysis need not be undertaken for solving the elastic small-deflection plate problems.

Figure 7.12 demonstrates the sequence of yielding of the ribs at discrete points within the plate boundary. First, yield occurs at the central point in the y-direction and subsequently propagates to adjacent nodal points at the central rib. The sequence of yielding demonstrates that the obtuse corner regions are usually the regions of higher stress intensity than the acute corner regions.

Figure 7.13 shows the distribution of membrane stresses at the terminal stage of loading. As in model plate no. 2, compressive membrane stresses occur at the acute corner regions and at the central line near the skew support whereas tensile membrane stresses exist in the vicinity of the obtuse corner.

Variation of effective depth with loading is shown in Fig. 7.14. As in plate model no. 1, it demonstrates the redistribution of stresses in the post-yield range due to the ductility of the material.

The experimental and theoretical deflection values at different nodal points are presented in Table 7.3. The ratio of maximum deflection at collapse load to deflection at first yield is of the order of 3.48 to 1; the corresponding ratio from experiments is 8.15 to 1. The results also appear to indicate, as in model plate no. 1 and no. 2, that if collapse is assumed to occur at a load factor of 2, then first yield occurs at a load factor of 0.85, indicating an inherent overload capacity of at least 15% which may be counted upon in the design of an orthotropic skew plate structure. This overload carrying capacity of the 45^{o} skew plate appears to be the same as for the rectangular plate panel of the same rigidity and almost the same aspect ratio.

7.4 Errors in the Experimental Investigation and Limitations of the Theoretical Assumptions

In spite of the proper care taken for maintaining an initial plane surface at the middle plane of the model plate during milling operation, an ideal uniform contact between support and test plate could not be achieved. This necessitated positioning shims of very fine thickness between the model plate and the supporting rods to obtain a uniform contact between them.

Instrumentation errors such as sensitivity and drag in mechanical dial gauges and pressure gauges, stability and errors in the installation of strain gauges and strain measuring instruments also contribute to some degree to the discrepancies noted.

The stress-strain curves from the four uniaxial tension tests, which demonstrated a close elastic-perfectly plastic material behaviour, was an idealization to suit the first theoretical basic assumption. However, strain-hardening was, in fact, observed at 1.45% elongation. Hence, during the continual plastification of the rib material, within certain region of the structural system, strain hardening in the ribs could have occurred resulting into higher stiffness properties and hence less deflections during the terminal stages of the load increments.

The discontinuity of the stiffening ribs and the deck plate structure, the rigidity of which is assumed to be uniformly distributed for the substitute orthotropic plate may be of some consequence in the determination of deflections as well as bending and membrane stresses in the structural system.

From the study of various graphs and tables it can be concluded that the maximum discrepancy of less than 10% between the theoretical and experimental results is partly due to the experimental errors involved and partly due to the fact that the present numerical solution is essentially based on a lower bound theorem satisfying the following conditions:

(a) Equilibrium and compatibility equations for each element of the plate have been satisfied,

(b) The stress-strain field is compatible with the specified boundary conditions, and

(c) Yield condition has nowhere been exceeded within the plate boundaries.

Hence, the present solution procedure developed herein could be a valuable aid to the minimization of reinforcing ribs with safety.

7.5 Study of the Effect of Skew in the Elasto-Plastic Analysis of Orthotropic Plate Structures

Although it is recognized that the collapse load of a structural system is unique so far as its physical

geometry is concerned, it is interesting to study the effect of skew on the collapse load estimated by the elasto-plastic solution procedure developed herein. The geometry of the skew model plate no. 2 is considered for this theoretical study. Theoretical solutions were obtained for orthotropic plate structure having 0^{o}, 30^{o} and 60^{o} angle of skew for comparison with the results of the experimental model plate no. 2 having a 45^{o} skew angle.

The load-deflection curves of orthotropic skew plates with different skew angles are shown in Figure 7.15. It is observed that as the angle of skew is increased, the collapse load also increases considerably. For the rectangular orthotropic plate, collapse load was found to be 14.59 p.s.i., with the corresponding values for 30^{o}, 45^{o} and 60^{o} skew plate structures being 15.52 p.s.i., 18.75 p.s.i. and 22.27 p.s.i., respectively; the percentage increases in collapse load are 6.5%, 25% and 52% based on the value for the rectangular plate structure. Figure 7.15 shows that at a certain intensity of load level, say 14.59 p.s.i., (which is the collapse load of the rectangular plate) the transverse displacements at centre of skew plate systems are relatively smaller in magnitude in comparison to those in the rectangular plate; the deflections decrease significantly with the increase in the angle of skew.

The distributions of membrane stresses at different collapse loads obtained by varying the angle of skew are presented in Figures 7.16 and 7.17. It can be observed that the rectangular orthotropic plate exhibits considerably higher values of tensile membrane stresses than the corresponding values for the skewed plate structure (Fig. 7.16); the membrane stresses decrease with increase in the skew angle. Compressive membrane stresses are found in the vicinity of the acute corner and close to the skew support (Fig. 7.17). For a high degree of skew angle ($\phi = 60^{o}$), compressive membrane stresses (σ_{y}^{m}) exist along the entire central span-length (Fig. 7.16b).

Figures 7.18 through 7.21 show the variation of effective bending rigidity at different nodal points along the central rib of orthotropic plates with varying angle of skew; it can be observed that considerable redistribution of stresses with progressive loading takes place, once yield is initiated at the section of maximum stress intensity. At the terminal stage of almost fully yielded ribs, the stiffened plate systems lose much of their bending load-carrying capacity and only the deck plate carries the additional load increments by membrane action. When compared to rectangular and even 30^{o} skewed plates, the 45^{o} and 60^{o} skewed plates exhibit a comparatively longer range of redistribution of stresses

after initiation of first yield (Figures 7.20 and 7.21). Hence the overload-carrying capacity (collapse load) of orthotropic skew plate structures increases with angle of skew.

7.6 Discussions of the Small Deflection Theoretical Solutions and the Experimental Results within the Elastic Stress Region

Typical results for the first sequence of testing of the plate models within the elastic domain are presented in Figures 7.22 through 7.38. Variation of moments M_y and deflections along the width and span-length of orthotropic rectangular plate model are shown in Figures 7.22(a) and 7.22(b), respectively. Comparisons of the present theoretical solution are also made with a series solution (86). Agreement between the theoretical solution and experimental results is found not to exceed 4%.

Figure 7.23 shows the variation of longitudinal moment M_x with span-length; the difference between the results from the experiment and theory is less than 2%. Figure 7.24 shows the variation of deflections under an asymmetric concentrated load. The linearity of the load-deflection curve within the elastic domain is demonstrated in Figure 7.25. Figures 7.26 and 7.27 show the variation of deflections and moments, respectively, under a concentrated load for the boundary condition of simple support on all sides. Figures 7.28 and 7.29 show the

comparisons between the theoretical and experimental results for deflections and moments, respectively. These test results were obtained under a concentrated lateral load with the boundary condition of simple supports along the two longer sides and free along the other two. Close agreement between the theory and experiment are found in all test results.

Variations of deflections and moments M_x and M_y with span-length and skew width for test plate no. 2 are shown in figures 7.30 and 7.31, respectively. The model plate is tested under a symmetric concentrated load with the boundary condition of simple supports on the two sides and free along the other two. Close agreement is found between experimental and theoretical results, the difference being less than 5% based on the experimental results. Figure 7.32 and 7.33 show the comparisons in moments and deflection values for model plate no. 2 under an asymmetric concentrated load with the same boundary condition. Variations of deflections and moments are shown in Fig. 7.34 for the test panel under a symmetric concentrated load with the boundary condition of simple support on all sides. As expected the obtuse corner regions of the skew plate are found to undergo more deflection and exhibit severe stress intensities compared to the acute corner region.

Figure 7.35 shows the variation of deflections with span-length and skew width for test plate no. 3 under a central concentrated lateral load with the boundary conditions of simple support on two sides and free along the other two. Figure 7.36 shows the variations of moments M_x and M_y with span-length. Figures 7.37 and 7.38 show the variations of deflections and moments under a concentrated lateral load with the boundary condition of simple support on all sides. Close agreement between the theoretical and experimental results are found in all cases, the maximum deviation being less than 5.5% based on the experimental results.

These discrepancies may be attributed to all the factors discussed in section 7.4 except the strain hardening effect.

CHAPTER 8

SUMMARY AND CONCLUSIONS

In this dissertation, a step by step solution procedure to trace the stress and deformation paths of orthotropic skew plates loaded into the elasto-plastic range is presented. The solution pertains to the boundary condition of simple support on all sides. The numerical method of analysis is based on finite difference approximations of the coupled sets of fourth order differential equations of equilibrium and compatibility describing the large deflection behaviour of orthotropic skew plates. The entire formulation of analysis is automated on a digital computer to investigate the structural response of orthotropic skew plates on the verge of collapse. The method is restricted in its applicability by a provision that no reversal of the stress intensity in the elasto-plastic stress domain may take place. The violation of this provision, however, would result in the estimation of a conservative collapse load. Comparisons are made with existing results for skewed plates with small deflection as well as for the limiting case of a rectangular plate with large deflection behaviour; good agreement is shown.

Theoretical solutions are also supported by experimental results obtained from tests on small scale model plates both in the elastic and elasto-plastic stress domain.

From this study, the following conclusions can be drawn concerning the elastic and elastic-plastic analysis of skew and rectangular orthotropic plates:

i. For a realistic analysis of structural responses of an orthotropic skew plate structure under lateral loading at or near its collapse load, it is necessary to consider the elasto-plastic behaviour of the plate undergoing large deflections.

ii. The concept of equivalent orthotropy as applied to the elastic stress-domain is also valid in the elasto-plastic stress regime under the condition that necessary modifications of the plate rigidities, owing to the yielding of discrete points, are taken into account. This is true both for orthogonal and skew orthotropic plate structures.

iii. The behaviour of orthotropic plate structures subjected to small lateral load in the elastic stress regime can be accurately predicted by considering only the equilibrium equation and neglecting the other non-linear terms used in the present solution procedure.

iv. Membrane stresses are insignificant up to the initiation of yield in the rib material; they become significant in the elasto-plastic regime,

particularly at the terminal stage of full yielding of ribs. The onset of compressive membrane action near the acute corner of an orthotropic skew plate is of interest owing to the introduction of skew in the geometry.

(v) Considering a conservative load factor of 2.0 at collapse load and a minimum load factor of 1.0 at the initiation of first yield, it appears that an overload-carrying capacity of at least 15% to 21% may be counted upon in the design of orthotropic plate systems within the ranges of the flexural rigidity ratio, aspect ratio and the skew angle considered herein.

(vi) The collapse load of an orthotropic skew plate structure increases considerably with increase in the angle of skew.

(vii) A minimum weight design of orthotropic skew plates seems to be an important natural extension of the newly developed elasto-plastic solution procedure as it predicts a lower-bound value of collapse load.

NOMENCLATURE

The notation and symbols used herein are summarized below:

a = one half length of plate in the x-direction.

b = one half length of plate in the v(skew) direction.

A_x, A_y = cross-sectional area of slab and beam portion of the repeating section in x- and y-direction, respectively.

B_x, B_y = membrane rigidities of plate and stiffener system defined by equations (3.23a) and (3.23b), respectively.

c_1, c_2 = spacing of x- and y-direction ribs.

D = flexural rigidity of plate.

D_x, D_y = orthotropic flexural rigidities per unit width in x- and y-direction, respectively.

D_1, D_2 = coupling rigidities - contribution of bending to torsional rigidity.

d_1, d_2 = depth of longitudinal and transverse ribs.

D_{xy}, D_{yx} = orthotropic torsional rigidity per unit width in x- and y-direction.

$D_t = (D_{xy} + D_{yx})/4.$

E = Young's Modulus of elasticity for isotropic material.

E_x, E_y = Young's Modul of elasticity of orthotropic material in x- and y-direction, respectively.

e_x, e_y = distances of the neutral surface of the repeating section from top fibre of plate in the longitudinal and transverse directions, respectively.

G = shear modulus of elasticity of isotropic material.

G_{xy}, G_{yx} = shear moduli of elasticity perpendicular to the z-axis in x- and y-direction.

$2H$ = plate torsional rigidity.

h = uniform plate thickness.

I_{ox}, I_{oy} = moment of inertia of longitudinal and transverse reinforcing ribs about neutral surface.

L_x, L_y = span-length and width of plate.

M_x, M_y, M_n = bending moment per unit width about y-, x- and v-axes, respectively.

M_{xy}, M_{yx} = twisting moment per unit width of a cross-section.

N_x, N_y = resultant in-plane axial force per unit distance in the x- and y-direction, respectively.

n_i = shape factor.

Q_x, Q_y = shear forces per unit length on planes perpendicular to the x- and y-axes.

$q(x,y)$ = distributed transverse loading.

t = deck plate thickness.

t_x, t_y = weighted x- and y- thickness of plate rib system.

u, v_1 = plate displacement in x- and y-direction, respectively.

v = oblique co-ordinate.

w = displacement component in the z-direction, w is called 'deflection'.

x, y, z = rectangular co-ordinates.

$\varepsilon_x^m, \varepsilon_y^m, \varepsilon_\eta^m$ = linear reference surface strains along x-, y- and η-direction, respectively.

ν_x, ν_y = Poisson's ratio associated with x- and y-direction.

σ_x^b, σ_y^b = bending stresses in the x- and y-direction, respectively.

σ^m_x, σ^m_y = membrane stresses in x- and y-direction, respectively.

$\tau^b_{xy}, \tau^m_{xy}, \tau^m_{\xi\eta}$ = shearing stress in plate developed by torsional moment and membrane action, per unit width of cross-section.

σ_p = yield point stress.

λ_u, λ_v = distance between node points in u- and v-direction, respectively.

λ_x, λ_y = distance between node points in x- and y-direction, respectively.

ϕ = angle of skew.

BIBLIOGRAPHY

1. Seely, F.B. and Smith, J.O., 'Advanced Mechanics of Material'. John Wiley and Sons Inc., New York, 1952, pp. 511-581.

2. Hodge, P.G. Jr., 'Plastic Analysis of Structures'. McGraw Hill Book Co. Inc., New York, 1959.

3. Wood, R.H. 'Plastic and Elastic Design of Slabs and Plates'. The Ronald Press Company, New York, 1961.

4. Troitsky, M.S., 'Orthotropic Bridges, Theory and Design'. The James F. Lincoln Arc Welding Foundation, October, 1968.

5. 'Orthotropic Steel Deck Bridges'. Design Manual of American Institute of Steel Construction. November, 1962.

6. William, M.L., 'Surface Stress Singularities Resulting from Various Boundary Conditions in Angular Corners of Plates Under Bending'. U.S. National Congress of App. Mech. 1951.

7. Vogt, H., 'Die Berechnung Schiefwinkliger platten und Plattenartiger Brückensysteme', Beton and Eisen, Vol. 39, No. 17, September 1940.

8. Jensen, V.P., 'Analysis of Skew Slab'. University of Illinois, Eng. Exp. Station. Bulletin No. 332, Sept. 1941.

9. Jensen, V.P. and Allen, J.W., "Studies of Highway Skew Slab Bridges with Curbs". Part I, Results of Analysis. Univ. of Illinois, Eng. Exp. Station, Bulletin No. 369, Sept. 1947.

10. Ehasz, F.L., "Structural Skew Plates". Proc. of ASCE, June 1945.

11. Robinson, K.E., "The Effect of Skew on the Behaviour of Simply Supported Bridge Slab". Cement and Concrete Association, London. Tech. Rep. TRB/271, July 1957.

12. Robinson, K.E., "The Behaviour of Single Span Skew Bridge Slabs Under Concentrated Loads". Cement and Concrete Association, London, Research Rep. No. 8, 1959.

13. Brewster, D.W., "Bending Moments in Elastic Skew Slabs". The Structural Engineer. Vol. 39, No. 11, Nov. 1961.

14. Yeginobali, A., "Analysis of Continuous Skewed Slab Bridge Decks". The Ohio State University. Eng. Exp. Station. Rep. No. EES 170-2. Aug. 1962.

15. Morley, L.S.D., "Bending of a Simply Supported Rhombic Plate Under Uniform Normal Loading". Quarterly Journal of Mechanics and Applied Mathematics, London, Vol. 15, 1962, P. 413.

16. Morley, L.S.D., "Skew Plates and Structures". The MacMillan Company, New York, Pergamon Press, 1963.

17. Naruoka, M. and Ohmura, H., "Digital Computer Analysis of Influence Coefficients for Deflection and Bending Moment of Orthotropic Parallelogram Plates". Mem. of Fac. of Eng., Kyoto Univ., Vol. 21, 1959.

18. Naruoka, M. and Yonezawa, H., "Uber die Anwendung der Biegungstheorie Orthotroper Platten auf die Berechnung Schiefer Balkenbrucken". Der Bauingenier, Vol. 32, P. 391, 1957.

19. Naruoka, M. and Ohmura, H., "On the Analysis of a Skew Girder Bridge by the Theory of Orthotropic Parallelogram Plate". Pub. of the Intn. Assoc. for the Bridge and Structural Eng., Vol. 19, 1959.

20. Basar, Y. and Yuksel, F., "Zur Berechnung Schiefwinkliger Orthotroper und Isotroper Platten". Beton and Stahlbetonbau, Nov. and Dec. 1961.

21. Cheung, Y., King, I., and Zienkiewicz, O., "Slab Bridge with Arbitrary Shape and Support Condition". Journal of the Institution of Civil Engineers, Vol. 40, May 1968, PP. 9-36.

22. Powell, G.H. and Ogden, D.W., "Analysis of Orthotropic Steel Plate Bridge Decks". ASCE, Proc. Vol. 95. J. Structural Division, No. ST5, May 1969.

23. Monforton, G.R., "Some Orthotropic Skew Plate Finite Element Results". J. of the Structural Division. Proc. ASCE Vol. 98, No. ST4, April 1972, PP. 955-960.

24. Kennedy, J.B. and Huggins, M.W., "Series Solution of Skewed Stiffened Plates". Journal of the Engineering Mechanics Division, ASCE, Vol. 90, No. EM1, Proc. Paper No. 3795, Feb. 1964, PP. 1-22.

25. Kennedy, J.B. and Ng, S.F., "Analysis of Skewed Plate Structures with Clamped Edges". Trans. of the Engineering Institute of Canada, Paper EIC-6S-BR & STR 9, Dec. 1965.

26. Kennedy, J.B., "On the Bending of Clamped Skew Plates Under Uniform Pressure". Journal of the Royal Aeronautics Society, May 1965.

27. Coull, A., "The Stress Analysis of Orthotropic Skew Bridge Deck". Structural Engineer, Vol. 42, No. 7, July 1964, PP. 235-241.

28. Coull, A., "Deformation of Orthotropic Skew Bridge Slab". Civil Engineering and Public Works Review". Vol. 63, No. 738, Jan. 1968, PP. 55-57.

29. Dorman, F.H., "The Thin Clamped Parallelogram Plate Under Uniform Normal Pressure". Dept. of Supply, Australia, A.R.L. Rep. SM.214, 1953.

30. Iyenger, K.T., Sundera Raja, Srinivason, R.S., and Sudara Rajan, C., "Some Studies on Skew Plates". The Aeronautical Journal of the Royal Aeronautical Society, Vol. 75, Feb. 1971. Technical notes. PP. 130-132.

31. Sampath, S.G., "Some Problems in the Flexure of the Rectilinear Plates". M.Sc. Thesis, Indian Institute of Science, 1966.

32. Aggarwala, B.D., "Bending of Parallelogram Plates". J. of the Engingering Mechanics Division, ASCE, Vol. 93, No. EM4, August 1967, PP. 9-18.

33. Argyris, J.H., "Matrix Displacement Analysis of Plates and Shells". Ingenieur Archiv. Vol. 35, 1966.

34. Karrholm, G., "Parallelogram Plates Analyzed by the Strip Method". Chalmers Technical University, Bul. No. 11, Goteborg, 1956,

35. Timoshenko, S. and Woinowsky-Kriegers, S., "Theory of Plates and Shells". 2nd Ed. McGraw-Hill, New York, 1959.

36. Kaiser, R., "Research and Experimental Study on Stresses and Deformations of Square Plates", Z. Angew. Math. Mech. PP. 73-98, No. 16, April 1936.

37. Wang, C.T., "Non-linear Large Deflection Boundary Value Problem of Rectangular Plates", N.A.C.A. Technical Note No. 1425. Washington, U.S. Government Printing Office, March, 1948.

38. Levy, S., "Bending of Rectangular Plates with Large Deflections". N.A.C.A. Technical Note No. 846, Washington, U.S. Government Printing Office, May, 1942.

39. Levy, S., "Square Plate with Clamped Edges Under Normal Pressure Producing Large Deflections". N.A.C.A. Technical Note No. 847. Washington, U.S. Government Printing Office, May, 1942.

40. Way, S., "Uniformly Loaded Clamped Rectangular Plates with Large Deflections". Proceedings, Fifth International Congress for Applied Mechanics, Cambridge, Massachusetts, 1938.

41. Bengston, H.W., "Ship Plating Under Compression and Hydrostatic Pressure". Trans. Society of Naval Architects and Marine Engineers, Vol. 47, 1939.

42. Yang, T.Y., "Finite Displacement Plate Flexure by the Use of Matrix Incremental Approach". International Journal for Numerical Methods in Engineering, Vol. 4, PP. 415-432, 1972.

43. Kennedy, J.B. and Ng, S., "Linear and Non-linear Analyses of Skew Plates". Trans. of A.S.M.E. Journal of App. Mech., June, 1967.

44. Lekhnitsky, S.G., "Anisotropic Plates", (Translation of 1947 edition by E.Z. Stowell). Published as one of the Series "Contribution to the Metallurgy of Steel". American Iron and Steel Institute, Number 50, June, 1956.

45. Yusuff, S., "Large Deflection Theory for Orthotropic Plates with Initial Curvatures". Thesis for the degree of Doctor of Aeronautical Engineering. Brooklyn Polytechnic Institute, June, 1949.

46. Otto Steinhardt and G. Abdel Sayed, "Zur Tragfahigkeit Von Versteinften Flachblechtafeln in Metallbau". Karlsruhe, 1963.

47. Soper, W.G., "Large Deflection of Stiffened Plates". A.S.M.E., Journal of Applied Mechanics, Vol. 25, Number 4, Dec., 1958.

48. Basu, A.K. and Chapman, J.C., "Large Deflection Behaviour of Transversely Loaded Rectangular Orthotropic Plates". Proc. Institute of Civil Engineers, 35, PP. 79-110, Sept. 1966.

49. Adotte, G.D., "Second Order Theory in Orthotropic Plates". Journal of the Structural Division, Proc., ASCE, No. ST5, Proc. Paper No. 5520, October 1967, PP. 343-362.

50. Vogel, V., "Der Biege-und Membranspannungszustand der Rechteckigen Orthotropen Platte mit Grosser Durchbiegung unter Gleichmassig Verteilter Vollast bei Navierschen Randbedingungen, Naherungswiese Behandelt mit Hilfe der Energie-Methode". Thesis presented to the Technische Hochschule, at Stuttgart, Germany, in partial fulfillment of the requirements for the degree of Doctor-Ingenieurs, Nov. 2, 1960.

51. Mader, F.W., Berechnung Orthotroper Platten Unter Flachenlasten, Randmomenten und Randdurchbiegungen". Stahlbau, Vol. 26, No. 5, May 1957, PP. 131-135.

52. Huber, H.T., "Die Theorie der Kreuzweise Bewehreten Eisenbeton Platten". Der Bauingenieur, Vol. 4, PP. 354-360, Germany 1923.

53. Ilyushin, A.A., "Some Problems in the Theory of Plastic Deformations". Translated from Prikladnaia Matematika i Mechanica, Vol. 7, 1943, PP. 245-272 by Grad. Div. Applied Math, Brown University, 1946.

54. Prager, W., "The Theory of Plasticity, A Survey of Recent Achievements". James Clayton Lecture, 1955, Inst. Mech. Engineer., London.

55. Hill, R., "The Mathematical Theory of Plasticity". Oxford University Press, 1950.

56. Tekinalp, B., "Elastic-Plastic Bending of Built-Up Circular Plate Under a Uniformly Distributed Load". J. Mech. Phys. Sol. 1957, Vol. 5, P. 135.

57. Haythornthwaite, R.M., "The Deflection of Plates in the Elastic-Plastic Range". Brown University, 1954.

58. Baker, Horne and Heyman, "The Steel Skeleton, Vol. II". Cambridge University Press.

59. Clarkson, J., "The Strength of Approximately Flat Long Rectangular Plates Under Lateral Pressure". Trans. North East Coast, Inst. of Engineers and Ship Builders, Vol. 74, Part I, P. 21, Nov. 1957.

60. Wah, T., "Large Deflection Theory of Elasto-Plastic Plates". Proc. ASCE, Vol. 84, EM4, Oct. 1958.

61. Lee, T., "Elastic-Plastic Analysis of Simply Supported Rectangular Plates Under Combined Axial and Lateral Loading". Ph.D. Dissertation, Lehigh University, 1961.

62. Lin, T.H. and Ho, E., "Elasto-Plastic Bending of a Rectangular Plate". Journal of Engineering Mechanics Division, Proc. ASCE, Vol. 94, EM1, PP. 199-210, Feb. 1968.

63. Bhaumic, A.K. and Hanley, J.T., "Elasto-Plastic Plates Analysis by Finite Differences". Journal of the Structural Division, Proc. ASCE, ST5, Oct. 1967, PP. 279-294.

64. Kagan, H.A. "Large Deflection, Elasto-Plastic Behaviour of Rectangular Two-Way Reinforced Plates". Thesis presented to the New York University at New York, in Partial Fulfillment of the Requirements for the degree of Doctor of Engineering Science, Dec. 1964.

65. Ang, A.H.S. and Lopez, L.A., "Discrete Model Analysis of Elastic-Plastic Plates". Journal of Engineering Mechanics Division, Proc. ASCE, Vol. 94, EM1, PP. 271-293, Feb. 1968.

66. Hopkins, H.G. and Prager, W., "The Load Carrying Capacities of Circular Plates". Journal of the Mechanics and Physics of Solids. Vol. 2, No. 1, 1953, PP. 1-13.

67. Hopkins, H.G. and Wang, A.J., "Load Carrying Capacities for Circular Plates of Perfectly Plastic Material with Arbitrary Yield Conditions". Journal of Mechanics and Physics of Solids, Vol. 3, 1954, PP. 117-129.

68. Hodge, P.G. Jr., "Plastic Bending of an Annular Plate". Journal of Mathematics and Physics, Vol. 36, No. 2, July 1957, PP. 130-137.

69. Prager, W., "The General Theory of Limit Design". Proceeding, 8th International Congress on Theory of Applied Mechanics, Istanbul, Vol. 2, 1952, PP. 65-72.

70. Johansen, K.W., "The Ultimate Strength of Reinforced Concrete Slab". Final Report, 3rd Congress, International Association for Bridge and Structural Engineering, Liege, Belgium, Sept. 1948, PP. 565-570.

71. Granholm, C.A. and Rowe, R.E., "The Ultimate Load of Simply Supported Skew Slab Bridges". C. and C.A. Res. Rep. No. 12, 1961.

72. Pfluger, A., "Zum Beulproblem der Anisotroper Bechtechplatte". Ingenieur, Archive No. 16, 1947.

73. Trenks, K., "Beitrag Zur Berechnung Orthogonal Anisotroper Rechtechsplatten". Der Bauingenieur, Vol. 29, No. 10, October 1954, PP. 372-440.

74. Bares, R. and Massonet, C., "Analysis of Beam Grids and Orthotropic Plates by the Guyon-Massonet-Bares Method". Frederick Unger Publishing Co., New York, 1968.

75. Ziegler, H., 'A Modification of Prager's Hardening Rule'. Quarterly of Applied Mathematics. Vol. 17, No. 1, 1959.

76. Mendelson, A., 'Plasticity: Theory and Application'. The MacMillan Co., New York, N.Y., 1968.

77. McLean, D., 'Mechanical Properties of Metals'. John Wiley, New York, 1962.

78. Beedle, L.S., 'Plastic Design of Steel Frames", John Wiley and Sons, Inc., New York, Nov. 1962.

79. Giencke, E., "Die Groundgleichungen fur die Orthotrope Platte mit Exzentrischen Steifen", Der Stahlbau, Vol. 24, June 1955, PP. 128-129.

80. Massonet, C., "Plaques et Coques Cylindriques Orthotropes a Nervures Dissymetriques", International Association for Bridge and Structural Engineering Publication, Vol. 19, 1959, PP. 201-230.

81. Schuman, H., "Zur Berechnung Orthogonal-Anisotroper Rechteckplatten unter Berucksichtung der diskontinuier-lichen Arordnung der Rippen". Stahlbau, Vol. 29, Number 10, Oct. 1960, PP. 302-309.

82. Hoffman, W.H., 'Bending of Orthogonally Stiffened Plates'. A.S.M.E. Journal of Applied Mechanics, Vol. 22, 1955.

83. Huffington, Jr., N.J., "Theoretical Determination of Rigidity Properties of Orthogonally Stiffened Plates". Doctoral Dissertation. The John Hopkins University, 1954.

84. Fung, Y.C. and Wittrick, W.H., "A Boundary Layer Phenomenon in the Large Deflection of Thin Plates". Quarterly Journal of Mechanics and Applied Mathematics, Vol. 8, 1955, PP. 191-210.

85. Gupta, D.S.R., "Orthotropic Continuous Skew Plates". Ph.D. Thesis, University of Windsor, 1974.

86. Szilard, R., "Theory and Analysis of Plates-Classical and Numerical Methods". Prentice-Hall Inc., 1974.

87. Kennedy, J.B. and Jain, S.C., "Ultimate Strength and Behaviour of Reinforced Concrete Slabs". Developments in Theoretical and Applied Mechanics, Vol. 6, 1972, PP. 671-694.

88. Hartmann, A.J., Kao, J.S. and Guzman-Barron, L., "Effect of Membrane Forces on Large Deflection of Simply Supported Rectangular Plates". Developments in Theoretical and Applied Mechanics, Vol. 6, 1972, PP. 581-595.

CHAPTER 9

APPENDICES

APPENDIX A

Transformation of the Orthotropic Plate Equations into Skew Co-ordinates

Basic transformation relations between the rectangular (x,y) and oblique (u,v) co-ordinate systems are:

$$u = x + y \tan \phi \tag{3.24}$$

and

$$v = y \sec \phi$$

Differentiating with respect to x and y, the following relations are obtained

$$u_{,x} = 1$$

$$u_{,y} = \tan \phi$$

$$v_{,x} = 0$$

$$v_{,y} = \sec \phi$$

$$w_{,x} = w_{,u}\, u_{,x} + w_{,v}\, v_{,x}$$

$$= w_{,u}$$

$$w_{,y} = w_{,u}\, u_{,y} + w_{,v}\, v_{,y}$$

$$= w_{,u} \tan \phi + w_{,v} \sec \phi$$

$$w_{,xx} = w_{,uu}$$

$$w_{,xy} = w_{,uu} \tan \phi + w_{,uv} \sec \phi$$

$$w_{,yy} = w_{,uu} \tan^2\phi + 2w_{,uv} \tan \phi \sec \phi + w_{,vv} \sec^2\phi$$

$$w_{,xxyy} = w_{,uuuu} \tan^2\phi + 2w_{,uuuv} \tan \phi \sec \phi + w_{,uuvv} \sec^2\phi$$

$$w_{,xxxx} = w_{,uuuu}$$

$$w_{,yyyy} = w_{,uuuu} \tan^4\phi + 4\, w_{,uuuv} \tan^3\phi \sec \phi$$

$$+ 6\, w_{,uuvv} \tan^2\phi \sec^2\phi + 4\, w_{,uvvv} \tan \phi \sec^3\phi$$

$$+ w_{,vvvv} \sec^4\phi$$

A set of similar expressions for derivatives of stress function F are obtained as follows:

$$F_{,x} = F_{,u}$$

$$F_{,y} = F_{,u} \tan \phi + F_{,v} \sec \phi$$

$$F_{,xx} = F_{,uu}$$

$$F_{,xy} = F_{,uu} \tan\phi + F_{,uv} \sec\phi$$

$$F_{,yy} = F_{,uu} \tan^2\phi + 2F_{,uv} \tan\phi \sec\phi + F_{,vv} \sec^2\phi$$

$$F_{,xxyy} = F_{,uuuu} \tan^2\phi + 2\, F_{,uuuv} \tan\phi \sec\phi + F_{,uuvv} \sec^2\phi$$

$$F_{,xxxx} = F_{,uuuu}$$

$$F_{,yyyy} = F_{,uuuu} \tan^4\phi + 4\, F_{,uuuv} \tan^3\phi \sec\phi + 6\, F_{,uuvv} \tan^2\phi \sec^2\phi + 4\, F_{,uvvv} \tan\phi \sec^3\phi + F_{,vvvv} \sec^4\phi$$

Substitution of fourth-order derivatives of w and F into equations (3.21) and (3.22) results in the derivation of the two basic equations (3.25) and (3.26) of orthotropic skew plate defining its large deflection behaviour.

APPENDIX B

FINITE DIFFERENCE EQUATIONS FOR LARGE DEFLECTION BEHAVIOUR OF ORTHOTROPIC SKEW PLATES

Finite difference expressions are derived in this section both for compatibility and equilibrium equations for different typical nodal points influenced by the plate boundary. These are: 1) general interior point, 2) interior point near the left simple support, 3) interior point near the right simple support, 4) interior point near the edge parallel to the x-axis, 5) interior point near the acute corner, and 6) interior point near the obtuse corner . These large deflection difference equations for an orthotropic skew plate pertain to the boundary condition of simple support on all sides.

For the linear (small-deflection) solution of the problem in which only the equilibrium equation is to be considered, difference equations are obtained for the boundary condition of a plate in which two opposite sides are simply supported and the other two sides are free. These expressions are presented in Appendix C.

B-1 Compatibility Equation at an Interior Point Near the Left Simple Support (Refer to EQU. 10.3)

Considering the first of the membrane boundary conditions, equation (4.19a) i.e. $\varepsilon_{\eta}^{m} = 0$, one obtains

$$\varepsilon_{y}^{m} \cos^2\phi + \varepsilon_{x}^{m} \sin^2\phi - \gamma_{xy}^{m} \sin\phi \cos\phi = 0 \qquad \text{(B-1.1)}$$

In terms of the stress function, equation (B-1.1) reduces to

$$a_{11} F_{,xx} + a_{12} F_{,yy} + a_{13} F_{,xy} = 0 \qquad \text{(B-1.2)}$$

where

$$a_{11} = \frac{t}{t_y E} (\cos^2\phi - \nu_y \sin^2\phi)$$

$$a_{12} = \frac{t}{t_x E} (\sin^2\phi - \nu_x \cos^2\phi) \qquad \text{(B-1.3)}$$

$$a_{13} = -\frac{1}{G} \sin\phi \cos\phi$$

In skew co-ordinates, equation (B-1.2) reduces to

$$a_{21} F_{,uu} + a_{22} F_{,uv} + a_{23} F_{,vv} = 0 \qquad \text{(B-1.4)}$$

where,

where

$$a_{21} = a_{11} + a_{12} \tan^2\phi - a_{13} \tan\phi$$

$$a_{22} = 2a_{12} \tan\phi \sec\phi - a_{13} \sec\phi \qquad \text{(B-1.5)}$$

$$a_{23} = a_{12} \sec^2\phi$$

Applying equation (B-1.4) at point (i-1,j), one obtains:

$$a_{31}F_{i-2,j} + a_{32}(-F_{i-2,j+1} + F_{i-2,j-1})$$

$$= -a_{31}(-2F_{i-1,j} + F_{i,j}) - a_{32}(F_{i,j+1} - F_{i,j-1})$$

$$-a_{33}(F_{i-1,j+1} - 2F_{i-1,j} + F_{i-1,j-1}) \qquad \text{(B-1.6)}$$

where

$$a_{31} = a_{21}\chi^2$$

$$a_{32} = a_{22}\frac{\chi}{4}\cos\phi \qquad \text{(B-1.7)}$$

$$a_{33} = a_{23}\cos^2\phi$$

and $$\chi = \frac{\lambda_y}{\lambda_x}$$

Considering the second of the membrane bboundary conditions, equation (4.19b), i.e. $\tau_{\xi\eta}^{m} = 0$, one obtains

$$-\sigma_{x}^{m}\tan\phi + \tau_{xy}^{m} = 0 \qquad \text{(B-1.8)}$$

Equ. (B-1.8) is transformed into skew co-ordinates as follows:

$$a_{41} F_{,uu} + a_{42} F_{,uv} + a_{43} F_{,vv} = 0 \qquad \text{(B-1.9)}$$

where

$$a_{41} = \frac{t}{t_x} \tan^3\phi + \tan\phi$$

$$a_{42} = 2 \frac{t}{t_x} \tan^2\phi \sec\phi + \sec\phi \qquad \text{(B-1.10)}$$

$$a_{43} = \frac{t}{t_x} \tan \sec^2\phi$$

Applying equation (B-1.9) at point (i-1,j) one obtains

$$a_{51} F_{i-2,j} + a_{52} (-F_{i-2,j+1} + F_{i-2,j-1})$$

$$= -a_{51} (-2F_{i-1,j} + F_{i,j}) - a_{52} (E_{i,j+1} - F_{i,j-1})$$

$$-a_{53} (F_{i-1,j+1} - 2F_{i-1,j} + F_{i-1,j-1}) \qquad \text{(B-1.11)}$$

where

$$a_{51} = a_{41} \varkappa^2$$

$$a_{52} = a_{42} \frac{\varkappa}{4} \cos\phi \qquad \text{(B-1.12)}$$

$$a_{53} = a_{43} \cos^2\phi$$

Applying these two boundary conditions at points (i-1,j+1) and (i-1,j-1), the following equations are obtained:

$$a_{31}\ R_{i-2,j+1} + a_{32}(-F_{i-2,j+2} + F_{i-2,j})$$

$$= -a_{31}(-2F_{i-1,j+1} + F_{i,j+1}) - a_{32}(F_{i,j+2} - F_{i,j})$$

$$-a_{33}(F_{i-1,j+2} - 2F_{i-1,j+1} + F_{i-1,j}) \qquad \text{(B-1.13)}$$

$$a_{31}\ F_{i-2,j-1} + a_{32}(-F_{i-2,j} + F_{i-2,j-2})$$

$$= -a_{31}(-2F_{i-1,j-1} + F_{i,j-1}) - a_{32}(F_{i,j} - F_{i,j-2})$$

$$-a_{33}(F_{i-1,j} - 2F_{i-1,j-1} + F_{i-1,j-2}) \qquad \text{(B-1.14)}$$

$$a_{51}\ F_{i-2,j+1} + a_{52}(-F_{i-2,j+2} + F_{i-2,j})$$

$$= -a_{51}(-2F_{i-1,j+1} + F_{i,j+1}) - a_{52}(F_{i,j+2} - F_{i,j})$$

$$-a_{53}(F_{i-1,j+2} - 2F_{i-1,j+1} + F_{i-1,j}) \qquad \text{(B-1.15)}$$

and

$$a_{51} F_{i-2,j-1} + a_{52}(-F_{i-2,j} + F_{i-2,j-2})$$

$$= -a_{51}(-2F_{i-1,j-1} + F_{i,j-1}) - a_{52}(F_{i,j} - F_{i,j-2})$$

$$-a_{53}(F_{i-1,j} - 2F_{i-1,j-1} + F_{i-1,j-2}) \qquad \text{(B-1.16)}$$

The exterior points outside the plate boundary associated with the coefficients of plate stiffness are:

$$(\alpha A' + \beta^2 Zx^2) F_{i-2,j} + \frac{\beta}{2}(\alpha B_y + A' + Zx^2) X$$

$$(-F_{i-2,j+1} + F_{i-2,j-1})$$

$$+ \beta^2 \frac{B_y}{4}(-2F_{i-2,j} + F_{i-2,j+2} + F_{i-2,j-2}) \qquad \text{(B-1.17)}$$

Eliminating exterior points in terms of interior points from the relations (B-1.6), (B-1.11), (B-1.13), (B-1.14), (B-1.15) and (B-1.16), after a few algebraic operations, expression (B-1.17) can be expressed as:

$$\text{(B-1.17)} = -G_5(-2F_{i-1,j} + F_{i,j}) + (G_6 + G_8 - G_4) X$$

$$(F_{i-1,j+1} - 2F_{i-1,j} + F_{i-1,j-1}) - G_7(F_{i,j+1} - F_{i,j-1})$$

$$-2G_2(-F_{i-1,j-1} + F_{i,j-1} + F_{i-1,j+1} - F_{i,j+1})$$

$$-G_1(2F_{i,j} - F_{i,j+2} - F_{i,j-2})$$

$$-G_3(-2F_{i-1,j-1} + F_{i-1,j-2} - F_{i-1,j+2} + 2F_{i-1,j+1})$$

$$\text{(B-1.18)}$$

where

$$G_1 = \beta^2 \frac{B_y}{4}$$

$$G_2 = G_1 \frac{a_{51}}{a_{52}}$$

$$G_3 = G_1 \frac{a_{53}}{a_{52}}$$

$$G_4 = G_2 \left(\frac{-a_{51}a_{33} + a_{31}a_{53}}{a_{32}a_{51} - a_{31}a_{52}} \right) \qquad \text{(B-1.19)}$$

$$G_5 = \alpha A' + \beta^2 \mathbb{Z}x^2$$

$$G_6 = G_5 \left(\frac{-a_{33}a_{52} + a_{32}a_{53}}{a_{31}a_{52} - a_{32}a_{51}} \right)$$

$$G_7 = \frac{\beta}{2} (\alpha B_y + A' + \mathbb{Z}x^2)$$

$$G_8 = G_7 \left(\frac{-a_{51}a_{33} + a_{31}a_{53}}{a_{32}a_{51} - a_{31}a_{52}} \right)$$

Substitution of relation (B-1.18) into equation (4.15) results into the compatibility equation near the left simple support.

A function for F must now be found that satisfies the boundary conditions for the simple support. The most general function of F is

$$F = A_n X^n + B_n Y^m + C_m X^n Y^m + D_n$$

An application of this Airy stress function to the simple support indicates that the nodal fictitious points $F_{i-2,j+2}$, $F_{i-2,j+1}$, $F_{i-2,j}$, $F_{i-2,j-1}$ and $F_{i-2,j-2}$ cannot be evaluated in terms of interior points from the assumed boundary conditions. On the other hand, if the stress function F is assumed to be an invariant with the x- and y-edge co-ordinates, i.e. F is a constant along the edges, the boundary conditions, equation (4.19) are satisfied at all points along the plate edge. This simplifies the expression for the stress function to the form $F = D_n$. Since D_n may have any value, for simplicity, it can be set equal to zero. This means that the Airy stress function F will be equal to zero for all edge points. This simplication of support restraint has the added advantage that the matrices associated with the equilibrium and compatibility equations are of consistent order. This assumption automatically reduces the size of the compatibility equation matrix and eliminates the cumbersome process of renumbering rows and columns.

Analytical results obtained with this assumption have been supported by Levy's classical series solutions for non-linear (large-deflection) elastic plate problems. Hence they are considered to be valid for large deflection elasto-plastic orthotropic skew plate analysis.

The compatibility equation near the left simple support is presented as a finite difference molecule in EQU. 10.3.

B-2 Compatibility Equation at an Interior Point Near The Right Simple Support (Refer to EQU. 10.4)

Adopting the same procedure as in section B-1, applying the membrane boundary conditions, the following six equations are obtained.

$$a_{31}F_{i+2,j} + a_{32}(F_{i+2,j+1} - F_{i+2,j-1})$$

$$= -a_{31}(F_{i,j} - 2F_{i+1,j}) - a_{32}(-F_{i,j+1} + F_{i,j-1})$$

$$- a_{33}(F_{i+1,j+1} - 2F_{i+1,j} + F_{i+1,j-1}) \qquad \text{(B-2.1)}$$

$$a_{31}F_{i+2,j+1} + a_{32}(F_{i+2,j+2} - F_{i+2,j})$$

$$= -a_{31}(F_{i,j+1} - 2F_{i+1,j+1}) - a_{32}(-F_{i,j+2} + F_{i,j})$$

$$- a_{33}(F_{i+1,j+2} - 2F_{i+1,j+1} + F_{i+1,j}) \qquad \text{(B-2.2)}$$

$$a_{31}F_{i+2,j-1} + a_{32}(F_{i+2,j} - F_{i+2,j-2})$$

$$= -a_{31}(F_{i,j-1} - 2F_{i+1,j-1}) - a_{32}(-F_{i,j} + F_{i,j-2})$$

$$- a_{33}(F_{i+1,j} - 2F_{i+1,j-1} + F_{i+1,j-2}) \qquad \text{(B-2.3)}$$

$$a_{51}F_{i+2,j} + a_{52}(F_{i+2,j+1} - F_{i+2,j-1})$$

$$= -a_{51}(F_{i,j} - 2F_{i+1,j}) - a_{52}(-F_{i,j+1} + F_{i,j-1})$$

$$-a_{53}(F_{i+1,j+1} - 2F_{i+1,j} + F_{i+1,j-1}) \qquad \text{(B-2.4)}$$

$$a_{51}F_{i+2,j+1} + a_{52}(F_{i+2,j+2} - F_{i+2,j})$$

$$= -a_{51}(F_{i,j+1} - 2F_{i+1,j+1}) - a_{52}(-F_{i,j+2} + F_{i,j})$$

$$-a_{53}(F_{i+1,j+2} - 2F_{i+1,j+1} + F_{i+1,j}) \qquad \text{(B-2.5)}$$

$$a_{51}F_{i+2,j-1} + a_{52}(F_{i+2,j} - F_{i+2,j-2})$$

$$= -a_{51}(F_{i,j-1} - 2F_{i+1,j-1}) - a_{52}(-F_{i,j} + F_{i,j-2})$$

$$-a_{53}(F_{i+1,j} - 2F_{i+1,j-1} + F_{i+1,j-2}) \qquad \text{(B-2.6)}$$

The exterior points outside the plate boundary associated with coefficients of plate stiffness are:

$$(\alpha A' + \beta^2 Zx^2)F_{i+2,j} + \frac{\beta}{2}(\alpha B_y + A' + Zx^2)x$$

$$(F_{i+2,j+1} - F_{i+2,j-1}) + \beta^2 \frac{B_y}{4}(F_{i+2,j+2}$$

$$- 2F_{i+2,j} + F_{i+2,j-2}) \qquad \text{(B-2.7)}$$

Eliminating the exterior points as in section B-1.1, the expression (B-2.7) can be expressed, by using relations (B-2.1), (B-2.2), (B-2.3), (B-2.4), (B-2.5) and (B-2.6) as follows:

$$
\begin{aligned}
(B\text{-}2.7) = & -G_5(F_{i,j} - 2F_{i+1,j+1}) + (G_6 \mp G_8 + G_4)\times \\
& (F_{i+1,j+1} - 2F_{i+1,j} + F_{i+1.j-1}) \\
& - G_7(-F_{i,j+1} + F_{i,j-1}) \\
& -2G_2(F_{i,j+1} - F_{i+1,j+1} - F_{i,j-1} + F_{i+1,j-1}) \\
& - G_1(-F_{i,j+2} + 2F_{i,j} - F_{i,j-2}) \\
& - G_3(F_{i+1,j+2} - 2F_{i+1,j+1} + 2F_{i+1,j-1} - F_{i+1,j-2})
\end{aligned}
$$

(B-2.8)

The compatibility equation at an interior point near the right simple support can be obtained by substituting the relation (B-2.8) into equation (4.15) which is presented as finite difference molecule in EQU. 10.4.

B-3 Compatibility Equation at an Interior Point Near the Edge Parallel to the x-axis (Refer to EQU. 10.5)

Applying the membrane boundary conditions Eq. (4.20) along the edge parallel to the x-axis; i.e

$$\tau_{xy}^{m} = 0$$

or

$$(F_{,xy})_{support} = 0 \qquad \text{(B-3.1)}$$

At point (i,j+1)

$$(F_{,xy})_{i,j+1} = \frac{\alpha}{\lambda_y^2}\left[\beta(F_{i-1,j+1} - 2F_{i,j+1} + F_{i+1,j+1}) + \tfrac{1}{4}(F_{i+1,j+2} - F_{i-1,j+2} + F_{i-1,j} - F_{i+1,j})\right] = 0$$

or

$$F_{i+1,j+2} - F_{i-1,j+2} = -4\beta(F_{i-1,j+1} - 2F_{i,j+1} + F_{i+1,j+1}) - (F_{i-1,j} - F_{i+1,j}) \qquad \text{(B-3.2)}$$

Similarly,

$$F_{i+2,j+2} - F_{i,j+2} = -4\beta(F_{i,j+1} - 2F_{i+1,j+1} + F_{i+2,j+1}) - (F_{i,j} - F_{i+2,j}) \qquad \text{(B-3.3)}$$

and

$$F_{i,j+2} - F_{i-2,j+2} = -4\beta(F_{i-2,j+1} - 2F_{i-1,j+1} + F_{i,j+1}) - (F_{i-2,j-1} - F_{i,j}) \qquad \text{(B-3.4)}$$

Applying the boundary condition $\varepsilon_x^m = 0$ along the edge, at point (i,j+1) one obtains

$$\gamma'(F_{i-1,j+1} + F_{i+1,j+1}) - 2(B_y + \gamma') F_{i,j+1}$$

$$+ \frac{\beta}{2} B_y (F_{i+1,j+2} - F_{i-1,j+2} + F_{i-1,j} - F_{i+1,j})$$

$$+ B_y (F_{i,j+2} + F_{i,j}) = 0 \qquad \text{(B-3.5)}$$

where $\gamma' = B_y \beta^2 - \nu_y B_x \alpha^2$

From (B-3.2) and (B-3.5) the following equation can be obtained

$$B_y F_{i,j+2} = -B_y F_{i,j} - \gamma' (F_{i-1,j+1} + F_{i+1,j+1})$$

$$+ 2(B_y + \gamma') F_{i,j+1} + 2\beta^2 B_y (F_{i-1,j+1} - 2F_{i,j+1}$$

$$+ F_{i+1,j+1}) \qquad \text{(B-3.6)}$$

From equations (B-3.3) and (B-3.4) it follows

$$F_{i+2,j+2} - 2F_{i,j+2} + F_{i-2,j+2}$$

$$= -4\beta (-2F_{i+1,j+1} + F_{i+2,j+1} - F_{i-2,j+1}$$

$$+ 2F_{i-1,j+1}) - (2F_{i,j} - F_{i-2,j} - F_{i+2,j}) \qquad \text{(B-3.7)}$$

External points associated with the in-plane stiffness coefficients in the general equations can now be related to the interior points by the following relations:

$$\beta^2 \frac{B_y}{4} (-2F_{i,j+2} + F_{i+2,j+2} + F_{i-2,j+2})$$

$$+ \beta B_y (F_{i+1,j+2} - F_{i-1,j+2}) + B_y F_{i,j+2}$$

$$= -\beta^3 B_y (-2F_{i+1,j+1} + F_{i+2,j+1} - F_{i-2,j+1} + 2F_{i-1,j+1})$$

$$- \beta^2 \frac{B_y}{4} (2F_{i,j} - F_{i-2,j} - F_{i+2,j})$$

$$- \beta B_y (F_{i-1,j} - F_{i+1,j}) - B_y F_{i,j}$$

$$- \gamma' (F_{i-1,j+1} + F_{i+1,j+1}) + 2(B_y + \gamma') F_{i,j+1}$$

$$- 2\beta^2 B_y (F_{i-1,j+1} - 2F_{i,j+1} + F_{i+1,j+1}) \qquad \text{(B-3.8)}$$

Substituting this relation into equation (4.15), the compatibility equation at an interior point near the edge parallel to the x-axis can be obtained. This equation is presented as a finite difference molecule in EQU. 10.5.

B-4 Compatibility Equation at an Interior Point Near an Acute Corner (Refer to EQU. 10.6)

Applying the membrane boundary condition

$$(\varepsilon_\eta^m)_{\text{support}} = 0$$

along the edge parallel to the v-axis, one obtains

@ node (i-1,j):

$$a_{31} F_{i-2,j} + a_{32}(-F_{i-2,j+1} + F_{i-2,j-1})$$

$$= -a_{31}(-2F_{i-1,j} + F_{i,j}) - a_{32}(F_{i,j+1} - F_{i,j-1})$$

$$- a_{33}(F_{i-1,j+1} - 2F_{i-1,j} + F_{i-1,j-1}) \qquad \text{(B-4.1)}$$

@ node (i-1,j-1):

$$a_{31} F_{i-2,j-1} + a_{32}(-F_{i-2,j} + F_{i-2,j-2})$$

$$= -a_{31}(-2F_{i-1,j-1} + F_{i,j-1}) - a_{32}(F_{i,j} - F_{i,j-2})$$

$$- a_{33}(F_{i-1,j} - 2F_{i-1,j-1} + F_{i-1,j-2}) \qquad \text{(B-4.2)}$$

@ node (i-1,j+1):

$$a_{31} F_{i-2,j+1} + a_{32}(F_{i,j+2} - F_{i-2,j+2} + F_{i-2,j})$$

$$+ a_{33} F_{i-1,j+2} = -a_{31}(-2F_{i-1,j+1} + F_{i,j+1})$$

$$- a_{32}(-F_{i,j}) - a_{33}(-2F_{i-1,j+1} + F_{i-1,j}) \qquad \text{(B-4.3)}$$

Applying the condition $(\tau_{\xi\eta})^{m_i}_{\text{support}} = 0$

@ node (i-1,j)

$$a_{51} F_{i-2,j} + a_{52}(-F_{i-2,j+1} + F_{i-2,j-1})$$

$$= -a_{51}(-2F_{i-1,j} + F_{i,j}) - a_{52}(F_{i,j+1} - F_{i,j-1})$$

$$- a_{53}(F_{i-1,j+1} - 2F_{i-1,j} + F_{i-1,j-1}) \qquad \text{(B-4.4)}$$

@ node (i-1,j-1):

$$a_{51} F_{i-2,j-1} + a_{52}(-F_{i-2,j} + F_{i-2,j-2})$$

$$= -a_{51}(-2F_{i-1,j-1} + F_{i,j+1}) - a_{52}(F_{i,j} - F_{i,j-2})$$

$$- a_{53}(F_{i-1,j} - 2F_{i-1,j-1} + F_{i-1,j-2}) \qquad \text{(B-4.5)}$$

@ node (i-1,j+1):

$$a_{51} F_{i-2,j+1} + a_{52}(F_{i,j+2} - F_{i-2,j+2} + F_{i-2,j})$$

$$+ a_{53} F_{i-1,j+2} = -a_{51}(-2F_{i-1,j+1} + F_{i,j+1})$$

$$- a_{52}(-F_{i,j}) - a_{53}(-2F_{i-1,j+1} + F_{i-1,j}) \qquad \text{(B-4.6)}$$

Applying the condition

$$(\varepsilon_x^m)_{\text{support}} = 0$$

along the edge parallel to the x-axis

@ node (i,j+1):

$$\frac{\beta}{2} B_y (F_{i+1,j+2} - F_{i-1,j+2}) + B_y F_{i,j+2} = -\gamma'(F_{i-1,j+1} + F_{i+1,j+1}) +$$

$$2(B_y + \gamma')F_{i,j+1} - \frac{\beta}{2} B_y (F_{i-1,j} - F_{i+1,j}) - B_y F_{i,j} \qquad \text{(B-4.7)}$$

@ node (i+1,j+1):

$$\frac{\beta}{2} B_y (F_{i+2,j+2} - F_{i,j+2}) + B_y F_{i+1,j+2}$$

$$= -\gamma' (F_{i,j+1} + F_{i+2,j+1}) + 2(B_y + \gamma') F_{i+1,j+1}$$

$$- \frac{\beta}{2} B_y (F_{i,j} - F_{i+2,j}) - B_y F_{i+1,j} \qquad \text{(B-4.8)}$$

@ node (i-1,j+1):

$$\frac{\beta}{2} B_y (F_{i,j+2} - F_{i-2,j+2} + F_{i-2,j}) + B_y F_{i-1,j+2}$$

$$+ \gamma' F_{i-2,j+1} = -\gamma' (F_{i,j+1}) + 2(B_y + \gamma') F_{i-1,j+1}$$

$$+ \frac{\beta}{2} B_y F_{i,j} - B_y F_{i-1,j} \qquad \text{(B-4.9)}$$

Applying the boundary condition $(\tau_{xy}^m)_{support} = 0$,

@ node (i+1,j+1):

$$F_{i+2,j+2} - F_{i,j+2} = -4\beta (F_{i,j+1} - 2F_{i+1,j+1} + F_{i+2,j+1})$$

$$- (F_{i,j} - F_{i+2,j}) \qquad \text{(B-4.10)}$$

@ node (i,j+1):

$$F_{i+1,j+2} - F_{i-1,j+2} = -4\beta (F_{i-1,j+1} - 2F_{i,j+1} + F_{i+1,j+1})$$

$$- (F_{i-1,j} - F_{i+1,j}) \qquad \text{(B-4.11)}$$

@ node (i-1,j+1):

$$F_{i,j+2} - F_{i-2,j+2} - 4\beta\,(F_{i-2,j+1}) + F_{i-2,j}$$

$$= -4\beta(-2F_{i-1,j+1} + F_{i,j+1}) - (-F_{i,j}) \qquad \text{(B-4.12)}$$

Eliminating the fictitious nodal point outside the plate boundary in terms of an interior point from the above equations, the following relations are obtained:

$$F_{i-2,j} = 2F_{i-1,j} - F_{i,j} + \frac{a_{33}a_{52} - a_{32}a_{53}}{a_{51}a_{32} - a_{31}a_{52}} \chi_1$$

$$(F_{i-1,j+1} - 2F_{i-1,j} + F_{i-1,j-1}) \qquad \text{(B-4.13)}$$

$$F_{i-2,j+1} = \frac{1}{\gamma' - 2\beta^2 B_y}\Big[-\gamma' F_{i,j+1} + 2\beta^2 B_y \chi$$

$$(F_{i,j+1} - 2F_{i-1,j+1}) + 2(\gamma' + B_y) F_{i-1,j+1}$$

$$- B_y\Big\{2F_{i-1,j} - 2F_{i+1,j} + 2\beta^2(F_{i,j+1}$$

$$- 2F_{i+1,j+1} + F_{i+2,j+1}) + 2\frac{(B_y + \gamma')}{B_y} F_{i+1,j+1}$$

$$- \frac{\gamma'}{B_y}(F_{i,j+1} + F_{i+2,j+1})$$

$$+ 4\beta(F_{i-1,j+1} - 2F_{i,j+1} + F_{i+1,j+1})\Big\}\Big] \qquad \text{(B-4.14)}$$

$$-F_{i-2,j+1} + F_{i-2,j-1} = -(F_{i,j+1} - F_{i,j-1})$$

$$- \frac{a_{51}a_{33} - a_{53}a_{31}}{a_{51}a_{32} - a_{31}a_{52}} (F_{i-1,j+1} - 2F_{i-1,j}$$

$$+ F_{i-1,j-1}) \qquad \text{(B-4.15)}$$

$$F_{i,j+2} = -F_{i,j} + 2\beta^2(F_{i-1,j+1} - 2F_{i,j+1} + F_{i+1,j+1})$$

$$+ 2 \frac{(B_y + \gamma')}{B_y} F_{i,j+1} - \frac{\gamma'}{B_y} (F_{i-1,j+1} + F_{i+1,j+1})$$

$$\text{(B-4.16)}$$

$$F_{i+1,j+2} = -F_{i+1,j} + 2\beta^2(F_{i,j+1} - 2F_{i+1,j+1} + F_{i+2,j+1})$$

$$+ 2 \frac{(B_y + \gamma')}{B_y} F_{i+1,j+1} - \frac{\gamma'}{B_y} \times$$

$$(F_{i,j+1} + F_{i+2,j+1}) \qquad \text{(B-4.17)}$$

$$F_{i-1,j+2} = -F_{i+1,j} + 2\beta^2(F_{i,j+1} - 2F_{i+1,j+1} + F_{i+2,j+1})$$

$$+ 2 \frac{(B_y + \gamma')}{B_y} F_{i+1,j+1} - \frac{\gamma'}{B_y} \times$$

$$(F_{i,j+1} + F_{i+2,j+1}) + 4\beta (F_{i-1,j+1}$$

$$- 2F_{i,j+1} + F_{i+1,j+1}) + F_{i-1,j} - F_{i+1,j}$$

$$\text{(B-4.18)}$$

and

$$F_{i-2,j-2} = 2F_{i-1,j+1} - 2F_{i,j} + \frac{a_{33}a_{52} - a_{32}a_{53}}{a_{51}a_{32} - a_{31}a_{52}} \times$$

$$(F_{i-1,j+1} - 2F_{i-1,j} + F_{i-1,j-1}) + F_{i,j-2}$$

$$- \frac{a_{51}}{a_{52}} \left[\frac{1}{\gamma' - 2\beta^2 B_y} \left\{ -\gamma' F_{i,j+1} + 2\beta^2 B_y \times \right.\right.$$

$$(F_{i,j+1} - 2F_{i-1,j+1}) + 2(\gamma' + B_y) F_{i-1,j+1}$$

$$- B_y \left(2F_{i-1,j} - 2F_{i+1,j} + 2\beta^2 (F_{i,j+1} - 2F_{i+1,j+1} \right.\right.$$

$$\left.\left. + F_{i+2,j+1}) \right) - 2(B_y + \gamma') F_{i+1,j+1}$$

$$+ \gamma' (F_{i,j+1} + F_{i+2,j+1}) - 4\beta B_y (F_{i-1,j+1}$$

$$\left.\left. - 2F_{i,j+1} + F_{i+1,j+1}) \right\} - F_{i,j+1} + F_{i,j-1} \right.$$

$$+ \frac{a_{51}a_{33} - a_{53}a_{31}}{a_{52}a_{31} - a_{51}a_{32}} (F_{i-1,j+1} - 2F_{i-1,j}$$

$$\left. + F_{i-1,j-1}) \right] - \frac{a_{51}}{a_{52}} (-2F_{i-1,j-1} + F_{i,j-1})$$

$$- \frac{a_{53}}{a_{52}} (F_{i-1,j} - 2F_{i-1,j-1} + F_{i-1,j-2})$$

(B-4.19)

The external points associated with in-plane stiffness coefficients in the compatibility equation near the edge parallel to the x-axis can be obtained in terms of interior points within the plate boundary, after a few algebraic operations, as follows:

$$\left(-\beta^2 \frac{B_y}{4} + \alpha A' + \varkappa^2\beta^2\right)F_{i-2,j} + \frac{\beta}{2}\left(\alpha B_y + A' + \varkappa^2\right)\times$$

$$\left(-F_{i-2,j+1} + F_{i-2,j-1}\right) + \beta^2 \frac{B_y}{4}\left(-2F_{i,j+2} + F_{i-2,j+2}\right.$$

$$\left. + F_{i+2,j+2}\right) + \beta^2 \frac{B_y}{4} F_{i-2,j-2} + \beta B_y\left(F_{i+1,j+2} - F_{i-1,j+2}\right)$$

$$+ B_y F_{i,j+2} = \left(-\beta^2 \frac{B_y}{4} + \alpha A' + \varkappa^2\beta^2\right)\left\{2F_{i-1,j} - F_{i,j}\right.$$

$$\left. + \frac{a_{33}a_{52} - a_{32}a_{53}}{a_{51}a_{32} - a_{31}a_{52}}\left(F_{i-1,j+1} - 2F_{i-1,j} + F_{i-1,j-1}\right)\right\}$$

$$+ \frac{\beta}{2}\left(\alpha B_y + A' + \varkappa^2\right)\left\{\left(-F_{i,j+1} + F_{i,j-1}\right)\right.$$

$$\left. + \frac{a_{33}a_{51} - a_{53}a_{31}}{a_{31}a_{52} - a_{51}a_{32}}\left(F_{i-1,j+1} - 2F_{i-1,j} + F_{i-1,j-1}\right)\right\}$$

$$- \beta^3 B_y\left(-2F_{i+1,j+1} + F_{i+2,j+1} + 2F_{i-1,j+1}\right)$$

$$+ \beta^3 \frac{B_y}{\gamma' - 2\beta^2 B_y}\left\{-\gamma' F_{i,j+1} + 2\beta^2 B_y\left(F_{i,j+1} - 2F_{i-1,j+1}\right)\right.$$

$$\left. + 2\left(\gamma' + B_y\right)F_{i-1,j+1} - B_y\left(2F_{i-1,j} - 2F_{i+1,j}\right)\right. \ldots \text{ con'd}$$

$$- 2\beta^2 B_y (F_{i,j+1} - 2F_{i+1,j+1} + F_{i+2,j+1})$$

$$- 2 (B_y + \gamma') F_{i+1,j+1} + \gamma' (F_{i,j+1} + F_{i+2,j+1})$$

$$- 4\beta B_y (F_{i-1,j+1} - 2F_{i,j+1} + F_{i+1,j+1})\Big\}$$

$$- \beta^2 \frac{B_y}{4} (2F_{i,j} - F_{i+2,j}) - 2\beta^2 B_y (F_{i-1,j+1} - 2F_{i,j+1}$$

$$+ F_{i+1,j+1}) - \beta B_y (F_{i-1,j} - F_{i+1,j}) - B_y F_{i,j}$$

$$+ 2(B_y + \gamma') F_{i,j+1} - \gamma' (F_{i-1,j+1} + F_{i+1,j+1})$$

$$+ \beta^2 \frac{B_y}{2} (2F_{i-1,j} - F_{i,j}) + \beta^2 \frac{B_y}{4} \frac{a_{33}a_{52} - a_{32}a_{53}}{a_{51}a_{32} - a_{31}a_{52}} \times$$

$$(F_{i-1,j+1} - 2F_{i-1,j} + F_{i-1,j-1}) + \beta^2 \frac{B_y}{4} F_{i,j-2}$$

$$- \beta^2 \frac{B_y}{4} \frac{a_{51}}{a_{52}} \frac{1}{\gamma' - 2\beta^2} \Big\{ - \gamma' F_{i,j+1} + 2\beta^2 B_y (F_{i,j+1}$$

$$- 2F_{i-1,j+1}) + 2(\gamma' + B_y) F_{i-1,j+1} - 2B_y (F_{i-1,j}$$

$$- F_{i+1,j}) - 2\beta^2 B_y (F_{i,j+1} - 2F_{i+1,j+1} + F_{i+2,j+1})$$

$$- 2(B_y + \gamma') F_{i+1,j+1} + \gamma' (F_{i,j+1} + F_{i+2,j+1})$$

$$- 4\beta B_y (F_{i-1,j+1} - 2F_{i,j+1} + F_{i+1,j+1})\Big\} \ldots \text{ con'd}$$

$$-\beta^2 \frac{B_y}{4} \frac{a_{51}}{a_{52}} \left\{ -F_{i,j+1} + F_{i,j-1} + \frac{a_{51}a_{33} - a_{53}a_{31}}{a_{52}a_{31} - a_{51}a_{32}} x \right.$$

$$\left. (F_{i-1,j+1} - 2F_{i-1,j} + F_{i-1,j-1}) \right\} - \beta^2 \frac{B_y}{4} \frac{a_{51}}{a_{52}} x$$

$$(-2F_{i-1,j-1} + F_{i,j-1}) - \frac{a_{53}}{a_{52}} \beta^2 \frac{B_y}{4} x$$

$$(F_{i-1,j} - 2F_{i-1,j-1} + F_{i-1,j-2}) \qquad \text{(B-4.20)}$$

Letting

$$\bar{A}_1 = -\beta^2 \frac{B_y}{4} + \alpha A' + \beta^2 Z\varkappa^2$$

$$\bar{A}_2 = \bar{A}_1 \frac{a_{33}a_{52} - a_{32}a_{53}}{a_{51}a_{32} - a_{31}a_{52}}$$

$$\bar{A}_3 = \frac{\beta}{2} (\alpha B_y + A' + Z\varkappa^2)$$

$$\bar{A}_4 = \frac{a_{33}a_{51} - a_{53}a_{31}}{a_{31}a_{52} - a_{51}a_{32}} \bar{A}_3$$

$$\bar{B}_1 = \beta^3 \frac{B_y}{\gamma' - 2\beta^2 B_y}$$

$$\bar{B}_2 = \beta^2 \frac{B_y}{4} \frac{a_{33}a_{52} - a_{32}a_{53}}{a_{51}a_{32} - a_{31}a_{52}}$$

$$\bar{B}_3 = \beta^2 \frac{B_y}{4} \frac{a_{51}}{a_{52}}$$

$$\bar{B}_4 = \bar{B}_3 \frac{a_{51}a_{33} - a_{53}a_{31}}{a_{52}a_{31} - a_{51}a_{32}}$$

$$\bar{B}_5 = \bar{B}_3 \frac{1}{\gamma' - 2\beta^2 B_y}$$

and substituting the relations of equation (B-4.20) into EQU. 9.5, the compatibility equation at an interior point near the acute corner can be obtained which is presented as a finite difference molecule in EQU. 10.6.

B-5 Compatibility Equation at an Interior Point Near an Obtuse Corner (Refer to EQU. 10.7)

Following the same procedure as in section B-4 of this Appendix, the exterior points may be evaluated in terms of interior points by applying the membrane boundary conditions, i.e. equations (4.19) and (4.20) and the resulting equation is presented as a finite difference molecule in EQU. 10.7.

B-6 Equilibrium Equation at an Interior Point Near the Left Simple Support (Refer to EQU. 10.8)

Applying the bending boundary conditions, equations (4.16) and (4.17) along the left simple support, we have:

$$w_{i-1,j+2} = w_{i-1,j+1} = w_{i-1,j} = w_{i-1,j-1} = w_{i-1,j-2} = 0 \qquad \text{(B-6.1)}$$

and

$$(M_x + M_y)_{\text{support}} = 0 \qquad \text{(B-6.2)}$$

Relation (B-6.2) leads to

$$K_x w_{,xx} + K_y w_{,yy} = 0 \qquad \text{(B-6.3)}$$

where

$$K_x = D_x + \nu_x D_y$$

$$K_y = D_y + \nu_y D_x$$

Substituting the difference expression of $w_{,xx}$ and $w_{,yy}$ at nodal point (i-1,j), one obtains

$$w_{i-2,j} + w_{i,j} = -K_y \frac{\beta}{2\delta} \left[w_{i,j+1} - w_{i-2,j+1} + w_{i-2,j-1} - w_{i,j-1} \right] \qquad \text{(B-6.4)}$$

where $\delta = K_x \alpha^2 + K_y \beta^2$

Condition of zero slope along the edge gives

$$\left(\frac{\partial w}{\partial v} \right)_{i-1,j} = \frac{1}{2} \left[\left(\frac{\partial w}{\partial v} \right)_{i-2,j} + \left(\frac{\partial w}{\partial v} \right)_{i,j} \right] = 0$$

In terms of difference equation, one obtains

$$-w_{i-2,j+1} + w_{i-2,j-1} = -w_{i,j-1} + w_{i,j+1} \qquad \text{(B-6.5)}$$

Substituting the relation (B-6.5) into equation (B-6.4) one obtains,

$$w_{i-2,j} = K_y \frac{\beta}{\delta} (w_{i,j-1} - w_{i,j+1}) - w_{i,j} \qquad \text{(B-6.6)}$$

In a similar manner, the following relations are obtained

$$\left.\begin{aligned} w_{i-2,j+1} &= K_y \frac{\beta}{\delta} (w_{i,j} - w_{i,j+2}) - w_{i,j+1} \\ w_{i-2,j+1} &= K_y \frac{\beta}{\delta} (w_{i,j-2} - w_{i,j}) - w_{i,j+1} \end{aligned}\right\} \quad \text{(B-6.7)}$$

$$\left.\begin{aligned} w_{i-2,j-1} &= K_y \frac{\beta}{\delta} (w_{i,j+2} - w_{i,j}) - w_{i,j-1} \\ w_{i-2,j-1} &= K_y \frac{\beta}{\delta} (w_{i,j} - w_{i,j-2}) - w_{i,j-1} \end{aligned}\right\} \quad \text{(B-6.8)}$$

$$w_{i-2,j+2} = K_y \frac{\beta}{\delta} (w_{i,j-1} - w_{i,j+1}) - w_{i,j+2} \quad \text{(B-6.9)}$$

$$w_{i-2,j-2} = K_y \frac{\beta}{\delta} (w_{i,j-1} - w_{i,j+1}) - w_{i,j-2}$$

The set of equations (B-6.7) and (B-6.8) which have different values for the same external point imposes a constraint $w_{i,j+2} - 2w_{i,j} + w_{i,j-2} = 0$, near the simple support. It is, however, assumed that this constraint near the simple support is valid as the deflection values close to supporting edges are small.

Substituting the relations (B-6.6) through (B-6.9) into the general equation of equilibrium Equ. (4.14), equilibrium equation near the left simple support can be deduced which is presented as a finite difference molecule in EQU. 10.8.

B-7 Equilibrium Equation at Interior Point Near the Right Simple Support (Refer to EQU. 10.9)

Adopting the same procedure as in preceding section B-6.1, the following expressions for exterior nodal point deflection in terms of interior point may be obtained

$$w_{i+2,j} = \beta \frac{K_y}{\delta} (w_{i,j+1} - w_{i,j-1}) - w_{i,j} \qquad \text{(B-7.1)}$$

$$\left.\begin{aligned} w_{i+2,j+1} &= \beta \frac{K_y}{\delta} (w_{i,j+2} - w_{i,j}) - w_{i,j+1} \\ w_{i+2,j+1} &= \beta \frac{K_y}{\delta} (w_{i,j} - w_{i,j-2}) - w_{i,j+1} \end{aligned}\right\} \qquad \text{(B-7.2)}$$

$$\left.\begin{aligned} w_{i+2,j-1} &= \beta \frac{K_y}{\delta} (w_{i,j+2} - w_{i,j}) - w_{i,j-1} \\ w_{i+2,j-1} &= \beta \frac{K_y}{\delta} (w_{i,j} - w_{i,j-2}) - w_{i,j-1} \end{aligned}\right\} \qquad \text{(B-7.3)}$$

$$w_{i+2,j+2} = \beta \frac{K_y}{\delta} (w_{i,j+1} - w_{i,j-1}) - w_{i,j+2} \qquad \text{(B-7.4)}$$

$$w_{i+2,j-2} = \beta \frac{K_y}{\delta} (w_{i,j+1} - w_{i,j-1}) - w_{i,j-2} \qquad \text{(B-7.5)}$$

Substituting the relations (B-7.1) through (B-7.5) into equilibrium equation (4.14), equilibrium equation near the right simple support can be obtained which is presented as a finite difference molecule in EQU. 10.9.

B-8 Equilibrium Equation at an Interior Point Near the Edge Parallel to the x-axis (Refer to EQU. 10.10)

Applying the boundary condition, equ. (4.18) for the simple support at $y = \pm b/2$, one obtains:

$$M_y = -D_y (w_{,yy} + \nu_x w_{,xx}) = 0$$

$$D_y w_{,yy} + \nu_x D_y w_{,xx} = 0$$

Adding and subtracting $D_x w_{,xx}$ to the above expression yields,

$$U_{edge} = (D_x - \nu_x D_y) w_{,xx_{edge}} \qquad (B\text{-}8.1)$$

At the support line $w_{i-2,j+1} = w_{i-1,j+1} = w_{i,j+1} = w_{i+1,j+1} = w_{i+2,j+1} = 0$. Hence

$$U_{i-1,j+1} = (D_x - \nu_x D_y) \frac{\alpha^2}{\lambda_y^2} (w_{i-2,j+1} - 2w_{i-1,j+1} + w_{i,j+1}) = 0$$

Similarly, $U_{i,j+1} = U_{i+1,j+1} = 0$.

From the expression of U in equations (4.10d), (4.10f) and (4.10g) and the above conditions, the following relations are obtained:

$$U_{i-1,j+1} = 0$$

or

$$\frac{\beta}{2} D_y(w_{i,j+2} - w_{i-2,j+2}) + D_y w_{i-1,j+2}$$

$$= - \frac{\beta}{2} D_y(w_{i-2,j} - w_{i,j}) - D_y w_{i-1,j} \qquad \text{(B-8.2)}$$

Similarly

$$\frac{\beta}{2} D_y(w_{i+1,j+2} - w_{i-1,j+2}) + D_y w_{i,j+2}$$

$$= - \frac{\beta}{2} D_y(w_{i-1,j} - w_{i+1,j}) - D_y w_{i,j} \qquad \text{(B-8.3)}$$

and

$$\frac{\beta}{2} D_y(w_{i+2,j+2} - w_{i,j+2}) + D_y w_{i+1,j+2}$$

$$= -\frac{\beta}{2} D_y(w_{i,j} - w_{i+2,j}) - D_y w_{i+1,j} \qquad \text{(B-8.4)}$$

The external points associated with the bending stiffness coefficients in the general equation are

$$\beta^2 \frac{D_y}{4} (-2w_{i,j+2} + w_{i+2,j+2} + w_{i-2,j+2})$$

$$+ \beta D_y(w_{i+1,j+2} - w_{i-1,j+2}) + D_y w_{i,j+2} \qquad \text{(B-8.5)}$$

From the relations (B-8.2) through (B-8.4), after a few algebraic operations, expression (B-8.5) can be related to the interior points as follows:

$$(B\text{-}8.5) = -D_y w_{i,j} + \beta^2 \frac{D_y}{4} (w_{i+2,j} - 2w_{i,j} + w_{i-2,j}) \qquad (B\text{-}8.6)$$

Substituting the relation (B-8.6) into the general equilibrium equation (4.14), equilibrium equation at an interior point can be obtained which is presented as finite difference molecule in EQU. 10.10.

B-9 Equilibrium Equation at an Interior Point Near the Acute Corner (Refer to EQU. 10.11)

From the bending boundary conditions, equation (4.16), one obtains

$$w_{i-1,j+1} = w_{i,j+1} = w_{i+1,j+1} = w_{i+2,j+1} = w_{i-1,j}$$

$$= w_{i-1,j-1} = w_{i-1,j-2} = 0$$

Applying the relations as derived in equations (B-6.3), through (B-6.9), the following relations are obtained:

$$w_{i-2,j} = K_y \frac{\beta}{\delta} (w_{i,j-1}) - w_{i,j} \qquad (B\text{-}9.1)$$

$$w_{i-2,j+1} = K_y \frac{\beta}{\delta} (w_{i,j-2} - w_{i,j}) \qquad (B\text{-}9.2)$$

$$w_{i-2,j-1} = K_y \frac{\beta}{\delta} (w_{i,j-2} - w_{i,j}) - w_{i,j-1} \qquad (B\text{-}9.3)$$

$$w_{i-2,j-2} = K_y \frac{\beta}{\delta} (w_{i,j-2}) - w_{i,j-2} \qquad (B\text{-}9.4)$$

From the relation (B-8.1) through (B-8.4), the following relations may be deduced.

$$U_{edge} = (D_x - \nu_x D_y) \frac{\partial^2 w}{\partial x^2}\Big|_{edge}$$

at node (i-1,j+1) :

$$U_{i-1,j+1} = \frac{\gamma}{\lambda_y^2} w_{i-2,j+1} \qquad \text{where } \gamma = (D_x - \nu_x D_y)\alpha^2$$

or

$$\frac{\beta}{2} D_y (w_{i,j+2} - w_{i-2,j+2}) + D_y w_{i-1,j+2} - (\gamma - A) w_{i-2,j+1}$$

$$= -\frac{\beta}{2} D_y (w_{i-2,j} - w_{i,j}) \qquad \text{(B-9.5)}$$

at node (i+1,j+1) :

$$U_{i+1,j+1} = 0$$

or

$$\frac{\beta}{2} D_y (w_{i+2,j+2} - w_{i,j+2}) + D_y w_{i+1,j+2} = -\frac{\beta}{2} D_y (w_{i,j} - w_{i+2,j}) - D_y w_{i+1,j} \qquad \text{(B-9.6)}$$

and

$$U_{i,j+1} = 0$$

or

$$\frac{\beta}{2} D_y (w_{i+1,j+2} - w_{i-1,j+2}) + D_y w_{i,j+2}$$

$$= \frac{\beta}{2} D_y w_{i+1,j} - D_y w_{i,j} \qquad \text{(B-9.7)}$$

Substituting expression (B-9.1) through (B-9.7) into EQU. **10.10**, the equilibrium equation at interior point near the acute corner is obtained. This is presented as a finite difference molecule in EQU. 10.11.

B-10 Equilibrium Equation at an Interior Point Near the Obtuse Corner

Following the same procedure as in the preceding section B-9, the equilibrium equation at an interior point near the obtuse corner can be obtained and is presented as a finite difference molecule in EQU. 10.12.

APPENDIX C

FINITE DIFFERENCE EQUATIONS FOR THE SMALL DEFLECTION BEHAVIOUR OF AN ORTHOTROPIC SKEW PLATE

As discussed in section 4.3.3, because of the various physical or mathematical restrictions for the validity of the governing equations at a free edge, the large deflection equations cannot be applied to a free edge. Nevertheless, within the elastic stress region, solutions of orthotropic plate problems may be well predicted by considering only the linear (small-deflection) theory of orthotropic plate. Since the theory can be effectively utilized at the free edge of the structural system, it was considered instructive to obtain test results from the model plates within the elastic range with the boundary conditions of simple support on two sides and free at the other two. For the elastic small deflection theory, the two governing equations are completely independent. Omitting the non-linear terms involving the stress functions from the equilibrium equation 10.1, 10.8 and 10.9, small deflection finite difference molecules can be obtained for (1) a general interior point, (2) an interior point near the left simple support and (3) an interior point near the right

simple support. These are presented as finite difference molecules in EQU. 11.1, EQU.11.2 and EQU. 11.3, respectively. In this section, difference equations will be obtained for: (4) an interior point near a free edge, (5) an interior point near the acute corner, (6) an interior point near the obtuse corner, (7) a general edge point, (8) an edge point near the acute corner, and (9) an edge point near the obtuse corner.

C.1 Interior Point Near a Free Edge (Refer to EQU. 11.4)

Utilizing the bending boundary condition (B-8.1) one obtains

$$U_{i-1,j+1} = \frac{\gamma}{\lambda_y^2}\left(w_{i-2,j+1} - 2\,w_{i-1,j+1} + w_{i,j+1}\right) \qquad \text{(C-1.1)}$$

$$U_{i,j+1} = \frac{\gamma}{\lambda_y^2}\left(w_{i-1,j+1} - 2\,w_{i,j+1} + w_{i+1,j+1}\right) \qquad \text{(C-1.2)}$$

$$U_{i+1,j+1} = \frac{\gamma}{\lambda_y^2}\left(w_{i,j+1} - 2\,w_{i+1,j+1} + w_{i+2,j+1}\right) \qquad \text{(c-1.3)}$$

Comparing equations (4.10d), (4.10f) and (4.10g) with the above equations, yields the following relations:

$$\frac{\beta}{2} D_y\left(-w_{i-2,j+2} + w_{i,j+2}\right) + D_y\, w_{i-1,j+2} = -D_y\, w_{i-1,j}$$
$$- \frac{\beta}{2} D_y\left(w_{i-2,j} - w_{i,j}\right) + 2(A + D_y - \gamma)\, w_{i-1,j+1}$$
$$+ (\gamma - A)\left(w_{i-2,j+1} + w_{i,j+1}\right) \qquad \text{(C-1.4)}$$

$$\frac{\beta}{2} D_y(-w_{i-1,j+2} + w_{i+1,j+2}) + D_y w_{i,j+2} = -D_y w_{i,j}$$

$$- \frac{\beta}{2} D_y(w_{i-1,j} - w_{i+1,j}) + 2(A + D_y - \gamma) w_{i,j+1}$$

$$+ (\gamma - A)(w_{i-1,j+1} + w_{i+1,j+1}) \qquad \text{(C-1.5)}$$

$$\frac{\beta}{2} D_y(-w_{i,j+2} + w_{i+2,j+2}) + D_y w_{i+1,j+2} = -D_y w_{i+1,j}$$

$$- \frac{\beta}{2} D_y(w_{i,j} - w_{i+2,j}) + 2(A + D_y - \gamma) w_{i+1,j+1}$$

$$+ (\gamma - A)(w_{i,j+1} + w_{i+2,j+1}) \qquad \text{(C-1.6)}$$

From the equations (C-1.4), (C-1.5) and (C-1.6) the following expression for an exterior point in terms of interior points can be deduced.

$$\beta^2 \frac{D_y}{4} (w_{i+2,j+2} + w_{i-2,j+2} - 2 w_{i,j+2})$$

$$+ \beta D_y(-w_{i-1,j+2} + w_{i+1,j+2}) + D_y w_{i,j+2}$$

$$= - D_y w_{i,j} + (\gamma - A)(w_{i-1,j+1} + w_{i+1,j+1})$$

$$+ 2(A + D_y - \gamma) w_{i,j+1} + \beta^2 \frac{D_y}{4} (w_{i-2,j} - 2w_{i,j} + w_{i+2,j})$$

$$+ \beta(A + D_y - \gamma)(w_{i+1,j+1} - w_{i-1,j+1})$$

$$+ \frac{\beta}{2} (\gamma - A)(w_{i+2,j+1} - w_{i-2,j+1}) \qquad \text{(C-1.7)}$$

Substituting the relations (C-1.7) into the general equilibrium equation at an interior point, i.e. EQU. 11.1, the equilibrium equation at an interior point near the free edge can be obtained. This is presented as a finite difference molecule in EQU. 11.4.

C.2 Interior Point Near an Acute Corner

Applying the relevant boundary conditions as deduced in equations (B-6.6) through (B-6.9) in conjunction with (C-1.4) through (C-1.6), the finite difference equations at an interior point near the acute corner is

obtained. This is presented as a finite difference molecule in EQU. 11.5.

C.3 Interior Point Near the Obtuse Corner

Following the same procedure as discussed in section C.2, difference equation at an interior point near the obtuse corner can be obtained which is presented as a finite difference molecule in EQU. 11.6.

C.4 General Free Edge Point (Refer to EQU. 11.7)

Neglecting the non-linear terms related to the stress function in the second of the equilibrium equations (4.3b), one obtains

$$\nabla\nabla w = U_{,xx} + U_{,yy} + DY_{,xx} = q(x,y) \qquad \text{(C-4.1)}$$

Following equation (4.6d), equation (C-4.1) reduces to

$$\frac{1}{\lambda_y^2}\left[\alpha(U_{i-1,j} + U_{i+1,j}) - 2(1+\alpha)\,U_{i,j}\right.$$

$$+ \frac{\beta}{2}\,(U_{i+1,j+1} - U_{i-1,j+1} + U_{i-1,j-1} - U_{i+1,j-1})$$

$$\left. + U_{i,j+1} + U_{i,j-1}\right] + D\,\frac{\varkappa^2}{\lambda_y^2}\left[Y_{i-1,j} - 2Y_{i,j} + Y_{i,j-1}\right]$$

$$= q(x,y) \qquad \text{(C-4.2)}$$

From the boundary condition (4.28a) at the free dge

$$M_y = - D_y \left(w_{,yy} + \nu_x w_{,xx}\right) = 0$$

one obtains:

$$(w_{,yy})_{edge} = - \nu_x (w_{,xx})_{edge}$$

or

$$Y_{i-1,j} = - \nu_x \frac{\varkappa^2}{\lambda_y^2} \left(w_{i-2,j} - 2 w_{i-1,j} + w_{i,j}\right)$$

$$Y_{i,j} = - \nu_x \frac{\varkappa^2}{\lambda_y^2} \left(w_{i-1,j} - 2 w_{i,j} + w_{i+1,j}\right) \qquad \text{(C-4.3)}$$

$$Y_{i+1,j} = - \nu_x \frac{\varkappa^2}{\lambda_y^2} \left(w_{i,j} - 2 w_{i+1,j} + w_{i+2,j}\right)$$

From the boundary condition (4.28b) at the free edge, one can deduce:

$$D_y \frac{\partial^3 w}{\partial y^3} + (2H - D_x \nu_y) \frac{\partial^3 w}{\partial x^2 \partial y} = 0 \qquad \text{(C-4.4)}$$

Since $$U = D_x \frac{\partial^2 w}{\partial x^2} + D_y \frac{\partial^2 w}{\partial y^2}$$

$$\frac{\partial U}{\partial y} = D_x \frac{\partial^3 w}{\partial x^2 \partial y} + D_y \frac{\partial^3 w}{\partial y^3} \qquad \text{(C-4.5)}$$

Equation (C-4.4) can now be written as

$$\frac{\partial U}{\partial y} + (2H - D_{xy} - D_x)\frac{\partial^3 w}{\partial x^2 \partial y} = 0 \qquad (C\text{-}4.6)$$

Let K(x,y) be a function of x and y. From the general edge point, a perpendicular is drawn parallel to the y-axis touching the network point t and s, respectively (EQU. 11.7). Hence $b_1 = \lambda_y \tan\phi$.

At point (i,j); Fig.C.1

$$\left(\frac{\partial K}{\partial y}\right)_{i,j} = \frac{K_t - K_s}{2\lambda_y}$$

By interpolation (Ref. 20)

$$K_t = K_{i,j+1} + \frac{K_{i+1,j+1} - K_{i-1,j+1}}{2\lambda_x}\chi$$

$$\lambda_y \tan\phi = K_{i,j+1} + \tfrac{1}{2}\beta\,(K_{i+1,j+1} - K_{i-1,j+1})$$

Similarly,

$$K_s = K_{i,j-1} - \tfrac{1}{2}\beta\,(K_{i+1,j-1} - K_{i-1,j-1})$$

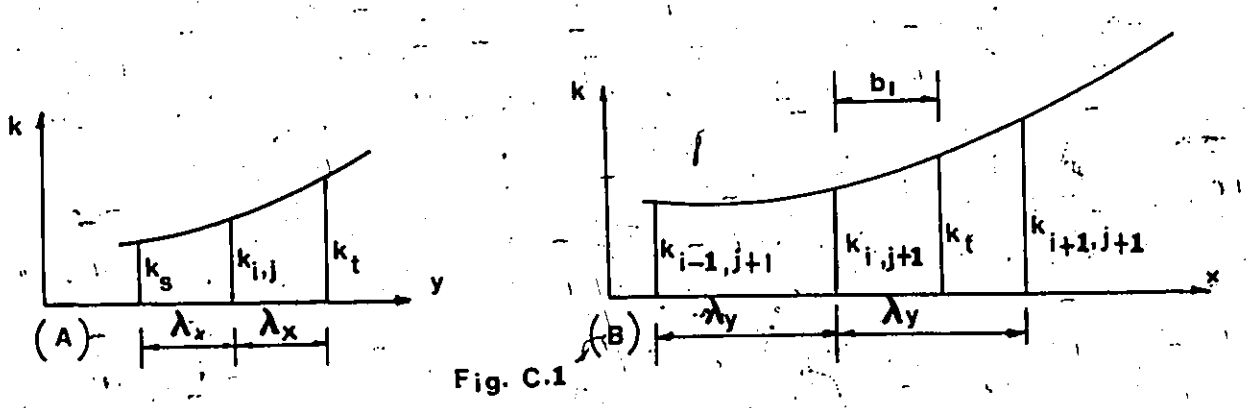

Fig. C.1

Hence

$$\left(\frac{\partial K}{\partial y}\right)_{i,j} = \frac{1}{2\lambda_y}\left[\left\{K_{i,j+1} + \tfrac{1}{2}\beta\,(K_{i+1,j+1} - K_{i-1,j+1})\right\}\right.$$

$$\left. - \left\{K_{i,j-1} - \tfrac{1}{2}\beta\,(K_{i+1,j-1} - K_{i-1,j-1})\right\}\right]$$

Following the same procedure, for the function U, one can deduce:

$$\left(\frac{\partial U}{\partial y}\right)_{i,j} = \frac{1}{2\lambda_y}\left[\left\{U_{i,j+1} + \tfrac{1}{2}\beta\,(U_{i+1,j+1} - U_{i-1,j+1})\right\}\right.$$

$$\left. - \left\{U_{i,j-1} - \tfrac{1}{2}\beta\,(U_{i+1,j-1} - U_{i-1,j-1})\right\}\right] \qquad \text{(C-4.7)}$$

Similarly,

$$\left\{\frac{\partial^3 w}{\partial x^2 \partial y}\right\}_{i,j} = \left\{\frac{\partial}{\partial y}\left(\frac{\partial^2 w}{\partial x^2}\right)\right\}_{i,j}$$

$$= \frac{\partial}{\partial y}\left\{\frac{\varkappa^2}{\lambda_y^2}\left(w_{i-1,j} - 2\,w_{i,j} + w_{i+1,j}\right)\right\}$$

$$= \frac{\varkappa^2}{2\lambda_y^3}\left[\left\{w_{i-1,j+1} + \tfrac{1}{2}\beta\left(w_{i,j+1} - w_{i-2,j+1}\right)\right\}\right.$$

$$- \left\{w_{i-1,j-1} - \tfrac{1}{2}\beta\left(w_{i,j-1} - w_{i-2,j-1}\right)\right\}$$

$$- 2\left\{w_{i,j+1} + \tfrac{1}{2}\beta\left(w_{i+1,j+1} - w_{i-1,j+1}\right)\right\}$$

$$+ 2\left\{w_{i,j-1} - \tfrac{1}{2}\beta\left(w_{i+1,j-1} - w_{i-1,j-1}\right)\right\}$$

$$+ \left\{w_{i+1,j+1} + \tfrac{1}{2}\beta\left(w_{i+2,j+1} - w_{i,j+1}\right)\right\}$$

$$\left. - \left\{w_{i+1,j-1} - \tfrac{1}{2}\beta\left(w_{i+2,j-1} - w_{i,j-1}\right)\right\}\right] \qquad \text{(C-4.8)}$$

Comparing equation (C-4.6) and (C-4.8) and substituting the relations (C-1.1) through (C-1.6) into equation (C-4.1), and after a few albegraic operations, the equation for the general edge point is obtained in finite difference molecule form EQU. 11.

C-5 Edge Point Near an Acute Corner (Refer to EQU. 11.8)

From the boundary conditions of section (B-1) and (C-4) it follows that:

$$w_{i-1,j} = w_{i-1,j-1} = w_{i-1,j-2} = 0 \qquad \text{(C-5.1)}$$

$$w_{i-2,j} = K_y \frac{\beta}{\delta} (w_{i,j-1} - w_{i,j+1}) - K_y \frac{1}{\delta} w_{i-1,j+1} - w_{i,j} \qquad \text{(C-5.2)}$$

$$w_{i-2,j-2} = K_y \frac{\beta}{\delta} (w_{i,j-1} - w_{i,j+1}) - K_y \frac{1}{\delta} w_{i-1,j+1} - w_{i,j-2} \qquad \text{(C-5.3)}$$

$$w_{i-2,j-1} = K_y \frac{\beta}{\delta} (w_{i,j-2} - w_{i,j}) - w_{i,j-1} \qquad \text{(C-5.4)}$$

$$w_{i-2,j+1} = K_y \frac{\beta}{\delta} (w_{i,j-2} - w_{i,j}) - w_{i,j+1} \qquad \text{(C-5.5)}$$

From the equation (C-1.1) and the relation

$$w_{i-2,j+1} = - w_{i,j+1} + w_{i-2,j-1} + w_{i,j-1} \qquad \text{(C-5.6)}$$

one can deduce

$$\beta\, w_{i,j+1} + w_{i-1,j+1} - \frac{(\gamma-A)}{D_y}\, w_{i-2,j}$$

$$= \beta\, w_{i,j-1} + \frac{\gamma-A}{D_y}\, w_{i,j} \qquad \text{(C-5.7)}$$

Comparing equations (C-5.2) and (C-5.7) it can be shown that

$$w_{i-2,j} = - w_{i,j}$$

Substituting these values into EQU. (10.7), the finite difference equation at an edge point near the acute corner is obtained. This is presented as a finite difference molecule in EQU. 11.8.

C-6 Edge Point Near the Obtuse Corner (Refer to EQU. 11.9)

Following the same procedure as in section C-5, the finite difference equation of an edge point near the obtuse corner is obtained. This is presented as a finite difference molecule in EQU. 11.9.

CHAPTER 10

Finite Difference Molecules for Compability and Equilibrium Equation.

Non-Linear (Large-Deflection) Theory

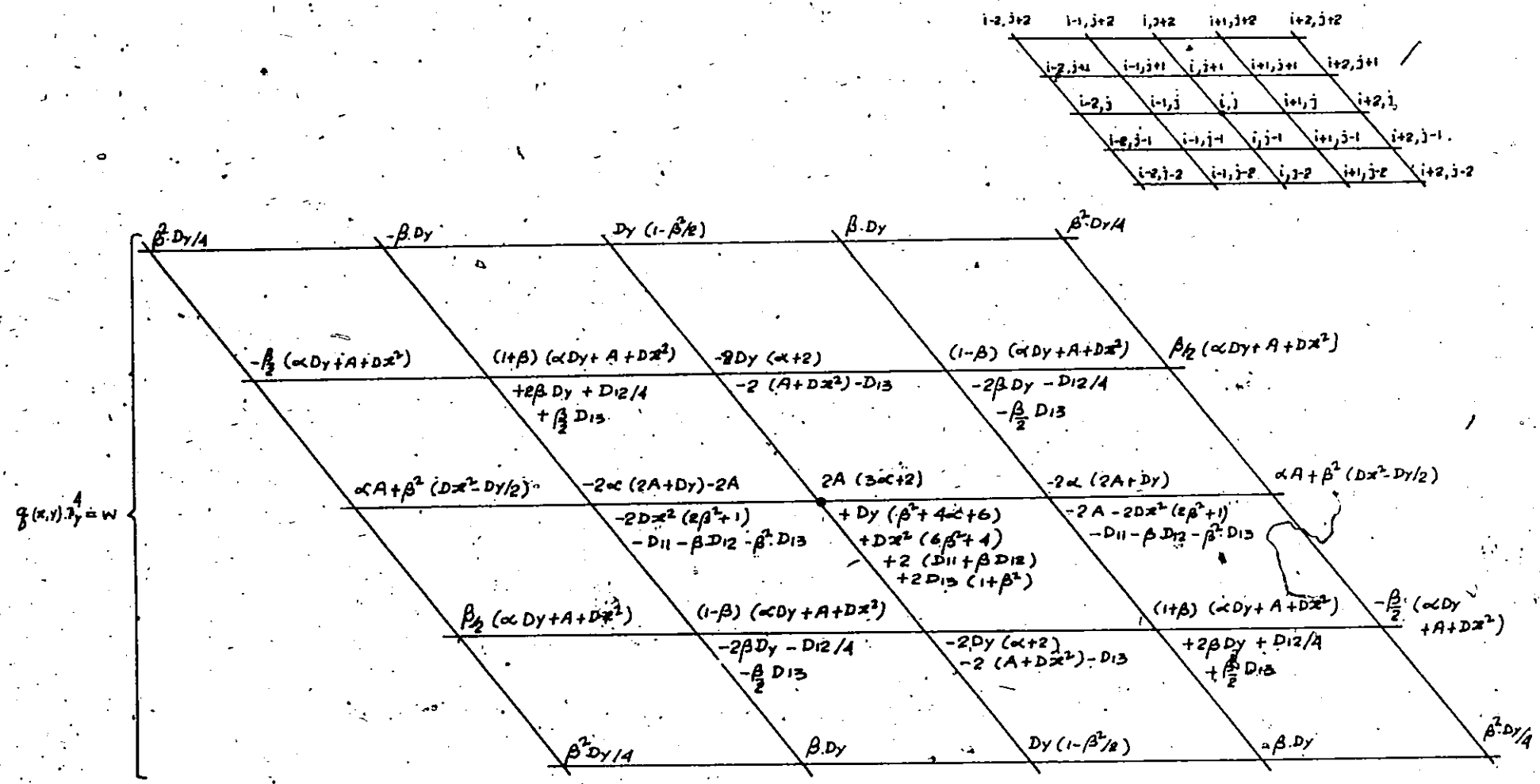

Where $(D_{11})_{i,j} = t\alpha^2\{\beta^2(F_{i-1,j} + F_{i+1,j}) - 2(1+\beta^2)F_{i,j} + \frac{\beta}{2}(F_{i+1,j+1} - F_{i-1,j+1} + F_{i-1,j-1} - F_{i+1,j-1}) + F_{i,j+1} + F_{i,j-1}\}$

$(D_{12})_{i,j} = -2t\alpha^2\{\beta(F_{i-1,j} - 2F_{i,j} + F_{i+1,j}) + \frac{1}{4}(F_{i+1,j+1} - F_{i-1,j+1} + F_{i-1,j-1} - F_{i+1,j-1})\}$

$(D_{13})_{i,j} = t\alpha^2(F_{i-1,j} - 2F_{i,j} + F_{i+1,j})$

EQU. 10.1 EQUILIBRIUM FINITE DIFFERENCE EQUATION AT GENERAL INTERIOR POINT

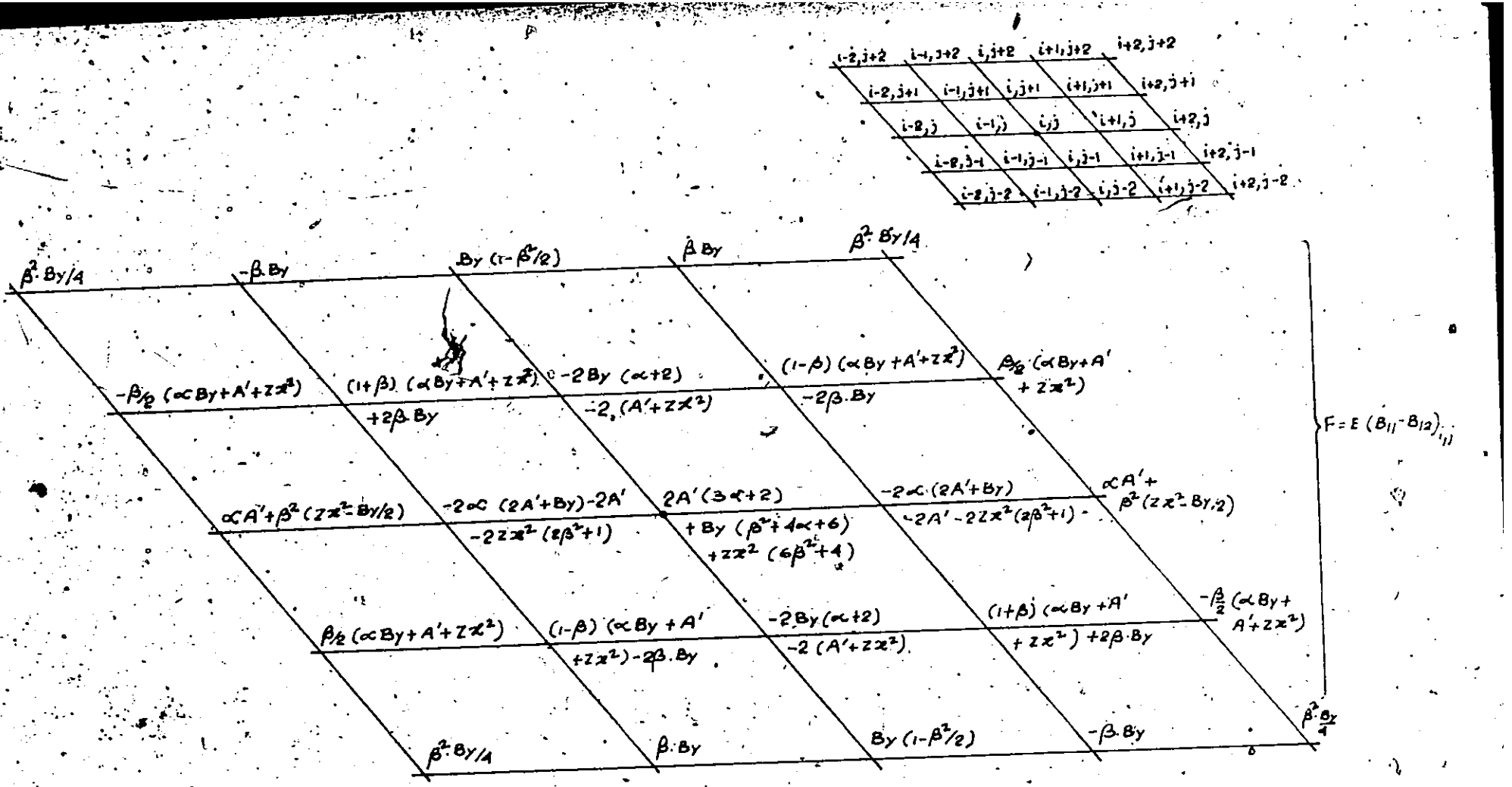

Where

$$(B_{11})_{i,j} = x^2\left\{\beta\left(w_{i-1,j} - 2w_{i,j} + w_{i+1,j}\right) + \tfrac{1}{4}\left(w_{i+1,j+1} - w_{i-1,j+1} + w_{i-1,j-1} - w_{i+1,j-1}\right)\right\}$$

$$(B_{12})_{i,j} = x^2\left(w_{i-1,j} - 2w_{i,j} + w_{i+1,j}\right)\left\{\beta^2\left(w_{i-1,j} + w_{i+1,j}\right) - 2\left(1+\beta^2\right)w_{i,j} + \beta/2\left(w_{i+1,j+1} - w_{i-1,j+1} + w_{i-1,j-1} - w_{i+1,j-1}\right) + w_{i,j+1} + w_{i,j-1}\right\}$$

EQU. 10.2 COMPATIBILITY FINITE DIFFERENCE EQUATION AT GENERAL INTERIOR POINT

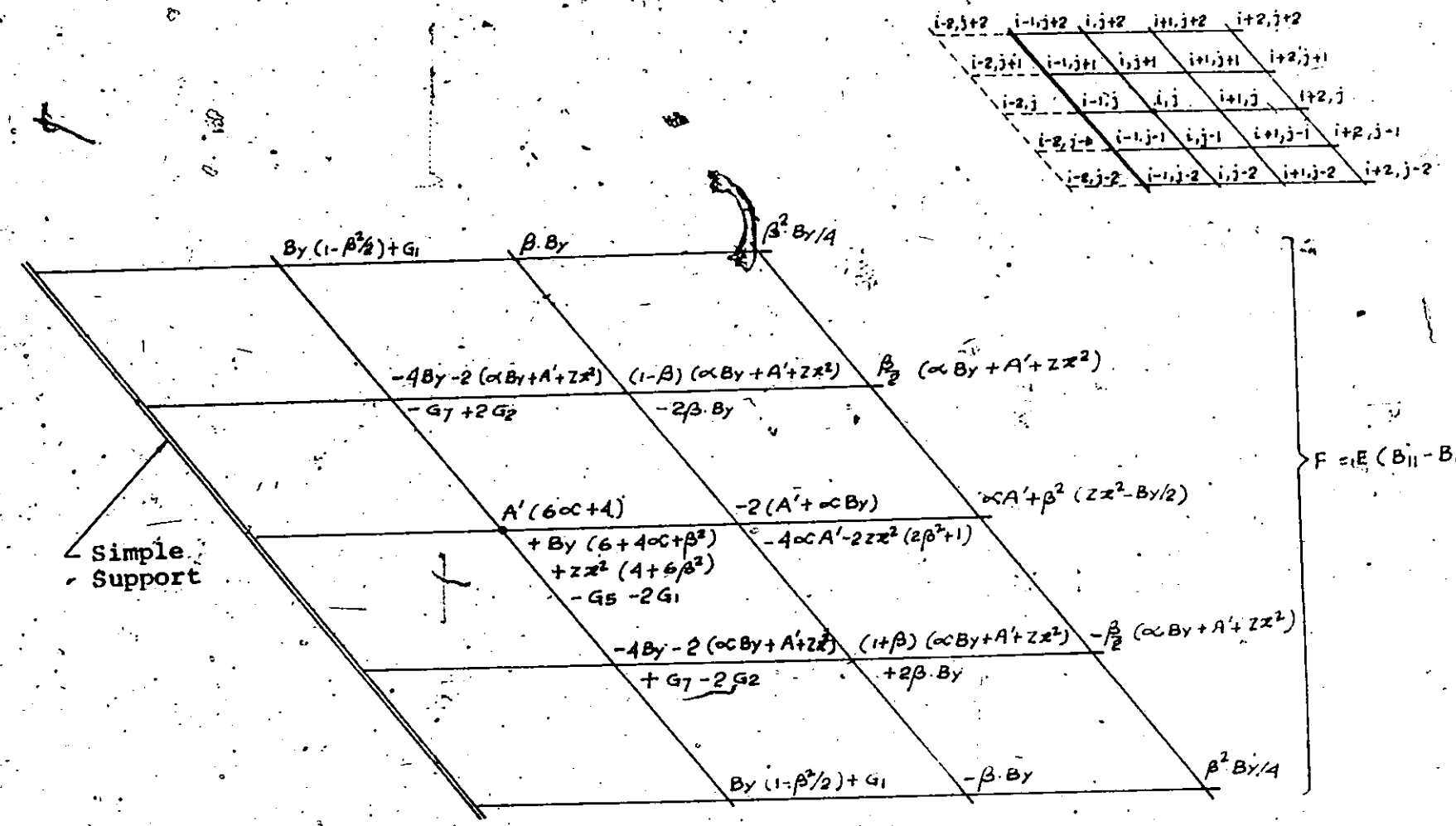

Where

$$(B_{11})_{i,j} = x^2\left\{\beta\,(-2\,W_{i,j} + W_{i+1,j}) + \tfrac{1}{4}\,(W_{i+1,j+1} - W_{i+1,j-1})\right\}$$

$$(B_{12})_{i,j} = x^2(-2\,W_{i,j} + W_{i+1,j})\left\{\beta^2 W_{i+1,j} - 2\,(1+\beta^2)\,W_{i,j} + \beta_2\,(W_{i+1,j+1} - W_{i+1,j-1}) + W_{i,j+1} + W_{i,j-1}\right\}$$

EQU. 10.3 COMPATIBILITY FINITE DIFFERENCE EQUATION AT INTERIOR POINT NEAR LEFT SIMPLE SUPPORT

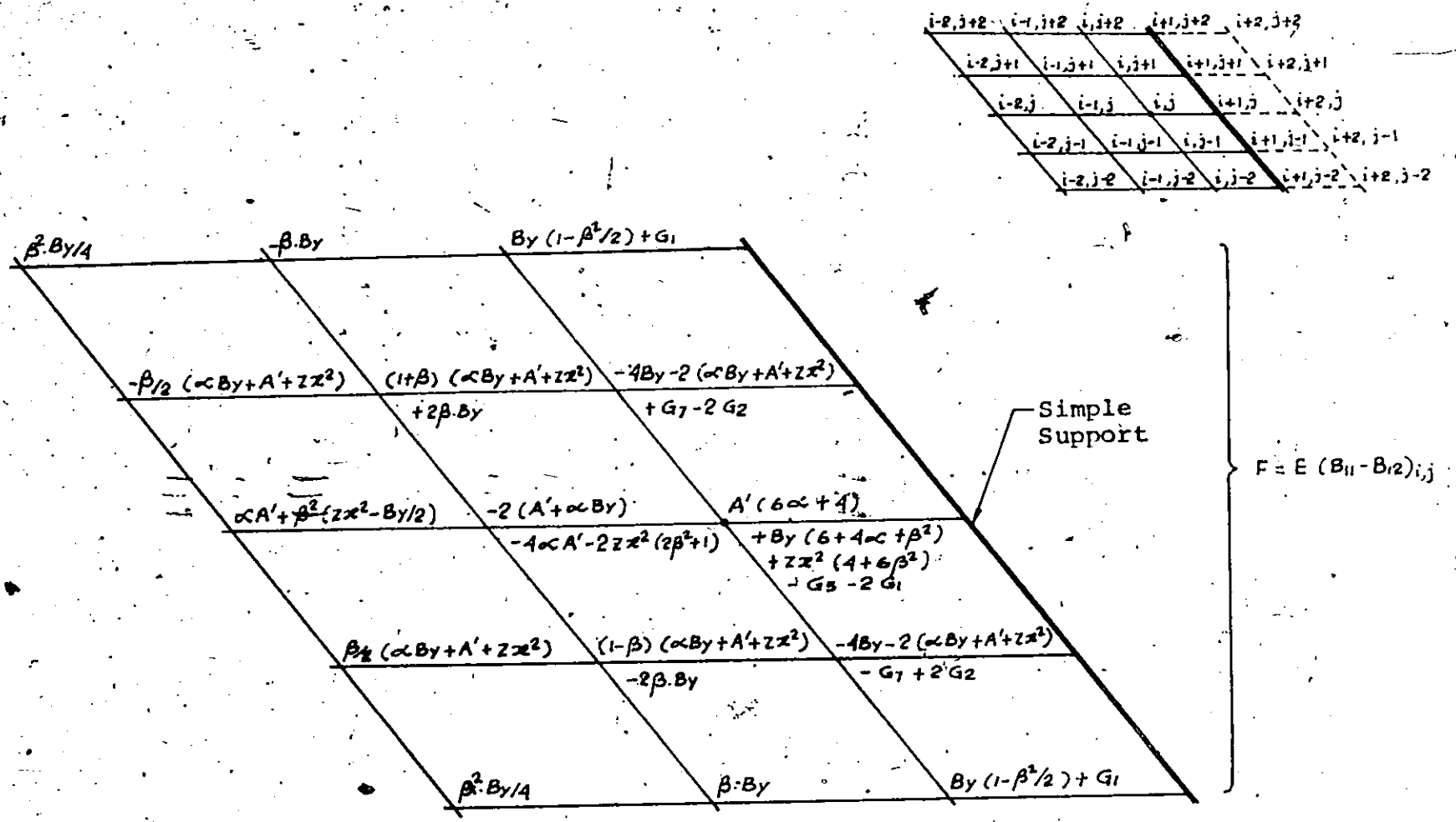

Where

$$(B_{11})_{i,j} = x^2\left\{\beta\,(w_{i-1,j} - 2w_{i,j}) + \tfrac{1}{4}\,(-w_{i-1,j+1} + w_{i-1,j-1})\right\}$$

$$(B_{12})_{i,j} = x^2(w_{i-1,j} - 2w_{i,j})\left\{\beta^2 w_{i-1,j} - 2(1+\beta^2)\,w_{i,j} + \beta/2\,(-w_{i-1,j+1} + w_{i-1,j-1}) + w_{i,j+1} + w_{i,j-1}\right\}$$

EQU. 10.4 COMPATIBILITY FINITE DIFFERENCE EQUATION AT INTERIOR POINT NEAR RIGHT SIMPLE SUPPORT

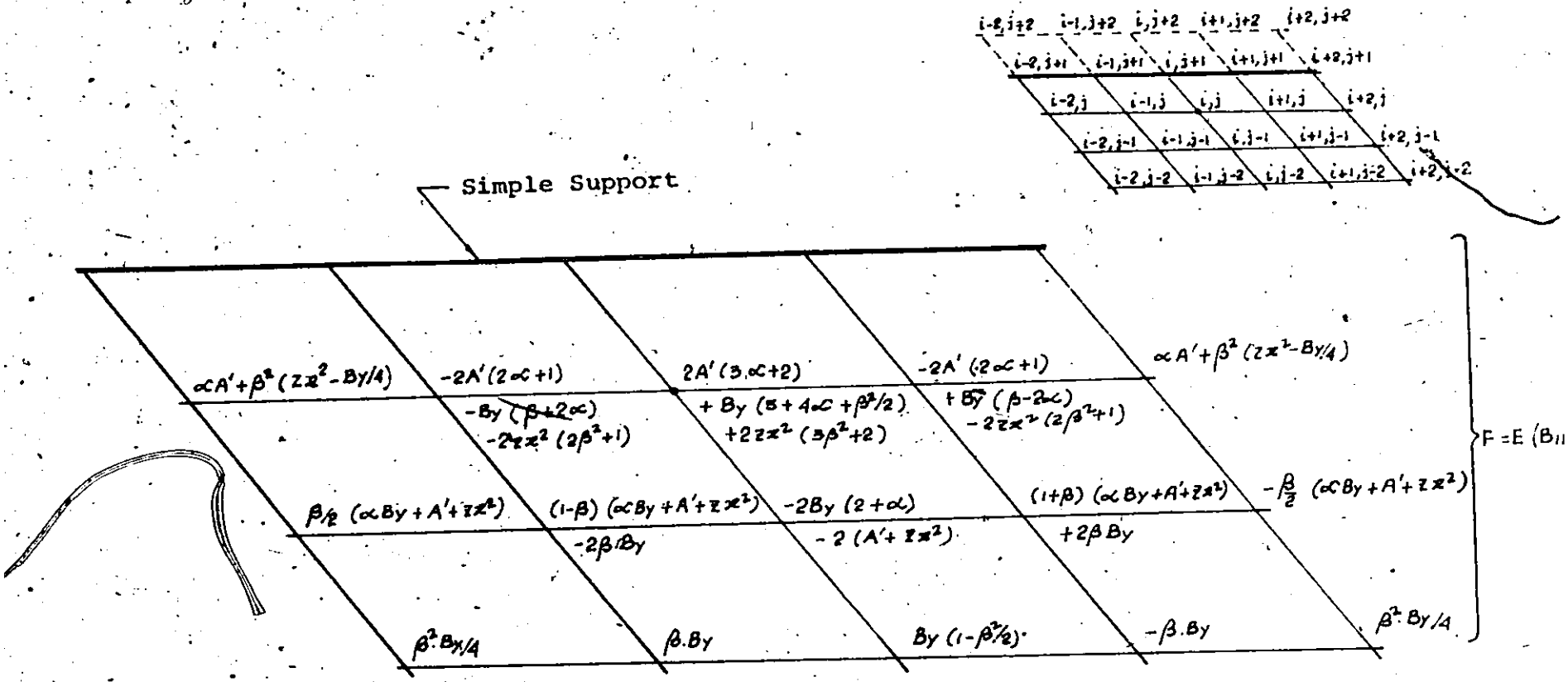

Where $(B_{11})_{i,j} = x^2\left\{\beta(W_{i-1,j} - 2W_{i,j} + W_{i+1,j}) + \tfrac{1}{4}(W_{i-1,j-1} - W_{i+1,j-1})\right\}$

$(B_{12})_{i,j} = x^2(W_{i-1,j} - 2W_{i,j} + W_{i+1,j})\left\{\beta^2(W_{i-1,j} + W_{i+1,j}) - 2(1+\beta^2)W_{i,j} + \frac{\beta}{2}(W_{i-1,j-1} - W_{i+1,j-1}) + W_{i,j-1}\right\}$

EQU. 10.5 COMPATIBILITY FINITE DIFFERENCE EQUATION AT INTERIOR POINT NEAR EDGE SUPPORT.

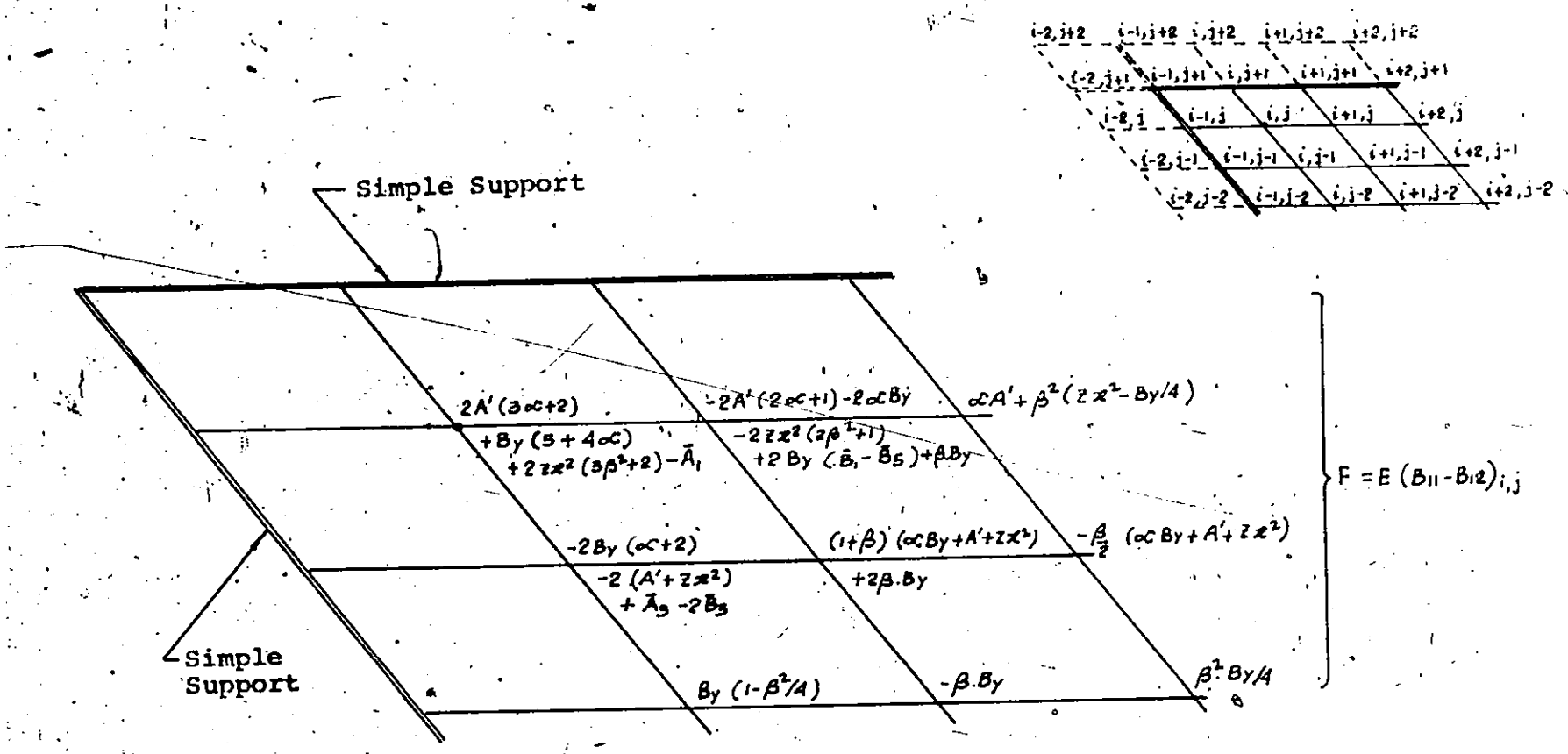

Where $(B_{11})_{i,j} = x^2\left\{\beta(-2W_{i,j} + W_{i+1,j}) + \frac{1}{4}(-W_{i+1,j-1})\right\}$

$(B_{12})_{i,j} = x^2\left(-2W_{i,j} + W_{i+1,j}\right)\left\{\beta^2 W_{i+1,j} - 2(1+\beta^2)W_{i,j} + \frac{\beta}{2}(-W_{i+1,j-1}) + W_{i,j-1}\right\}$

EQU. 10.6 COMPATIBILITY FINITE DIFFERENCE EQUATION AT INTERIOR POINT NEAR ACUTE CORNER..

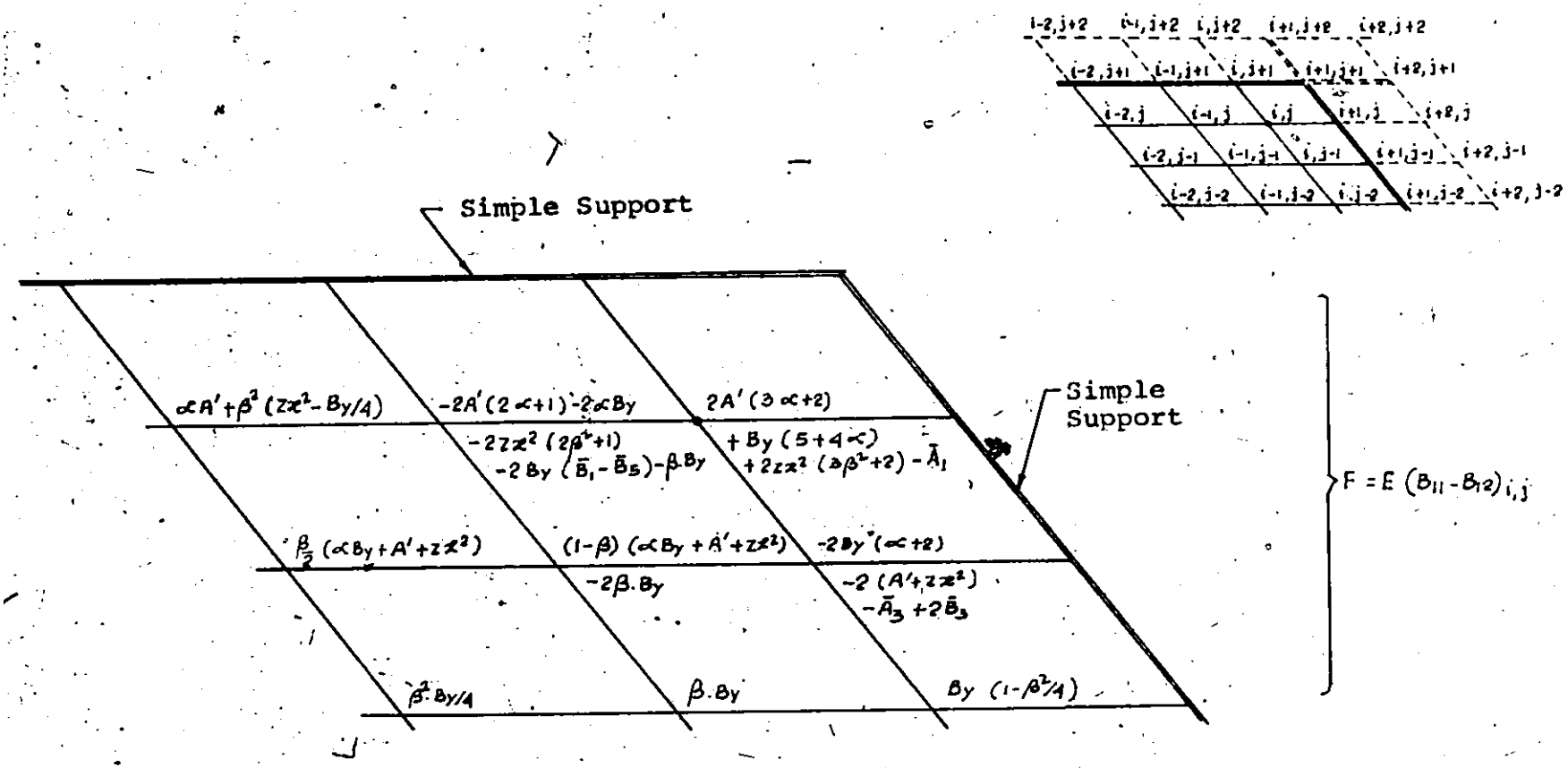

Where $(B_{11})_{i,j} = \alpha^2 \left\{ \beta (w_{i-1,j} - 2w_{i,j}) + \frac{1}{4} w_{i-1,j-1} \right\}$

$(B_{12})_{i,j} = \alpha^2 (w_{i-1,j} - 2w_{i,j}) \left\{ \beta^2 w_{i-1,j} - 2(1+\beta^2) w_{i,j} + \frac{\beta}{2} w_{i-1,j-1} + w_{i,j-1} \right\}$

EQU. 10.7 COMPATIBILITY FINITE DIFFERENCE EQUATION AT INTERIOR POINT NEAR OBTUSE CORNER

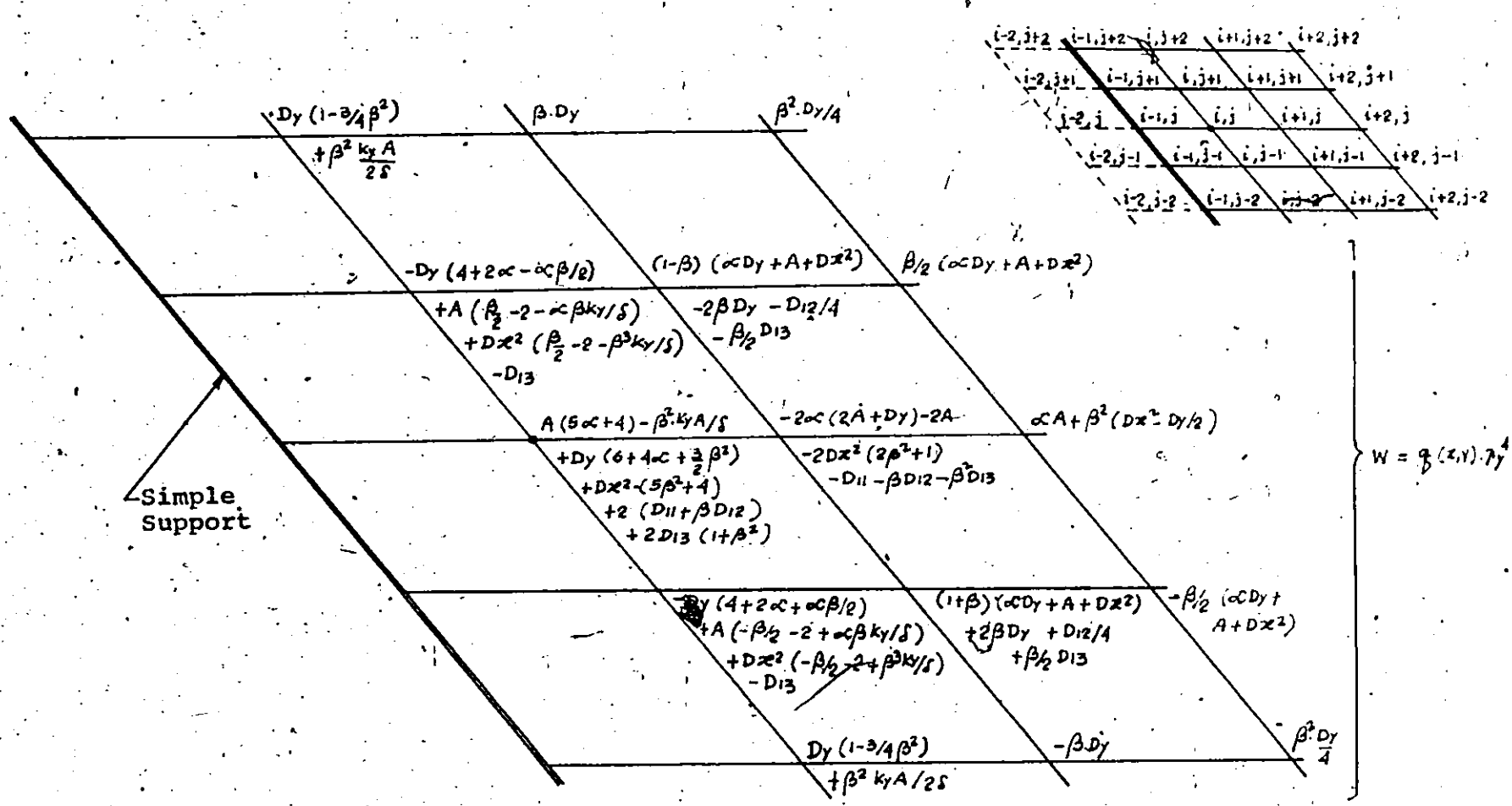

Where

$$(D_{11})_{i,j} = t\Delta x^2 \left\{ \beta^2 F_{i+1,j} - 2(1+\beta^2) F_{i,j} + \frac{\beta}{2} (F_{i+1,j+1} - F_{i+1,j-1}) + F_{i,j+1} + F_{i,j-1} \right\}$$

$$(D_{12})_{i,j} = -2t\Delta x^2 \left\{ \beta (-2F_{i,j} + F_{i+1,j}) + \tfrac{1}{4} (F_{i+1,j+1} - F_{i+1,j-1}) \right\}$$

$$(D_{13})_{i,j} = t\Delta x^2 (-2F_{i,j} + F_{i+1,j})$$

EQU. 10.8 EQUILIBRIUM FINITE DIFFERENCE EQUATION AT INTERIOR POINT NEAR LEFT SIMPLE SUPPORT

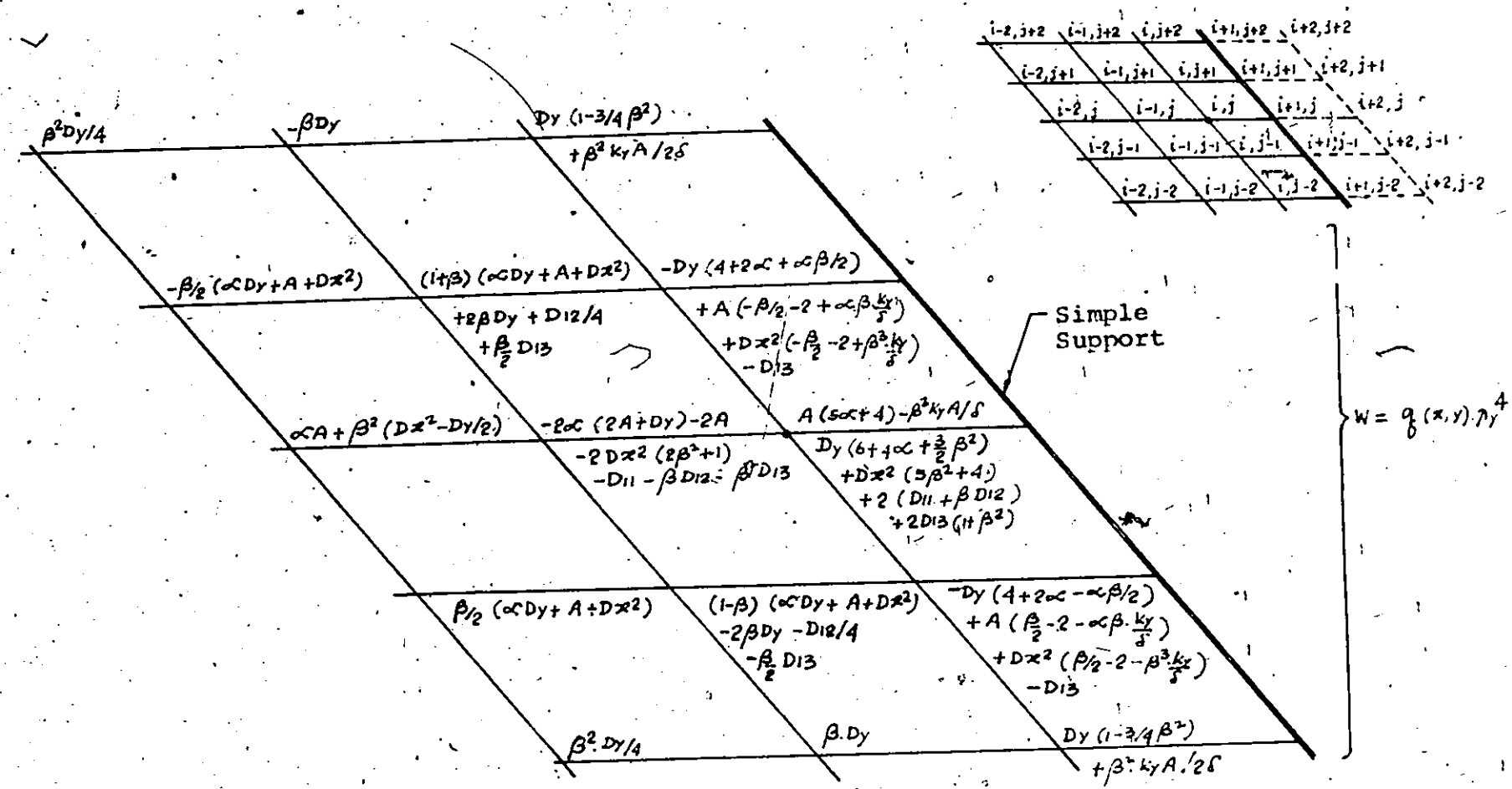

Where,

$$(D_{11})_{i,j} = t x^2 \left\{ \beta^2 F_{i-1,j} - 2(1+\beta^2) F_{i,j} + \frac{\beta}{2} (-F_{i-1,j+1} + F_{i-1,j-1}) + F_{i,j+1} + F_{i,j-1} \right\}$$

$$(D_{12})_{i,j} = -2 t x^2 \left\{ \beta (F_{i-1,j} - 2F_{i,j}) + 1/4 (-F_{i-1,j+1} + F_{i-1,j-1}) \right\}$$

$$(D_{13})_{i,j} = t x^2 (F_{i-1,j} - 2F_{i,j})$$

EQU. 10.9 EQUILIBRIUM FINITE DIFFERENCE EQUATION AT INTERIOR POINT NEAR RIGHT SIMPLE SUPPORT.

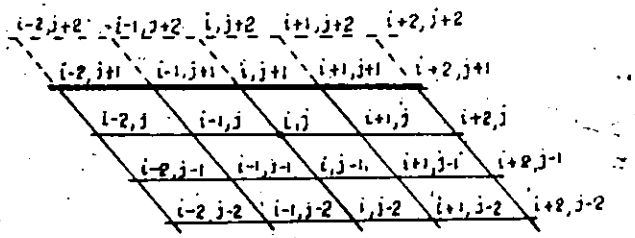

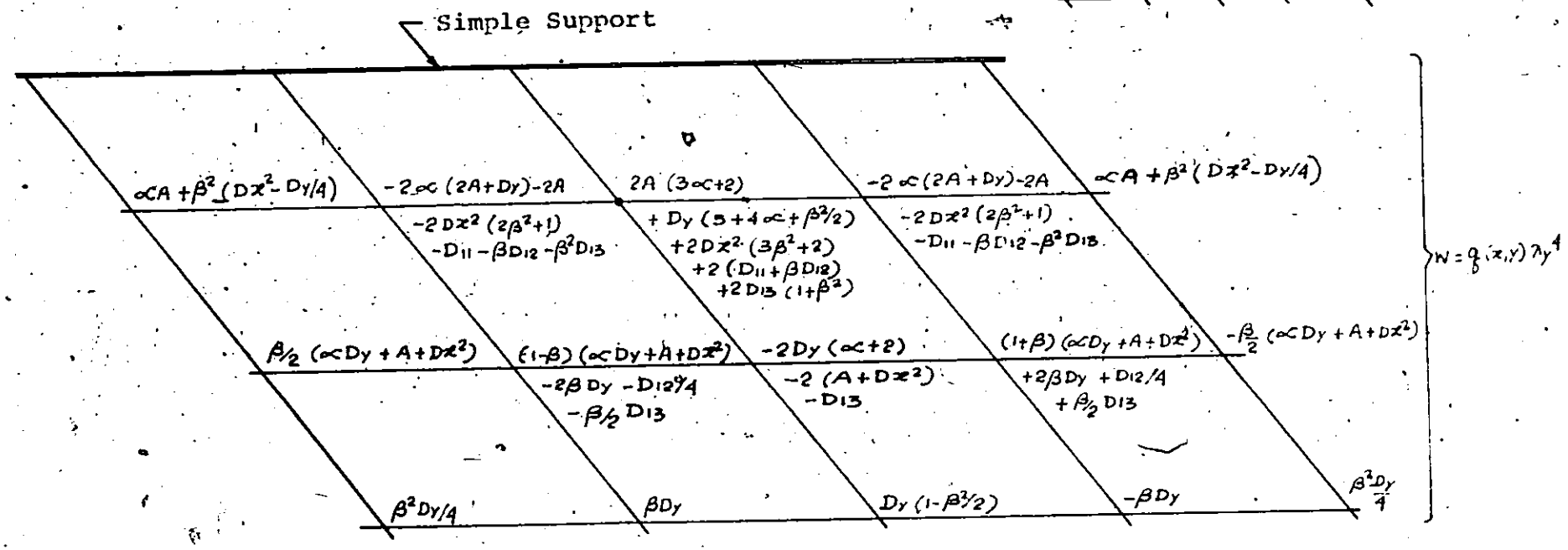

Where

$$(D_{11})_{i,j} = tx^2\left\{\beta^2(F_{i-1,j}+F_{i+1,j}) - 2(1+\beta^2)F_{i,j} + \frac{\beta}{2}(F_{i-1,j-1} - F_{i+1,j-1}) + F_{i,j-1}\right\}$$

$$(D_{12})_{i,j} = -2tx^2\left\{\beta(F_{i-1,j} - 2F_{i,j} + F_{i+1,j}) + \frac{1}{4}(F_{i-1,j-1} - F_{i+1,j-1})\right\}$$

$$(D_{13})_{i,j} = tx^2\left(F_{i-1,j} - 2F_{i,j} + F_{i+1,j}\right)$$

EQU. 10.10 EQUILIBRIUM FINITE DIFFERENCE EQUATION AT INTERIOR POINT NEAR THE EDGE PARALLEL TO X-AXIS.

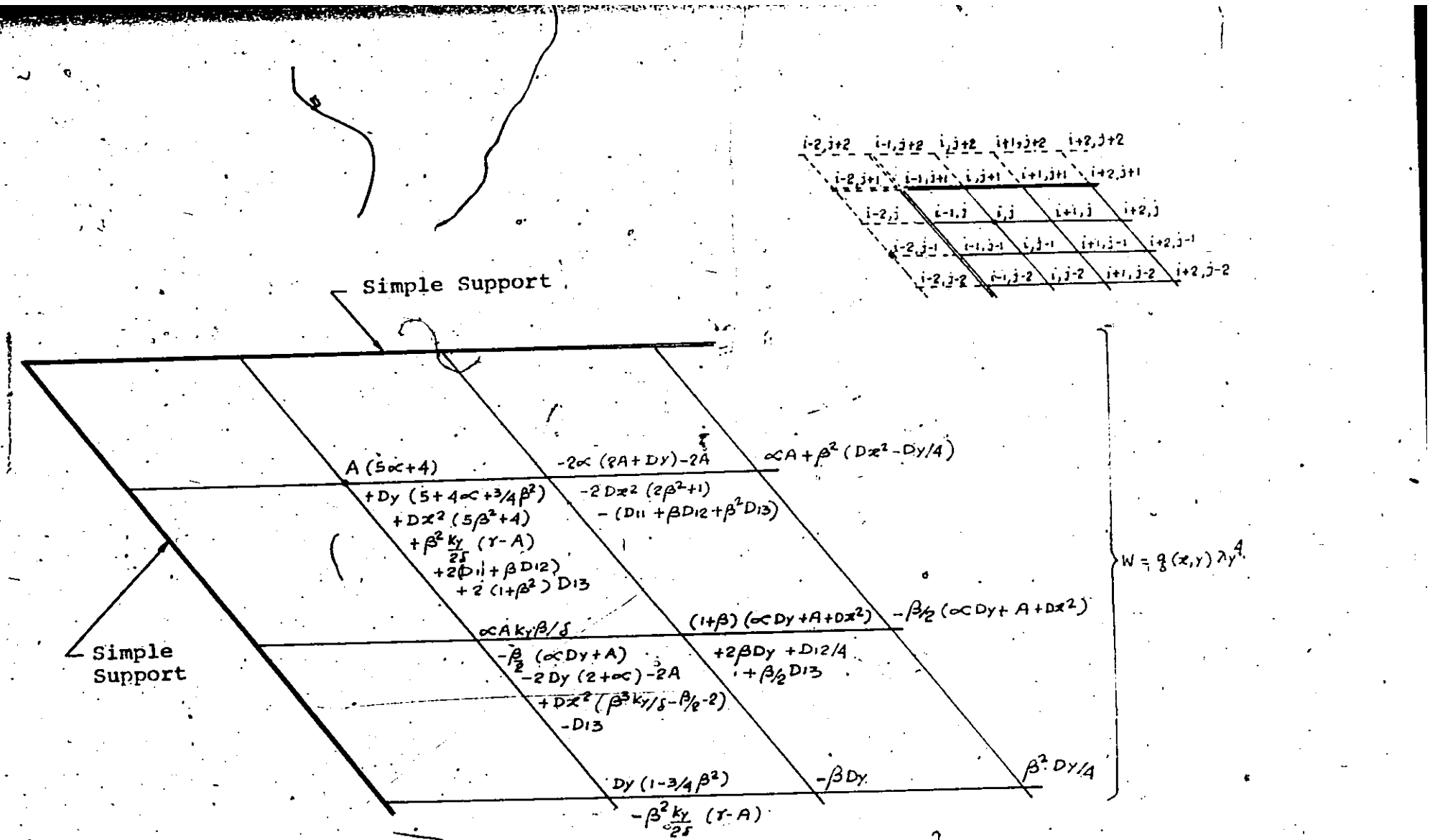

Where
$$(D_{11})_{i,j} = tx^2\left\{\beta^2 F_{i+1,j} - 2(1+\beta^2)F_{i,j} + \frac{\beta}{2}(-F_{i+1,j-1}) + F_{i,j-1}\right\}$$
$$(D_{12})_{i,j} = -2tx^2\left\{\beta(-2F_{i,j} + F_{i+1,j}) + \tfrac{1}{4}(-F_{i+1,j-1})\right\}$$
$$(D_{13})_{i,j} = tx^2(-2F_{i,j} + F_{i+1,j})$$

EQU. 10.11 EQUILIBRIUM FINITE DIFFERENCE EQUATION AT INTERIOR POINT NEAR ACUTE CORNER

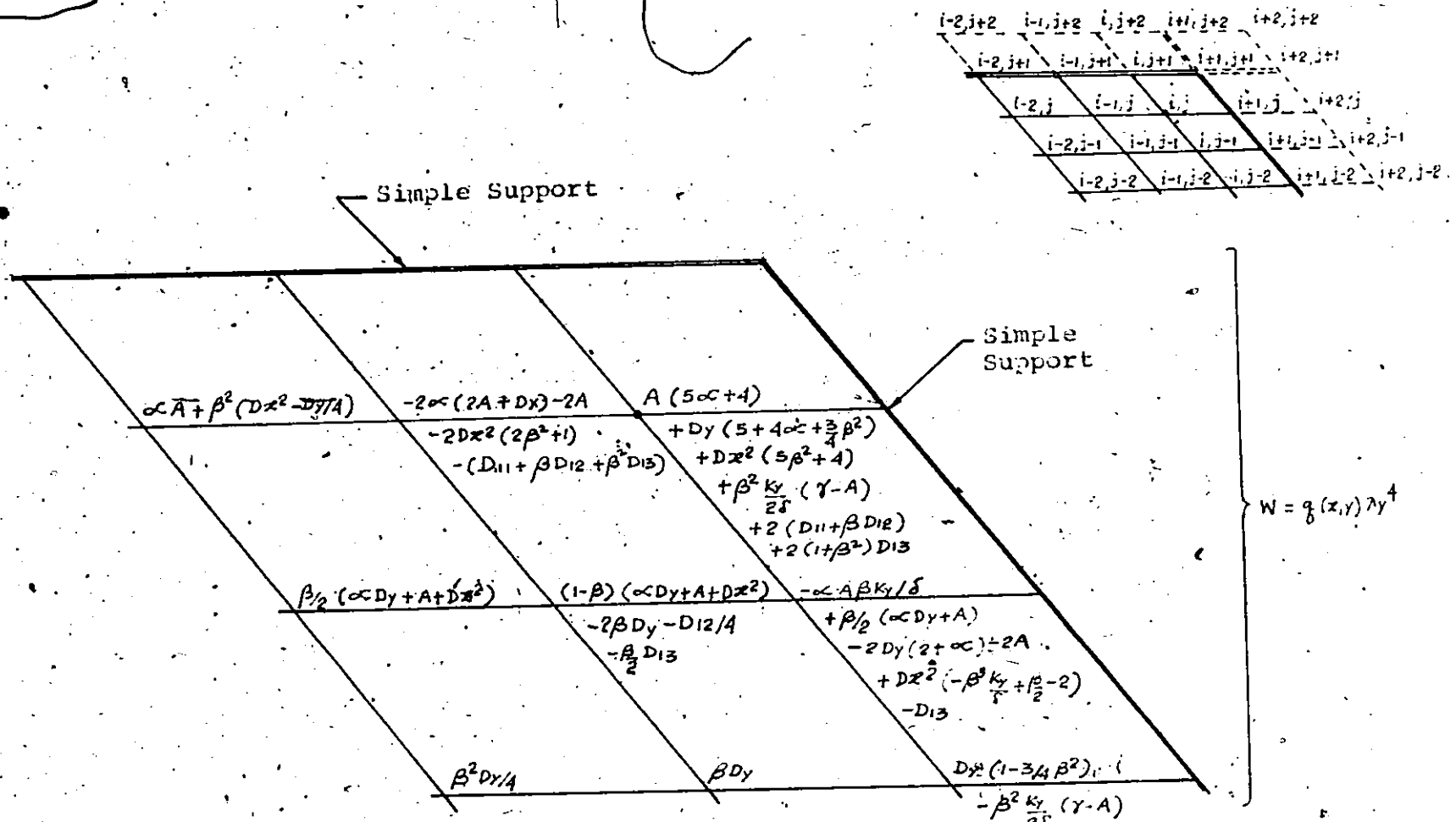

Where:

$$(D_{11})_{i,j} = tx^2\left\{\beta^2 F_{i-1,j} - 2(1+\beta^2)F_{i,j} + \frac{\beta}{2}F_{i-1,j-1} + F_{i,j-1}\right\}$$

$$(D_{12})_{i,j} = -2tx^2\left\{\beta(F_{i-1,j} - 2F_{i,j}) + \tfrac{1}{4}F_{i-1,j-1}\right\}$$

$$(D_{13})_{i,j} = tx^2(F_{i-1,j} - 2F_{i,j})$$

EQU. 10.12 EQUILIBRIUM FINITE DIFFERENCE EQUATION AT INTERIOR POINT NEAR OBTUSE CORNER.

CHAPTER 11

Finite Difference Molecules for Equilibrium Equation.

Linear (Small-Deflection) Theory.

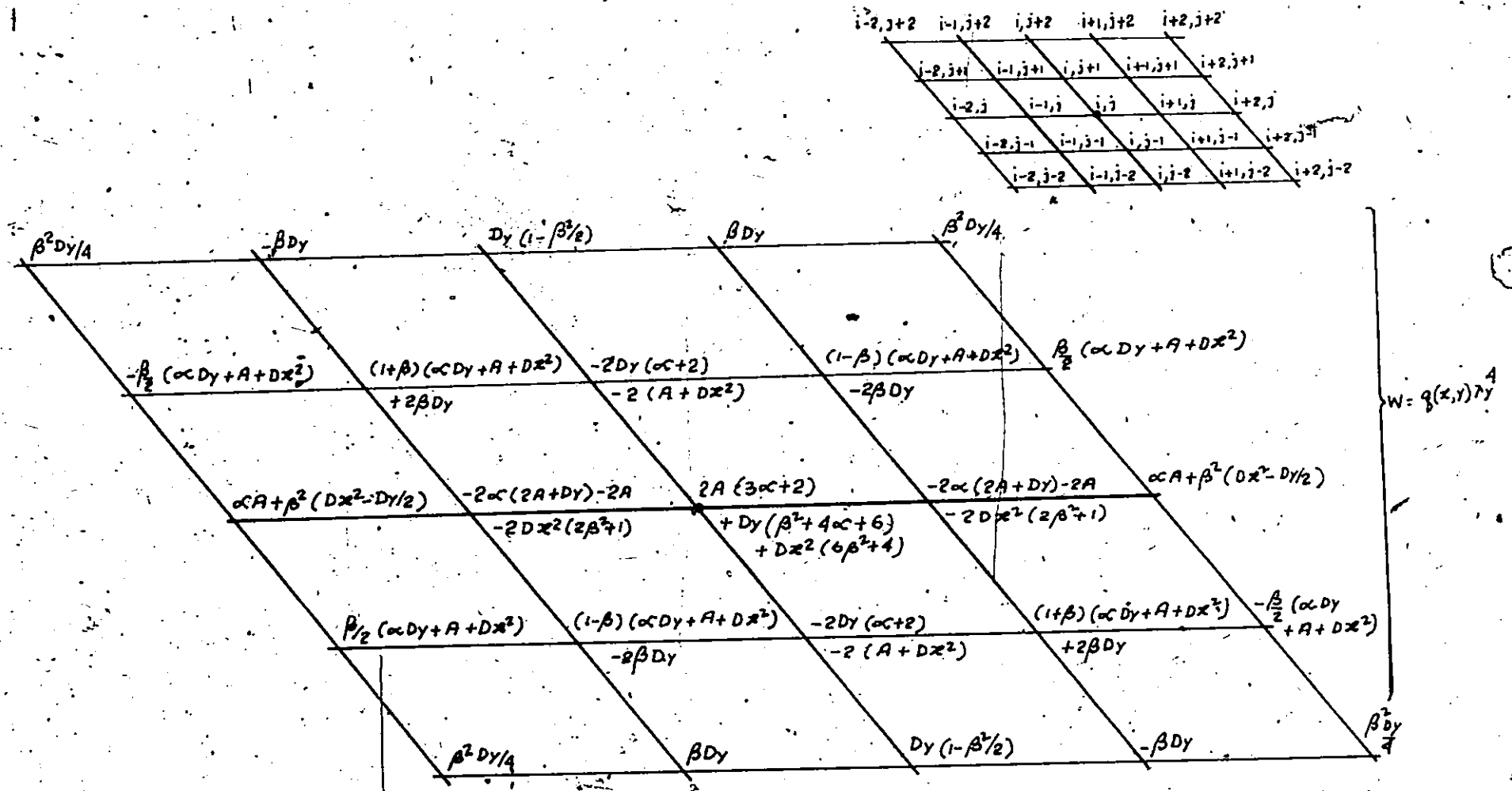

EQU. 11.1 FINITE DIFFERENCE EQUATION AT GENERAL INTERIOR POINT

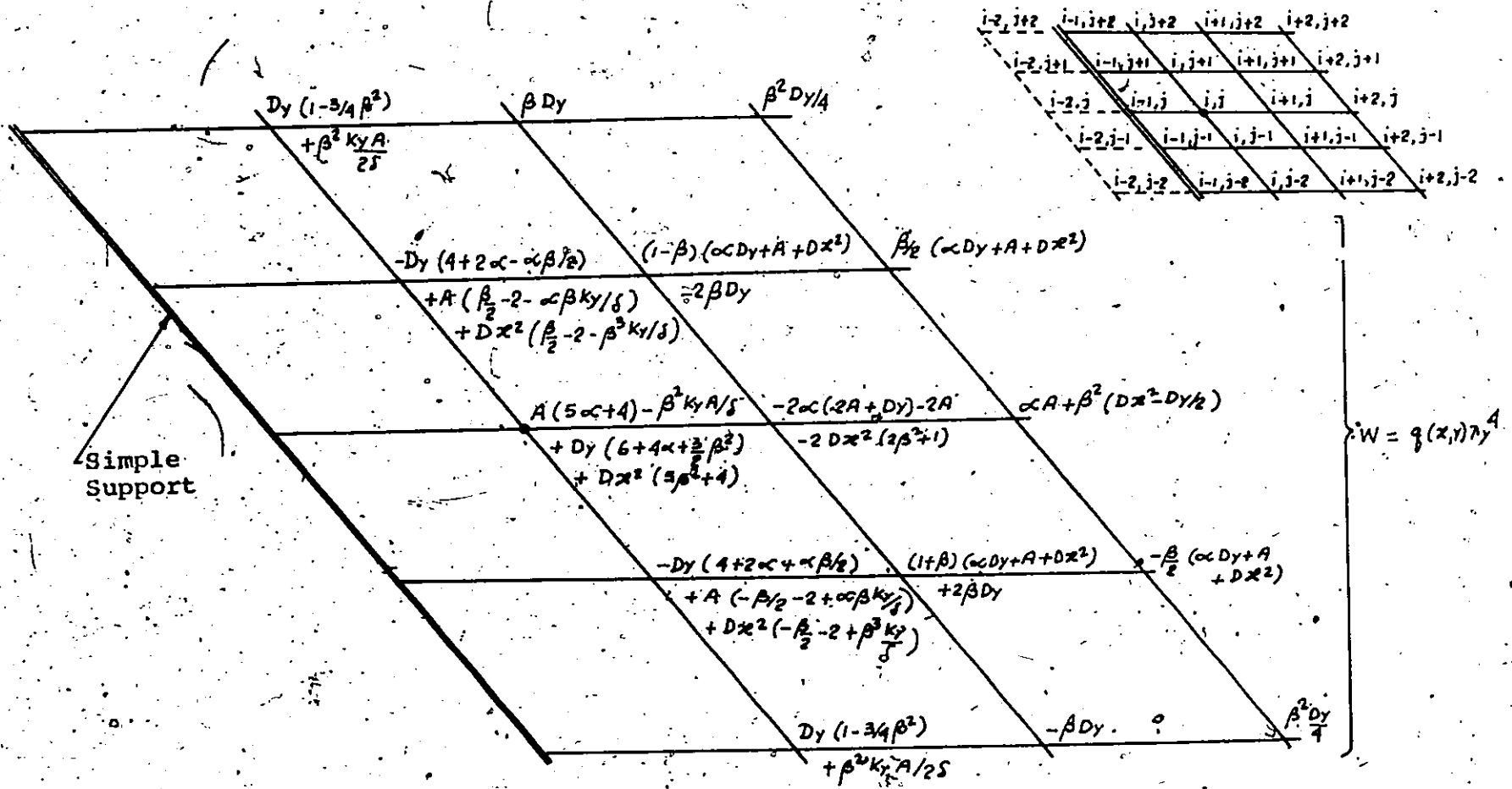

EQU. 11.2 FINITE DIFFERENCE EQUATION AT INTERIOR POINT NEAR LEFT SIMPLE SUPPORT.

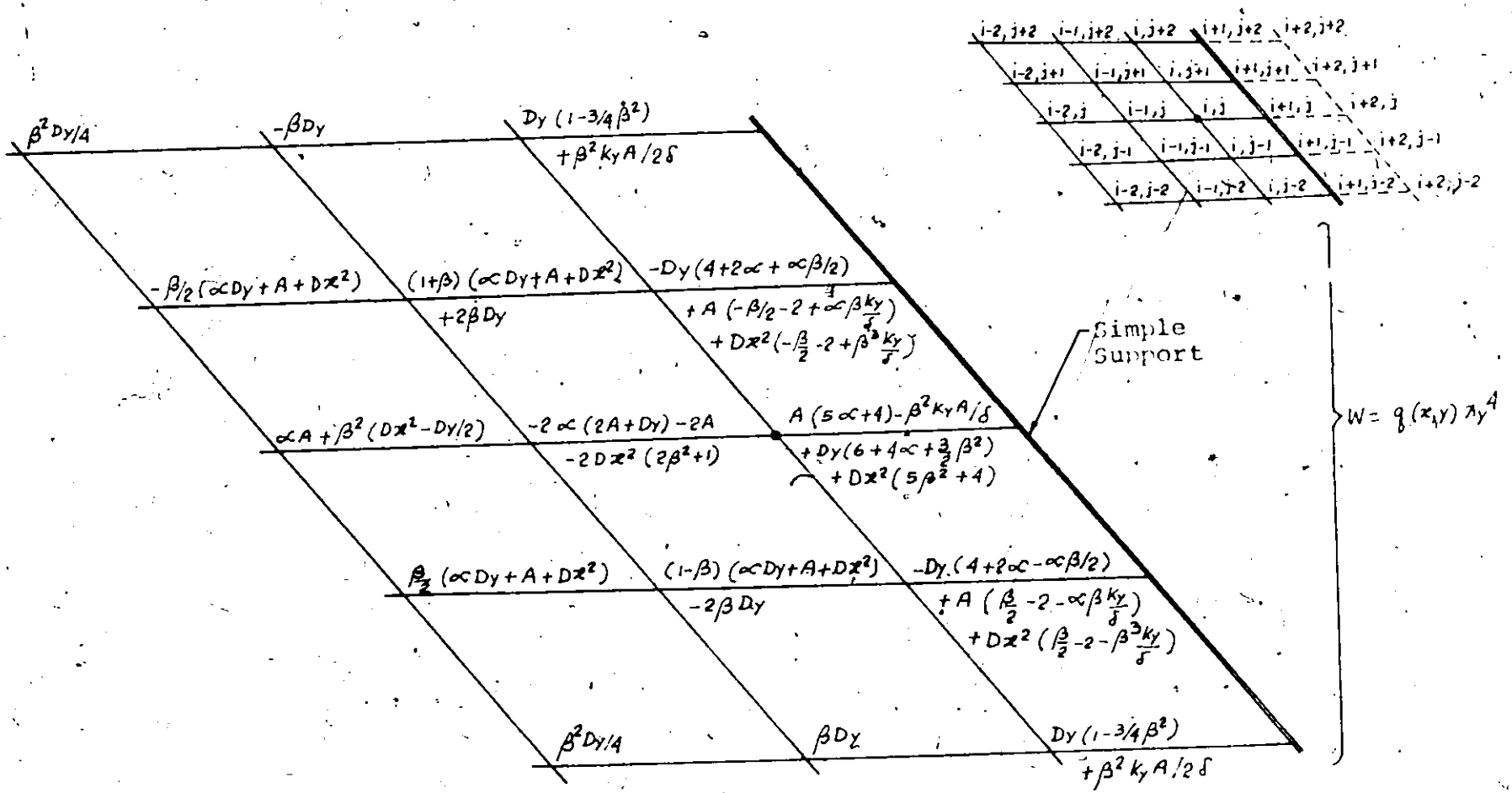

EQU. 11.3 FINITE DIFFERENCE EQUATION AT INTERIOR POINT NEAR RIGHT SIMPLE SUPPORT.

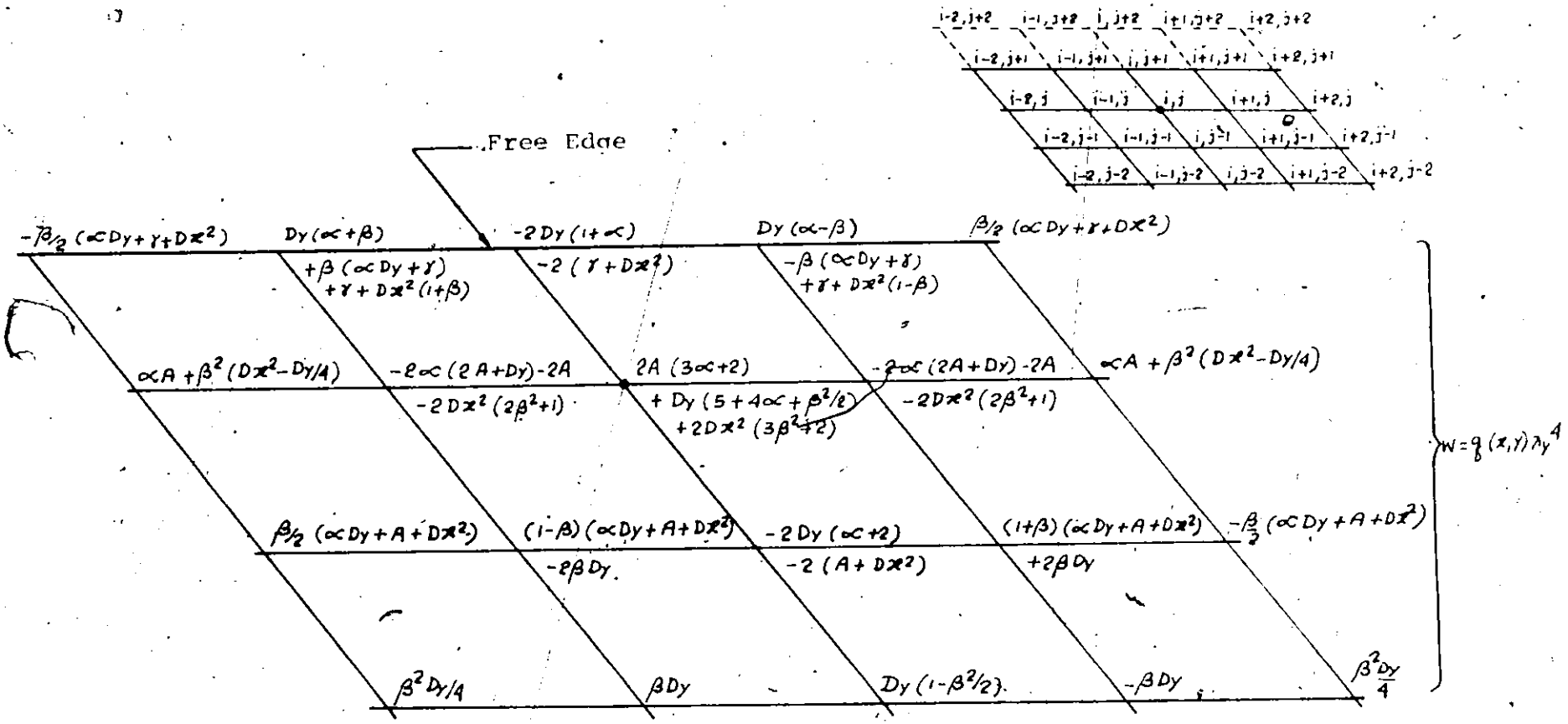

EQU. 11.4 FINITE DIFFERENCE EQUATION AT INTERIOR POINT NEAR FREE EDGE.

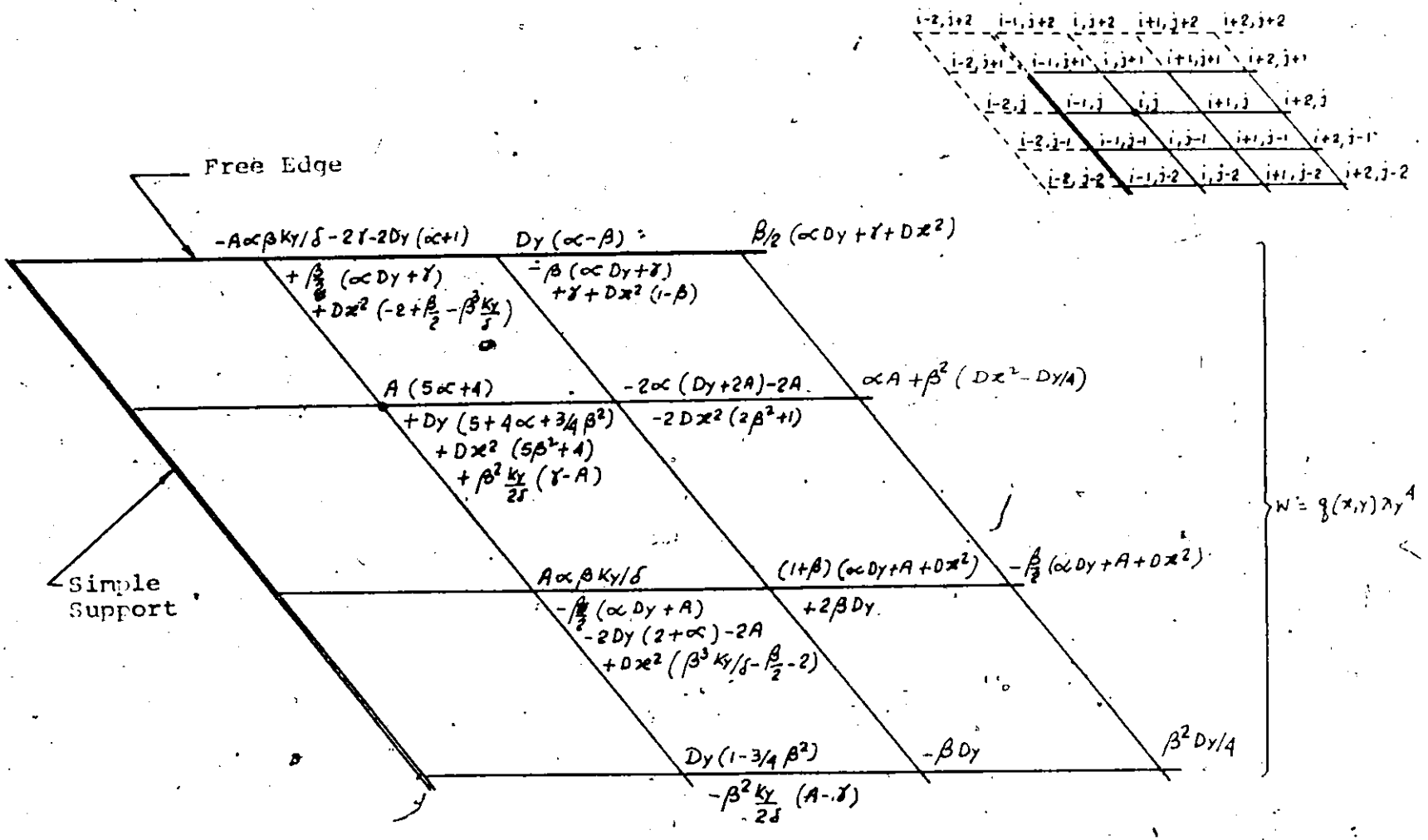

EQU. 11.5 FINITE DIFFERENCE EQUATION AT INTERIOR POINT NEAR ACUTE CORNER.

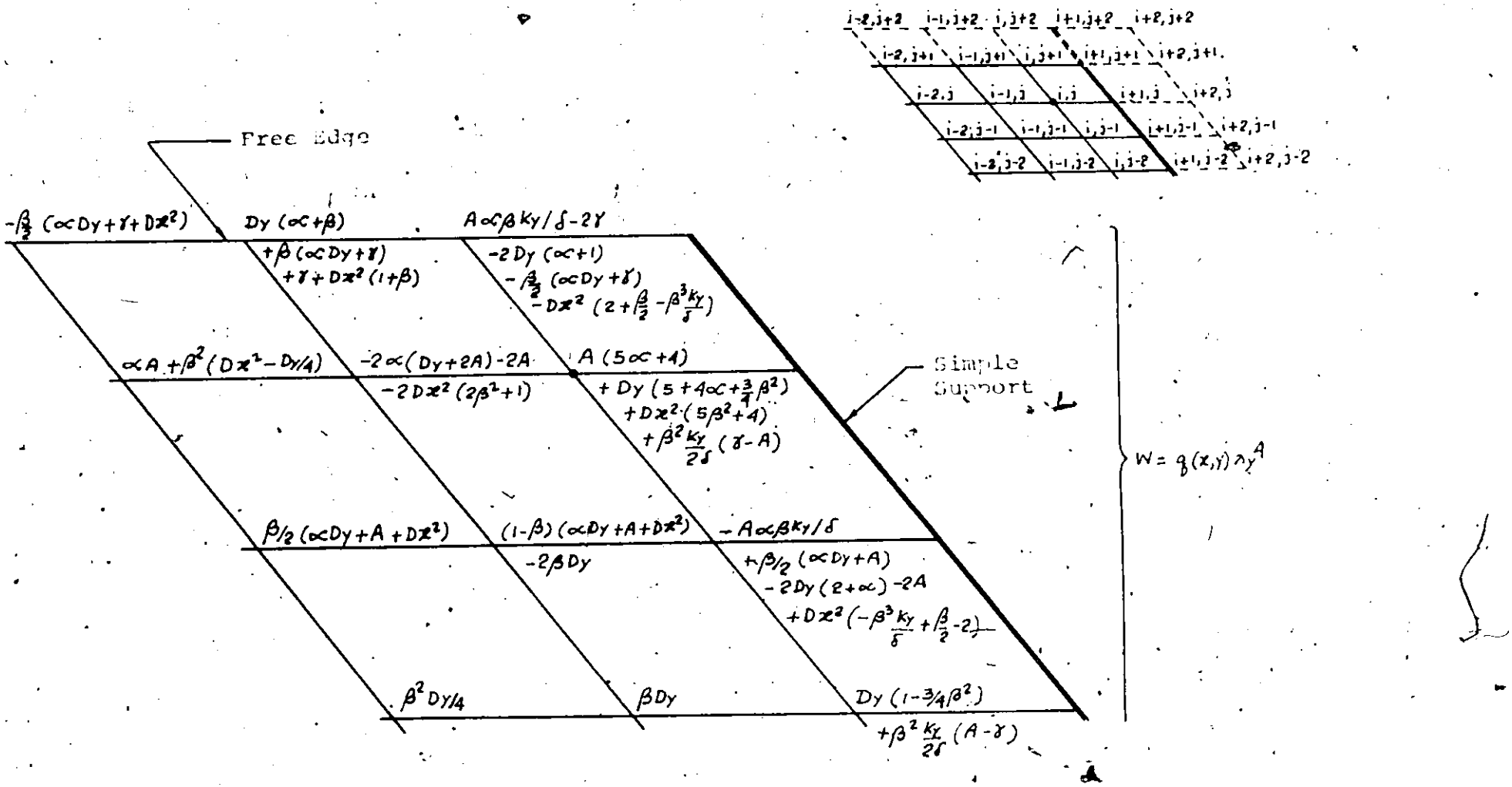

EQUATION 1.6 FINITE DIFFERENCE EQUATION AT INTERIOR POINT NEAR OUTER EDGE

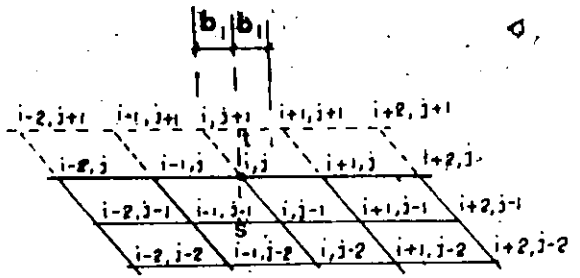

Free Edge

$\alpha\gamma/2 + \psi(A-\gamma)/2D_y$ $\quad -\gamma(2\alpha+1) - \psi$ $\quad 3\alpha\gamma + 3\psi(A-\gamma)/D_y$ $\quad -\gamma(2\alpha+1) - \psi$ $\quad \alpha\gamma/2 + \psi(A-\gamma)/2D_y$

$-\beta^2 D_y/4 - Dx^4 dx/2$ $\quad -2\psi(A-\gamma)/D_y + 2Dx^4 dx$ $\quad +2(\psi+\gamma) + D_y(1+\beta^2/2) - 3Dx^4 dx$ $\quad -2\psi(A-\gamma)/D_y + 2Dx^4 dx$ $\quad -\beta^2 D_y/4 - Dx^4 dx/2$

$\beta/2\,(A+\psi)$ $\quad (A+\psi)(1-\beta)$ $\quad -2(A+D_y+\psi)$ $\quad (A+\psi)(1+\beta)$ $\quad -\frac{\beta}{2}(A+\psi)$

$-\beta D_y$ $\quad +\beta D_y$

$\beta^2 D_y/4$ $\quad \beta D_y$ $\quad D_y(1-\beta^2/2)$ $\quad -\beta D_y$ $\quad \beta^2 D_y/4$

$W = q(x,y)\lambda^4 y/2$

Where $\psi = 2H - d_y D_x - D_x$

EQU. 11.7 FINITE DIFFERENCE EQUATION AT GENERAL EDGE POINT

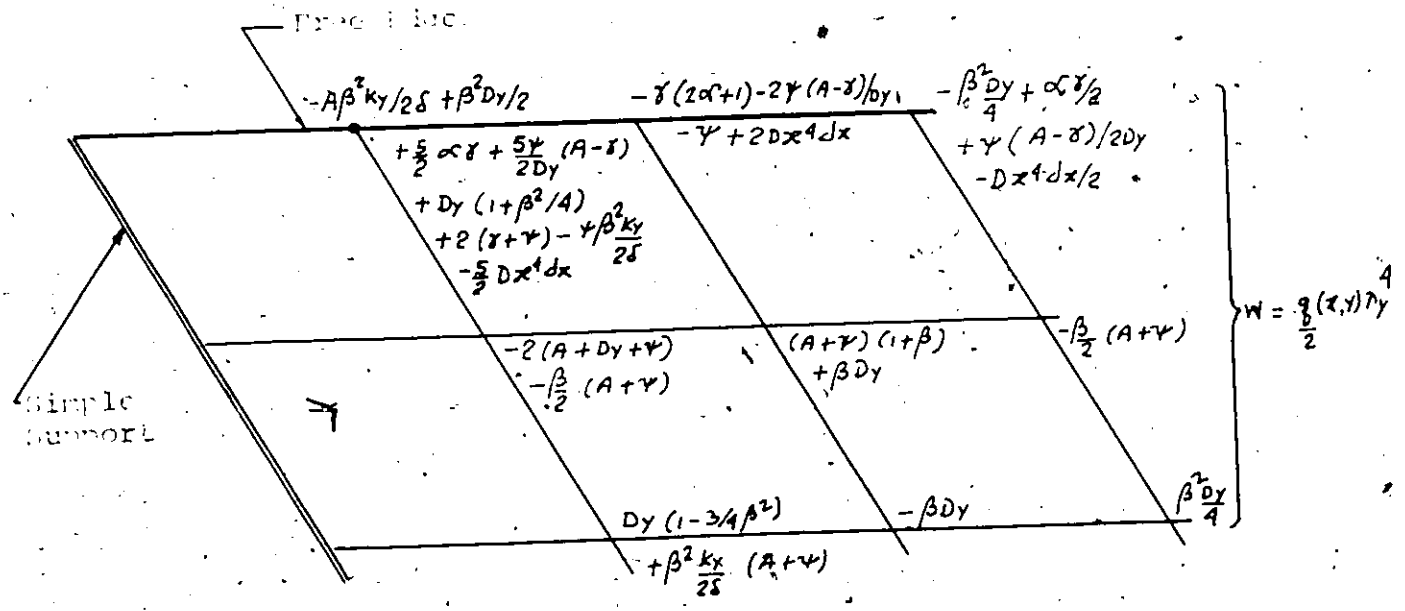

FIG. 11.8 FINITE DIFFERENCE EQUATION FOR EDGE POINT NEAR ACUTE CORNER.

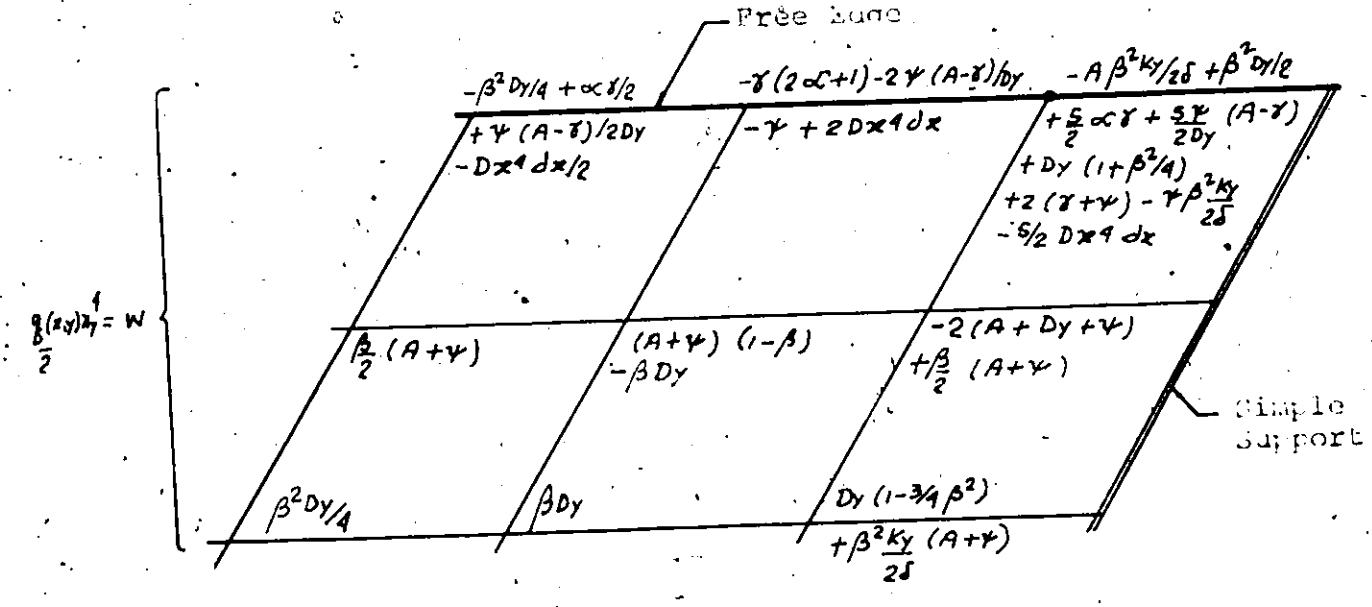

FIG. 11.9 FINITE DIFFERENCE EQUATION FOR EDGE POINT NEAR OBTUSE CORNER.

CHAPTER 12

TABLES

TABLE 5.1

DEFLECTIONS AND MOMENTS AT CENTRE OF SIMPLY SUPPORTED ORTHOTROPIC SKEW PLATE UNDER UNIFORM LOADING

$b/a = 1$; $D_x/D_y = 10$; $D_1 = D_2 = D_y/3$; $D_{xy} = D_{yx} = D_y$

(Linear Analysis)

Skew Angle ϕ, in degrees	Authors	Deflections x $10\ D_x/q \cdot b^4$	Max. Moment x $10/qb^2$
30°	Author Monforton Gupta	1.445 1.452 1.457	3.63 3.79 3.66
45°	Author Monforton Gupta	0.915 0.922 0.940	2.47 2.58 2.51

Author: Finite difference method.

Monforton: Finite element method.

Gupta: Series solution.

TABLE 5.2

DEFLECTIONS AND MOMENTS AT CENTRE OF SIMPLY SUPPORTED ISOTROPIC SKEW PLATES UNDER UNIFORM LOADING

$b/a = 1$, $\nu = 0.3$; $Q = 4b^2\cos\phi$

(Linear Analysis)

Skew Angle ϕ, in Degrees	Authors and Methods	Deflections x $10\ D/Qb^2$	Principal Moments	
			$M_1 \times 10/Q$	$M_2 \times 10/Q$
10°	Author	0.1551	0.489	0.451
	Iyenger	0.1574	0.493	0.456
	Sampath	0.1575	0.493	0.457
	Gupta	0.1589	0.498	0.461
	Morley	0.1572	0.494	0.461
30°	Author	0.1134	0.483	0.375
	Gupta	0.1206	0.497	0.394
	Sampath	0.1181	0.495	0.384
	Aggarwala	0.1178	0.488	0.383
	Morley	0.1182	0.491	0.385
45°	Author	0.0761	0.455	0.301
	Iyenger	0.0770	0.465	0.323
	Gupta	0.0790	0.472	0.334
	Sampath	0.0751	0.457	0.313
	Angyris	0.0735	0.459	0.303

Author: Finite Difference
Iyenger: Fourier Series
Sampath: Polar function and Taylor expansion
Aggarwala: Conformal mapping
Morley: Corner function
Gupta: Series solution
Argyris: Finite element

TABLE 5.3

COMPARISON OF PRESENT SOLUTIONS WITH THOSE OF LEVY'S SOLUTIONS

$b/a = 1$; $\nu = 0.316$; $E = 30 \times 10^6$ P.S.I.

(Non-Linear Analysis)

Skew Angle ϕ	qa^4/Eh^4	W_{centre}/h (Levy)	W_{centre}/h (Author)	Percentage Difference based on Levy's Solution
0^o	12.1	0.486	0.479	1.5
	29.4	0.962	0.943	2.0
	56.9	1.424	1.342	5.8
	99.4	1.870	1.791	4.2
	161	2.307	2.209	4.3
	247	2.742	2.589	5.6
	358	3.174	2.973	6.3

Author: Finite difference

Levy: Series solution

TABLE 6.1

GEOMETRIES OF MODEL TEST PLATES

Geometry	Model Plate No. 1	Model Plate No. 2	Model Plate No. 3
Skew Angle ϕ in degrees	0	45	45
L_x, inches	36.5	27.5	44
L_y, inches	24.5	19.0	22.0
C_1, inches	6.125	3.166	5.5
C_2, inches	4.563	x-direction rib only	5.5
t_1, inches	0.25	0.25	0.1875
t_2, inches	0.25	0.00	0.25
d_1, inches	0.75	0.75	0.75
d_2, inches	0.75	0.125	0.75
t, inches	0.125	0.125	0.125

where
L_x = span-length in the x-direction = 2a.
L_y = span-length in the y-direction = 2b cosϕ.
C_1, C_2 = spacing of x- and y-direction ribs.
t_1, t_2 = rib thicknesses in x- and y-direction.
d_1, d_2 = x- and y-direction plate-rib depth.
t = deck plate thickness.

TABLE 6.2

EXPERIMENTS IN ELASTIC STRESS REGION

Plates	Experiment Nos.	Loading	Location of Loading	Boundary Condition
Model Plate No. 1 $\phi = 0^{o}$	1	Point Load	@ centre (x=0, y=0)	All sides simply supported (s.s.)
	2	DO	@ centre	Longer sides s.s. shorter sides free
	3	DO	@ centre	Shorter sides s.s. longer sides free
	4	DO	@ (-a/4,0)	All sides s.s.
	5	DO	@ (0,-b/4)	Longer sides s.s. shorter sides free
	6	DO	@ (-a/4,0)	Shorter sides s.s. Longer sides free
	7	DO	@ (-a/2,0)	All sides s.s.
	8	DO	@ (0,-b/2)	Longer sides s.s. shorter sides free
	9	DO	@ (-a/2,0)	Shorter sides s.s. Longer sides free
	10	U.D.L.	Entire Plate	All sides s.s..

TABLE 6.2 con'd

Plates	Experiment Nos.	Loading	Location of Loading	Boundary Condition
Model Plate No. 2 $\phi = 45^{o}$	11	Point Load	@ centre (u=0, v=0)	Two opposite sides s.s. Other two sides free
	12	DO	@ (0,-b/3)	DO
	13	DO	@ centre (u=0,v=0)	All sides s.s.
	14	DO	@ (0,-b/3)	DO
	15	DO	@ (0,-2b/3)	DO
	16	U.D.L.	Entire Plate	DO
Model Plate No. 3 $\phi=45^{o}$	17	Point Load	@ centre (u=0,v=0)	All sides s.s.
	18	DO	@ centre (u=0,v=0)	Shorter sides s.s. Longer sides free
	19	DO	@ (-a/4,0)	DO
	20	U.D.L.	Entire Plate	All sides s.s.

TABLE 6.3

EXPERIMENTS IN ELASTIC-PLASTIC STRESS DOMAIN

Plates	Experiment Nos.	Loading	Boundary Condition
Model Plate No. 1	21	U.D.L.	All sides simply supported.
Model Plate No. 2	22	DO	DO
Model Plate No. 3	23	DO	DO

TABLE 6.4

LOCATIONS OF STRAIN GAGES

Plate No. 1	Bottom Strain Gages		Top Strain Gages	
Point	x(in.)	y(in.)	x(in.)	y(in.)
A	-13.69	-6.12	-13.69	-6.12
B	-9.12	0.0	-9.12	0.0
C	0.0	0.0	0.0	0.0
D	0.0	6.12	0.0	6.12
E	4.56	0.0	4.56	0.0
F	0.0	3.062	-	-
G	2.28	6.12	-	-
H	-	-	0.0	12.25
I	-	-	-18.25	0.0
Plate No. 2	u(in.)	v(in.)	u(in.)	v(in.)
A	0.0	0.0	0.0	0.0
B	-4.58	0.0	-4.58	0.0
C	0.0	4.48	0.0	4.48
D	4.58	8.96	4.58	8.96
E	-9.16	8.96	-9.16	8.96
F	-	-	0.0	13.44
Plate No. 3	u(in.)	v(in.)	u(in.)	v(in.)
A	0.0	0.0	0.0	0.0
B	-5.5	0.0	-5.5	0.0
C	0.0	7.78	0.0	7.78
D	5.5	7.78	5.5	7.78
E	-16.5	7.78	-16.5	7.78
F	-2.28	0.0	-	-
G	0.0	3.89	-	-
H	-	-	-5.5	15.55

TABLE 7.1

COMPARISON OF LATERAL DEFLECTIONS (INCHES)
FOR MODEL PLATE NO. 1

Load p.s.i.	Point 11, x=0, y=0		Point 9, x=9.126, y=0		Point 4, x=0, y=6.125	
	Expt.	Theory	Expt.	Theory	Expt.	Theory
1.0	0.025	0.026	0.021	0.019	0.020	0.019
2.0	0.051	0.052	0.041	0.039	0.039	0.037
3.0	0.075	0.078	0.060	0.058	0.058	0.056
4.0	0.100	0.104	0.079	0.077	0.073	0.074
5.0	0.125	0.128	0.100	0.097	0.092	0.092
6.0	0.149	0.152	0.120	0.114	0.109	0.109
6.25*	0.156	0.158	0.127	0.118	0.112	0.113
6.52	0.159	0.165	0.129	0.123	0.115	0.118
6.89	0.173	0.175	0.142	0.131	0.129	0.125
7.26	0.187	0.186	0.149	0.138	0.135	0.133
7.64	0.195	0.197	0.160	0.147	0.145	0.141
7.90	0.201	0.205	0.164	0.153	0.148	0.147
8.28	0.215	0.218	0.173	0.162	0.155	0.153
8.65	0.225	0.231	0.184	0.171	0.164	0.165
8.92	0.240	0.242	0.196	0.179	0.176	0.172
9.29	0.255	0.258	0.208	0.190	0.188	0.183
9.56	0.265	0.271	0.220	0.199	0.198	0.193
9.94	0.286	0.292	0.232	0.214	0.205	0.207
10.31	0.305	0.317	0.246	0.231	0.220	0.225
10.57	0.323	0.337	0.253	0.245	0.236	0.238
10.83	0.340	0.359	0.275	0.260	0.256	0.253
11.09	0.365	0.385	0.288	0.278	0.266	0.271
11.34	0.390	0.416	0.310	0.299	0.282	0.292

...con'd

TABLE 7.1 con'd

Load p.s.i.	Point 11, x=0, y=0		Point 9, x=9.126, y=0		Point 4, x=0, y=6.125	
	Expt.	Theory	Expt.	Theory	Expt.	Theory
11.60	0.430	0.452	0.320	0.324	0.300	0.317
11.86	0.469	0.494	0.341	0.354	0.327	0.346
12.12	0.521	0.543	0.361	0.388	0.365	0.381
12.38	0.565	0.599	0.402	0.427	0.395	0.416
12.63	0.634	0.664	0.451	0.471	0.442	0.464
12.89	0.689	0.730	0.478	0.519	0.479	0.513
13.15	0.741	0.805	0.521	0.572	0.532	0.566
13.41	0.801	0.884	0.563	0.629	0.568	0.623
13.66	0.887	0.967	0.613	0.689	0.623	0.683
13.92	0.969	1.054	0.675	0.752	0.671	0.745
14.18	1.041	1.143	0.725	0.816	0.730	0.809
14.44	1.127	1.234	0.802	0.883	0.785	0.875
14.70**	1.219	1.327	0.871	0.952	0.871	0.943

*Theoretical first yield in y-direction at central point.
**Rib at node 11 has fully yielded in y-direction.

TABLE 7.2

COMPARISON OF LATERAL DEFLECTIONS (INCHES)
MODEL PLATE NO. 2

Load p.s.i.	Point 13, u=0, v=0		Point 12, u=-4.583, v=0		Point 8, u=0, v=4.48	
	Expt.	Theory	Expt.	Theory	Expt.	Theory
1.0	0.017	0.018	0.014	0.016	0.015	0.016
2.0	0.033	0.036	0.029	0.031	0.030	0.032
3.0	0.051	0.054	0.042	0.046	0.045	0.048
4.0	0.067	0.071	0.058	0.062	0.059	0.064
5.0	0.083	0.089	0.071	0.077	0.074	0.079
6.0	0.098	0.106	0.085	0.092	0.089	0.095
7.0	0.115	0.123	0.097	0.106	0.103	0.110
7.41*	0.121	0.129	0.103	0.112	0.110	0.116
7.67	0.125	0.134	0.110	0.116	0.113	0.120
8.04	0.133	0.142	0.117	0.123	0.117	0.127
8.31	0.140	0.148	0.122	0.128	0.124	0.133
8.57	0.148	0.156	0.129	0.135	0.130	0.139
8.83	0.157	0.164	0.135	0.142	0.138	0.148
9.08	0.166	0.174	0.143	0.151	0.148	0.157
9.34	0.177	0.185	0.152	0.161	0.158	0.167
9.60	0.189	0.196	0.163	0.171	0.167	0.177
9.85	0.201	0.206	0.173	0.179	0.175	0.187
10.13	0.210	0.218	0.181	0.189	0.184	0.197
10.39	0.221	0.229	0.190	1.199	0.194	0.207
10.66	0.230	0.242	0.198	0.210	0.203	0.218
10.92	0.240	0.255	0.206	0.221	0.213	0.230
11.30	0.257	0.275	0.216	0.238	0.224	0.247
11.56	0.268	0.289	0.229	0.251	0.236	0.261

con'd ...

TABLE 7.2 con'd

Load p.s.i.	Point 13, u=0, v=0		Point 12, u=-4.583, v=0		Point 8, u=0, v=4.48	
	Expt.	Theory	Expt.	Theory	Expt.	Theory
11.94	0.289	0.312	0.240	0.271	0.251	0.280
12.20	0.308	0.329	0.255	0.285	0.271	0.295
12.58	0.329	0.354	0.278	0.307	0.283	0.317
12.84	0.358	0.373	0.308	0.323	0.299	0.333
13.22	0.383	0.401	0.325	0.347	0.318	0.357
13.59	0.404	0.430	0.346	0.371	0.334	0.383
13.97	0.426	0.460	0.371	0.398	0.356	0.409
14.34	0.459	0.491	0.399	0.425	0.383	0.436
14.72	0.486	0.524	0.430	0.453	0.423	0.465
14.98	0.516	0.548	0.451	0.473	0.458	0.485
15.25	0.541	0.572	0.470	0.494	0.474	0.506
15.52	0.558	0.596	0.485	0.515	0.501	0.527
15.78	0.588	0.621	0.507	0.536	0.520	0.549
16.05	0.618	0.646	0.521	0.558	0.541	0.571
16.31	0.640	0.673	0.540	0.579	0.561	0.593
16.58	0.663	0.698	0.561	0.602	0.580	0.615
16.84	0.683	0.724	0.580	0.624	0.603	0.638
17.11	0.699	0.750	0.601	0.647	0.623	0.660
17.38	0.725	0.777	0.625	0.669	0.648	0.684
17.64	0.755	0.803	0.651	0.692	0.673	0.707
17.91	0.780	0.830	0.676	0.715	0.692	0.730
18.19	0.805	0.859	0.698	0.739	0.712	0.755
18.47	0.830	0.888	0.717	0.796	0.732	0.780
18.75**	0.855	0.917	0.742	0.789	0.751	0.805

*Theoretical first yield in the x-direction at central point.
**Terminal stage of complete yielding of ribs at node 13 in the x-direction.

TABLE 7.3

COMPARISON OF LATERAL DEFLECTIONS (INCHES)
FOR MODEL PLATE NO. 3

Load p.s.i.	Point 11, u=0, v=0		Point 9, u=-11.0, v=0		Point 4, u=0, v=7.78	
	Expt.	Theory	Expt.	Theory	Expt.	Theory
1.0	0.016	0.017	0.011	0.012	0.010	0.012
2.0	0.031	0.034	0.021	0.024	0.020	0.024
3.0	0.048	0.052	0.031	0.035	0.030	0.036
4.0	0.064	0.069	0.043	0.047	0.041	0.047
5.0	0.082	0.086	0.054	0.059	0.053	0.059
6.0	0.097	0.103	0.065	0.071	0.640	0.708
6.91*	0.111	0.118	0.078	0.081	0.074	0.081
7.28	0.116	0.124	0.082	0.086	0.080	0.089
7.65	0.124	0.131	0.085	0.091	0.084	0.090
8.03	0.131	0.139	0.089	0.095	0.089	0.095
8.40	0.138	0.146	0.095	0.101	0.094	0.101
8.78	0.146	0.154	0.100	0.106	0.099	0.105
9.04	0.153	0.160	0.105	0.109	0.103	0.109
9.42	0.160	0.169	0.110	0.116	0.107	0.116
9.69	0.167	0.176	0.116	0.120	0.112	0.120
10.06	0.174	0.187	0.122	0.127	0.118	0.128
10.44	0.183	0.199	0.128	0.135	0.124	0.135
10.70	0.191	0.209	0.134	0.141	0.131	0.142
11.08	0.204	0.224	0.141	0.150	0.139	0.151
11.45	0.219	0.240	0.149	0.160	0.148	0.162
11.83	0.234	0.260	0.161	0.173	0.159	0.175
12.09	0.247	0.275	0.171	0.182	0.170	0.185
12.34	0.271	0.292	0.182	0.192	0.180	0.196

...con'd

TABLE 7.3 con'd

Load p.s.i.	Point 11, u=0, v=0		Point 9, u=-11.0, v=0		Point 4, u=0, v=7.78	
	Expt.	Theory	Expt.	Theory	Expt.	Theory
12.60	0.284	0.311	0.192	0.204	0.191	0.209
12.86	0.299	0.333	0.202	0.218	0.203	0.223
13.12	0.326	0.358	0.215	0.233	0.215	0.239
13.38	0.347	0.387	0.228	0.251	0.229	0.258
13.63	0.380	0.419	0.250	0.271	0.248	0.279
13.89	0.417	0.457	0.276	0.294	0.273	0.304
14.15	0.459	0.501	0.301	0.321	0.301	0.333
14.41	0.495	0.548	0.326	0.352	0.331	0.365
14.66	0.546	0.601	0.354	0.387	0.359	0.401
14.92	0.601	0.659	0.381	0.425	0.401	0.440
15.18	0.645	0.727	0.423	0.467	0.445	0.482
15.44	0.701	0.787	0.463	0.511	0.491	0.527
15.70	0.773	0.857	0.501	0.558	0.529	0.574
15.95	0.829	0.928	0.558	0.608	0.571	0.623
16.21**	0.915	1.001	0.602	0.658	0.625	0.674

*Theoretical first yield in the y-direction at central point.
**Rib at node 13 has fully yielded in the y-direction.

CHAPTER 13

FIGURES

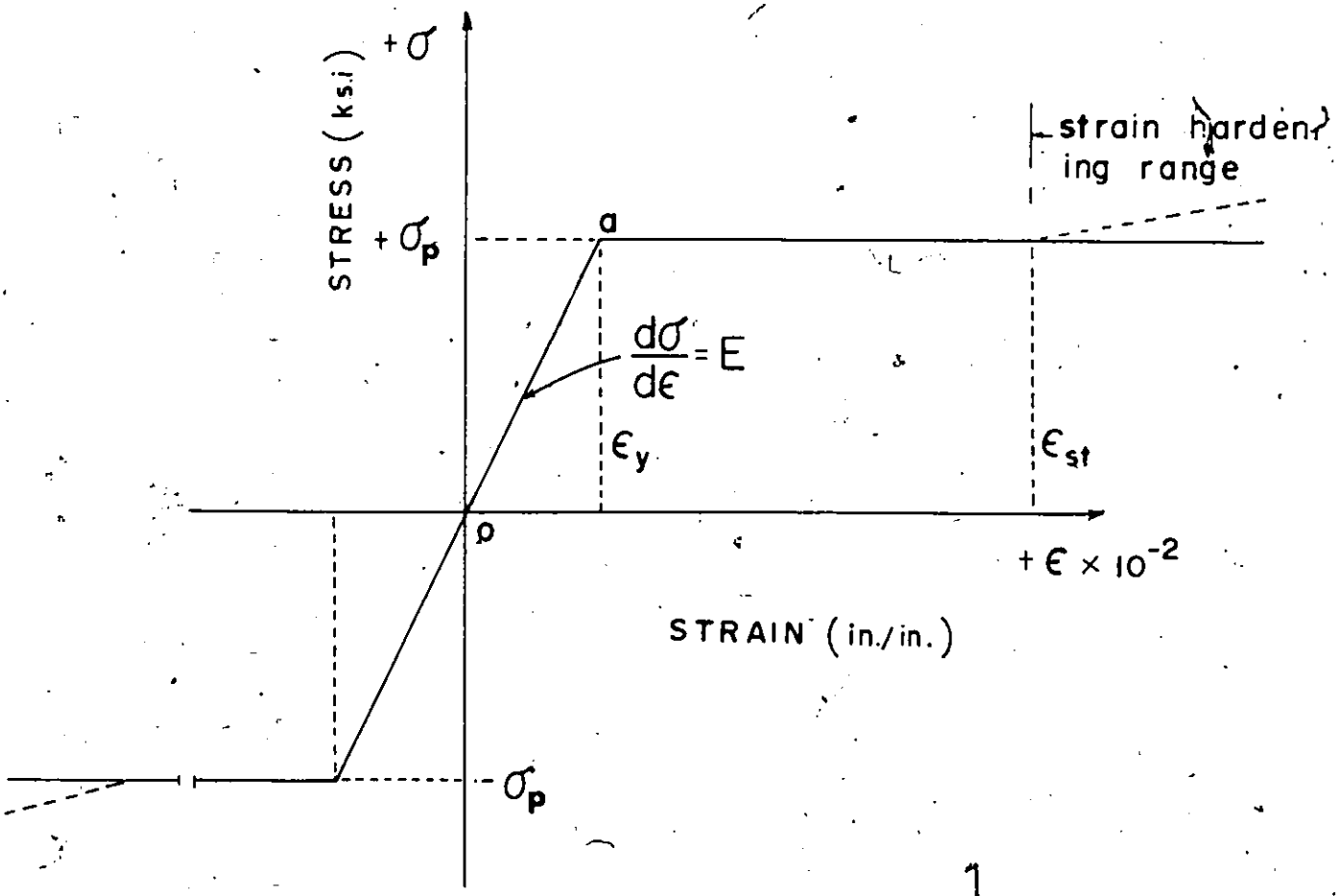

SPECIMEN : STRUCTURAL STEEL ASTM A-441

EXPERIMENTAL VALUES (Average) :

$\sigma_p = 50.0$ k.s.i

$E = 30.0 \times 10^3$ k.s.i

$\nu = 0.3$

$\epsilon_{st} = 1.45 \times 10^{-2}$

Figure 3.1 IDEALIZED STRESS-STRAIN CURVE FOR AN ELASTIC-PERFECTLY PLASTIC MATERIAL

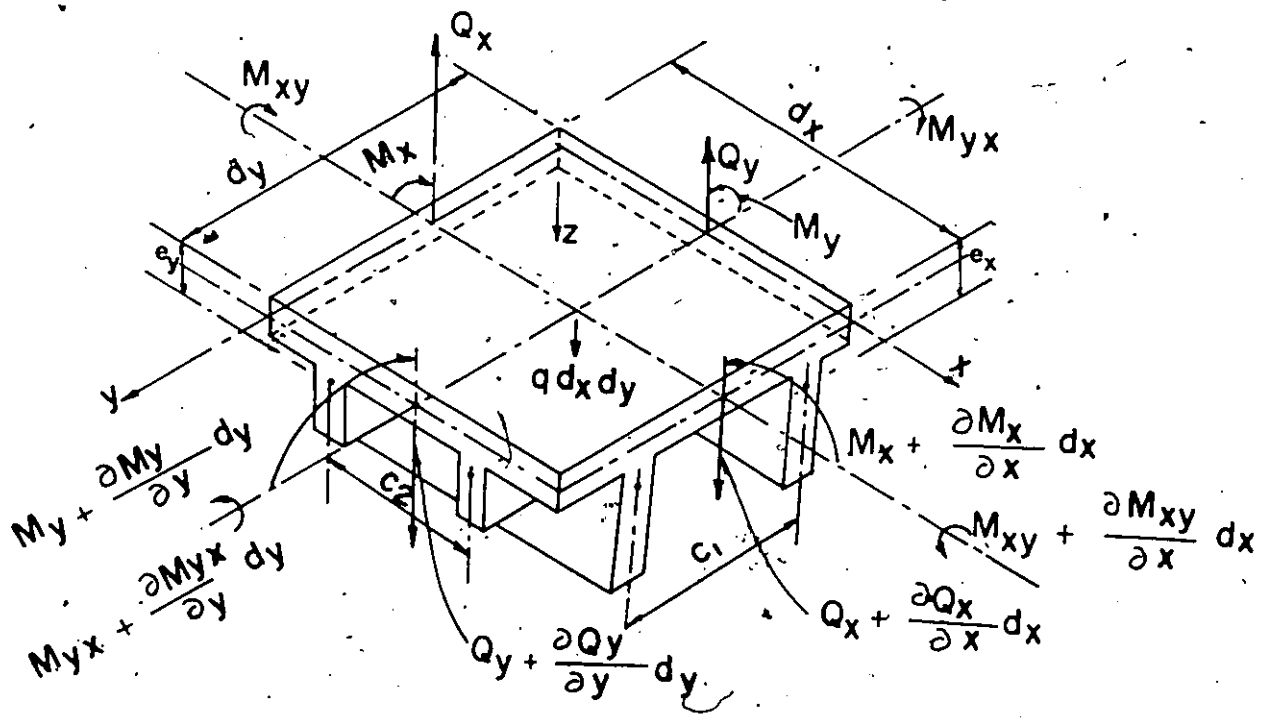

(a) BENDING FORCES

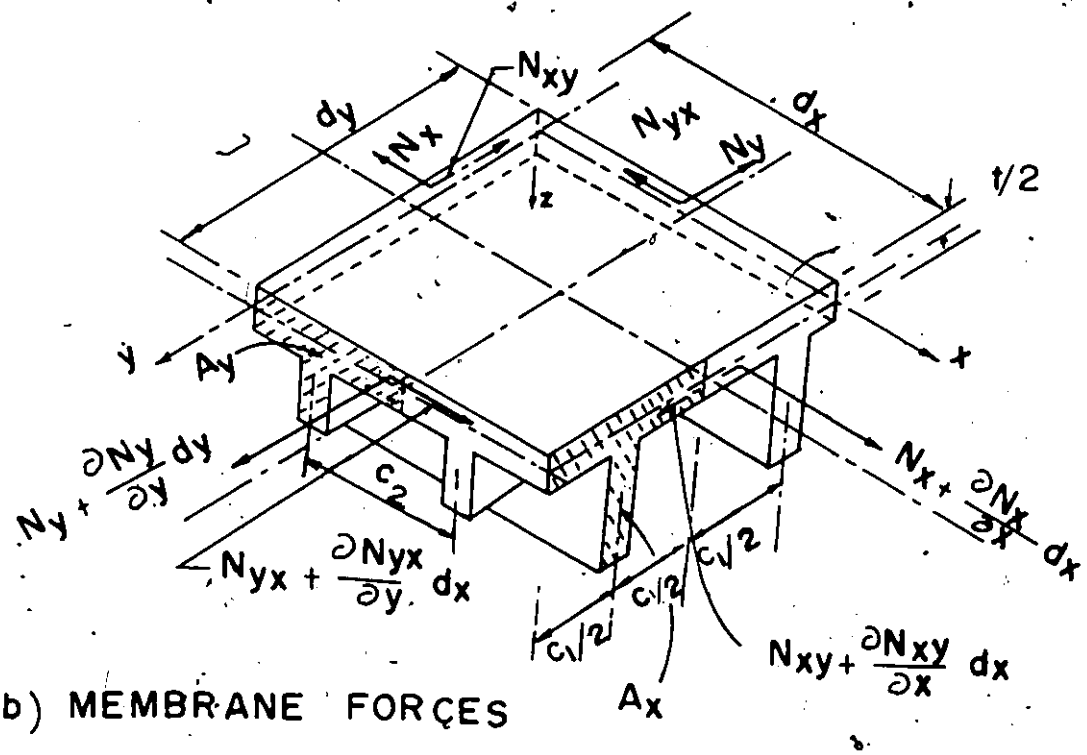

(b) MEMBRANE FORCES

Figure 3.2 ORTHOTROPIC PLATE ELEMENT UNDER BENDING AND MEMBRANE FORCES.

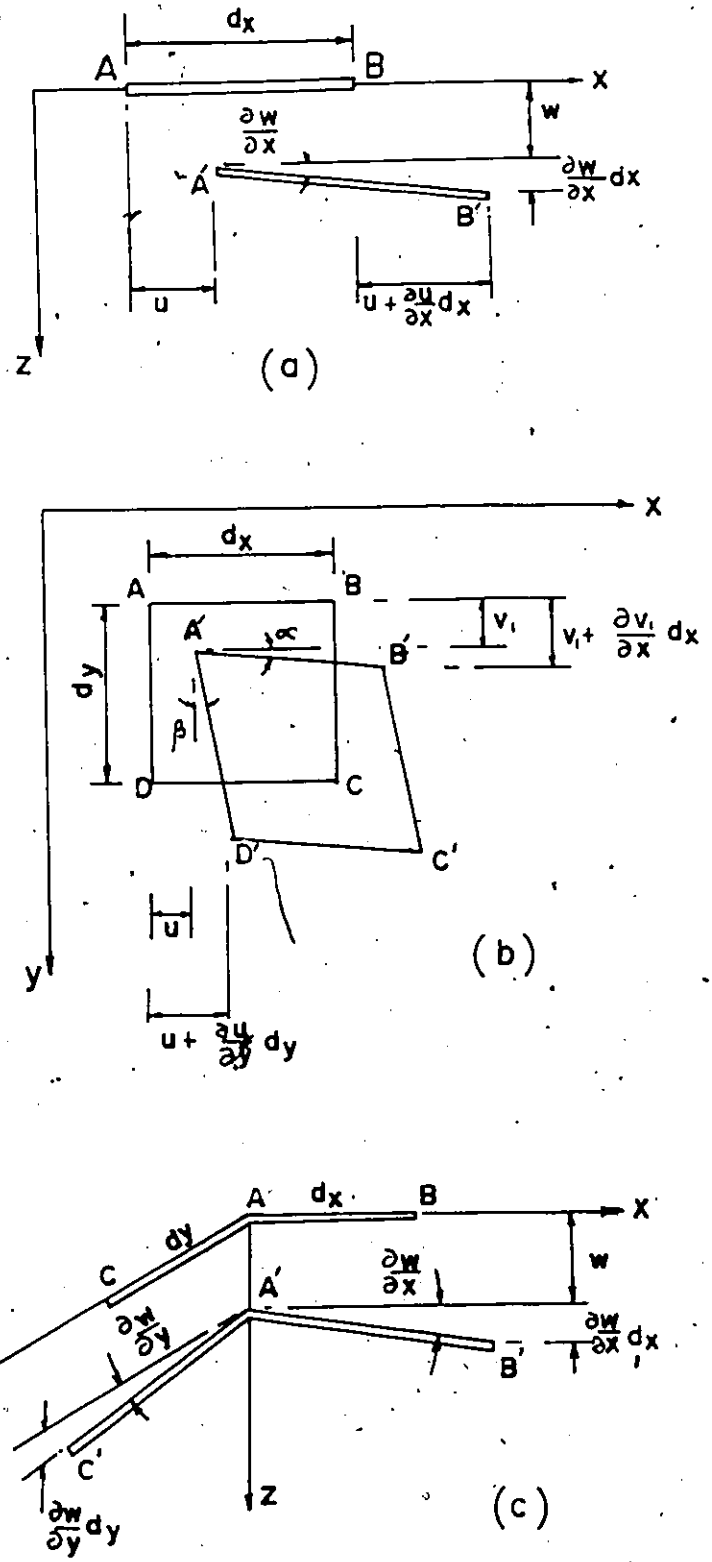

Figure 3.3 DEFORMATION DUE TO MEMBRANE ACTION.

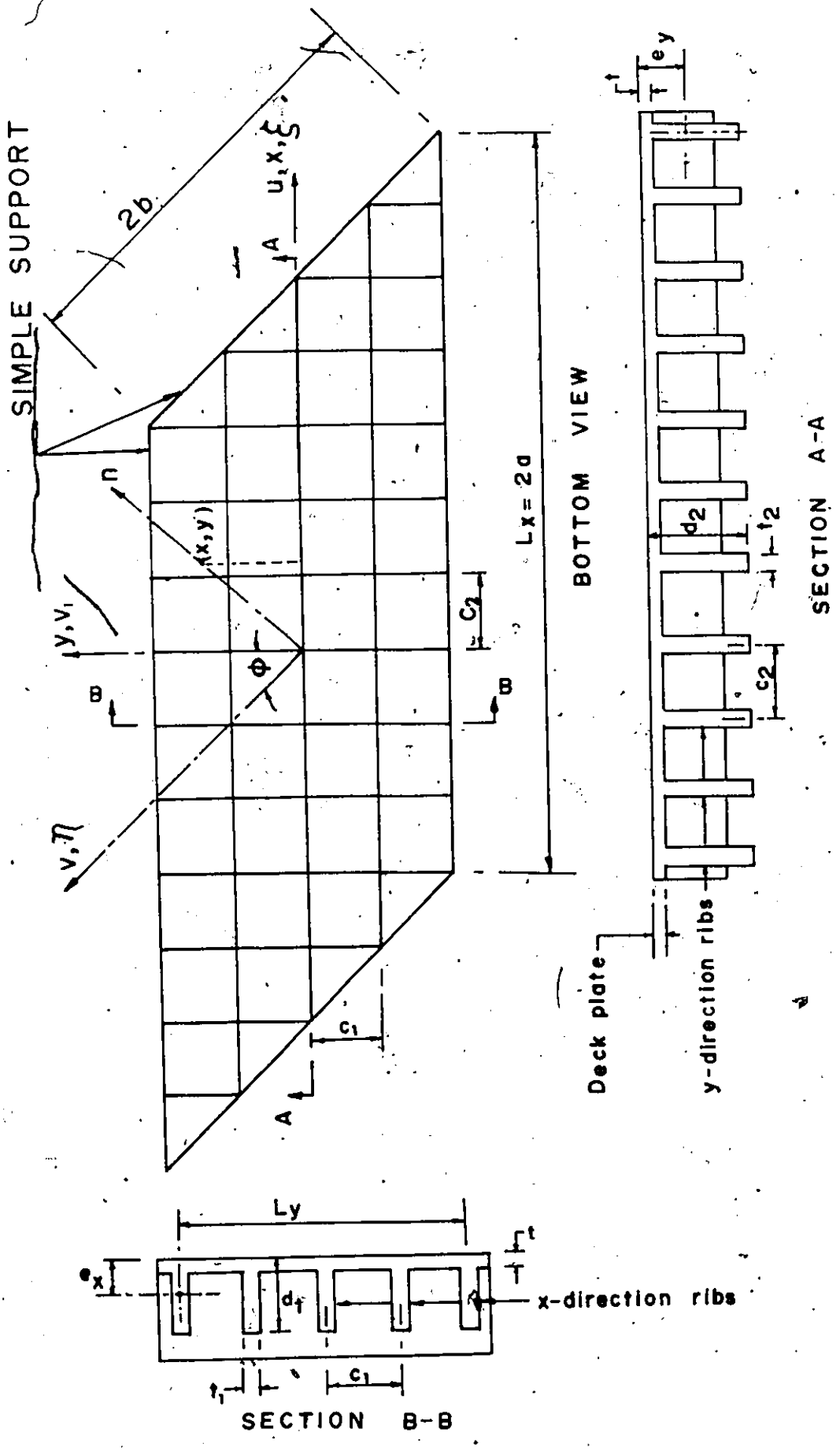

Figure 3.4 ORTHOTROPIC SKEW PLATE AND CO-ORDINATE SYSTEM.

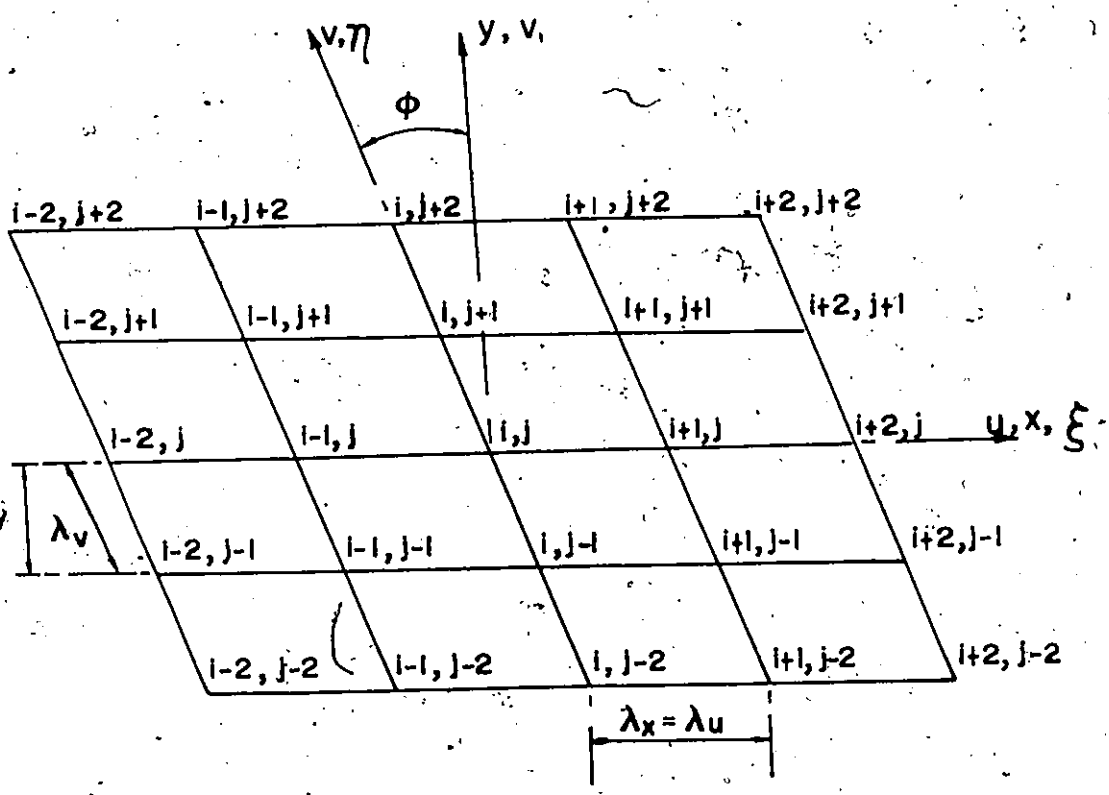

Figure 4.1 Favre's Finite Difference Network With Modified Nodal Point Notation.

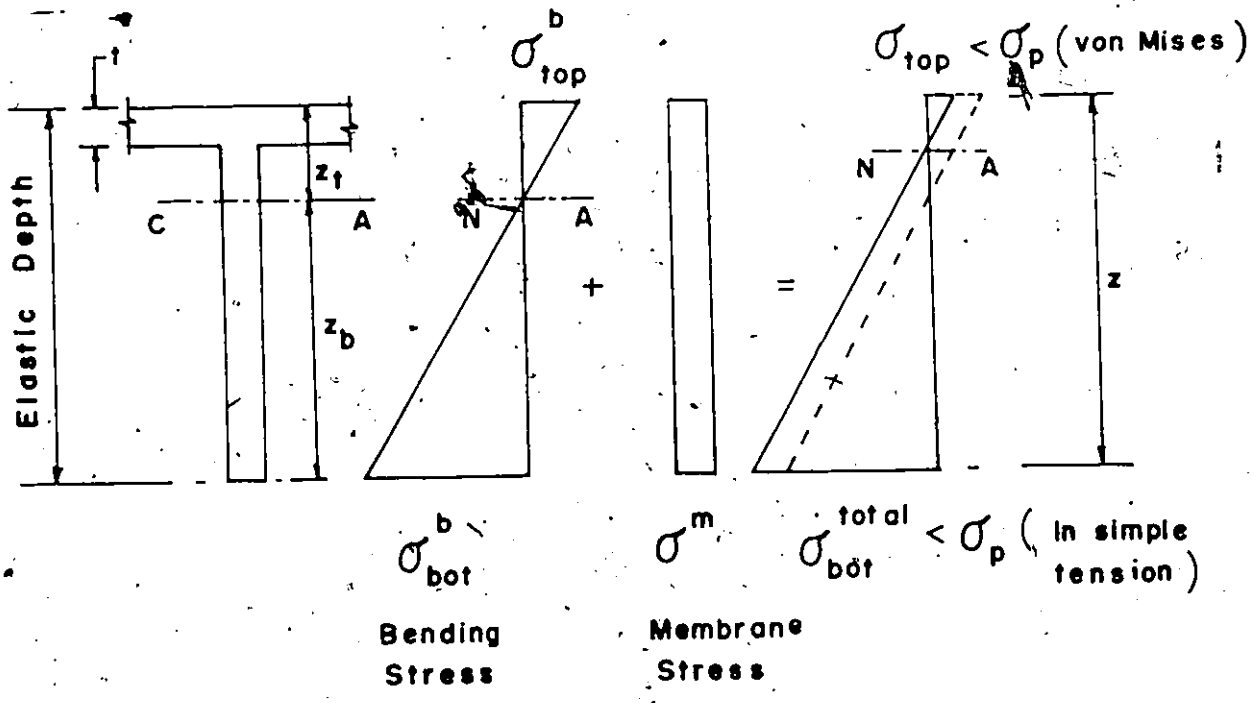

Figure 5.1 Elastic Stress Distribution

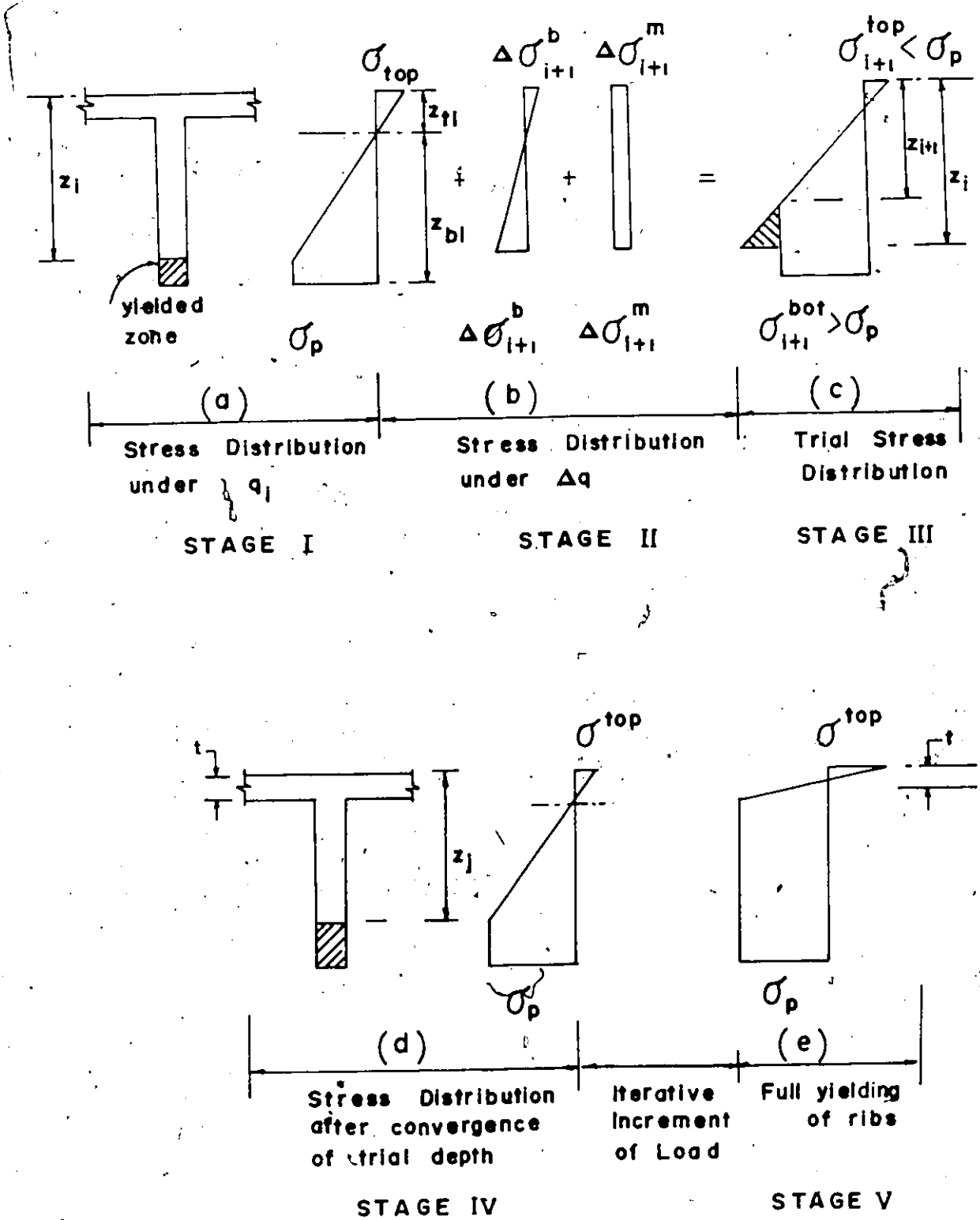

Figure 5·2 Stress Distribution in Post-Yield Range.

Fig. 5·3 FLOW DIAGRAM FOR ELASTO-PLASTIC ANALYSIS OF ORTHOTROPIC SKEW PLATES.

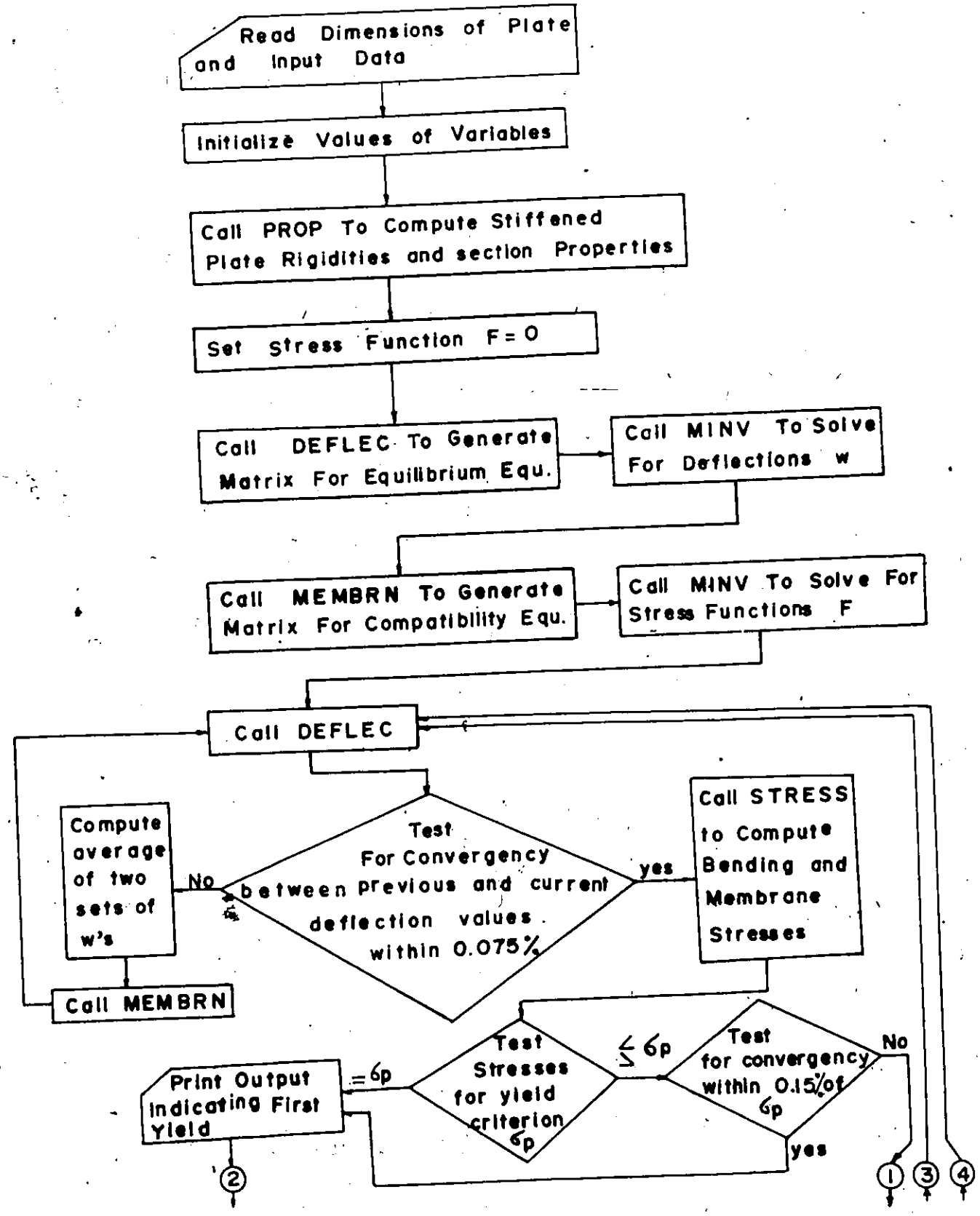

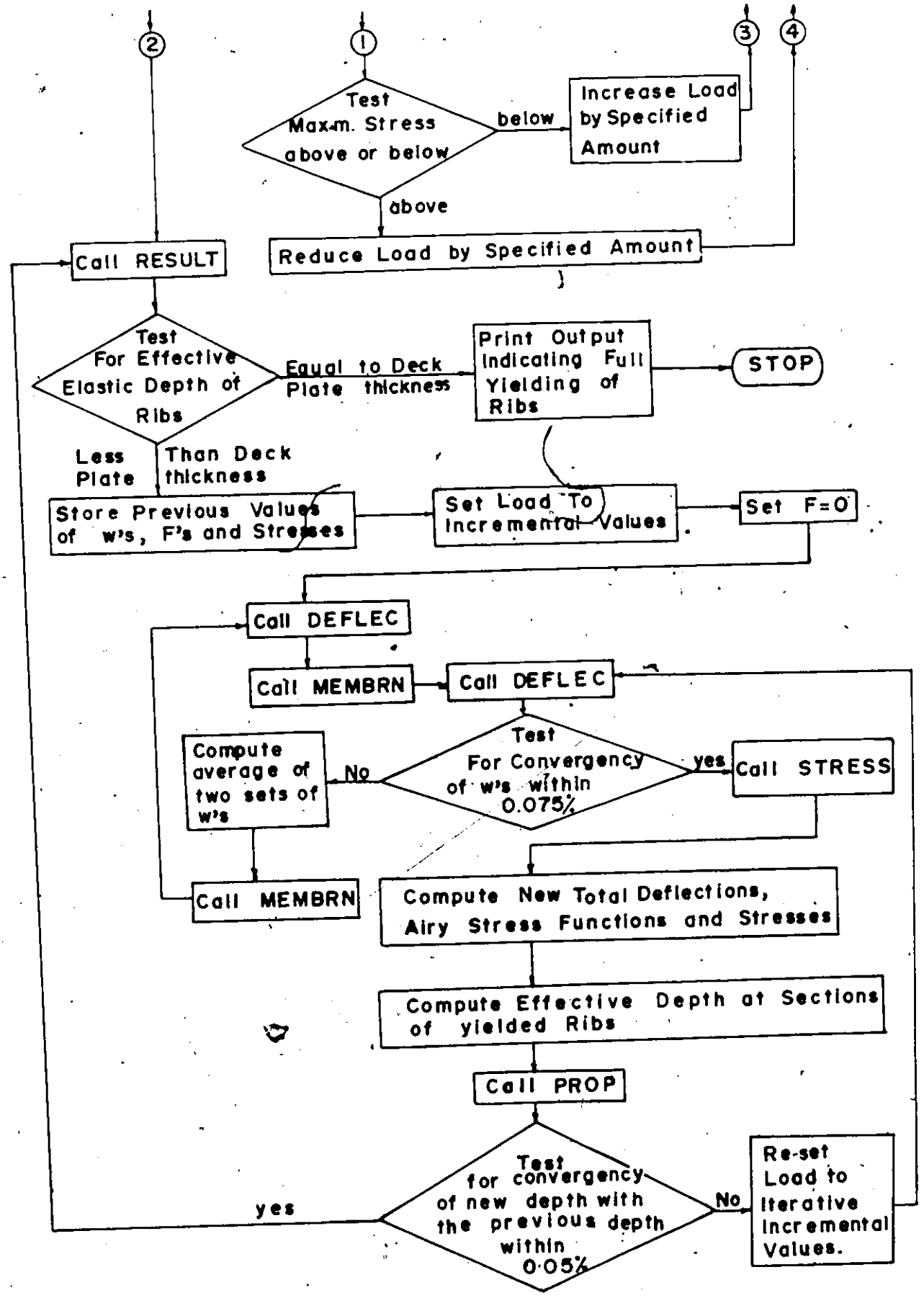
2
1
3
4
Test Max.m. Stress above or below
below
Increase Load by Specified Amount
above
Reduce Load by Specified Amount
Call RESULT
Test For Effective Elastic Depth of Ribs
Equal to Deck Plate thickness
Print Output Indicating Full Yielding of Ribs
STOP
Less Than Deck Plate thickness
Store Previous Values of w's, F's and Stresses
Set Load To Incremental Values
Set F=0
Call DEFLEC
Call MEMBRN
Call DEFLEC
Compute average of two sets of w's
No
Test For Convergency of w's within 0.075%
yes
Call STRESS
Call MEMBRN
Compute New Total Deflections, Airy Stress Functions and Stresses
Compute Effective Depth at Sections of yielded Ribs
Call PROP
Test for convergency of new depth with the previous depth within 0.05%
yes
No
Re-set Load to Iterative Incremental Values.

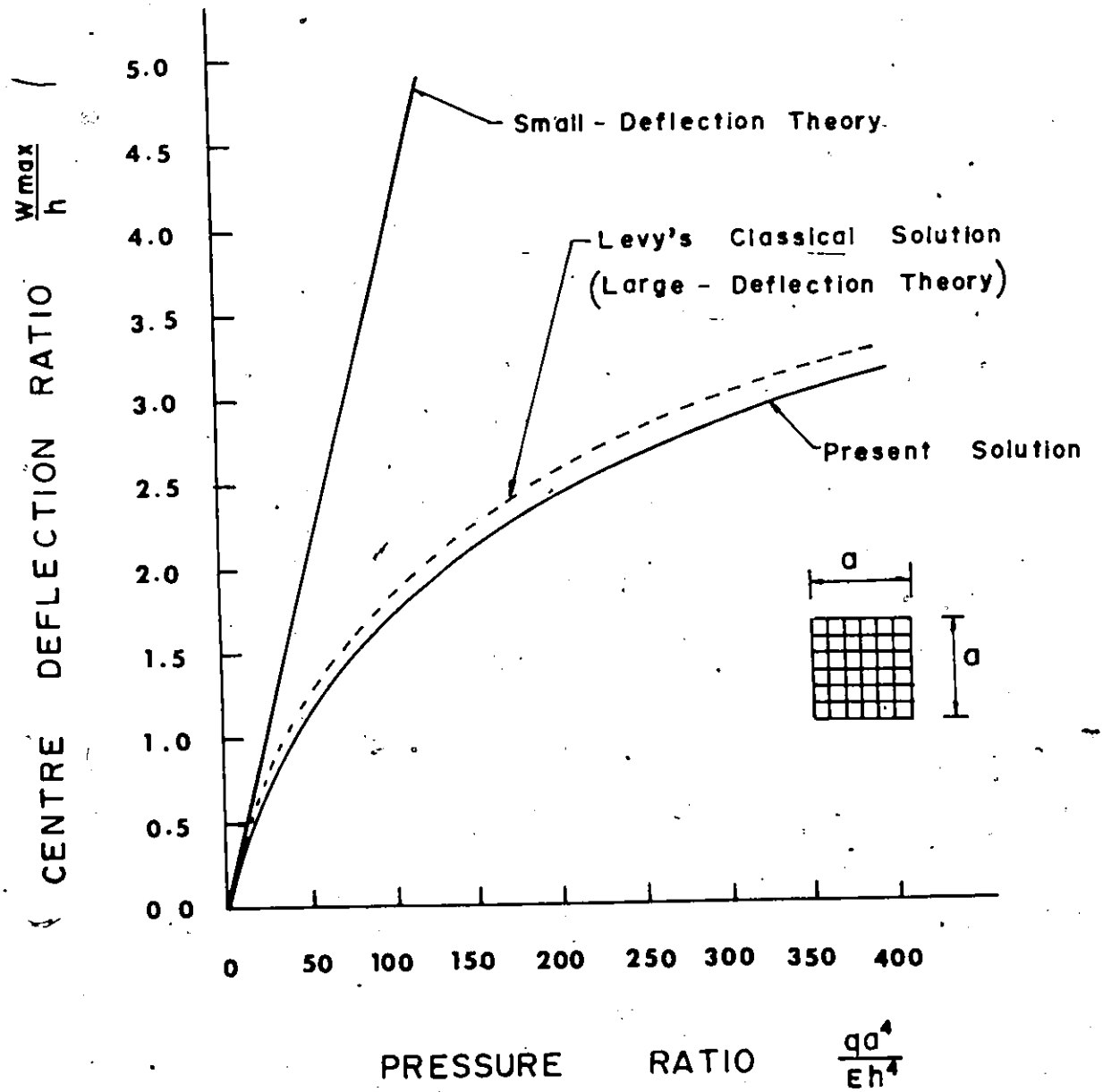

Figure 5·4 LOAD DEFLECTION DIAGRAM FOR A UNIFORMLY LOADED SIMPLY SUPPORTED SQUARE PLATE.

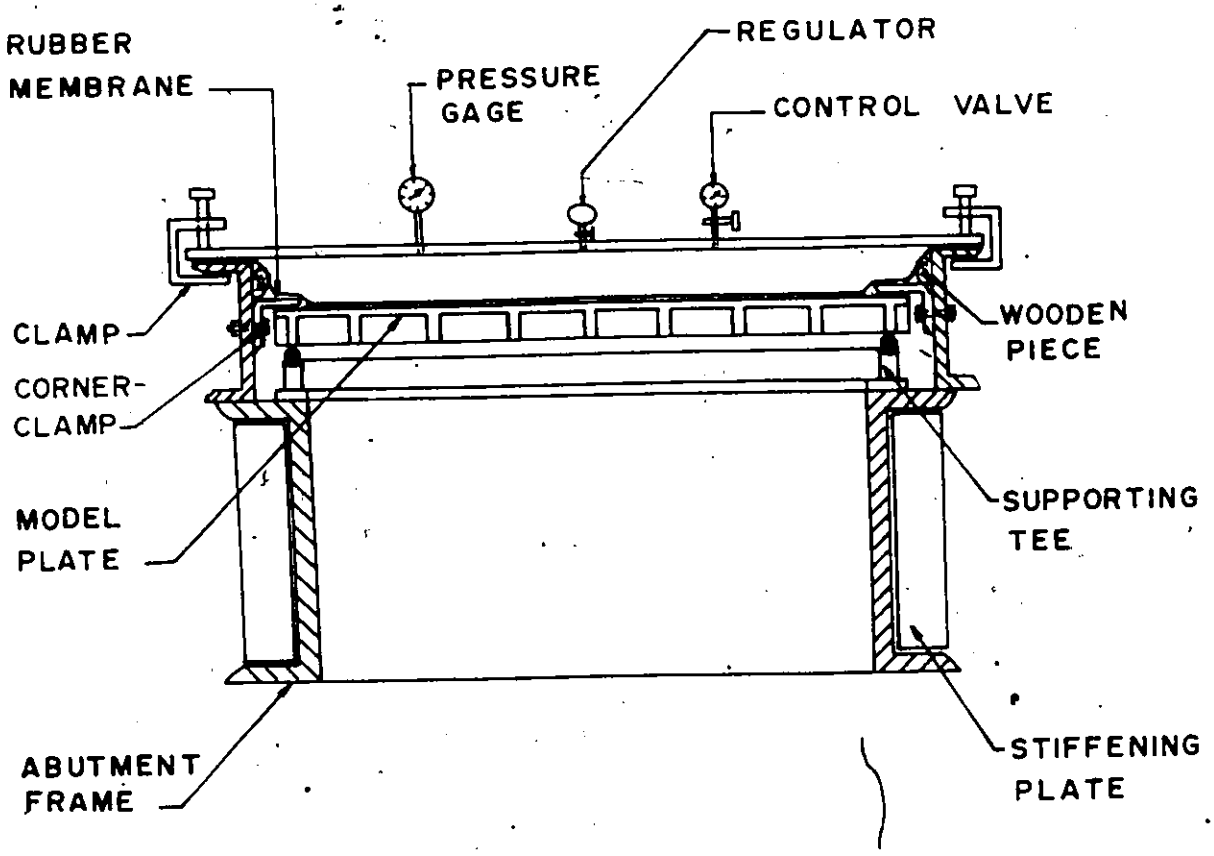

Figure 6·1 Loading Device and Abutment Frame

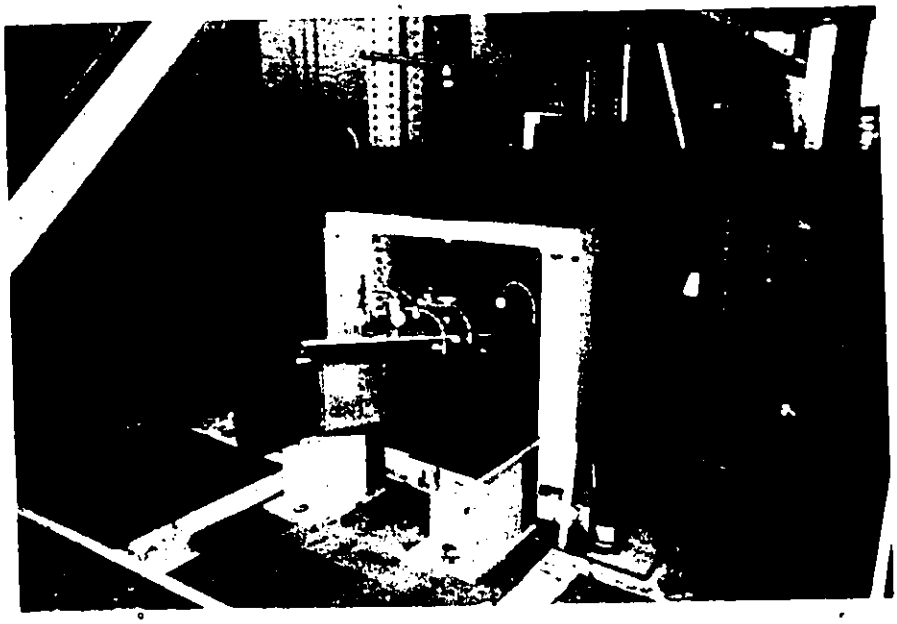

Figure 6.2 Application of Point Load in the Elastic Stress Region.

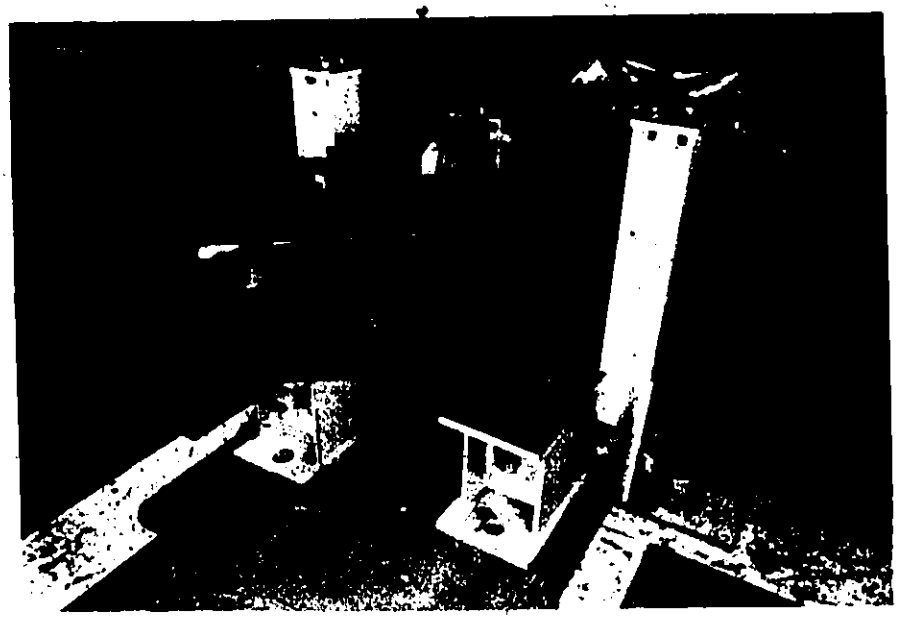

Figure 6.3 Uniformly Distributed Loading Test Set-Up in the Elastic and Elasto-Plastic Stress Domain.

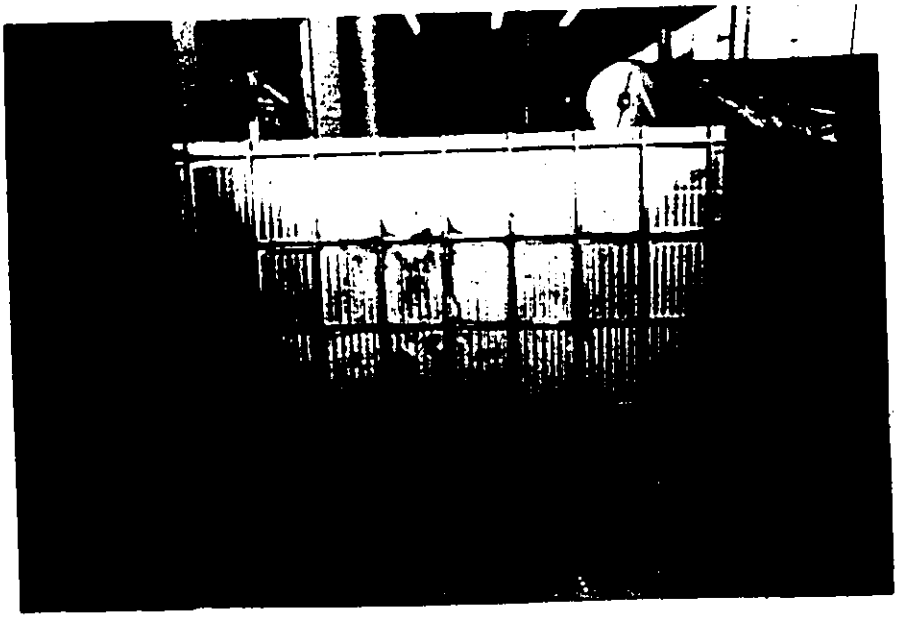

Figure 6·4 Model Plate No. 1 Showing the Integral System Of Ribs And Deck Plate.

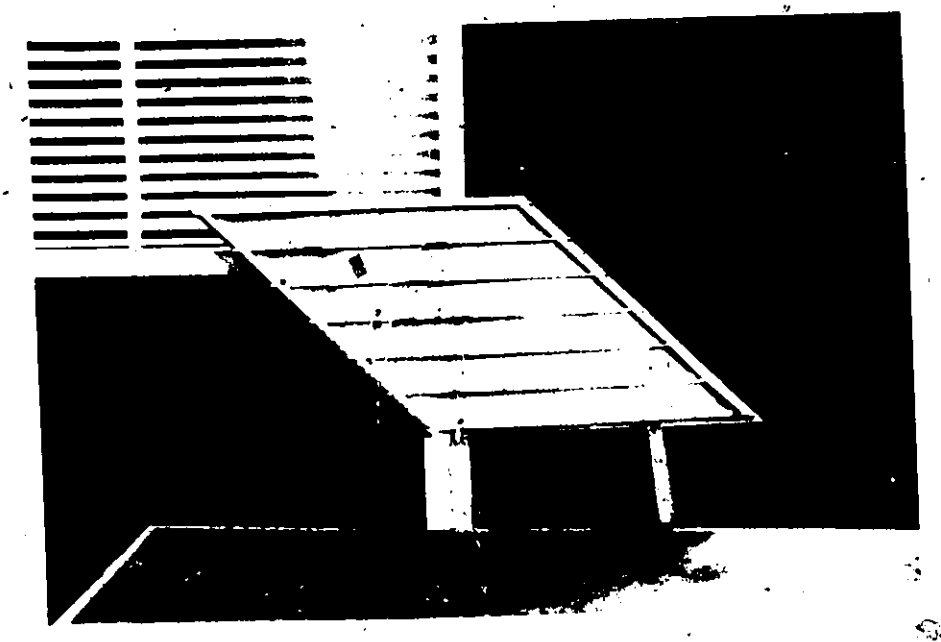

Figure 6·5 Model Plate No. 2 With Unidirectional Ribs.

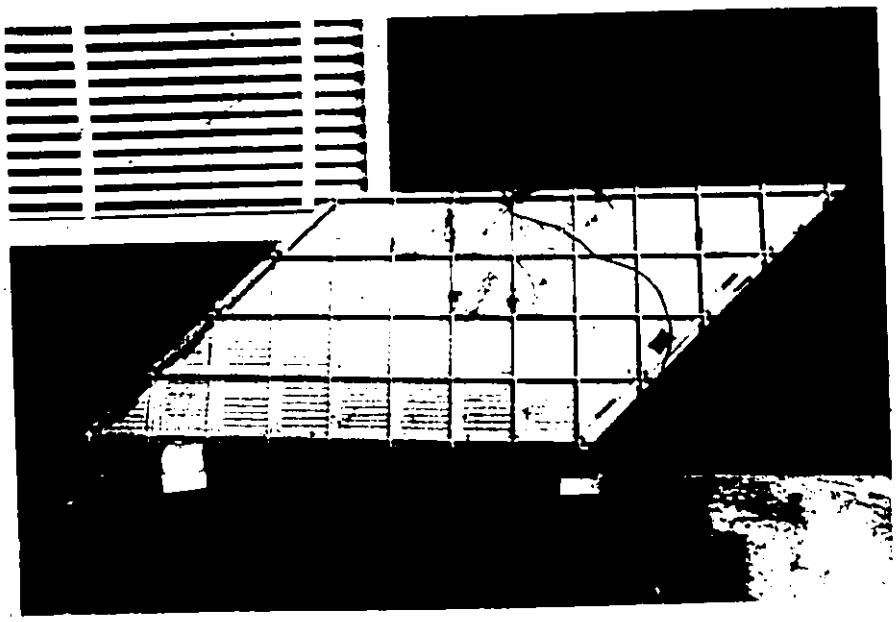

Figure 6·6 Skew Model Plate No. 3 With Ribs in both Principal (x - , y -) Directions.

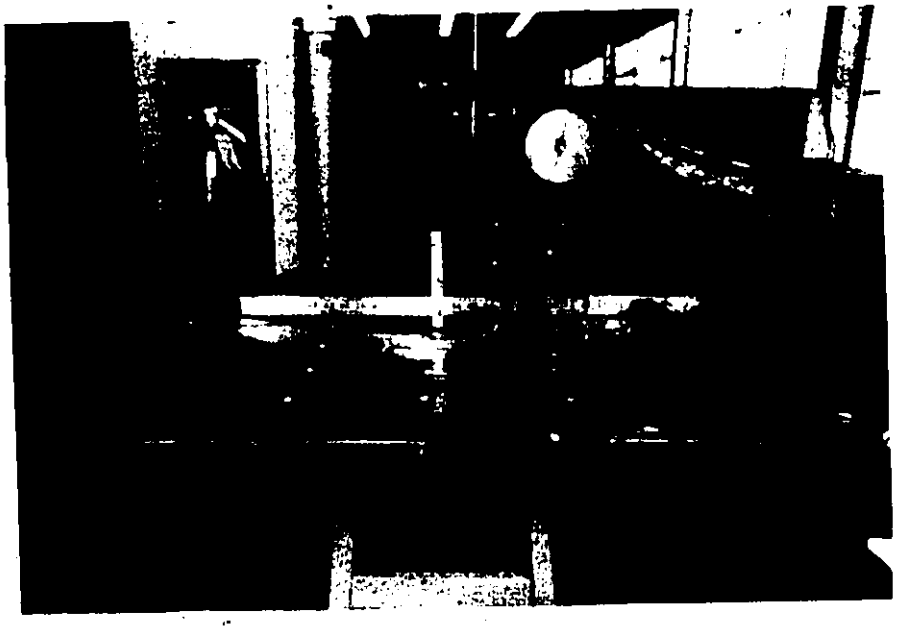

Figure 6·7 Permanent Deformation in Model Plate No. 1

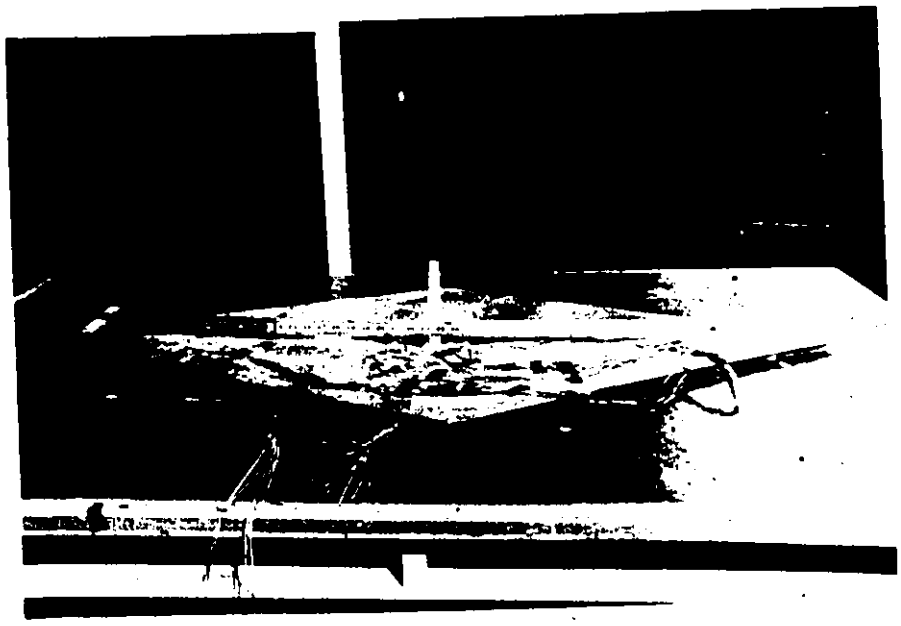

Figure 6-8 Permanent Deformation in Model Plate No. 3

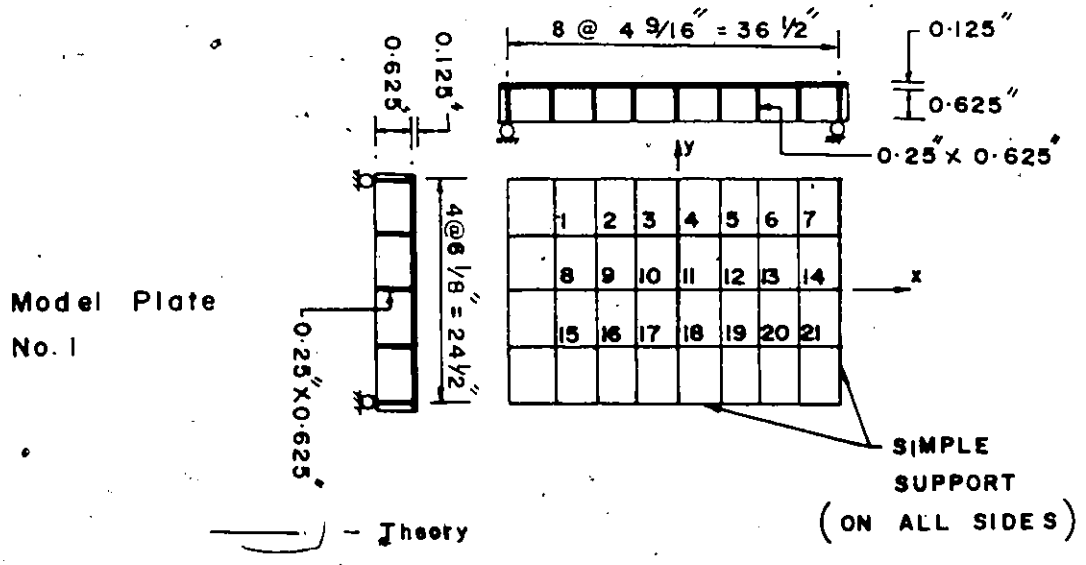

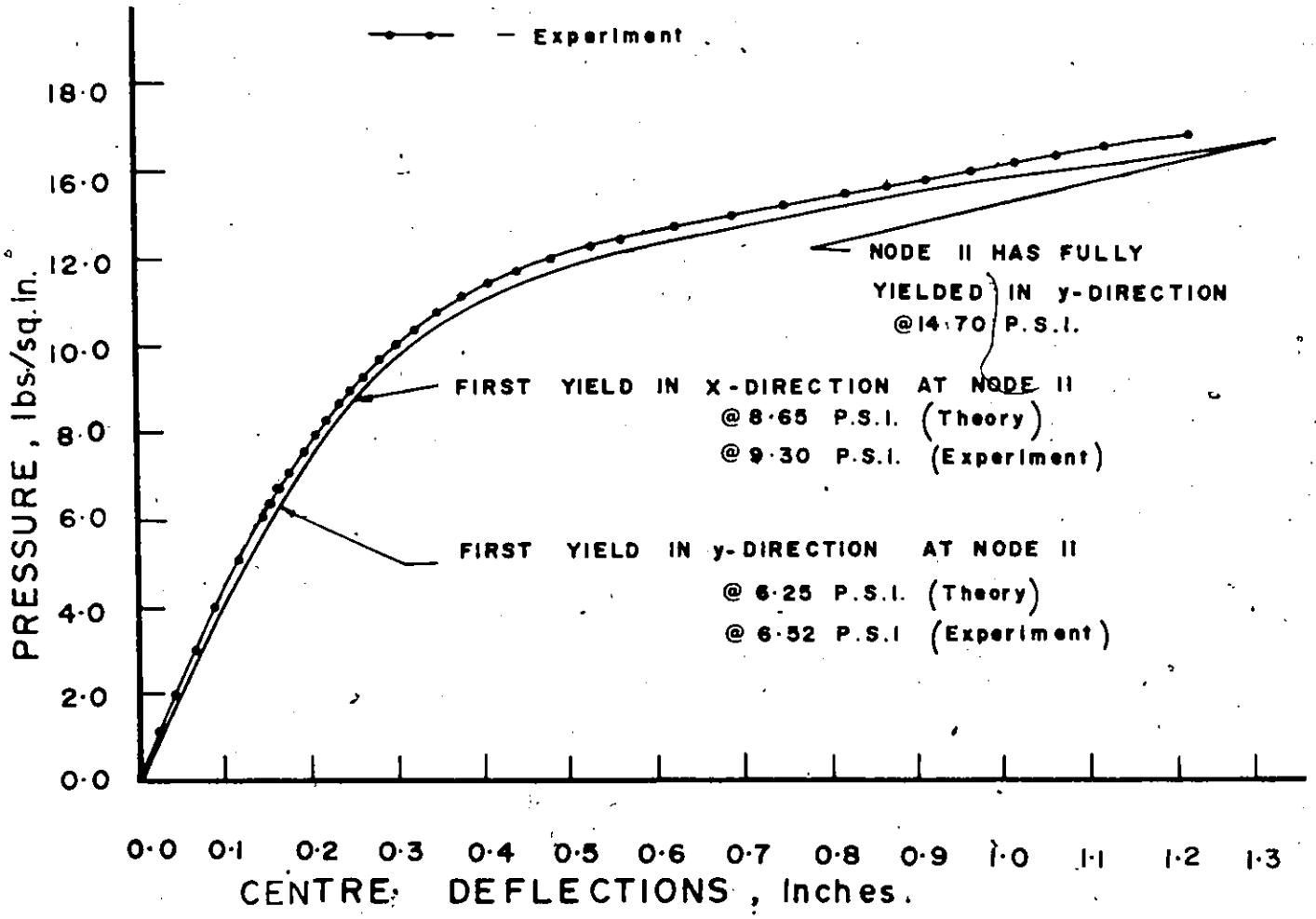

Figure 7·1 COMPARISON OF THEORETICAL AND EXPERIMENTAL DEFLECTIONS AT CENTRAL POINT.

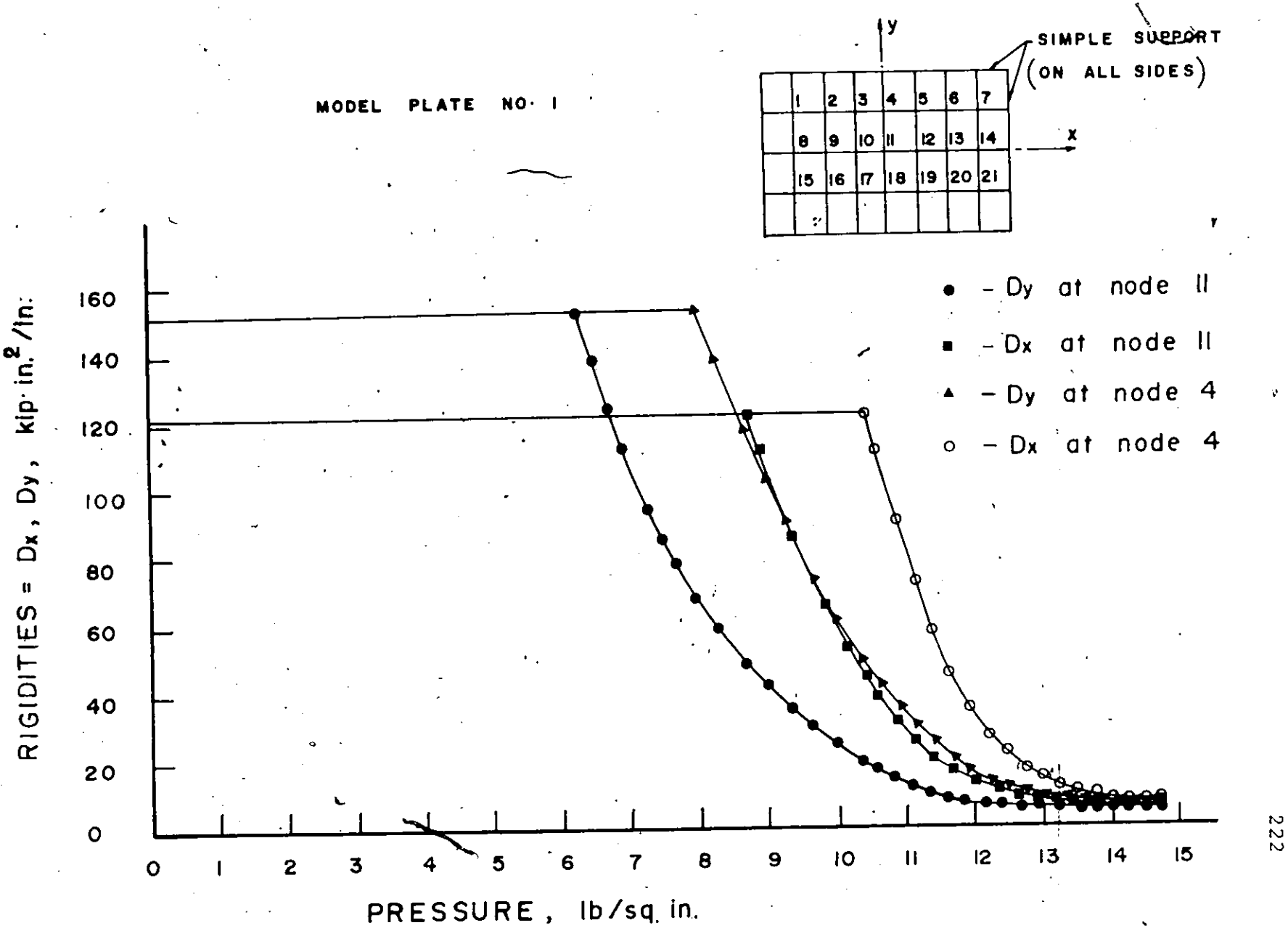

Figure 7·2 VARIATION OF EFFECTIVE RIGIDITIES WITH PRESSURE

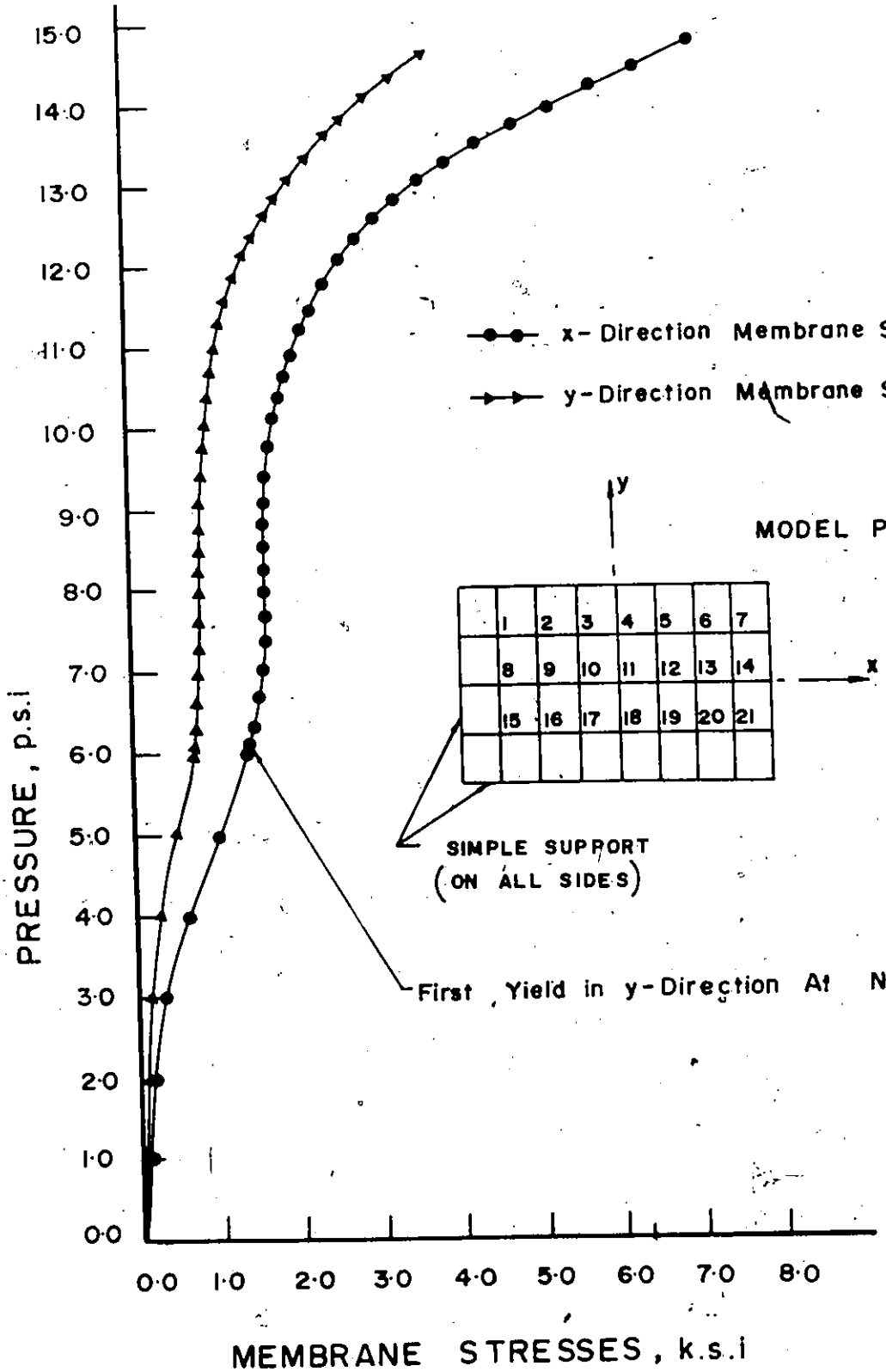

Figure 7·3 Variation Of Membrane Stresses With Pressure At Centre.

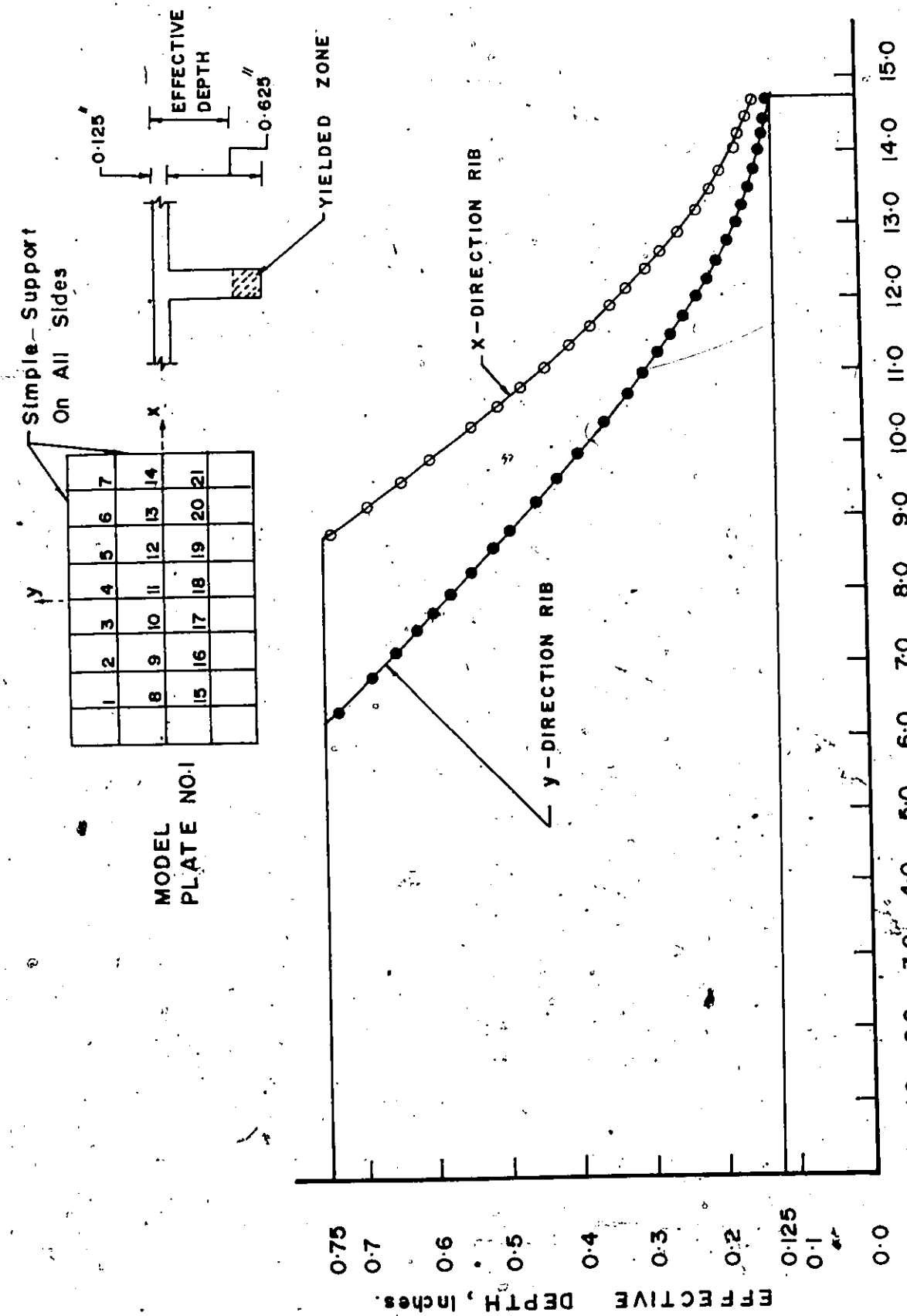

Figure 7·4 Variation Of Effective Depth At Centre With Load.

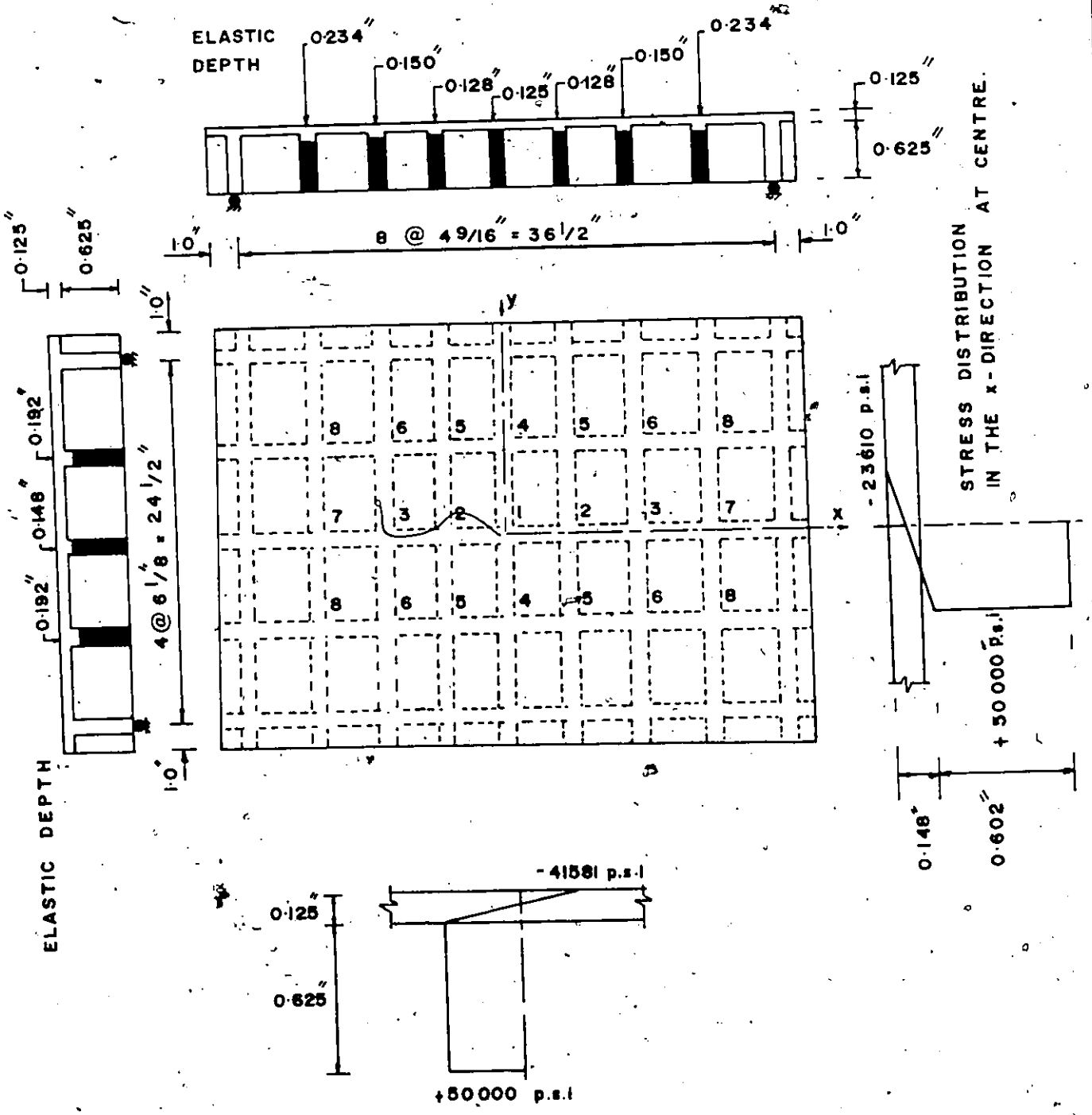

STRESS DISTRIBUTION IN THE y-DIRECTION AT CENTRE.

Figure 7·5 SEQUENCES OF YIELDING OF RIBS ALONG y- AND x- CENTRAL AXES

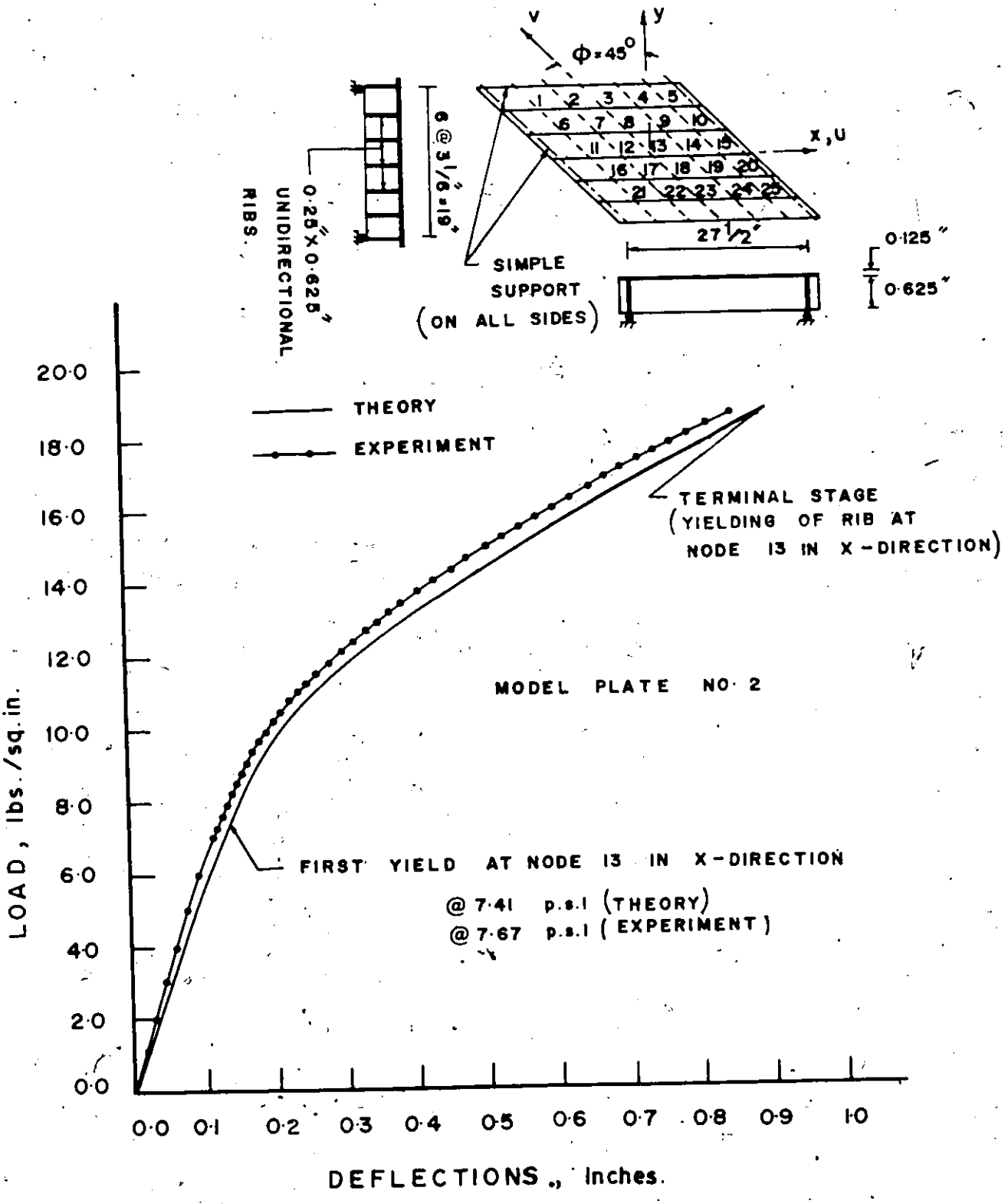

Figure 7.6 LOAD VERSUS CENTRE DEFLECTION

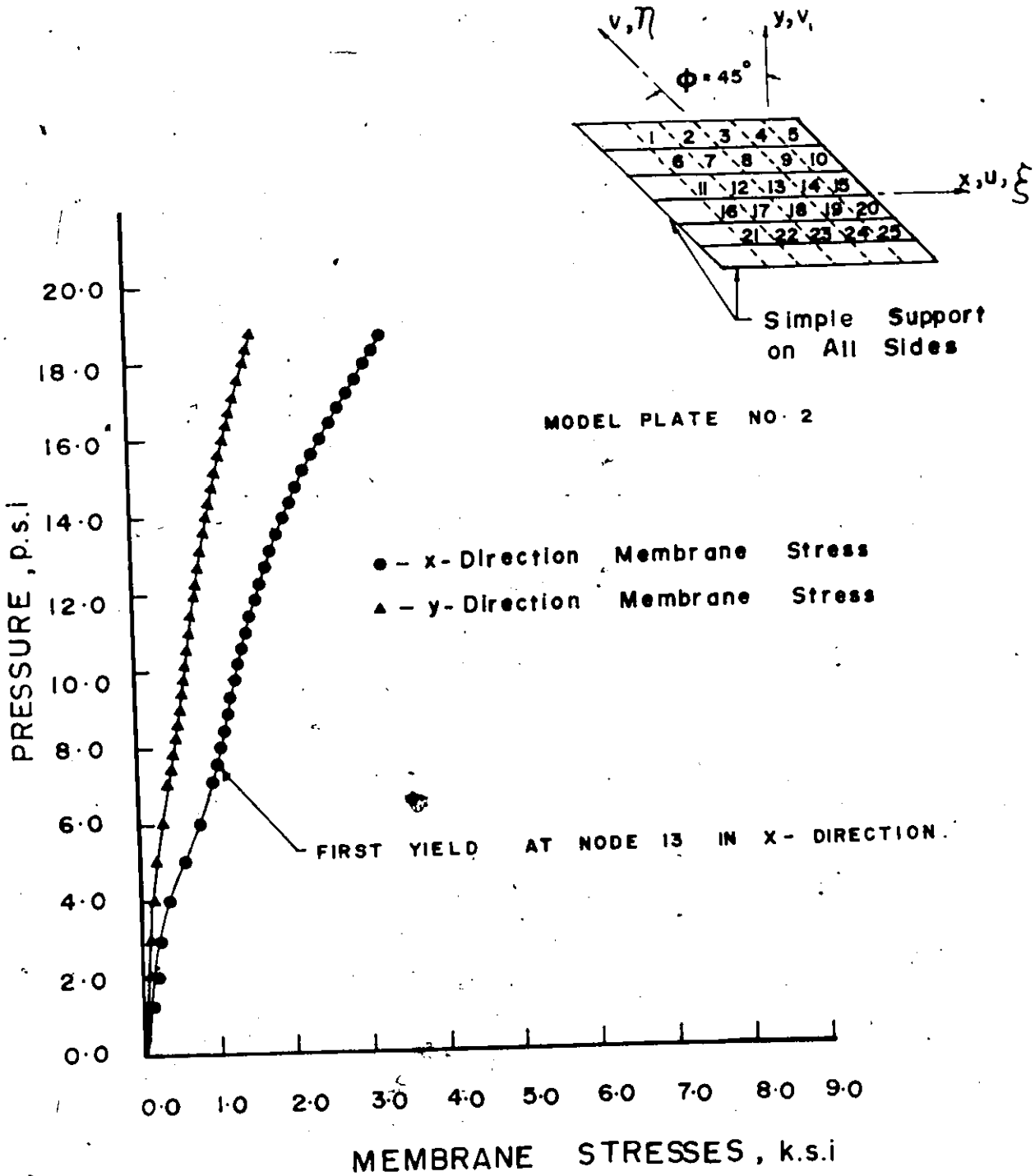

Figure 7·7 VARIATION OF MEMBRANE STRESSES AT CENTRE WITH PRESSURE.

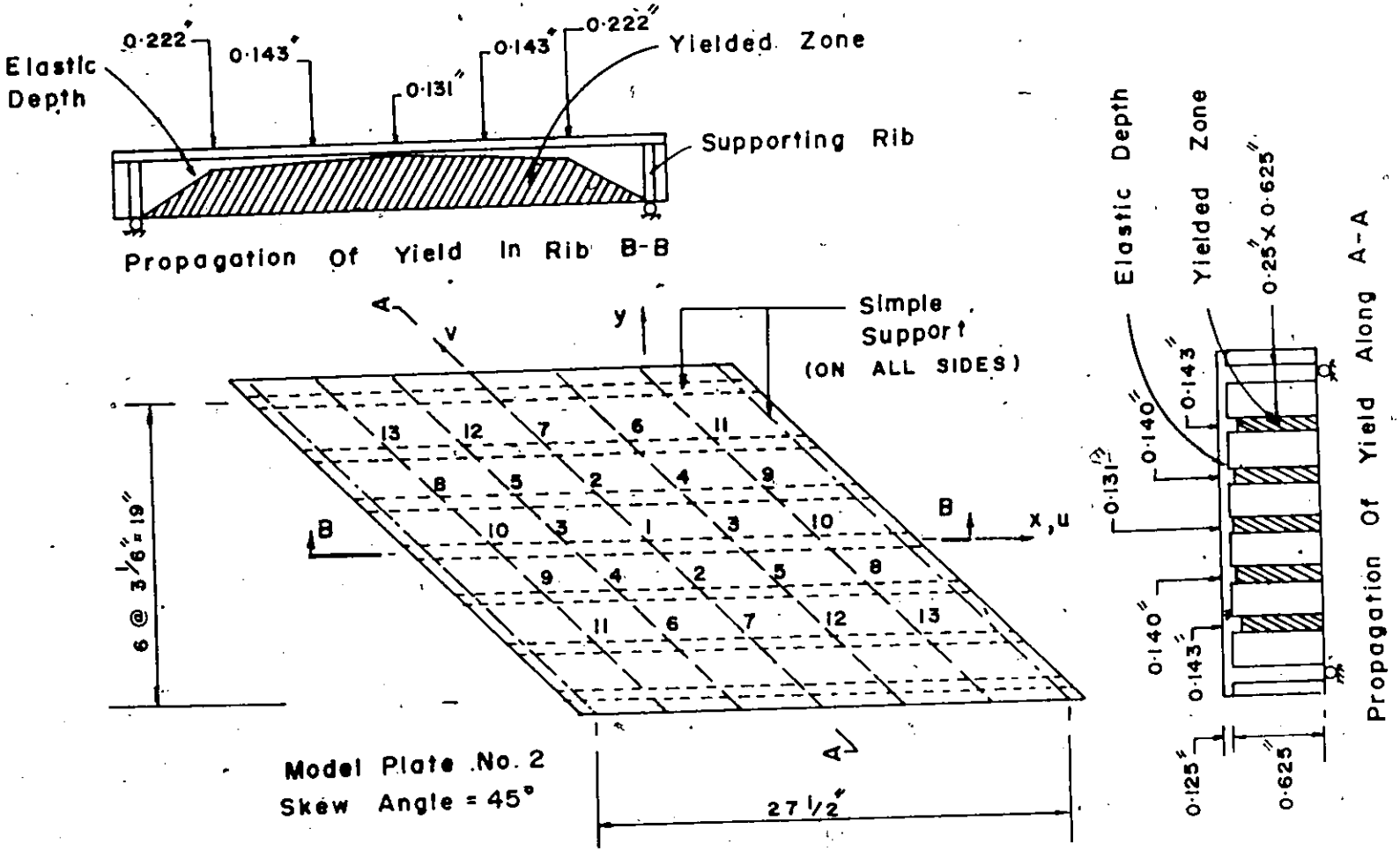

Figure 7·8 SEQUENCES OF YIELDING OF RIBS AT DISCRETE POINTS.

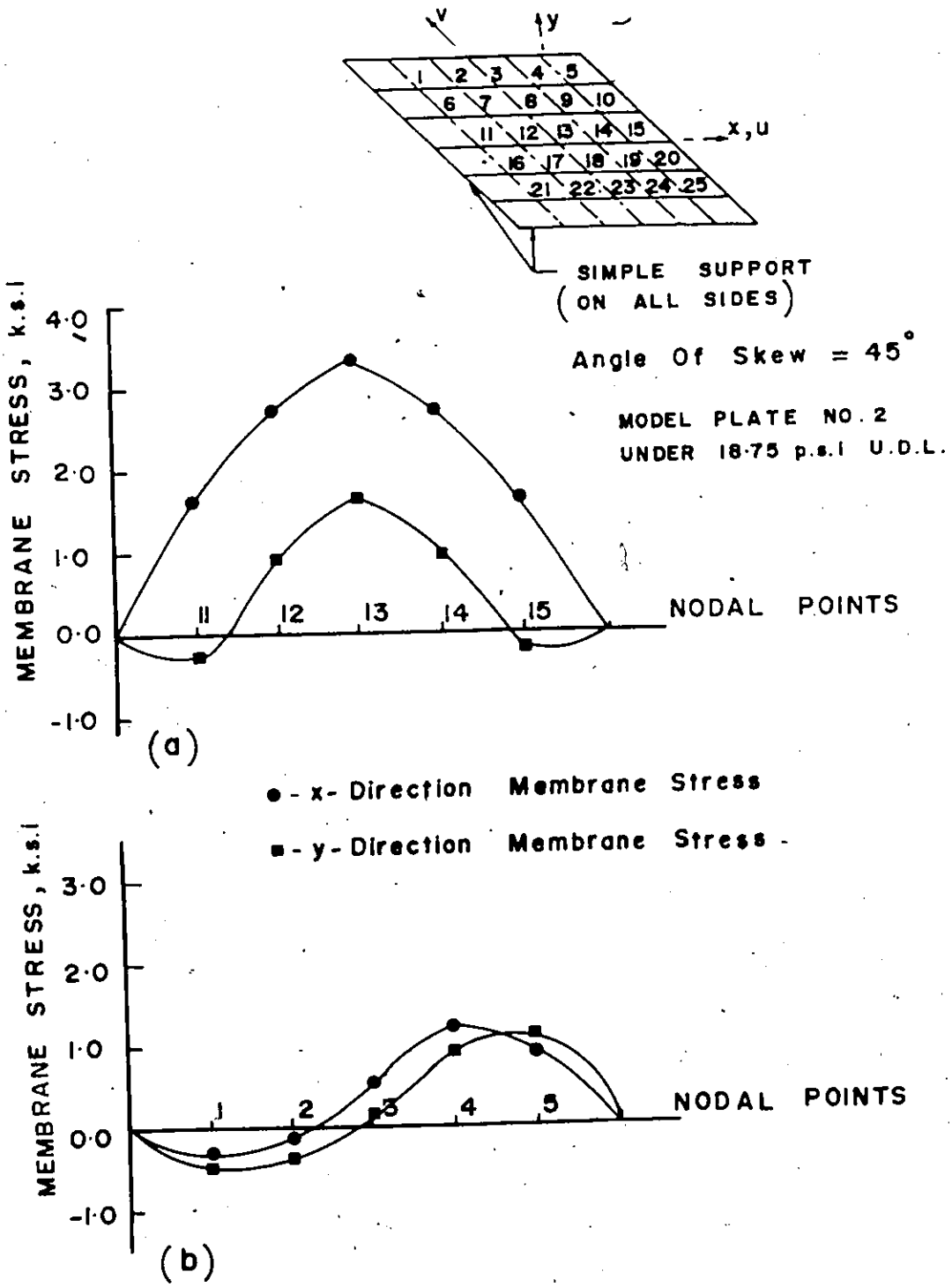

Figure 7·9 Distribution Of Membrane Stresses.

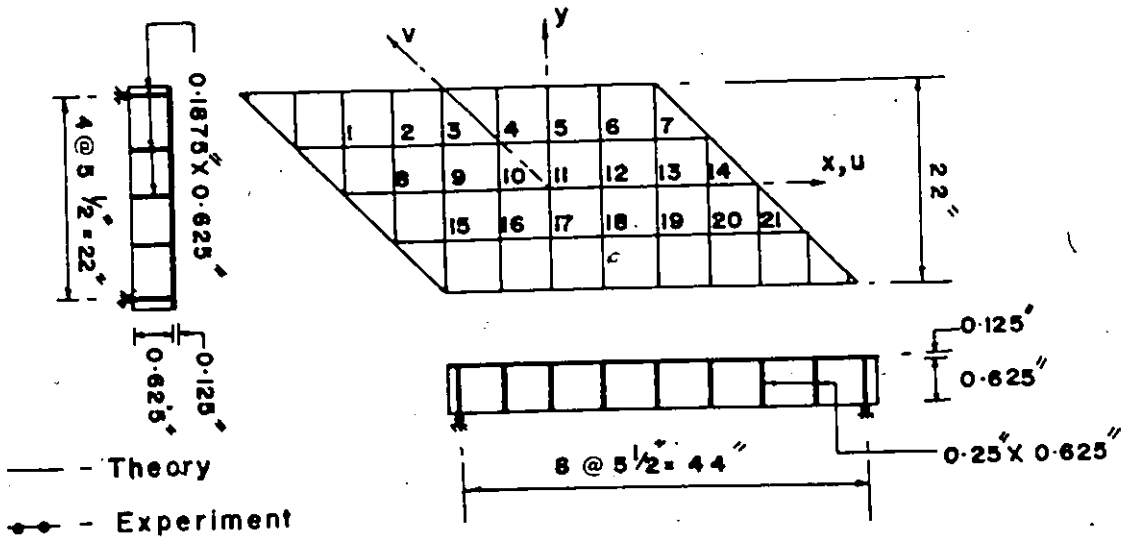

Angle of Skew = 45°

Model Plate No. 3

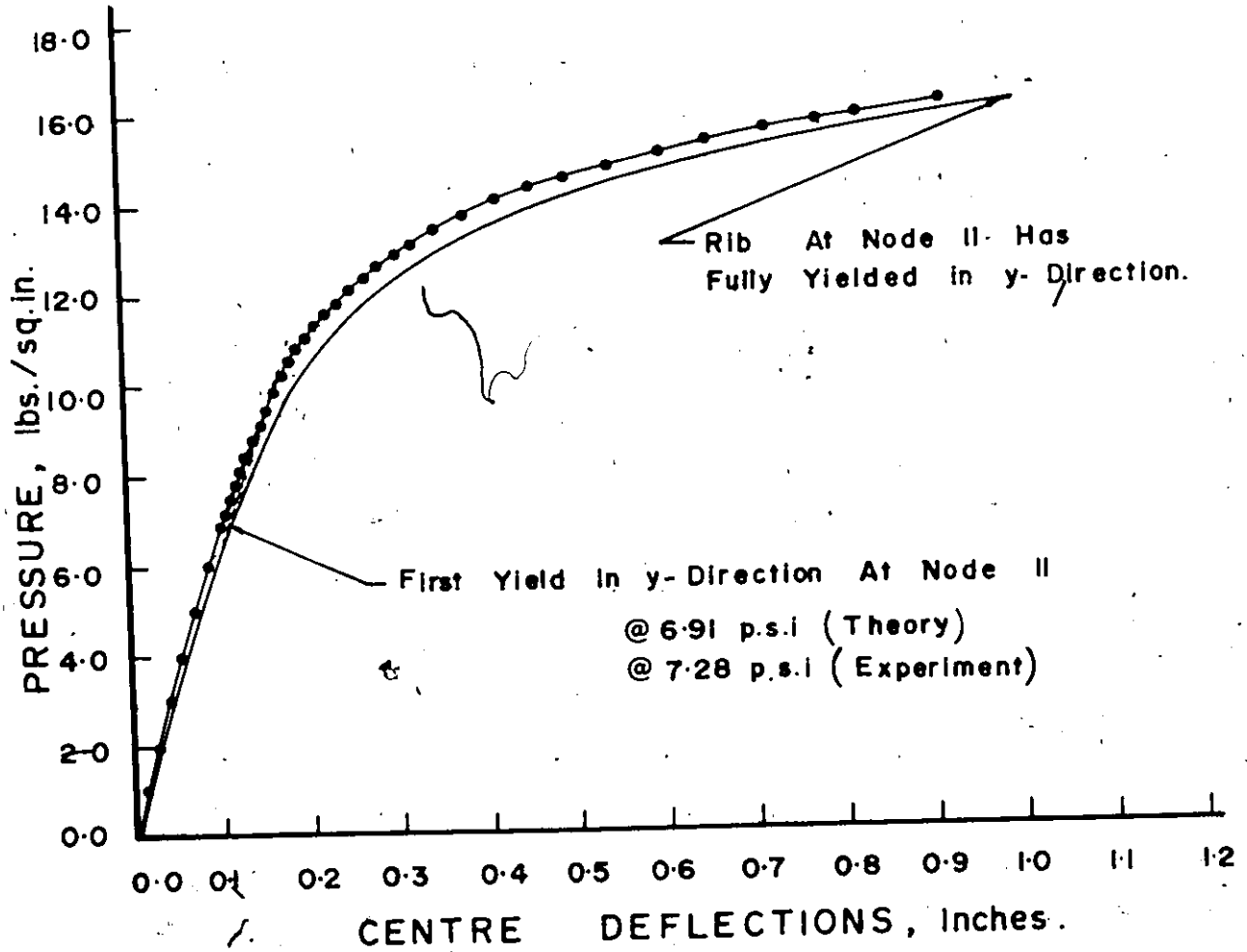

Fig. 7·10 COMPARISON OF THEORETICAL AND EXPERIMENTAL DEFLECTIONS AT NODE 11.

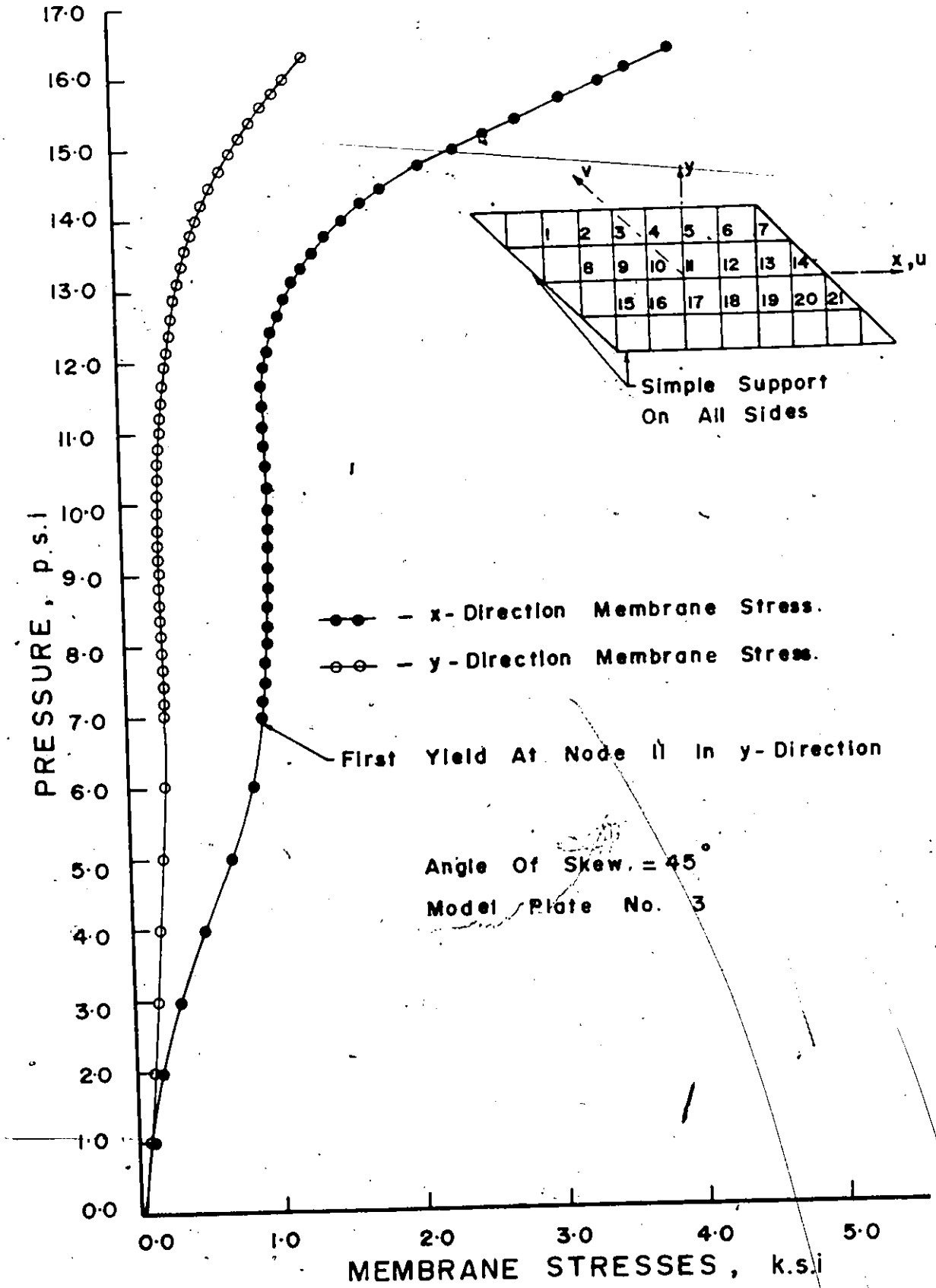

Figure 7·11 Variation Of Membrane Stresses At Centre With Pressure.

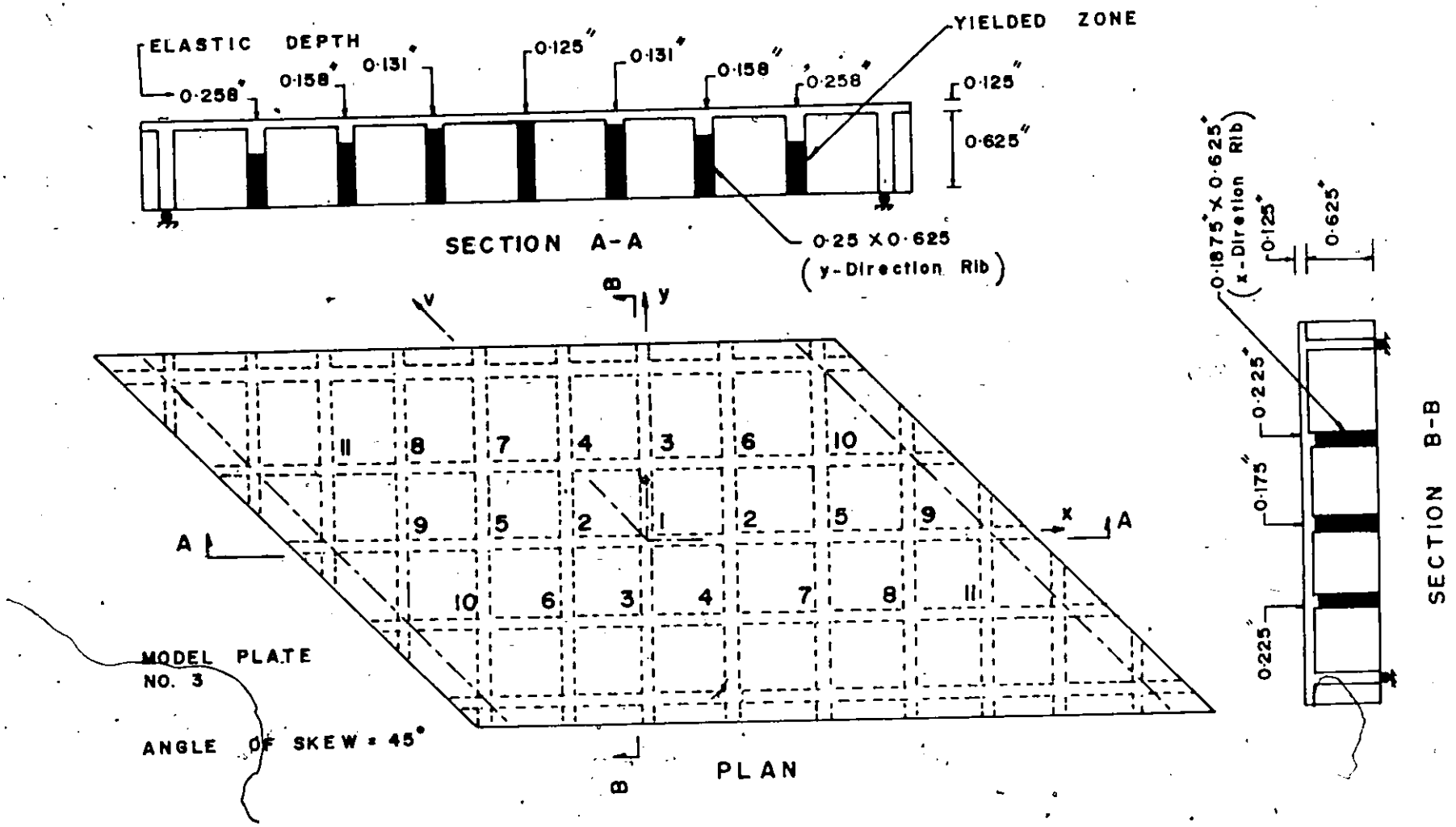

Figure 7·12 Sequences Of Yielding Of Ribs In the y- And x- Directions.

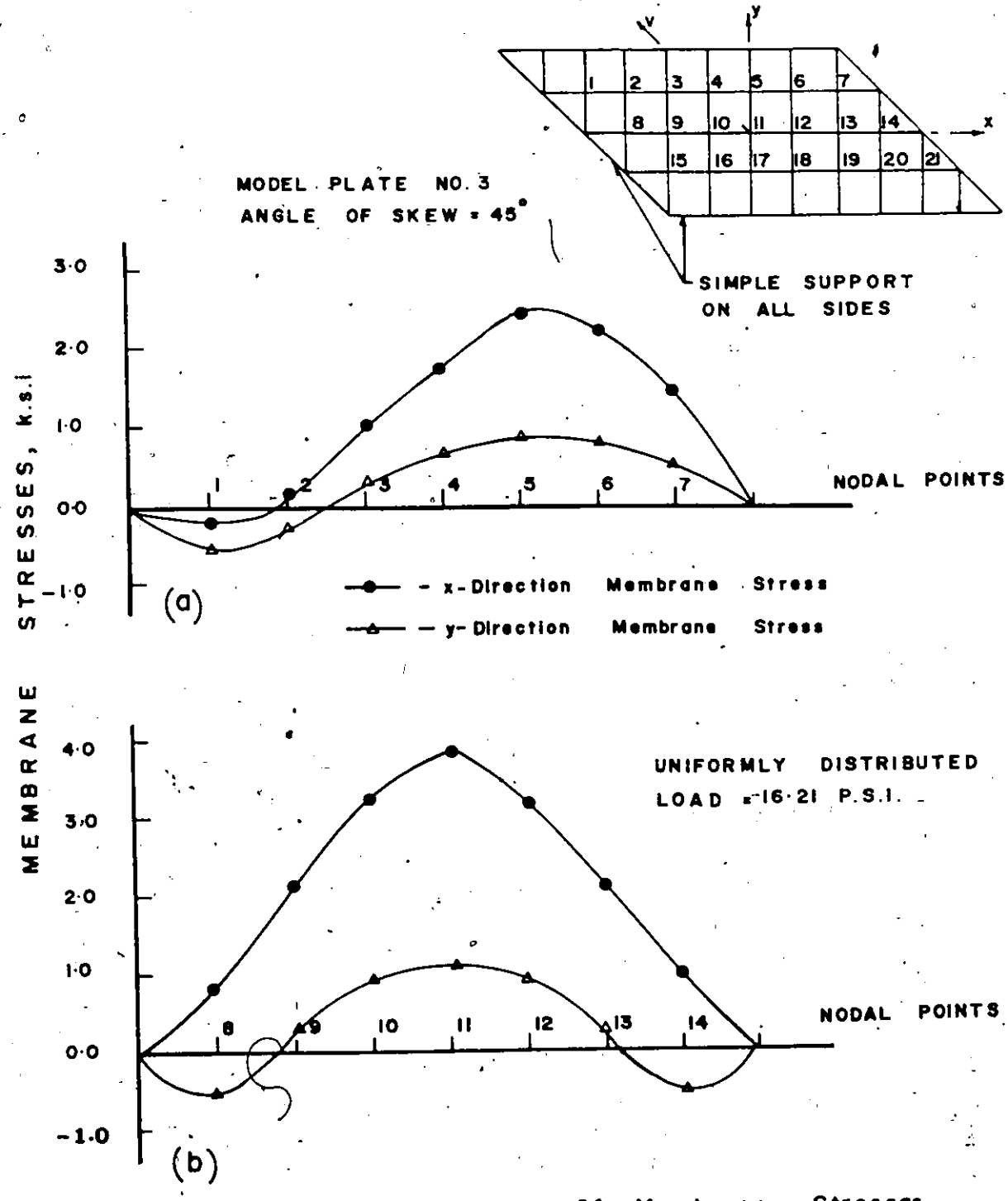

Figure 7·13 Variation Of Membrane Stresses.

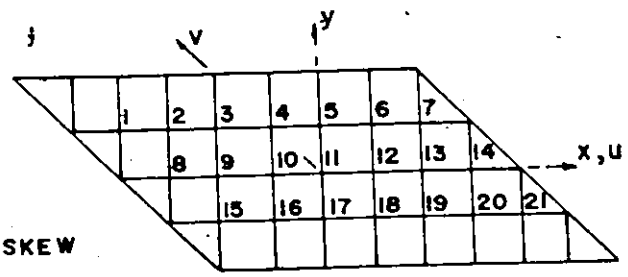

ANGLE OF SKEW
= 45°
MODEL PLATE NO. 3

— y-Direction Effective Depth At Node 11
— x-Direction Effective Depth At Node 11
— y-Direction Effective Depth At Node 5
— x-Direction Effective Depth At Node 5

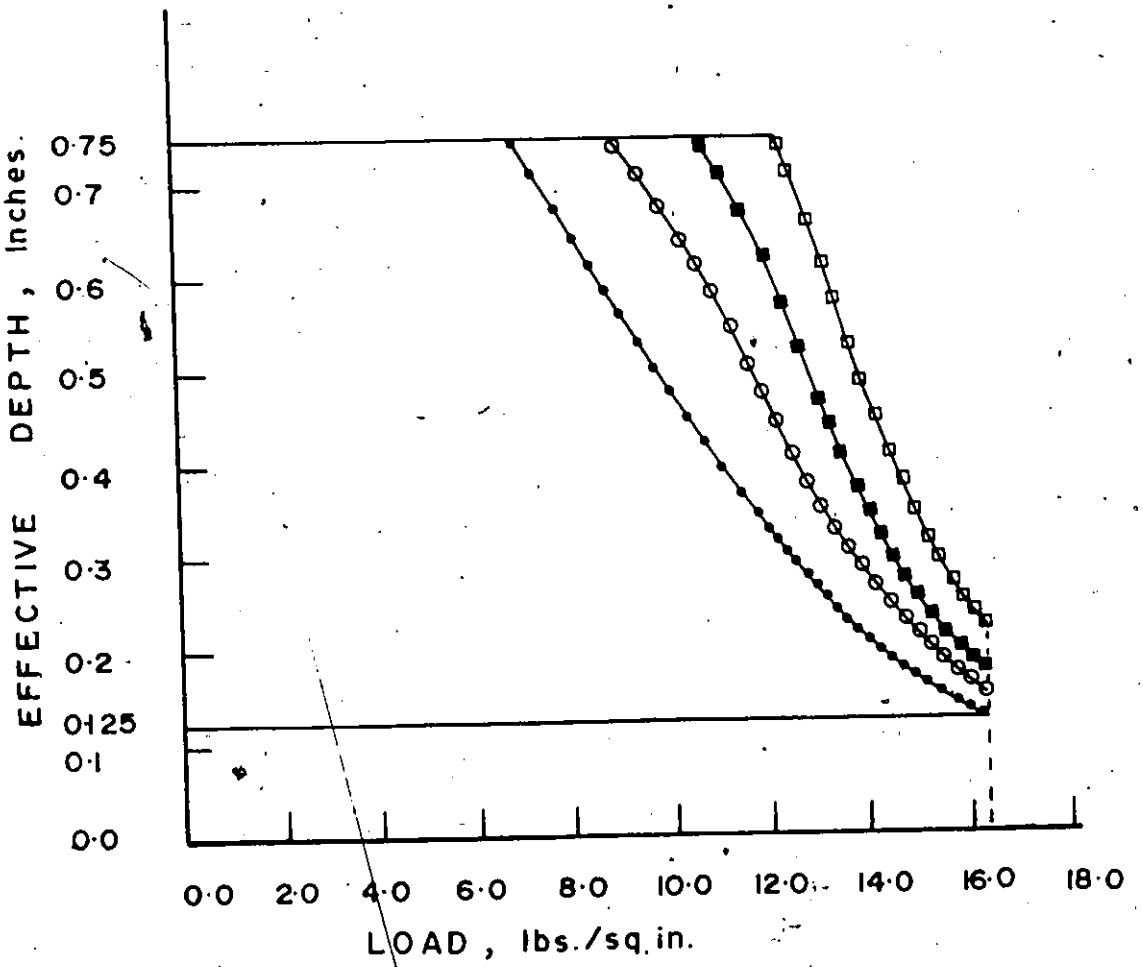

Figure 7·14 Variation Of Effective Depth With Load.

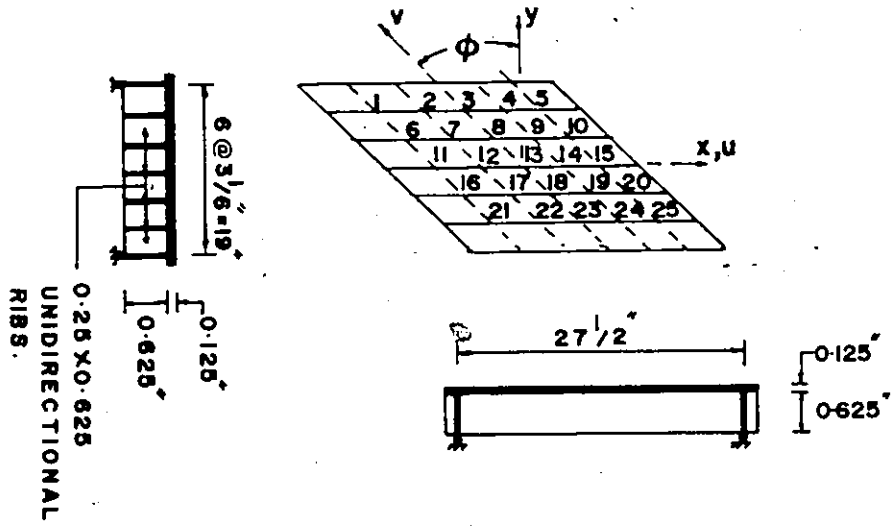

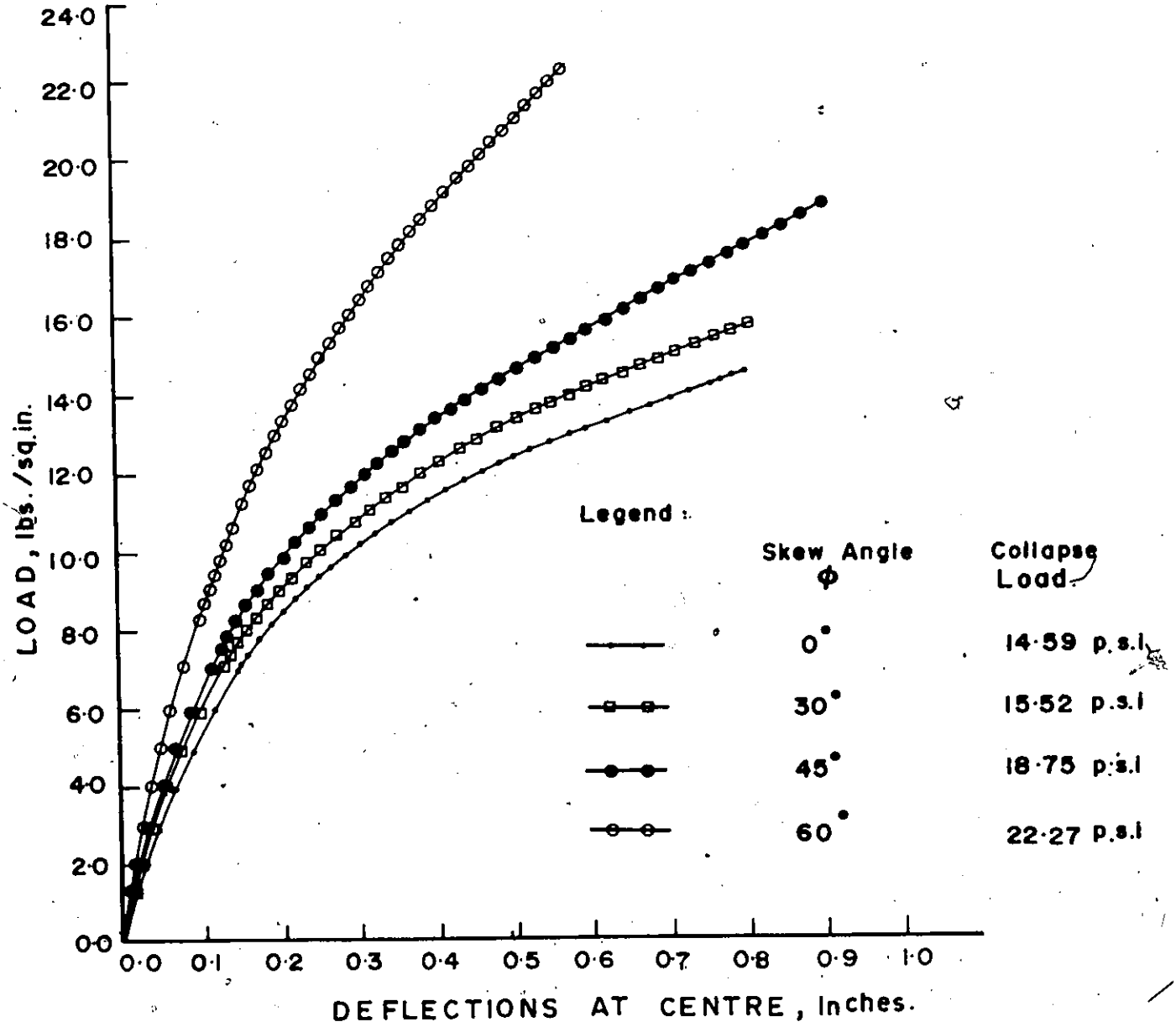

Figure 7·15 Load Versus Centre Deflections.

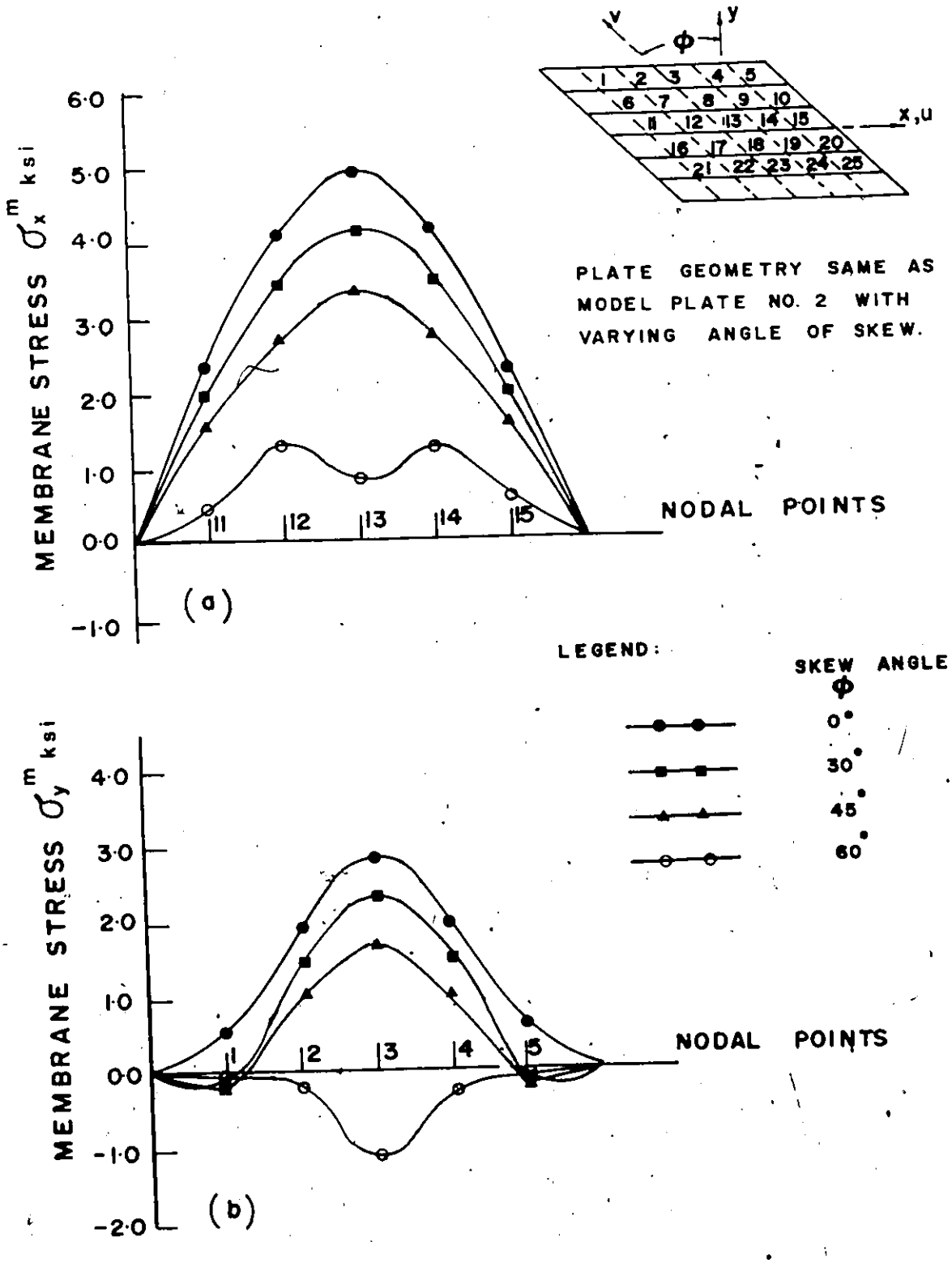

Figure 7·16 Variation Of Membrane Stresses. At Collapse Loads in Fig. 7·15

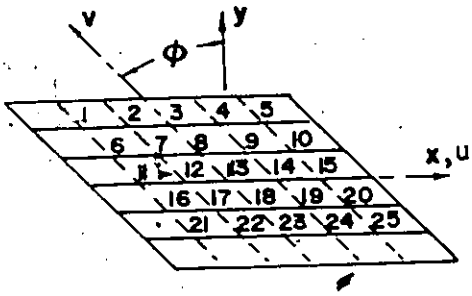

PLATE GEOMETRY SAME AS MODEL PLATE NO. 2 WITH VARYING ANGLE OF SKEW.

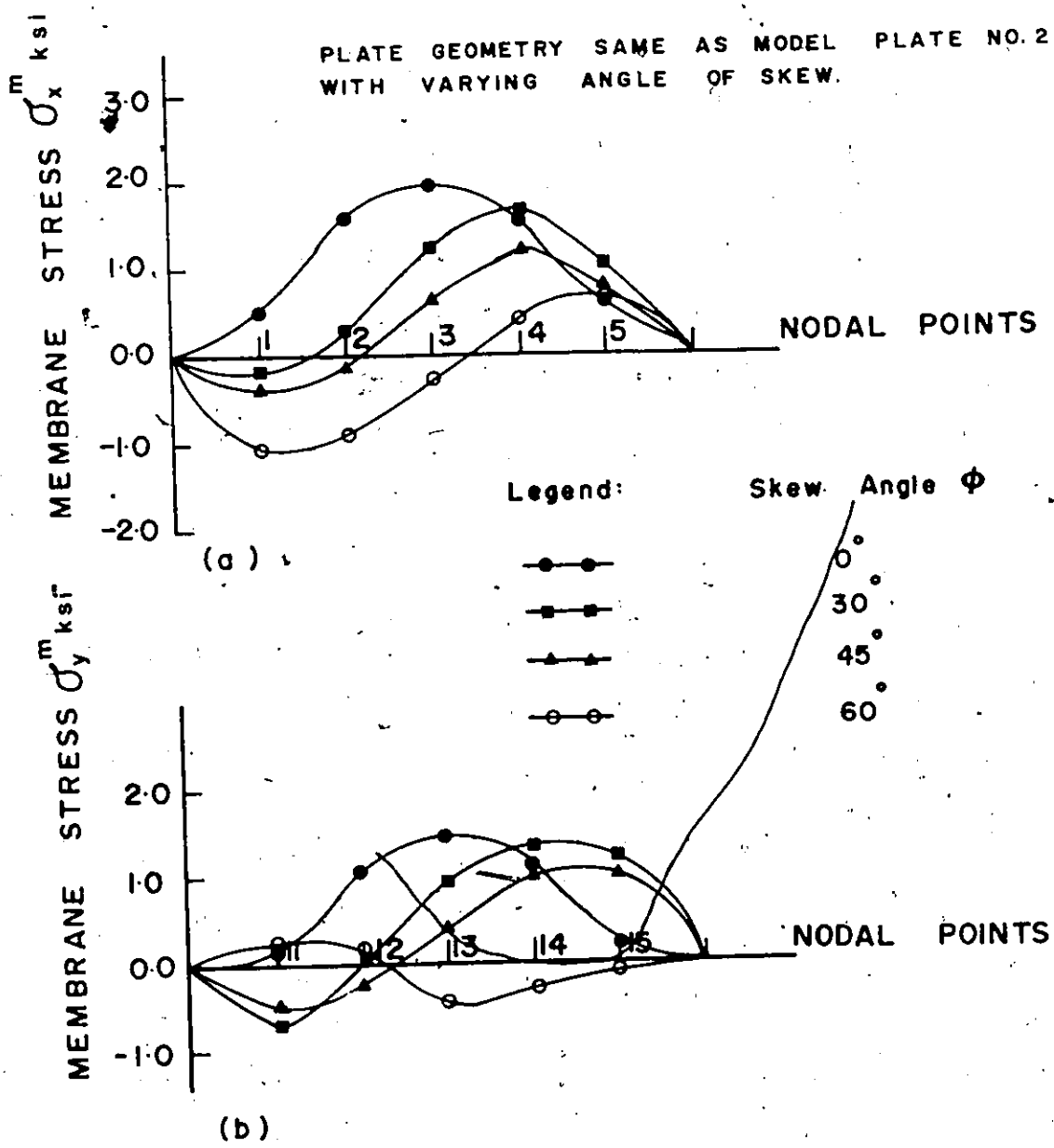

Figure 7·17 Variation Of Membrane Stresses.

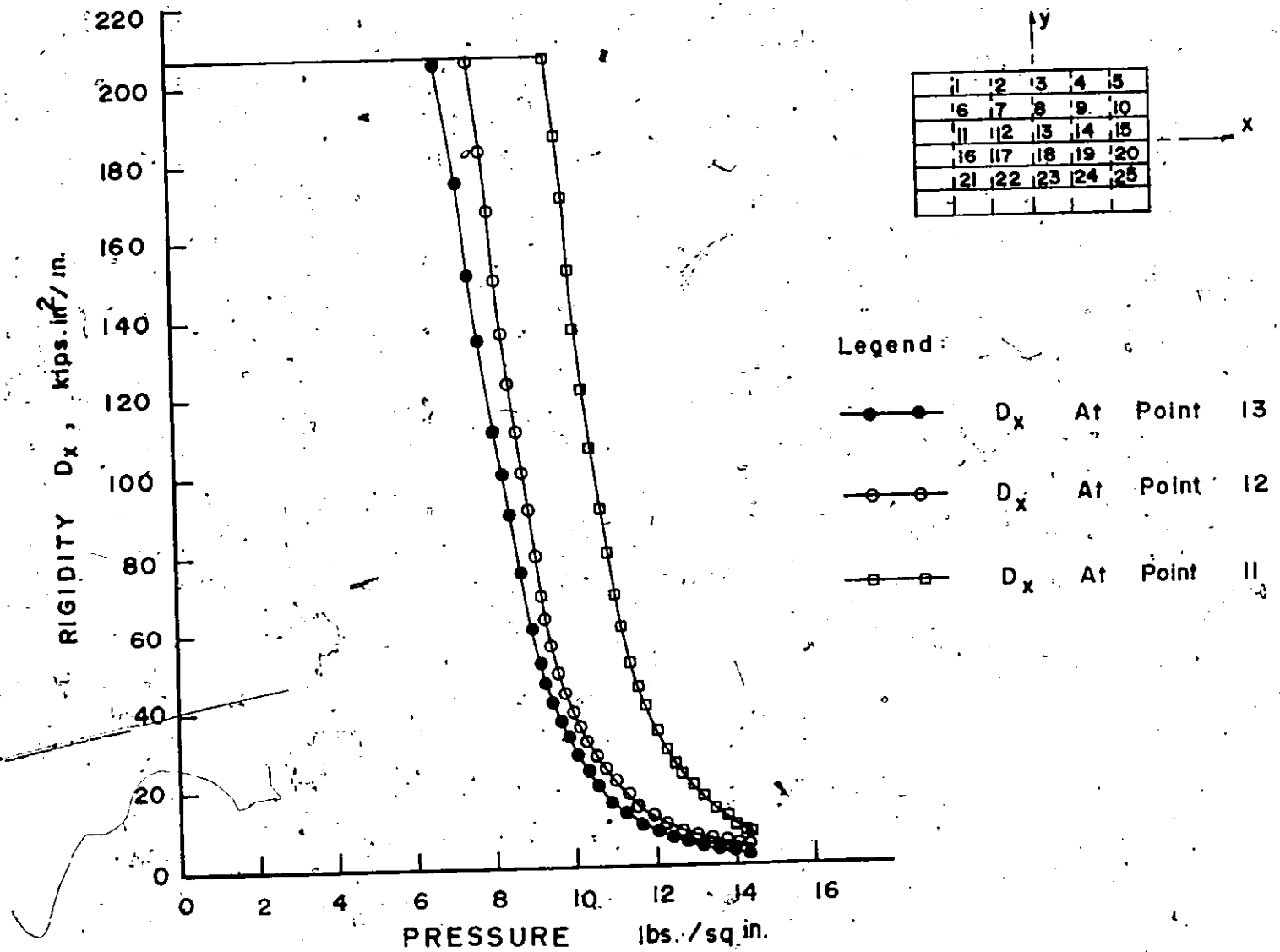

Figure 7.18 Variation Of Effective Rigidity With Pressure

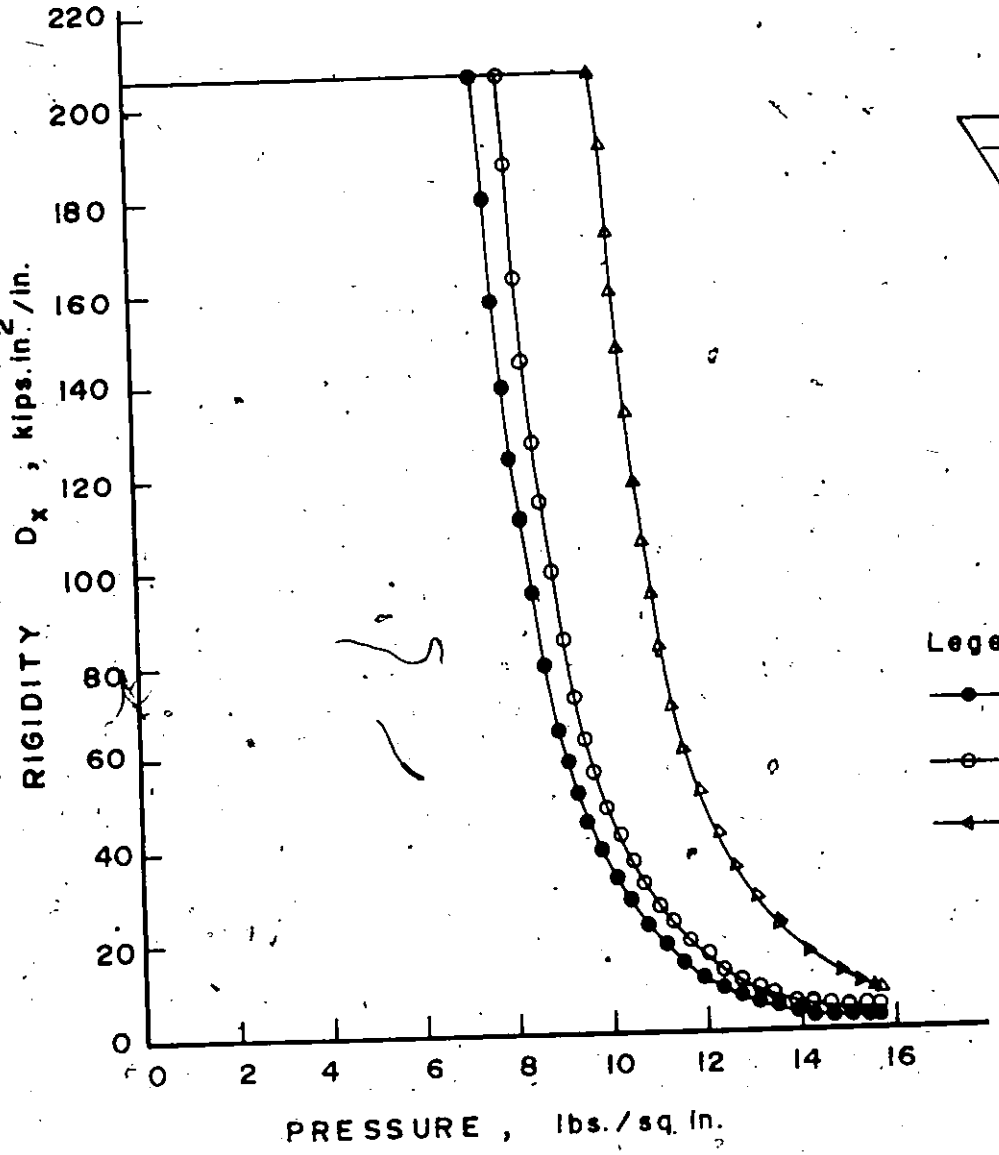

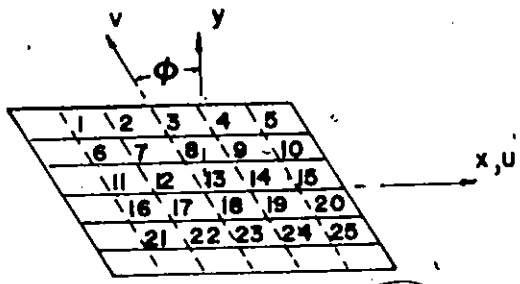

SKEW ANGLE $\Phi = 30^\circ$

Legend :

D_x At Point 13

D_x At Point 12

D At Point 11

Figure 7·19 Variation Of Effective Rigidity With Pressure

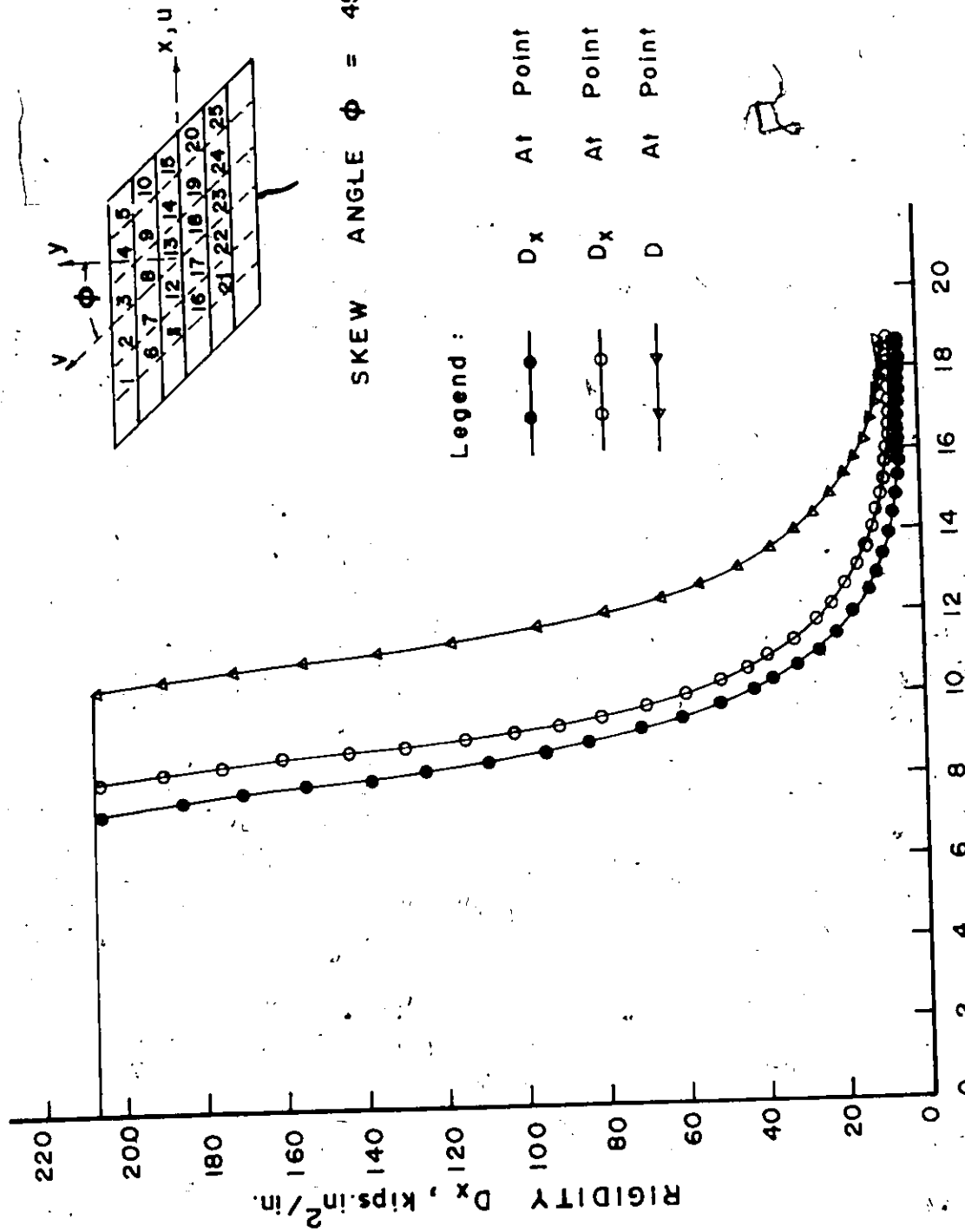

Figure 7.20 Variation Of Effective Rigidity With Pressure.

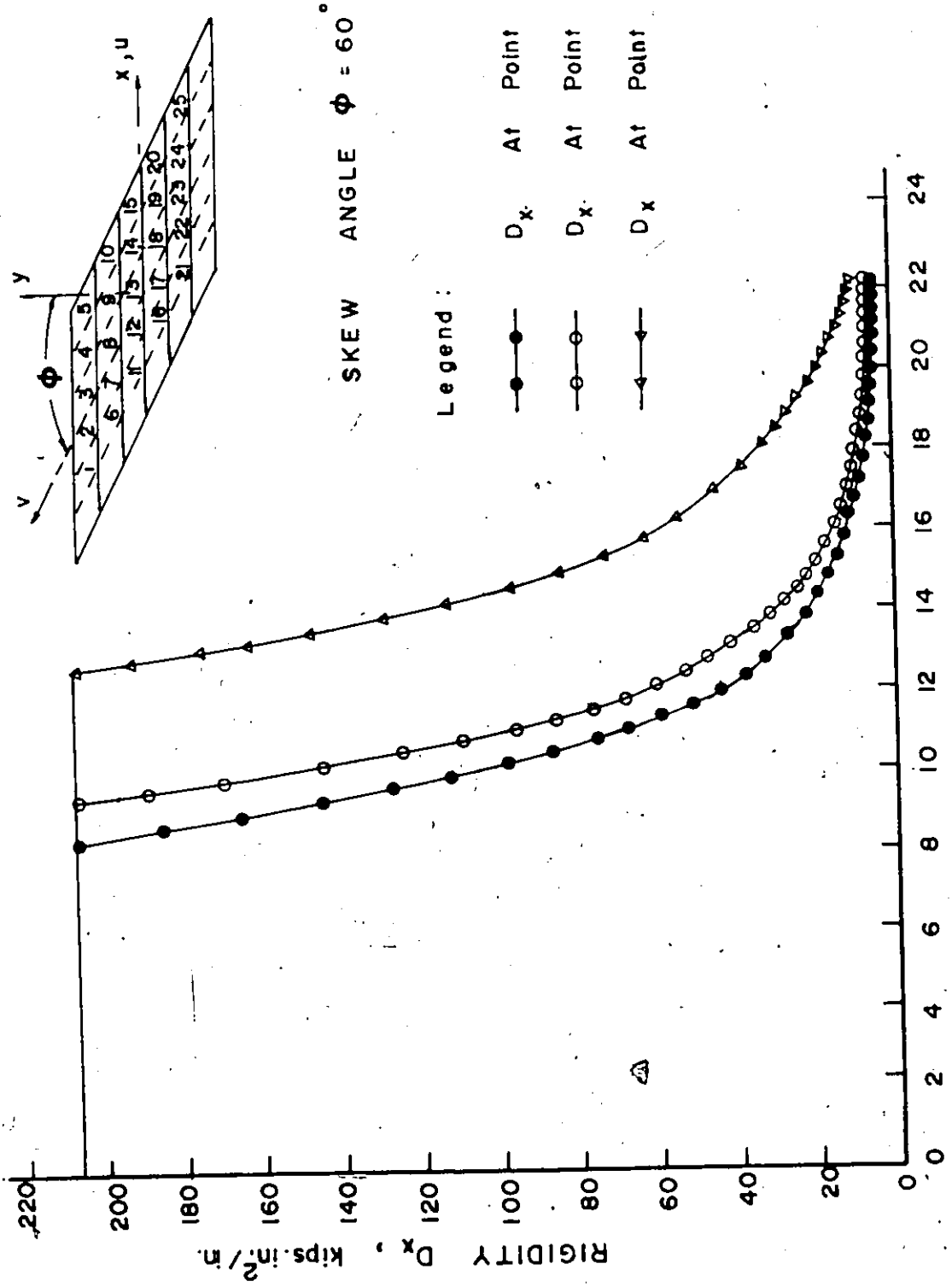

Figure 7·21 Variation Of Effective Rigidity With Pressure.

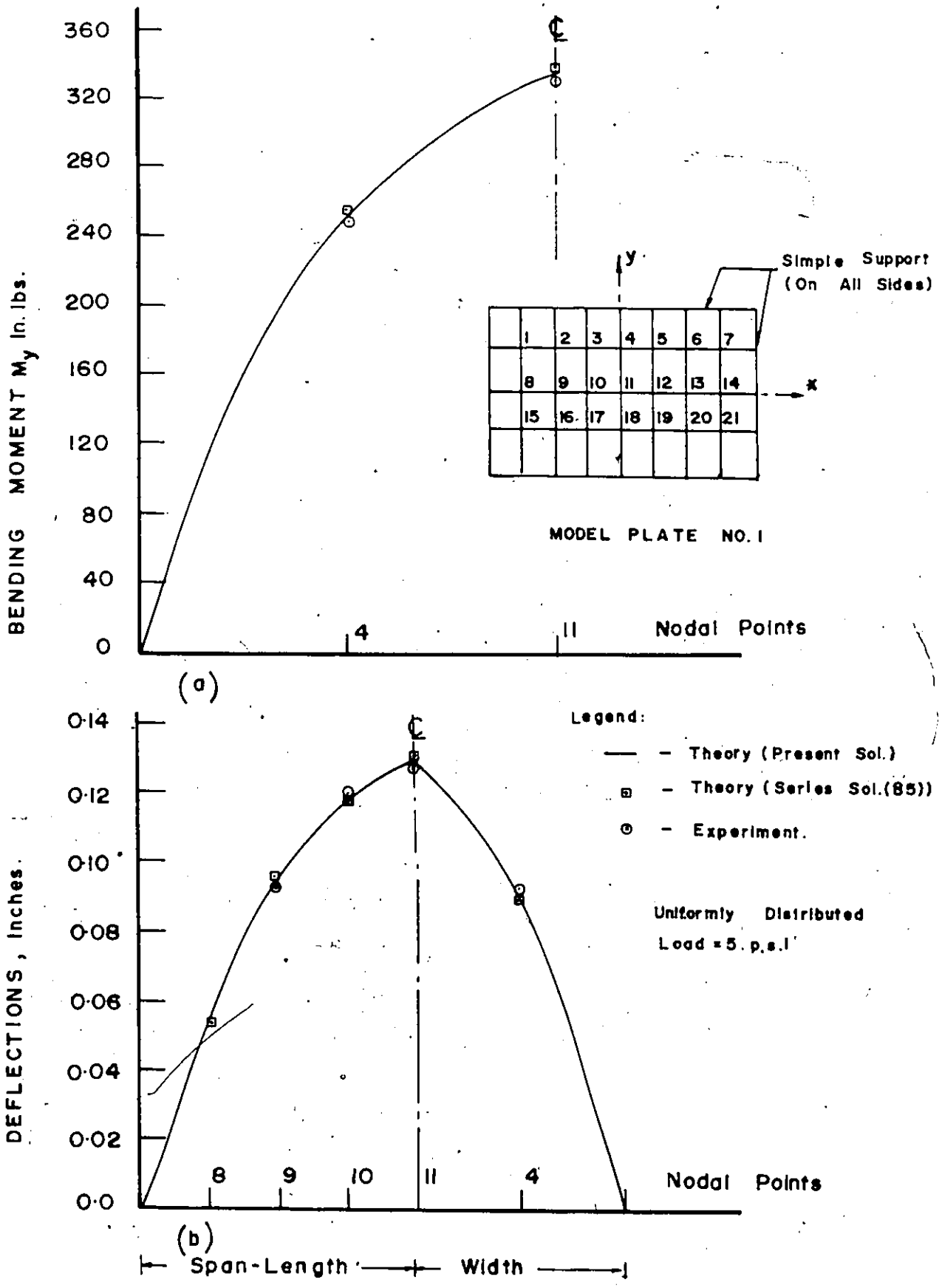

Figure 7·22 Variation Of(a) M_y & (b) Deflections.

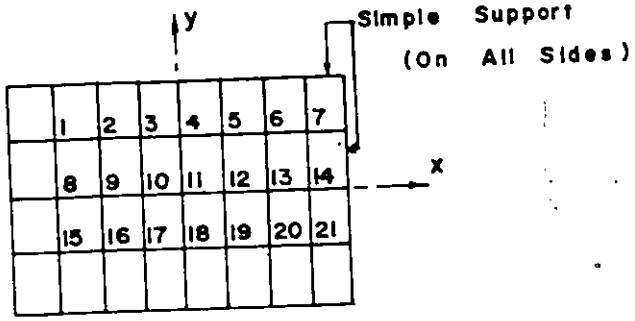

MODEL PLATE NO. 1

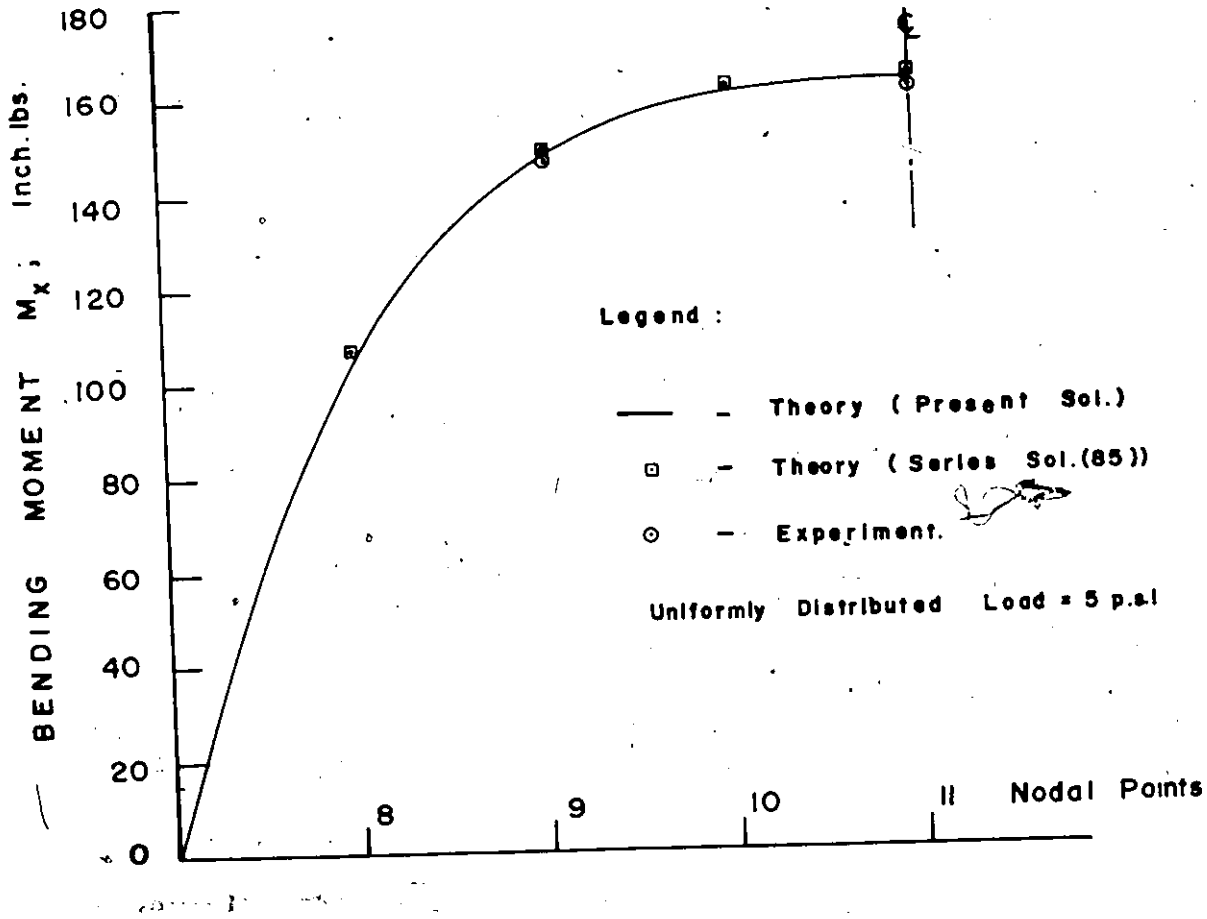

Figure 7·23 Variation Of M_x

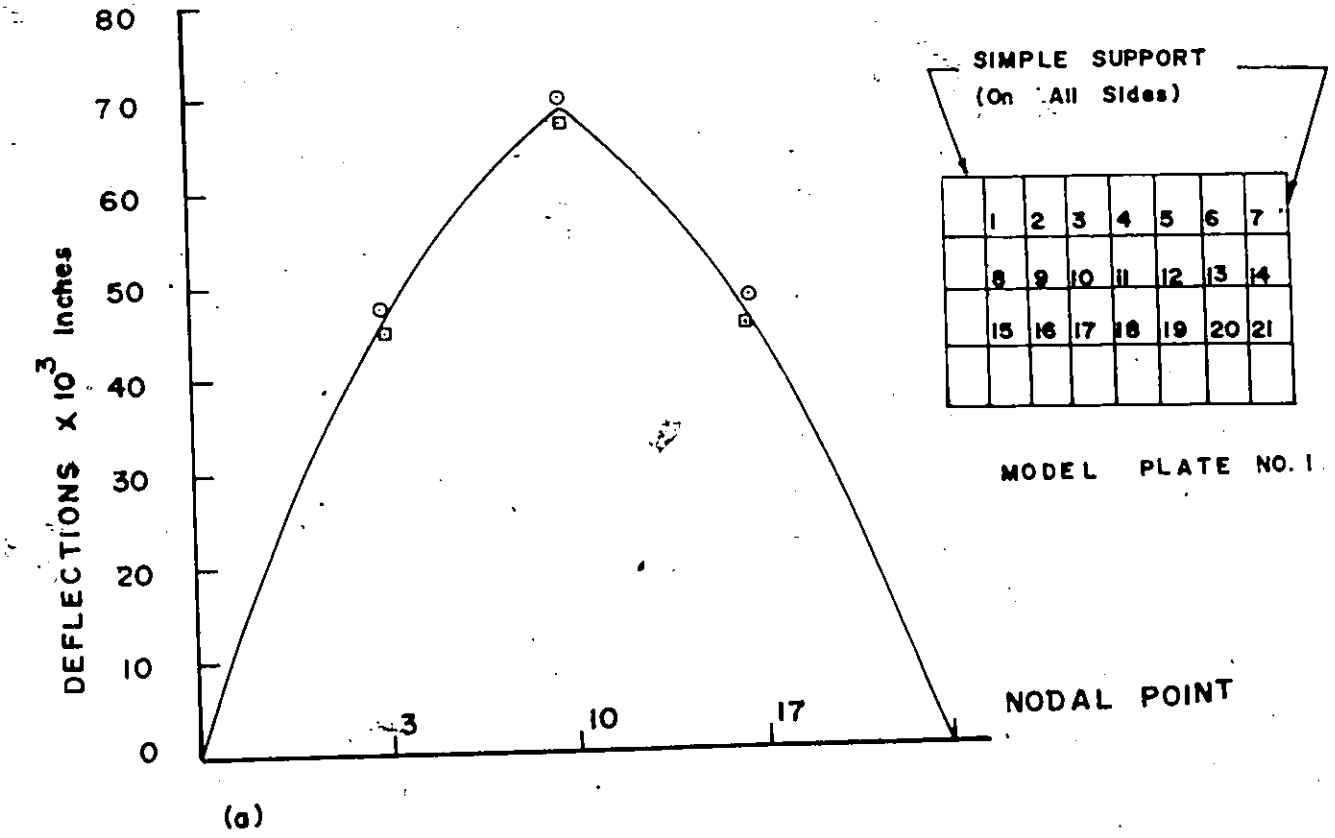

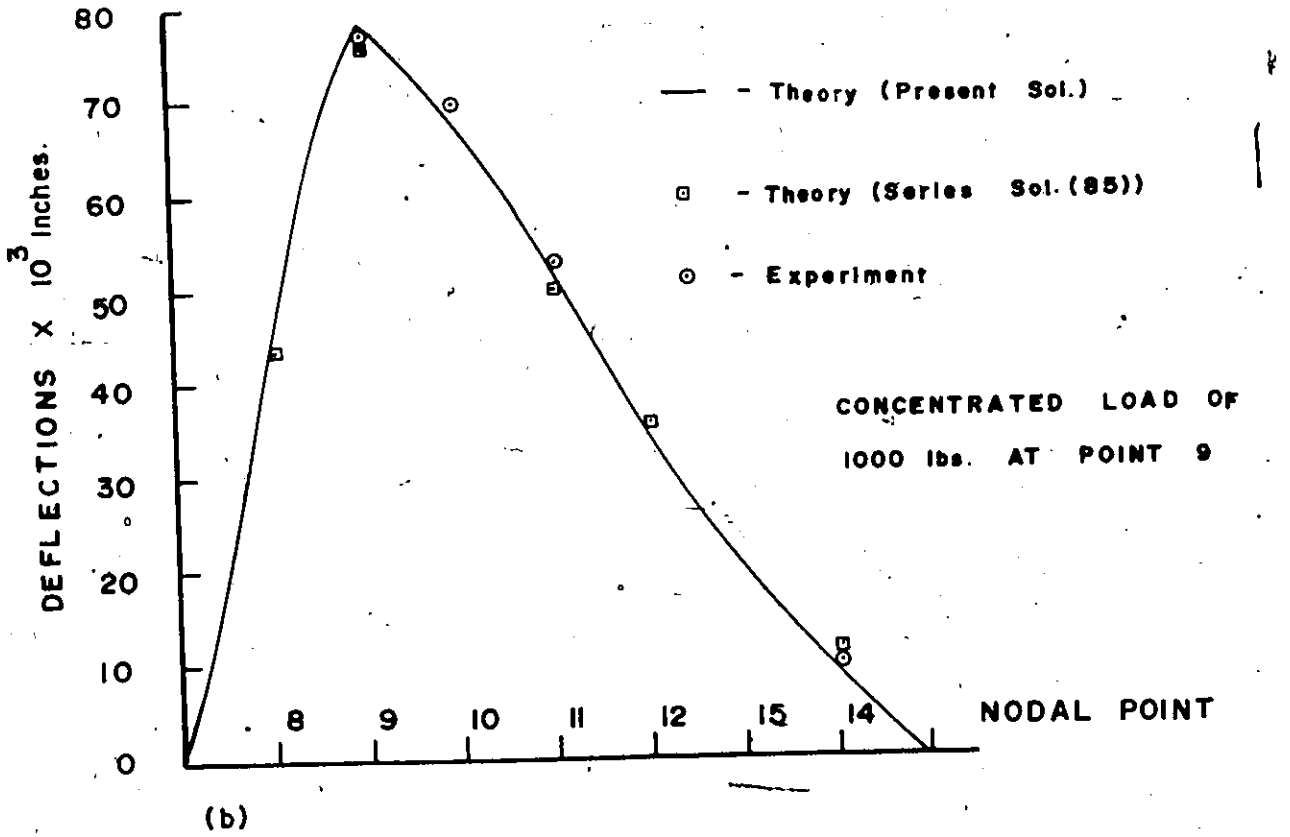

Fig. 7-24 Variation Of Deflection.

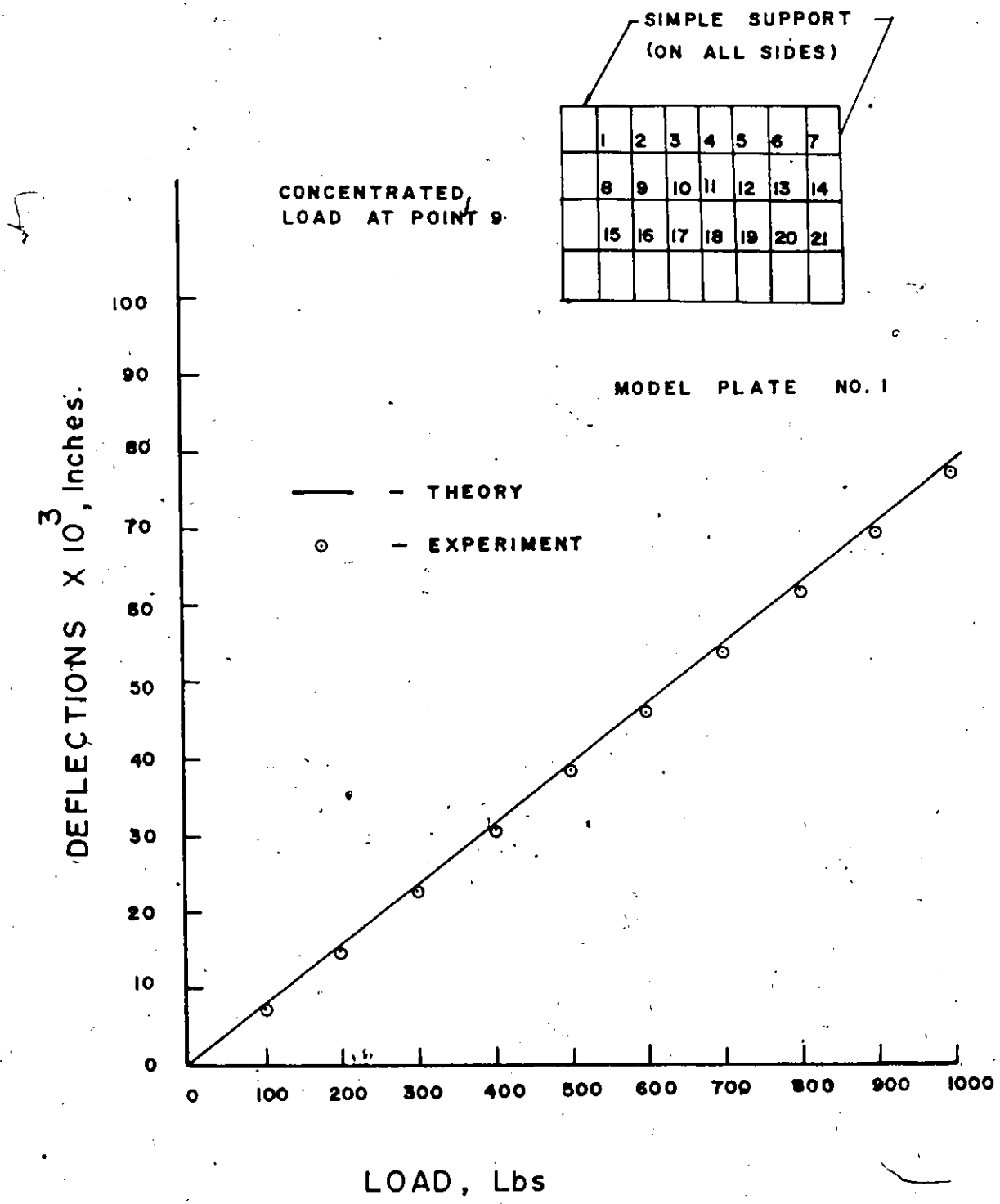

Figure 7·25 LOAD VERSUS DEFLECTION AT POINT 9

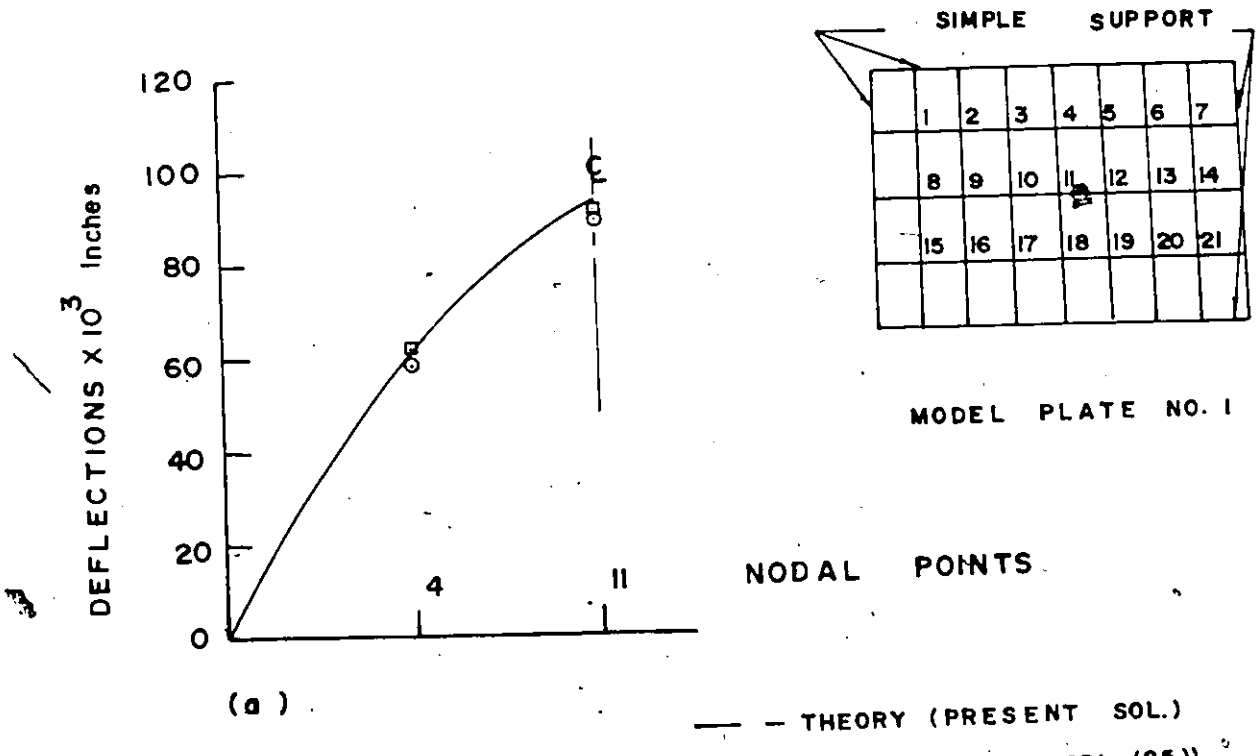

Figure 7·26 Variation Of Deflections.

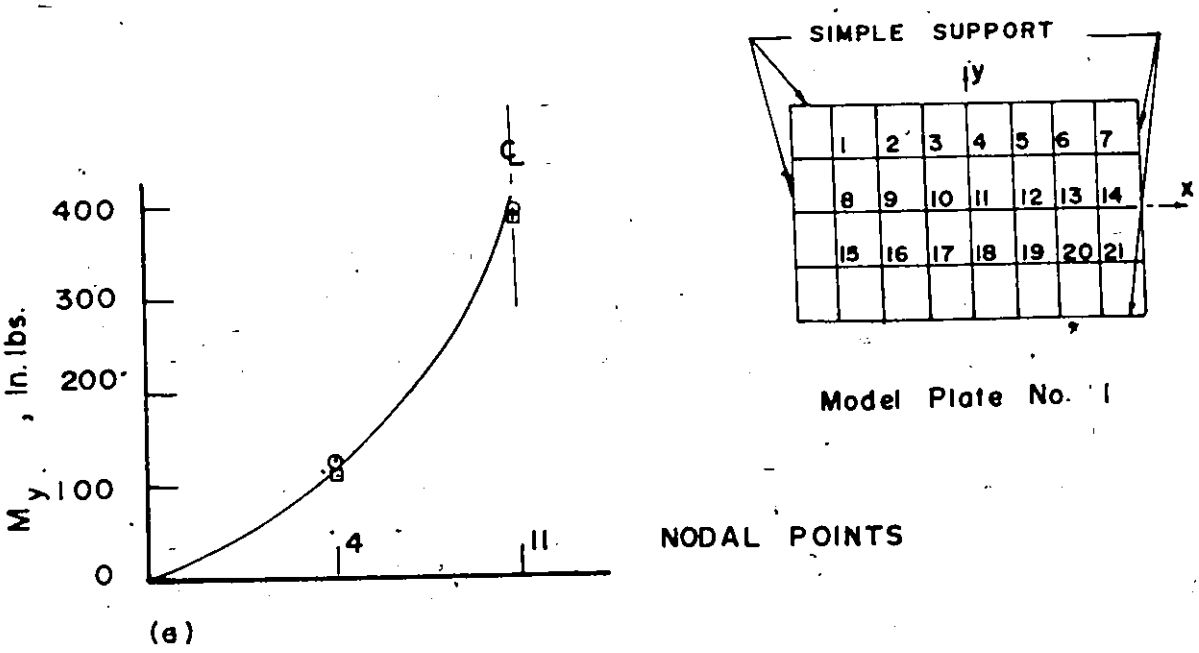

Fig. 7·27 Variation Of Bending Moments.

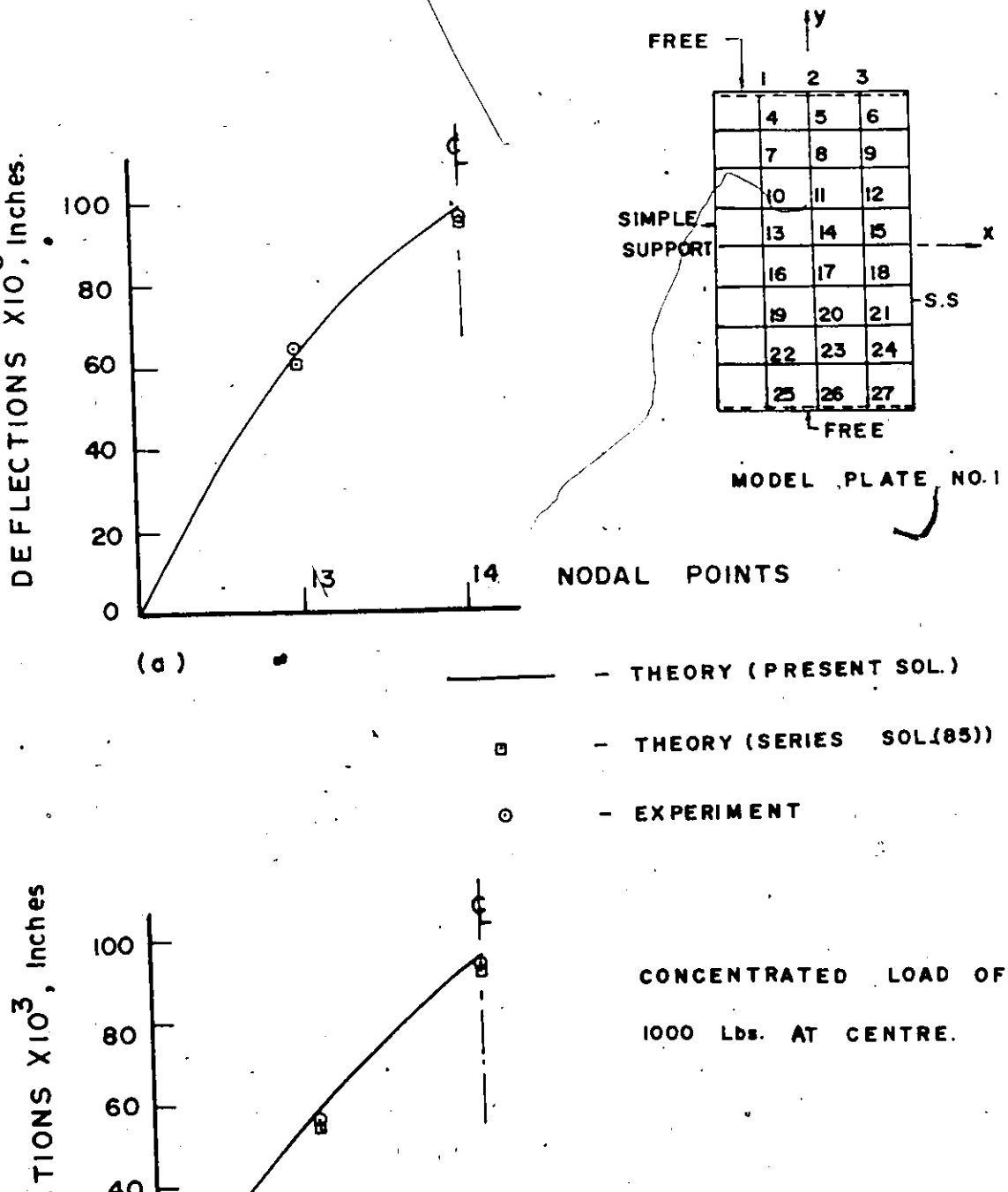

Fig. 7·28 Variation Of Deflections.

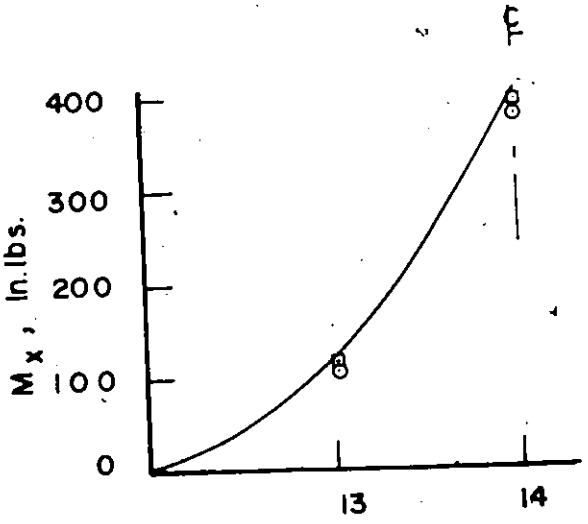

(a)

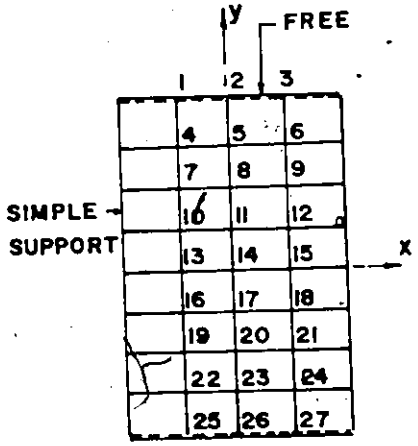

Model plate No.1

— THEORY(PRESENT SOL.)

⊡ — THEORY(SERIES SOL. (85))

⊙ — EXPERIMENT.

CONCENTRATED LOAD OF 1000 lbs AT CENTRE.

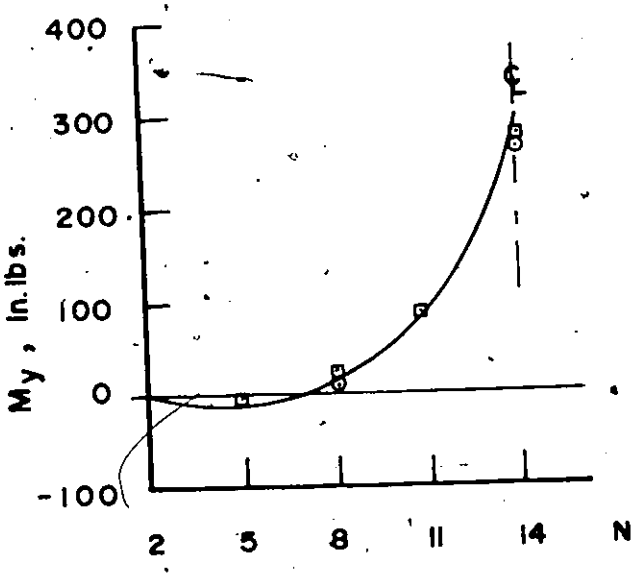

(b)

Figure 7·29 Variation Of Bending Moments.

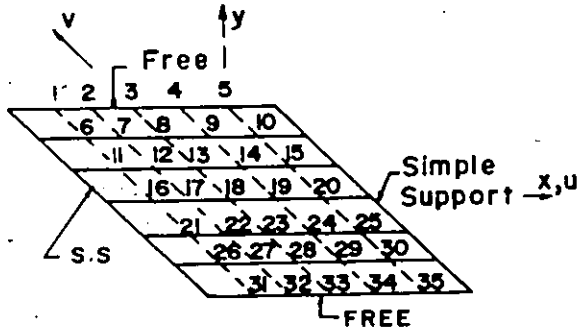

Model Plate No. 2

SKEW ANGLE = 45°

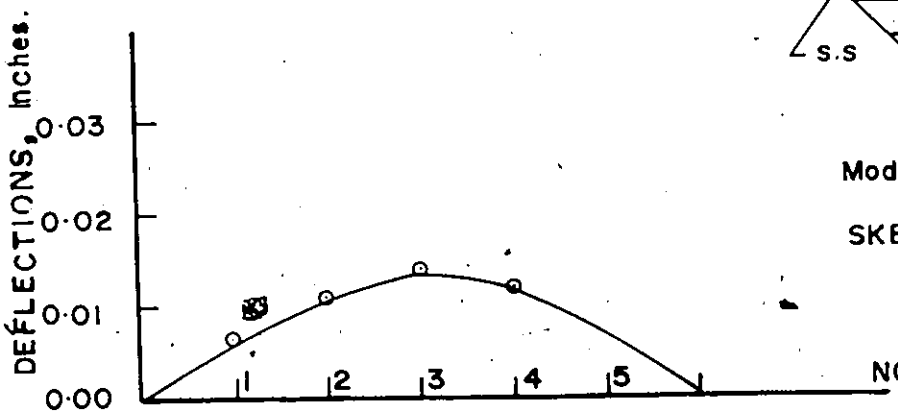

Span - Length At Free Edge

(b)

Concentrated Load Of 500 lbs. At Centre.

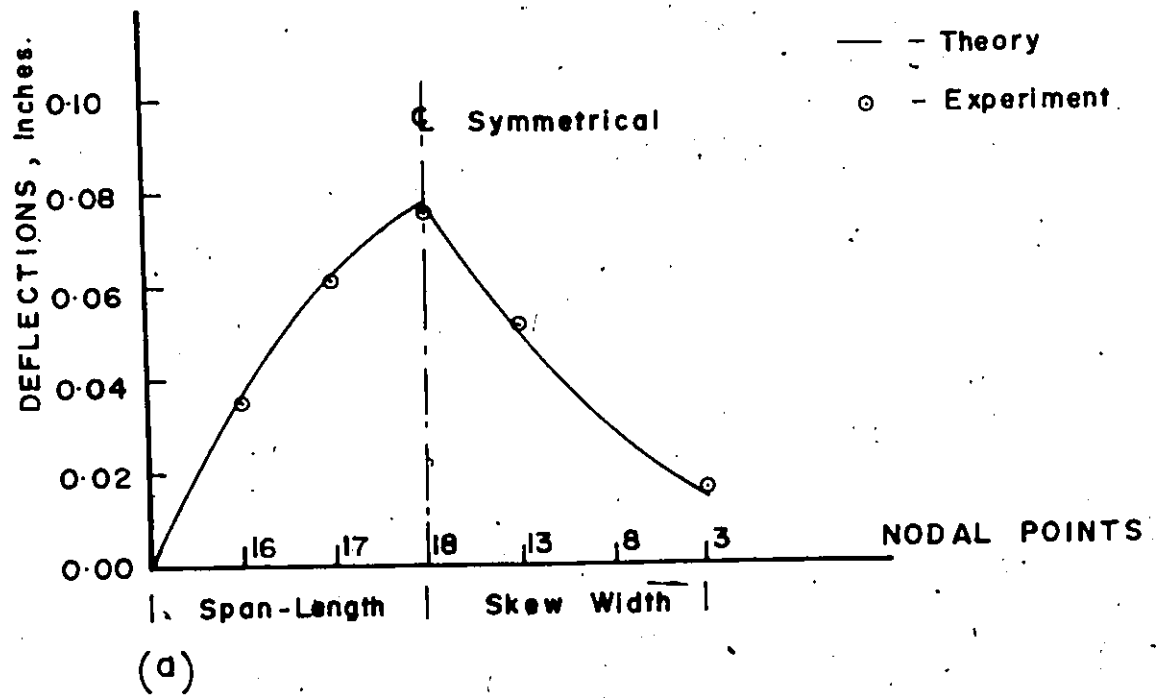

(a)

Figure 7·30 Variation Of Deflections

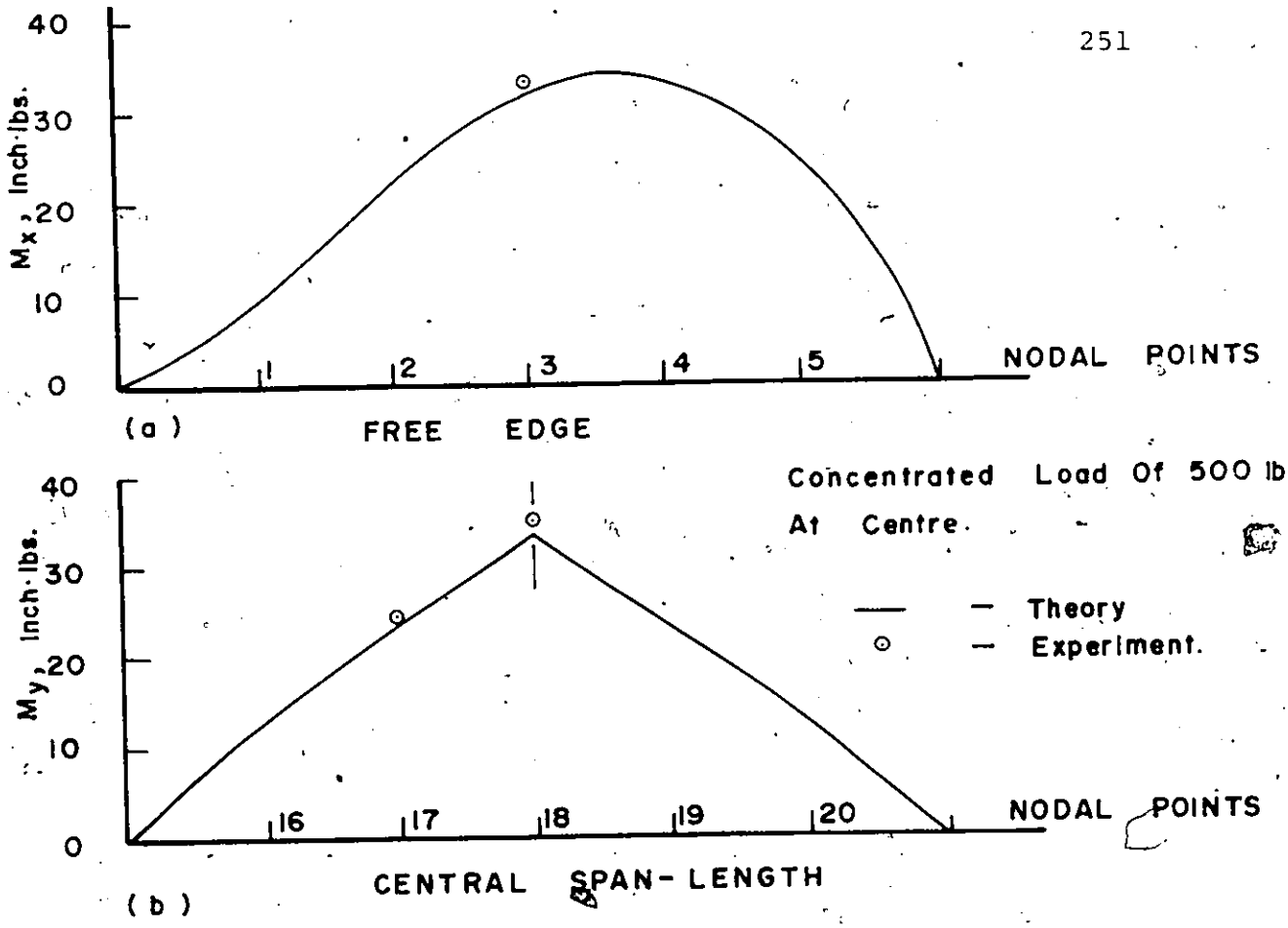

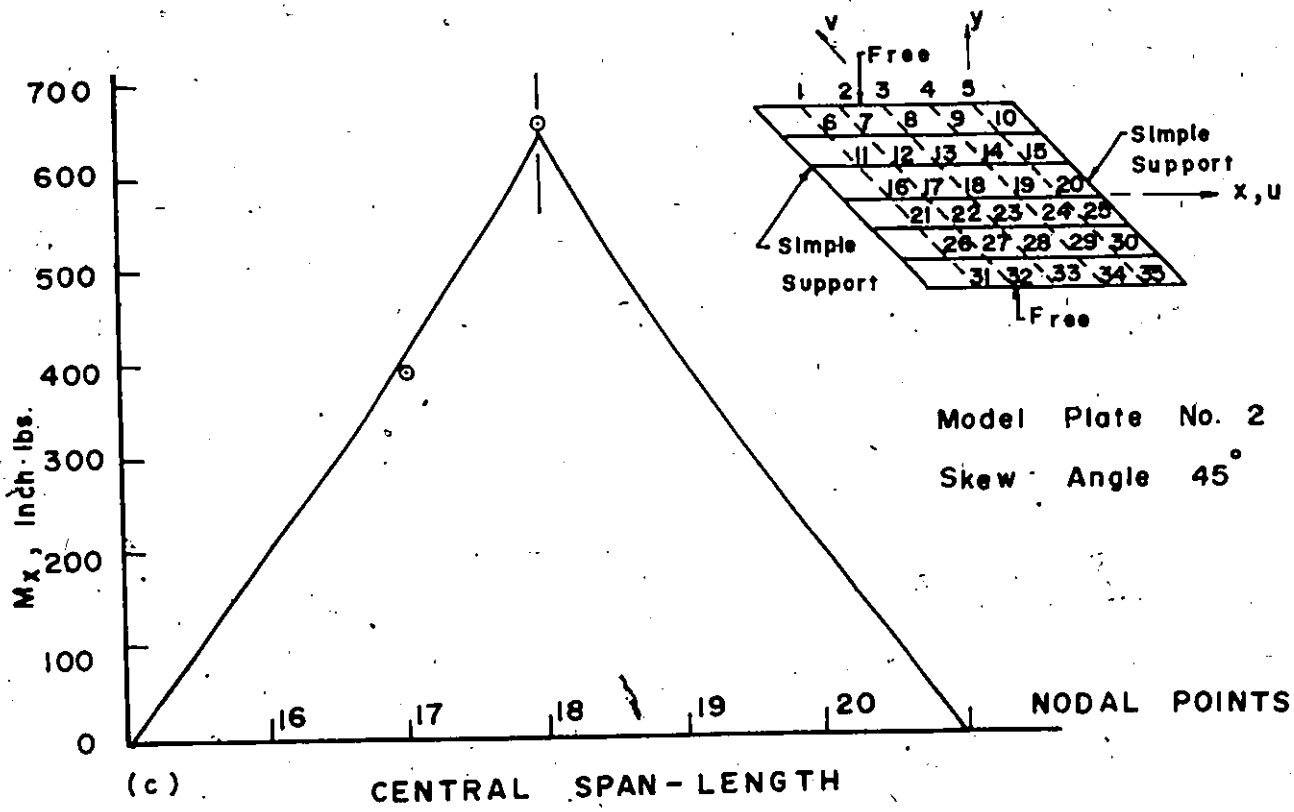

Figure 7·31 Variations Of Moments With Span-Length

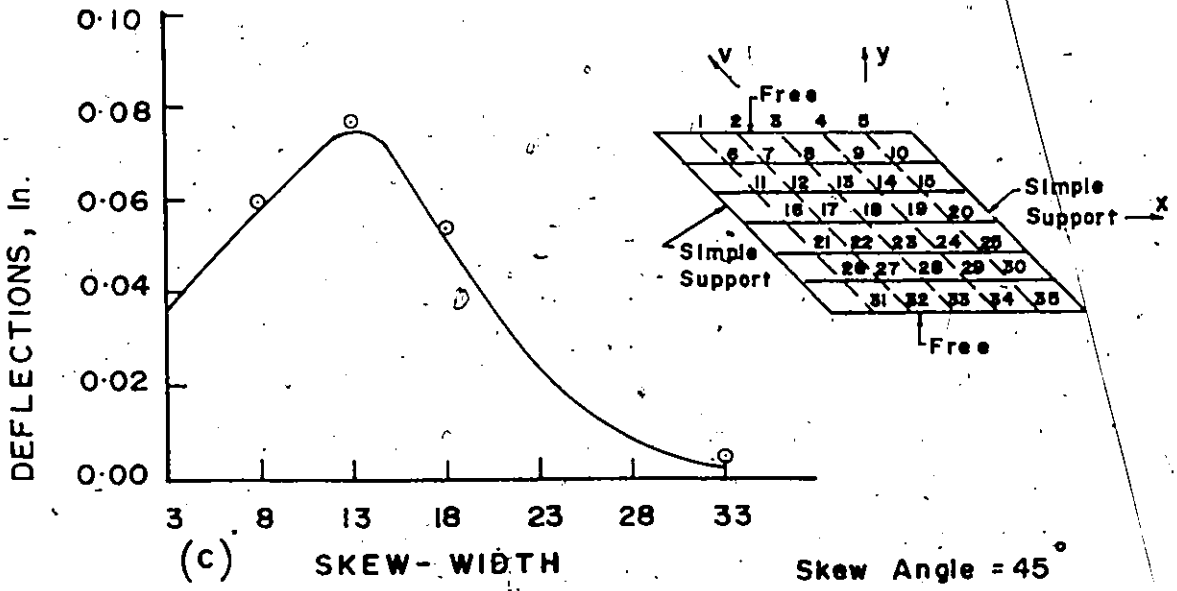

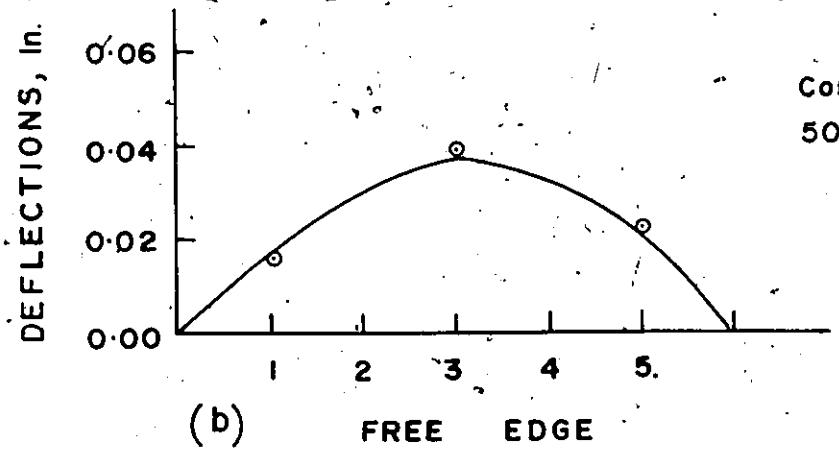

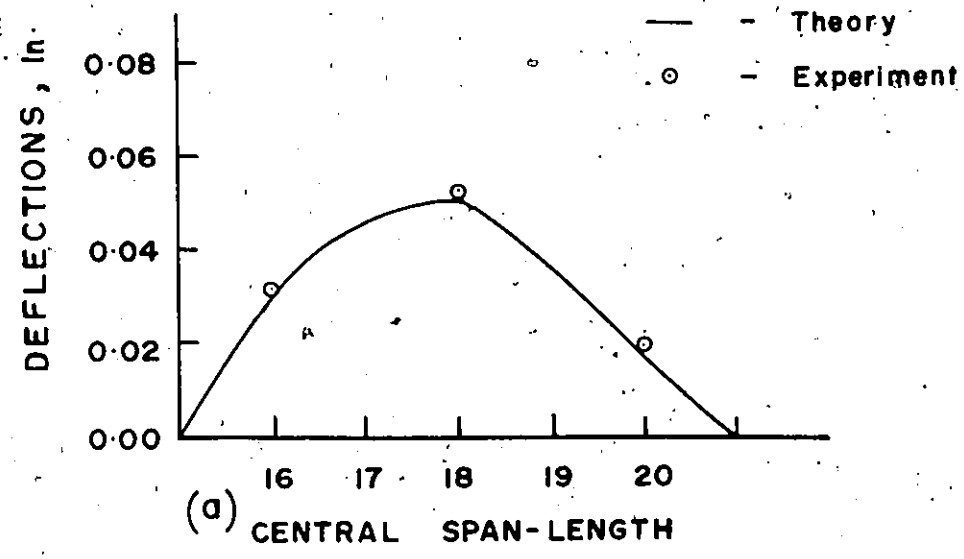

Fig· 7·32 Variations Of Deflections With Span-Length And Skew-Width.

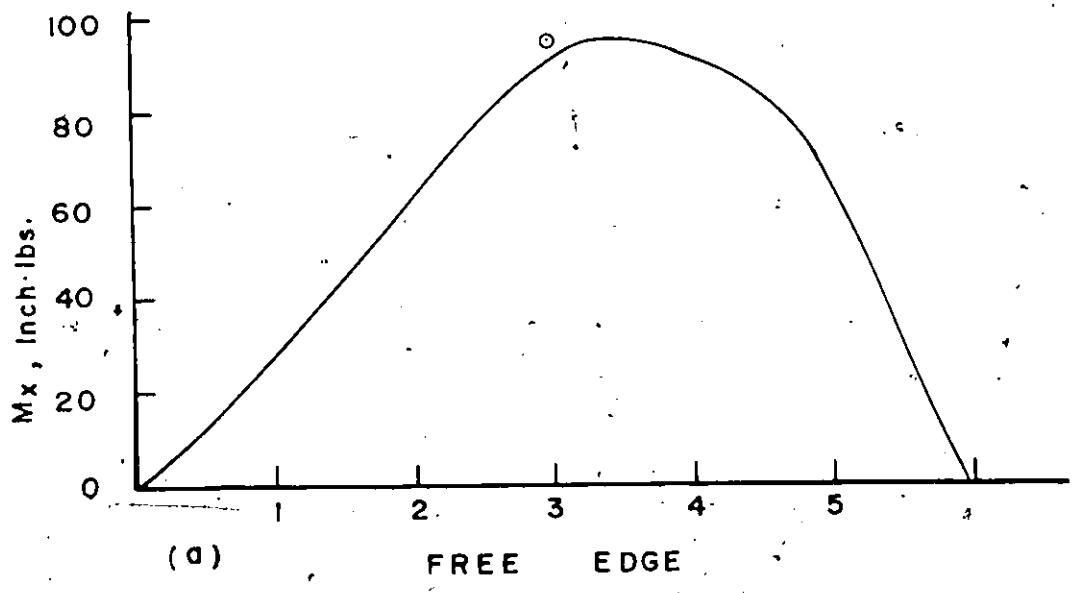

Concentrated Load Of 500 lbs. At Pt. 13

Refer To Fig. 7.32

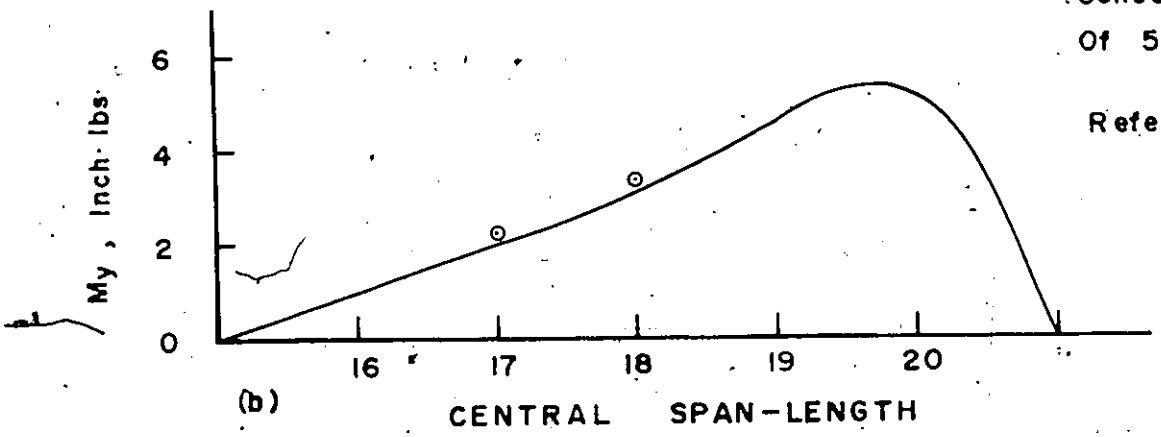

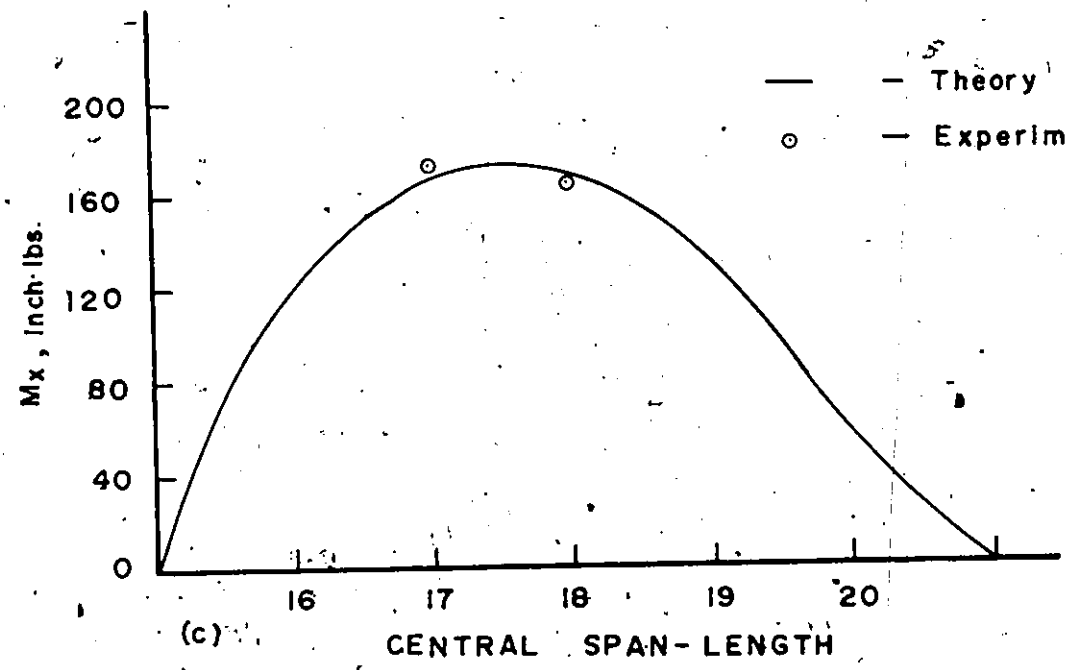

Figure 7.3 ...ortions Of Moments With Span-Length.

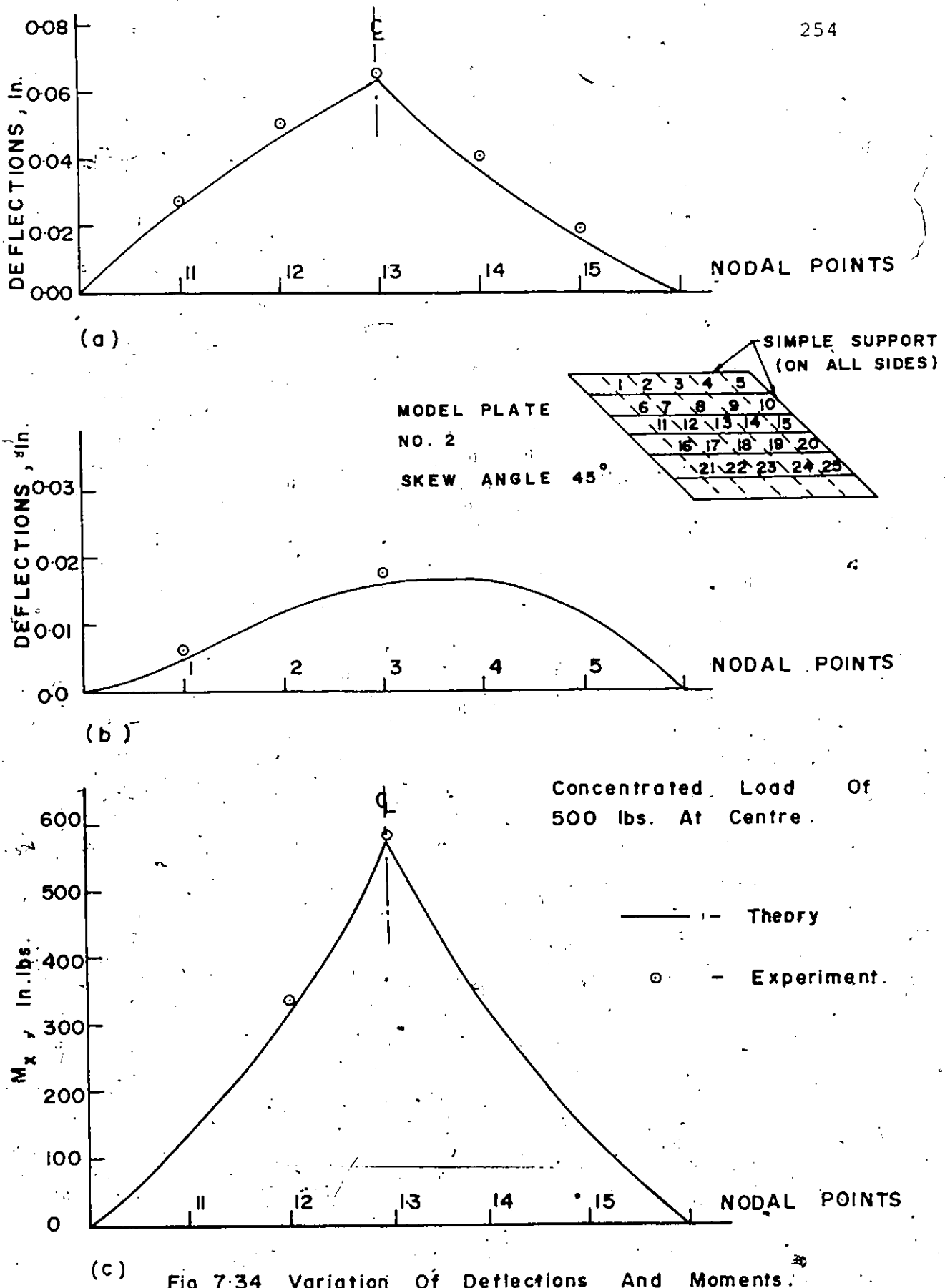

Fig. 7·34 Variation Of Deflections And Moments.

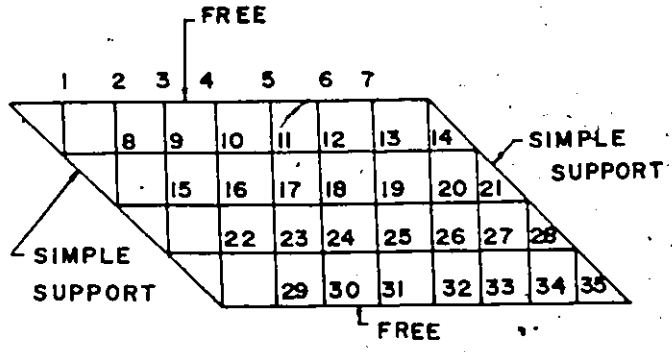

MODEL PLATE NO.3

SKEW ANGLE = 45°

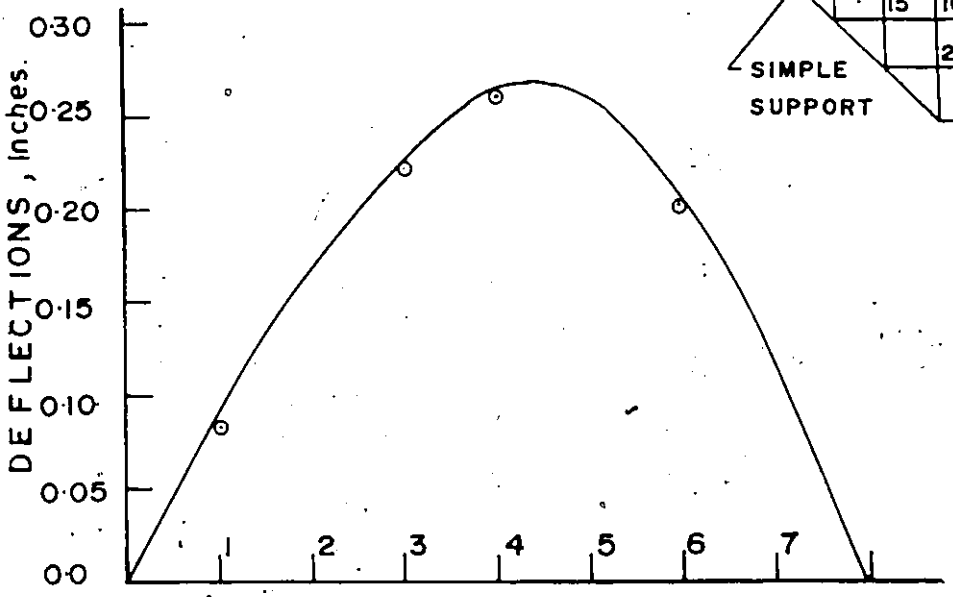

(a)

CONCENTRATED LOAD OF 400 Lbs AT CENTRE

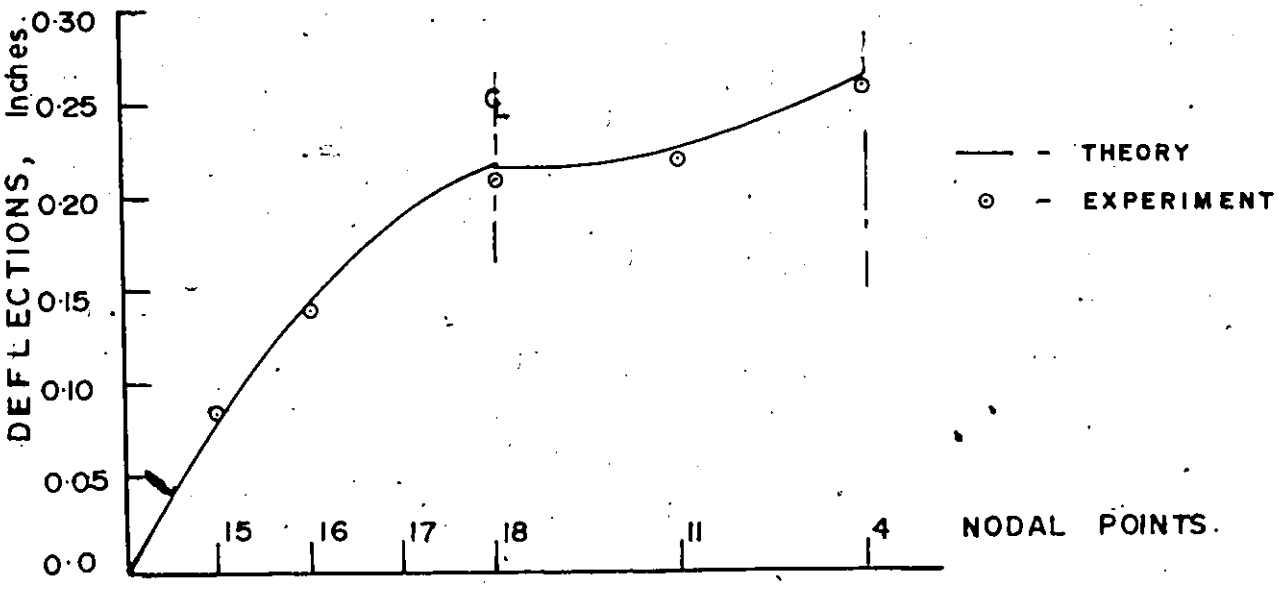

(b)

Fig. 7·35 Variation Of Deflections

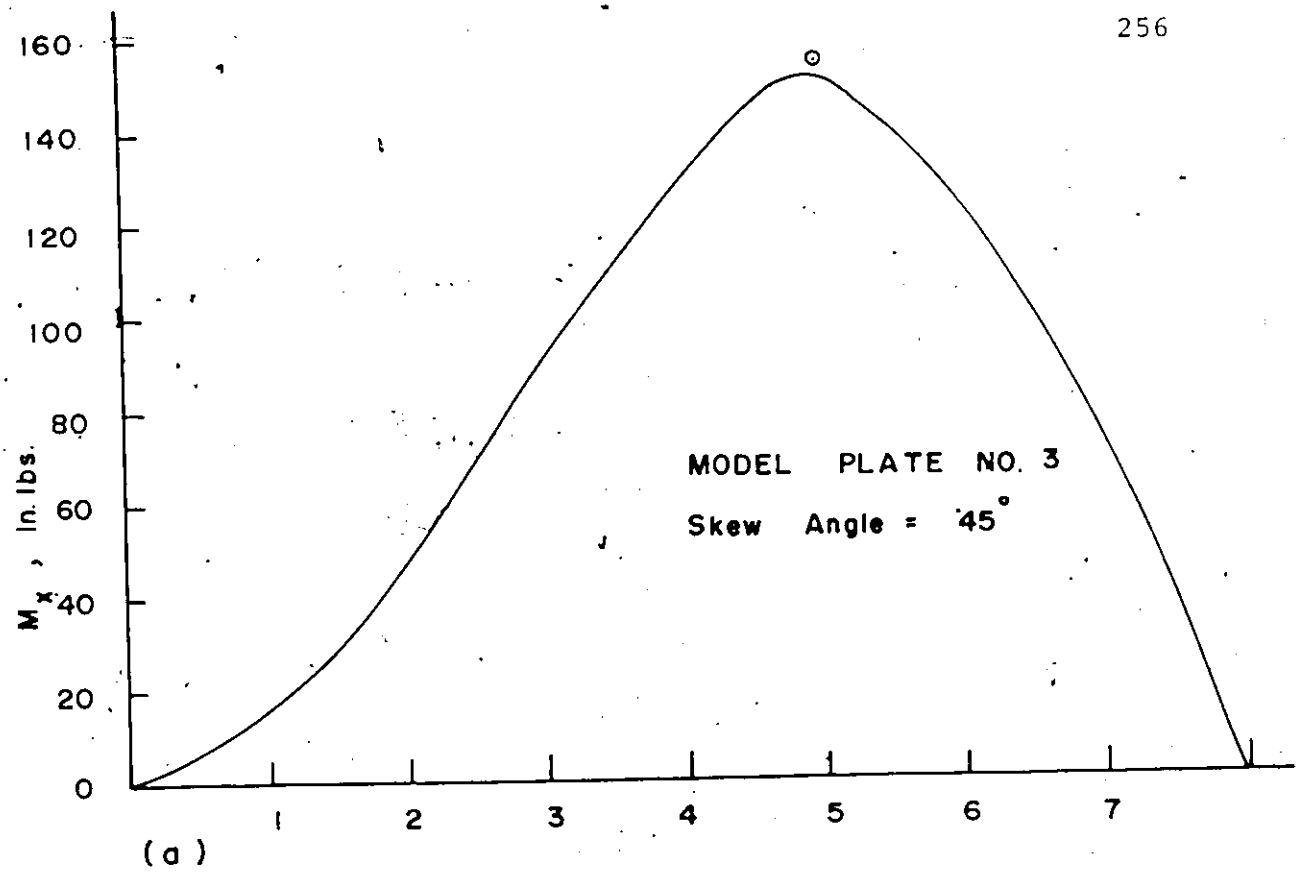

(a)

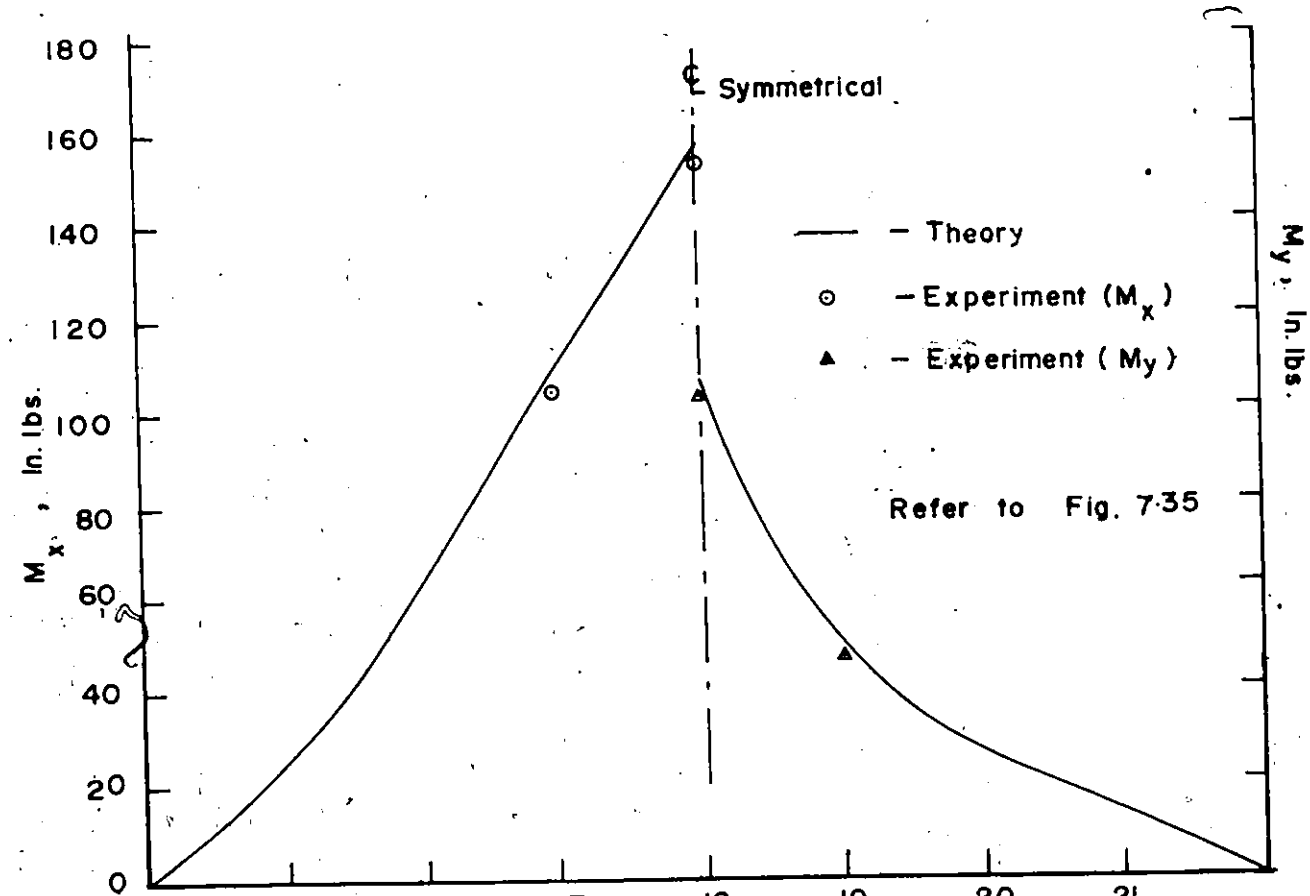

(b)

Fig. 7·36 Variation Of Moments.

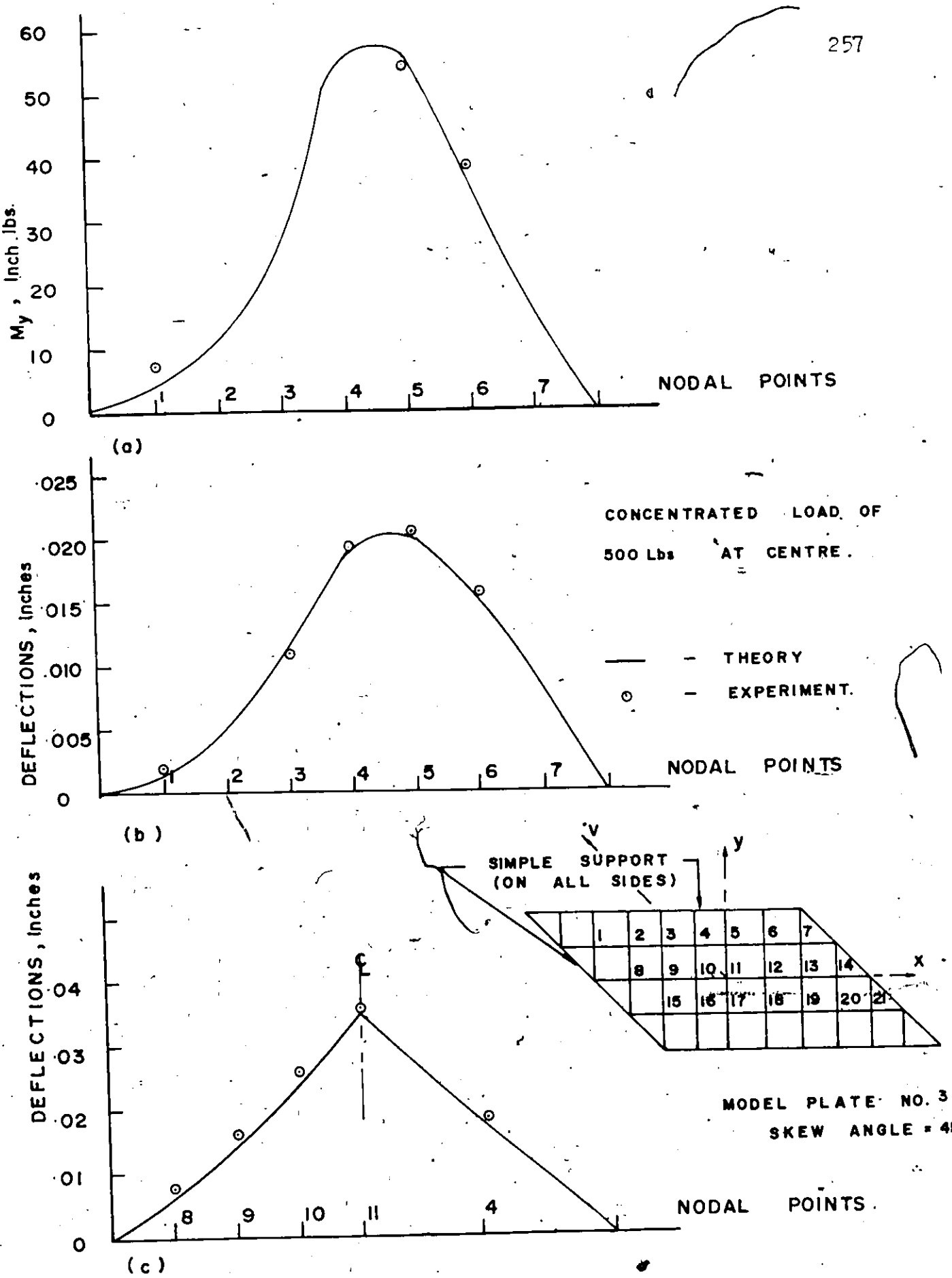

Fig. 7·37 Variation Of Deflections And Moments.

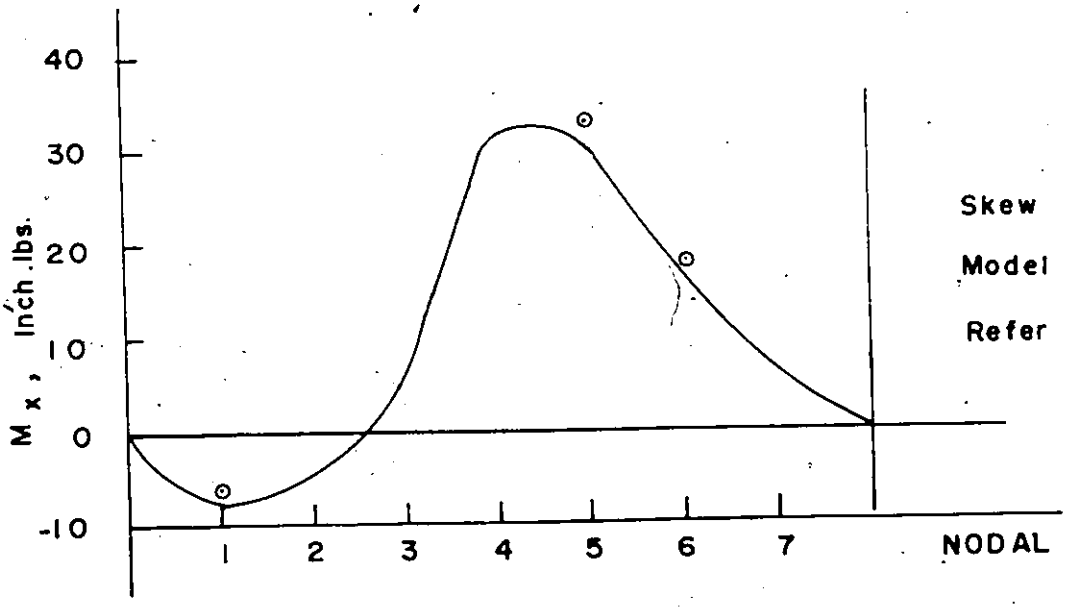

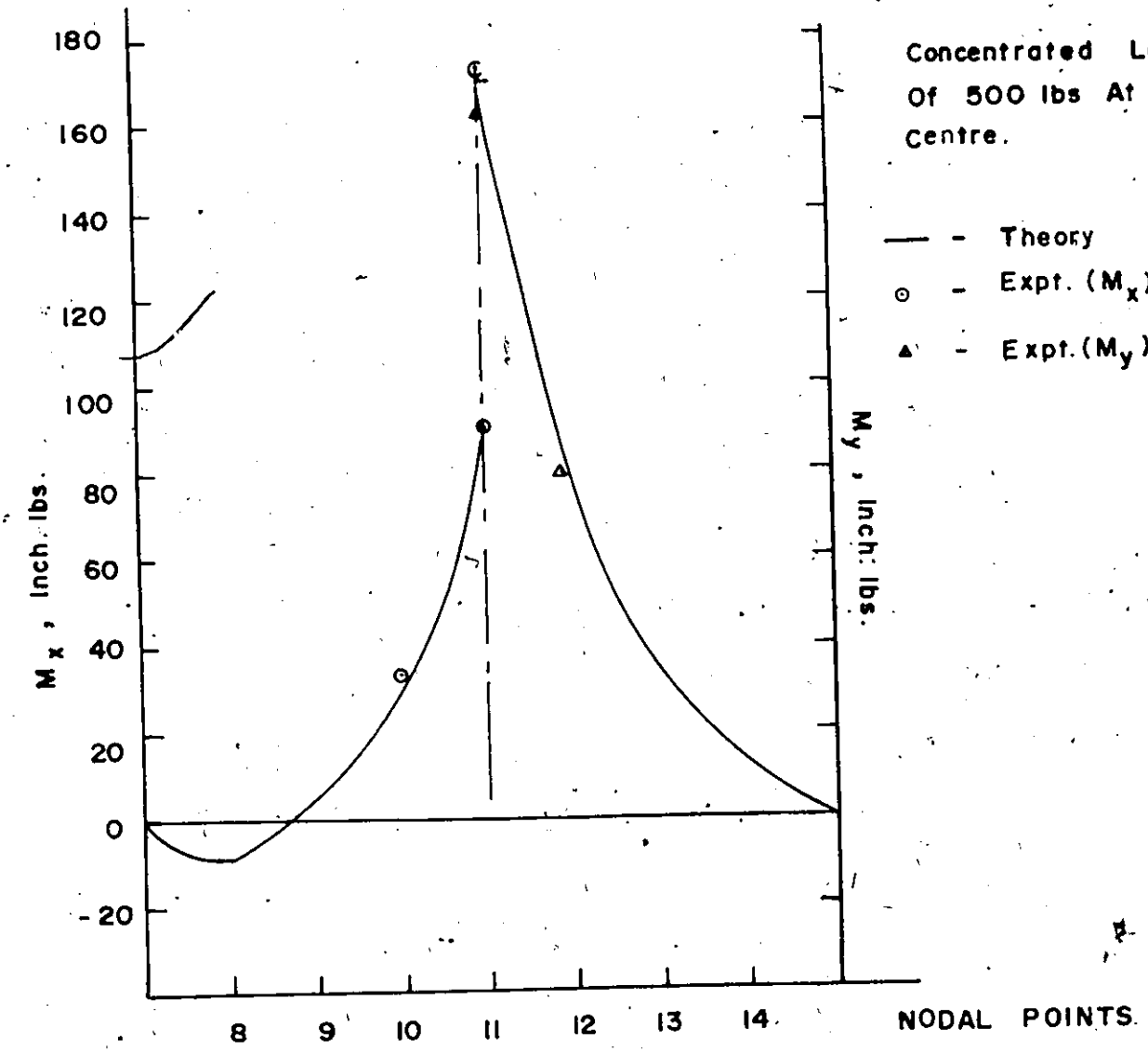

Fig· 7·38 Variation Of Moments.

CHAPTER 14

COMPUTER PROGRAM

```
C     PLASTI - PLASTIC ANALYSIS OF ORTHOTROPIC SKEW PLATES.
C     BIJUSH K. CHOWDHURY
C     M = NO. OF DISCRETE POINTS IN THE X,U - DIRECTION
C     N = NO. OF DISCRETE POINTS IN THE Y - DIRECTION
C     TL = SPAN - LENGTH IN X - DIRECTION
C     TB = WIDTH OF PLATE IN Y - DIRECTION
C     ANG = ANGLE OF SKEW
C     Z1,Z2 = DEPTH OF PLASTIC RIB IN X- , Y- DIRECTIONS, RESPECTIVELY
C     EX,EY = X-,Y- DIRECTION RIB THICNESS, RESPECTIVELY
C     THIC = DECK PLATE THICKNESS
C     A IS A TWO DIMENSIONAL ARRAY OF DIMENSION (M*N,9*N) TO STORE
C          EQUILIBRIUM MATRIX EQUATIONS
C     B IS A TWO DIMENSIONAL ARRAY OF DIMENSION (M*N,1*N) TO STORE
C          COMPATIBILITY MATRIX EQUATIONS
C     PL IS A LOAD VECTOR OF DIMENSION (M*N)
      DIMENSION XI(25),YI(25),YMU(25),BMX(25),DX(25),BMY(25),DY(25),BMXY
     1(25),CX(25),BY(25),BX(25),ZTX(25),ZTY(25),SIY(25),SIX(25),GX(25),
     2GY(25),FT(25),FP(25),BXY(25),BYX(25),H(25),D(25),GAM(25),AX(25),
     3XK(25),YK(25),DEL(25),SI(25),AAX(25),AAY(25),TX(25),TY(25),CH(25),
     4B3(25),B4(25),B5(25),B(25,25),C(25),B11(25),B12(25)
      DIMENSION TSXTN(25),TSXBN(25),TSYBN(25),TXYTN(25),TSYTN(25),
     1ZX(25),ZY(25),T(25),XMU(25),ZBX(25),ZBY(25),F(25),W(25),WN(25),W1(
     225),W2(25),ZXN(25),ZYN(25),XMS(25),YMS(25),XBSB(25),YBSB(25),XBST(
     325),YBST(25),BTXY(25),TXYM(25),SIGMA(25),TSXB(25
     4),TSYB(25),TSXT(25),TSYT(25),TXYT(25),XMSN(25),YMSN(25),G(25)
      DIMENSION CAX(25),CD(25),CGAM(25),A(25,25),D11(25),D12(25),D13(25)
     1,PL(25),L(25),M1(25),IR(25),IC(25),A11(25),A12(25),A13(25),
     2A21(25),A22(25),A23(25),A31(25),A32(25),A33(25),A41(25),A42(25),
     3A43(25),A51(25),A52(25),A53(25),G1(25),G2(25),G3(25),G4(25),G5(25)
     4,G6(25),G7(25),G8(25),A1(25),A2(25),A3(25),A4(25),B1(25),B2(25)
      COMMON/AA/W,F,PL,L,M1,BMX,BMY,BMXY,WN,W1,W2,ZX,ZY,ZBX,
     1ZBY,ZTX,ZTY,XMU,YMU,M,N,T
      COMMON/BB/AX,DX,H,SI,GAM,D,XK,YK,DEL,DY,BXY,BYX,FT,FP,SIX,SIY,XI,
     1YI,GX,GY,CX,AAX,AAY,TX,TY,CH,BX,BY,CGAM,CD,CAX
      COMMON/CC/XMS,YMS,XBSB,YBSB,XBST,YBST,TSXB,TSYB,TSXT,TSYT,SIGMA,
     1BTXY,TXYM,TXYT
      COMMON/DD/AM,AN,YIELD,EX,EY,EX,EY,C,FI,Z1,Z2,THIC,AL,AB,ZETA,ANU,
     1EXA,AS,BET,ALP,TL,TB,ANG
      COMMON/EE/N1,N2,N3,N4,N5,N7,N8,N9,N11,N12,N13,N14,M2,M3,M4,M5,M7,
     1M8,M9,M10,M12,M13,M14,M15,M17,M18,M19,M20,K1,K2,K3,K4,K6,K7,K8,K9,
     2K11,K12,K13,K14,K16,K17,K18,K19,K21,K22,K23,K24,K26,K27,K28,K29,
     3K31,K32,K33,K34,K36,K37,K38,K39
      READ 190,TL,TB,AM,AN,ANG
  190 FORMAT (5E15.6)
      READ 191,EX,XPOIS,YIELD,D,DD,EN
  191 FORMAT (6E11.4)
      READ 192,Z1,Z2,EX,EY,THIC
  192 FORMAT (5E15.6)
      READ 193,LINE,M,N
  193 FORMAT (3I5)
      AL=TL/(M+1)
      AB=TB/(N+1)
      N1=M+1
      N2=M+2
      N3=M+3
      N4=M+4
      N6=2*M+1
      N7=2*M+2
      N8=2*M+3
      N9=2*M+4
      N11=3*M+1
      N12=3*M+2
      N13=3*M+3
      N14=3*M+4
      M2=M-3
      M3=M-2
      M4=M-1
      M5=M
      M7=2*M-3
      M8=2*M-2
      M9=2*M-1
      M10=2*M
      M12=3*M-3
      M13=3*M-2
      M14=3*M-1
      M15=3*M
      M17=4*M-3
      M18=4*M-2
```

```
      M19=4*M-1
      M20=4*M
      K1=M*N
      K2=M*N-1
      K3=M*N-2
      K4=M*N-3
      K6=(N-1)*M+1
      K7=(N-1)*M+2
      K8=(N-1)*M+3
      K9=(N-1)*M+4
      K11=(N-1)*M
      K12=(N-1)*M-1
      K13=(N-1)*M-2
      K14=(N-1)*M-3
      K16=(N-2)*M+1
      K17=(N-2)*M+2
      K18=(N-2)*M+3
      K19=(N-2)*M+4
      K21=(N-2)*M
      K22=(N-2)*M-1
      K23=(N-2)*M-2
      K24=(N-2)*M-3
      K26=(N-3)*M+1
      K27=(N-3)*M+2
      K28=(N-3)*M+3
      K29=(N-3)*M+4
      K31=(N-3)*M
      K32=(N-3)*M-1
      K33=(N-3)*M-2
      K34=(N-3)*M-3
      K36=(N-4)*M+1
      K37=(N-4)*M+2
      K38=(N-4)*M+3
      K39=(N-4)*M+4
      FI=ANG*3.141592/180.
      AB=TB/(TL*COS(FI))
      AS=AB/AL
      ANU=AS**2/(1.+AB**2)
      BET=AS*TAN(FI)
      ALP=BET**2+AS**2
      EXA=1./(AB**2)
      ZETA=-2.*AB*EXA
      EY=EX
      LINK=0
      DO 300 I=1,K1
      TSXTN(I)=0.
      TSXBN(I)=0.
      TSYBN(I)=0.
      TXYTN(I)=0.
300   TSYTN(I)=0.
      DO 301 I=1,K1
      ZX(I)=Z1
      ZY(I)=Z2
      T(I)=THIC
      XMU(I)=XPOIS
      ZBX(I)=0.
301   ZBY(I)=0.
      CALL PROP
      DO 305 I=1,K1
305   F(I)=0.
      CALL DEFLEC
      DO 306 I=1,K1
306   W(I)=WN(I)
      CALL MEMBRN
      DO 307 I=1,K1
307   W1(I)=W(I)
1000  CALL DEFLEC
      DO 308 I=1,K1
      IF (WN(I)-W1(I)) 310,311,312
310   IF(((WN(I)-W1(I))/WN(I))+.00075)313,311,311
312   IF(((WN(I)-W1(I))/WN(I))-.00075)311,311,313
313   DO 314 K=1,K1
314   W(K)=.5*(W1(K)+WN(K))
      DO 315 J=1,K1
315   W1(J)=WN(J)
      CALL MEMBRN
      GO TO 1000
311   CONTINUE
```

```
  303 CONTINUE
      DO 1001 I=1,K1
      ZXN(I)=Z1
      ZYN(I)=Z2
      XMS(I)=0.
      YMS(I)=0.
      XBST(I)=0.
      YBST(I)=0.
      XBST(I)=0.
      YBST(I)=0.
      QTXY(I)=0.
 1001 TXYM(I)=0.
      CALL STRESS
      DO 440 I=1,K1
      IF (YIELD-SIGMA(I))441,440,440
  441 PRINT 710,I,SIGMA(I)
  710 FORMAT(//22H DECK PLATE STRESS AT I5,8H EQUALS E15.6,
     123H IS ABOVE YIELD.STOP THE RUN.)
      CALL RESULT
      CALL EXIT
  440 CONTINUE
      DO 511 K=1,K1
      IF (YIELD-TSXB(K))512,513,514
  512 IF (((YIELD-TSXB(K))/YIELD)+.0015)515,513,513
  514 IF (((YIELD-TSXB(K))/YIELD)-.0015)513,513,511
  515 PRINT 519,K,Q,TSXB(K)
  519 FORMAT (//27H HAVE PASSED YIELD AT NODE I5,15H IN X-DIRECTION,
     110X,5H Q = E15.6,5X,11H TSXB(K) = E15.6)
      GO TO 520
  513 PRINT 723,K
  723 FORMAT(////21H FIRST YIELD AT NODE I5,15H IN X-DIRECTION)
      GO TO 524
  511 CONTINUE
      DO 611 I=1,K1
      IF (YIELD-TSYB(I)) 612,613,614
  612 IF (((YIELD-TSYB(I))/YIELD)+.0015)615,613,613
  614 IF (((YIELD-TSYB(I))/YIELD)-.0015)613,613,611
  615 PRINT 619,I,Q,TSYB(I)
  619 FORMAT (//27H HAVE PASSED YIELD AT NODE I5,15H IN Y-DIRECTION,
     110X,5H Q = E15.6,5X,11H TSYB(I) = E15.6)
      GO TO 520
  613 PRINT 623,I
  623 FORMAT (////21H FIRST YIELD AT NODE I5,15H IN Y-DIRECTION)
      GO TO 524
  611 CONTINUE
      IF (Q-PN) 1120,1121,1121
 1121 CALL RESULT
      GO TO 9999
 1120 Q=Q+DQ
      GO TO 1000
  520 DQ=DQ/2.
      Q=Q-DQ
      GO TO 1000
C     STEP BY STEP SOLUTION PROCEDURE WITH ITERATIVE INCREMENTAL
C          LOADING STARTS
  524 CALL RESULT
      Q1=Q
      GO TO 931
 1111 CONTINUE
      Q=Q1+Q
      CALL RESULT
      Q1=Q
      DO 903 I=1,K1
      IF (ZX(I)-T(I))1716,1716,903
 1716 PRINT 1717,I
 1717 FORMAT (//13H BEAM AT NODE I5,'HAS FULLY YIELDED IN X-DIRECTION')
      CALL EXIT
  903 CONTINUE
  931 CONTINUE
      DQ=.5
      Q=.5
      LINK=LINK+1
      IF(LINE-LINK) 1876,1876,1879
 1876 PRINT 1877,LINK
 1877 FORMAT (///'HAVE GONE THROUGH REQUESTED NUMBER OF INCREMENTS.
     1 LINK =',I5)
      GO TO 9999
 1879 CONTINUE
```

```
      DO 935 I=1,K1
      W2(I)=WN(I)
      G(I)=F(I)
      TSXBN(I)=TSXB(I)
      TSYBN(I)=TSYB(I)
      TSXTN(I)=TSXT(I)
      TSYTN(I)=TSYT(I)
      TXYTN(I)=TXYT(I)
      XMSN(I)=XMS(I)
      YMSN(I)=YMS(I)
  935 F(I)=0.
 9111 CALL DEFLEC
      DO 936 I=1,K1
  936 W(I)=WN(I)
      CALL MEMBRN
      DO 937 I=1,K1
  937 W1(I)=W(I)
 9211 CALL DEFLEC
      DO 831 I=1,K1
      IF (WN(I)-W1(I)) 830,831,832
  830 IF (((WN(I)-W1(I))/WN(I))+.00075)833,831,831
  832 IF (((WN(I)-W1(I))/WN(I))-.00075)831,831,833
  831 CONTINUE
      GO TO 835
  833 DO 839 I=1,K1
  839 W(I)=.5*(W1(I)+WN(I))
      DO 834 I=1,K1
  834 W1(I)=WN(I)
      CALL MEMBRN
      GO TO 9211
  835 CALL STRESS
      DO 836 I=1,K1
      WN(I)=WN(I)+W2(I)
      TSXB(I)=TSXB(I)+TSXBN(I)
      TSYB(I)=TSYB(I)+TSYBN(I)
      TSXT(I)=TSXT(I)+TSXTN(I)
      TSYT(I)=TSYT(I)+TSYTN(I)
      TXYT(I)=TXYT(I)+TXYTN(I)
      XMS(I)=XMS(I)+XMSN(I)
      YMS(I)=YMS(I)+YMSN(I)
      SIGMA (I)=SQRT(TSXT(I)**2+TSYT(I)**2-TSXT(I)*TSYT(I)
     1+TXYT(I)**2*3.)
  836 F(I)=F(I)+G(I)
      CALL STRESS
      DO 1510 I=1,K1
      IF(TSXT(I))1600,1601,1601
 1600 ZX(I)=ZX(I)-(ZX(I)/(-TSXT(I)+TSXB(I)))*(TSXB(I)-YIELD)
      GO TO 1602
 1601 ZX(I)=ZX(I)-(ZX(I)/(TSXT(I)-TSXB(I)))*(-TSXB(I)-YIELD)
 1602 IF(TSYT(I))1603,1604,1604
 1603 ZY(I)=ZY(I)-(ZY(I)/(-TSYT(I)+TSYB(I)))*(TSYB(I)-YIELD)
      GO TO 1510
 1604 ZY(I)=ZY(I)-(ZY(I)/(TSYT(I)-TSYB(I)))*(-TSYB(I)-YIELD)
 1510 CONTINUE
      DO 942 I=1,K1
      IF (Z1-ZX(I)) 943,942,942
  943 ZX(I)=Z1
  942 CONTINUE
      DO 944 I=1,K1
      IF (Z2-ZY(I)) 953,944,944
  953 ZY(I)=Z2
  944 CONTINUE
      CALL PROP
      DO 946 I=1,K1
      IF (ZXN(I)-ZX(I))947,946,948
  947 IF (((ZXN(I)-ZX(I))/ZXN(I))+.0005)949,946,949
  948 IF (((ZXN(I)-ZX(I))/ZXN(I))-.0005)946,946,949
  949 GO TO 954
  946 CONTINUE
      DO 950 I=1,K1
      IF (ZYN(I)-ZY(I))951,950,952
  951 IF (((ZYN(I)-ZY(I))/ZYN(I))+.0005)953,950,950
  952 IF (((ZYN(I)-ZY(I))/ZYN(I))-.0005)950,950,953
  953 GO TO 954
  950 CONTINUE
      GO TO 1111
  954 DO 955 I=1,K1
      TSXBN(I)=TSXBN(I)*ZX(I)/ZXN(I)
```

```
      TSY3N(I)=TSY3N(I)*ZY(I)/ZYN(I)
      ZXN(I)=ZX(I)
  950 ZYN(I)=ZY(I)
      DR=DR/2.
      D=D-DR/2.
      DO 950 I=1,K1
  950 F(I)=0.
      GO TO 9111
 9999 STOP
      END
```

```
      SUBROUTINE RESULT
C     SOLUTIONS OF ORTHOTROPIC PLATE PROBLEM AT DIFFERENT STAGES OF
C          LOADING
      DIMENSION XI(25),YI(25),YMU(25),BMX(25),DX(25),BMY(25),DY(25),BMXY
     1(25),CX(25),BY(25),BX(25),ZTX(25),ZTY(25),SIY(25),SIX(25),GX(25),
     2GY(25),ET(25),EP(25),BXY(25),BYX(25),H(25),D(25),GAM(25),AX(25),
     3XK(25),YK(25),DEL(25),SI(25),AAX(25),AAY(25),TX(25),TY(25),CH(25),
     4B3(25),B4(25),B5(25),B(25,25),C(25),B11(25),B12(25)
      DIMENSION TSXTN(25),TSXBN(25),TSYBN(25),TXYTN(25),TSYTN(25),
     1ZX(25),ZY(25),T(25),XMU(25),ZBX(25),ZBY(25),F(25),W(25),WN(25),WL(
     225),W2(25),ZXN(25),ZYN(25),XMS(25),YMS(25),XBS(25),YBS(25),XBST(
     325),YBST(25),STXY(25),TXYM(25),SIGMA(25),TSXB(25
     4),TSYB(25),TSXT(25),TSYT(25),TXYT(25),XMSN(25),YMSN(25),G(25)
      DIMENSION CAX(25),CO(25),CGAM(25),A(25,25),D11(25),D12(25),D13(25),
     1,BL(25),L(25),M1(25),I2(25),IC(25),A11(25),A12(25),A13(25),
     2A21(25),A22(25),A23(25),A31(25),A32(25),A33(25),A41(25),A42(25),
     3A43(25),A51(25),A52(25),A53(25),G1(25),G2(25),G3(25),G4(25),G5(25)
     4,G6(25),G7(25),G8(25),A1(25),A2(25),A3(25),A4(25),B1(25),B2(25)
      COMMON/AA/W,F,BL,L,M1,BMX,BMY,BMXY,WN,W1,W2,ZX,ZY,ZBX,
     1ZBY,ZTX,ZTY,XMU,YMU,M,N,T
      COMMON/BB/AX,DX,H,SI,GAM,D,XK,YK,DEL,DY,BXY,BYX,ET,EP,SIX,SIY,XI,
     1YI,GX,GY,CX,AAX,AAY,TX,TY,CH,BX,BY,CGAM,CO,CAX
      COMMON/CC/XMS,YMS,XBS3,YBS3,XBST,YBST,TSXB,TSYB,TSXT,TSYT,SIGMA,
     1BTXY,TXYM,TXYT
      COMMON/DD/AM,AN,YIELD,PX,PY,EX,EY,C,E1,Z1,Z2,THIC,AL,AP,ZETA,ANU,
     1EXA,AS,BET,ALP,TL,TB,ANG
      COMMON/EE/N1,N2,N3,N4,N6,N7,N8,N9,N10,N11,N12,N13,N14,M2,M3,M4,M5,M7,
     1M8,M9,M10,M12,M13,M14,M15,M17,M18,M19,M20,K1,K2,K3,K4,K5,K7,K8,K9,
     2K11,K12,K13,K14,K16,K17,K18,K19,K21,K22,K23,K24,K26,K27,K28,K29,
     3K31,K32,K33,K34,K36,K37,K38,K39
      PRINT 1201
 1201 FORMAT (1H ,20X,24H COMPUTATION OF STRESSES////)
      PRINT 999
  999 FORMAT (//' ANGLE OF SKEW      TL              TB')
      PRINT 998,ANG,TL,TB
  998 FORMAT (E15.8,4X,E15.8,4X,E15.8)
      PRINT 1202
 1202 FORMAT (' NODE          LOAD C        DEFLECTION',5X,' AIRY STRESS
     1 FUNCTION')
      PRINT 1203,(I,C,WN(I),F(I),I=1,K1)
 1203 FORMAT (I5,4X,E12.4,3X,E15.8,5X,E15.8)
      PRINT 1206,YIELD,PX,PY,AM,AN
 1206 FORMAT (//16H YIELD STRESS = E15.6,5X,29H X-DIRECTION RIB THICKNES
     1S = E15.6,5X,29H Y-DIRECTION RIB THICKNESS = E15.6/27H X-DIRECTION
     2 RIB SPACING = E15.6,5X,27H Y-DIRECTION RIB SPACING = E15.6//)
      PRINT 1207,Z1,Z2
 1207 FORMAT (//10H DEPTHX = E15.6,5X,10H DEPTHY = E15.6//)
      PRINT 1208
 1208 FORMAT (//5H NODE,10X,6H IX(I),13X,6H IY(I),12X,7H ZBX(I),12X,
     17H ZBY(I),11X,8H DEPX(I),11X,8H DEPY(I))
      PRINT 1209,(I,XI(I),YI(I),ZBX(I),ZBY(I),ZX(I),ZY(I),I=1,K1)
 1209 FORMAT(I5,4X,E15.8,4X,E15.8,4X,E15.8,4X,E15.8,4X,E15.8,4X,E15.8,4X,E15.8)
      PRINT 1212
 1212 FORMAT (//'      NODE',5X,'X-DIRECTION MEMBRANE STRESS',5X,'Y-DIR
     1ECTION MEMBRANE STRESS')
      PRINT 1213,(I,XMS(I),YMS(I),I=1,K1)
 1213 FORMAT (I10,8X,E15.8,10X,E15.8)
      PRINT 1216
 1216 FORMAT(//' NODE          TSXB(I)          TSYB(I)          TSXT(
     1I)          TSYT(I)')
      PRINT 1217,(I,TSXB(I),TSYB(I),TSXT(I),TSYT(I),I=1,K1)
 1217 FORMAT(I5,4X,E15.8,4X,E15.8,4X,E15.8,4X,E15.8)
      PRINT 1218
 1218 FORMAT(' NODE          DX(I)          DY(I)          H(I)')
      PRINT 1219,(I,DX(I),DY(I),H(I),I=1,K1)
 1219 FORMAT(I5,4X,E15.8,4X,E15.8,4X,E15.8)
      RETURN
      END
```

```
      SUBROUTINE STRESS
C     COMPUTATION OF MOMENT TENSOR, BENDING AND MEMBRANE STRESS TENSOR AND
C          STRESS COMPUTATION FOR COMPARISON WITH VON MISSES YIELD CRITERION
      DIMENSION XI(25),YI(25),YMU(25),BMX(25),DX(25),BMY(25),DY(25),BMXY
     1(25),CX(25),BY(25),BX(25),ZTX(25),ZTY(25),SIY(25),SIX(25),GX(25),
     2GY(25),FT(25),FP(25),BXY(25),BYX(25),D(25),GAM(25),AX(25),
     3XK(25),YK(25),DEL(25),SI(25),AAX(25),AAY(25),TX(25),TY(25),CH(25),
     4B3(25),B4(25),B5(25),B(25,25),C(25),B11(25),B12(25)
      DIMENSION TSXTN(25),TSXBN(25),TSYBN(25),TXYTN(25),TSYTN(25),
     1ZX(25),ZY(25),T(25),XMU(25),ZBX(25),ZBY(25),F(25),W(25),WN(25),W1(
     225),W2(25),ZXN(25),ZYN(25),XMS(25),YMS(25),XBSB(25),YBSB(25),XBST(
     325),YBST(25),BTXY(25),BTXYM(25),SIGMA(25),TSXB(25
     4),TSYB(25),TSXT(25),TSYT(25),TXYT(25),XMSN(25),YMSN(25),G(25)
      DIMENSION CAX(25),CO(25),GGAM(25),A(25,25),D11(25),D12(25),D13(25)
     1,PL(25),L(25),M1(25),I3(25),IC(25),A11(25),A12(25),A13(25),
     2A21(25),A22(25),A23(25),A31(25),A32(25),A33(25),A41(25),A42(25),
     3A43(25),A51(25),A52(25),A53(25),G1(25),G2(25),G3(25),G4(25),G5(25)
     4,G6(25),G7(25),G8(25),A1(25),A2(25),A3(25),A4(25),B1(25),B2(25)
      COMMON/AA/W,F,PL,L,M1,BMX,BMY,BMXY,WN,W1,W2,ZX,ZY,ZBX,
     1ZBY,ZTX,ZTY,XMU,YMU,M,N,T
      COMMON/BB/AX,DX,H,SI,GAM,D,XK,YK,DEL,DY,BXY,BYX,FT,FP,SIX,SIY,XI,
     1YI,GX,GY,CX,AAX,AAY,TX,TY,CH,BX,BY,CGAM,CO,CAX
      COMMON/CC/XMS,YMS,XBSB,YBSB,XBST,YBST,TSXB,TSYB,TSXT,TSYT,SIGMA,
     1BTXY,TXYM,TXYT
      COMMON/DD/AM,AN,YIELD,FX,FY,SX,SY,O,FI,Z1,Z2,THIC,AL,AB,ZETA,ANU,
     1EXA,AS,BET,ALP,TL,TB,ANG
      COMMON/EE/N1,N2,N3,N4,N6,N7,N8,N9,N11,N12,N13,N14,M2,M3,M4,M5,M7,
     1M8,M9,M10,M12,M13,M14,M15,M17,M18,M19,M20,K1,K2,K3,K4,K6,K7,K8,K9,
     2K11,K12,K13,K14,K16,K17,K18,K19,K21,K22,K23,K24,K26,K27,K28,K29,
     3K31,K32,K33,K34,K36,K37,K38,K39
      NS=(N-2)*M
      DO 501 I=1,K1
      BMX(I)=0.
      BMY(I)=0.
      XMS(I)=0.
      YMS(I)=0.
  501 TXYM(I)=0.
      BMX(1)=-DX(1)*EXA*(-2.*(AS**2+YMU(1)+BET**2*YMU(1))*WN(1)+(AS**2+
     1BET**2*YMU(1))*WN(2)+BET*.5*YMU(1)*(-WN(N2))+YMU(1)*WN(N1))
      BMY(1)=-DY(1)*EXA*(-2.*(1.+BET**2+AS**2*XMU(1))*WN(1)+(BET**2+AS**
     12*XMU(1))*WN(2)+BET*.5*(-WN(N2))+WN(M1))
      BMXY(1)=ZETA*CX(1)*(BET*(-2.*WN(1)+WN(2))+.25*(-WN(N2)))
      XMS(1)=BY(1)*EXA*(BET**2*F(2)-2.*(1.+BET**2)*F(1)+BET*.5*(-F(N2))+
     1F(N1))
      YMS(1)=BX(1)*ANU*(-2.*F(1)+F(2))
      TXYM(1)=-AS*EXA*(BET*(-2.*F(1)+F(2))+.25*(-F(N2)))
      DO 505 I=2,M4
      BMX(I)=-DX(I)*EXA*(-2.*(AS**2+YMU(I)+BET**2*YMU(I))*WN(I)+(AS**2+
     1BET**2*YMU(I))*(WN(I-1)+WN(I+1))+BET*.5*YMU(I)*(WN(I+M4)-WN(I+N1))
     2+YMU(I)*WN(I+M)
      BMY(I)=-DY(I)*EXA*(-2.*(1.+BET**2+AS**2*XMU(I))*WN(I)+(BET**2+
     1AS**2*XMU(I))*(WN(I-1)+WN(I+1))+BET*.5*(WN(I+M4)-WN(I+N1))+WN(I+M)
     1)
      BMXY(I)=ZETA*CX(I)*(BET*(WN(I-1)-2.*WN(I)+WN(I+1))
     1+.25*(WN(I+M4)-WN(I+N1)))
      XMS(I)=BY(I)*EXA*(BET**2*(F(I-1)+F(I+1))-2.*(1.+BET**2)*F(I)+BET*.
     15*(F(I+M4)-F(I+N1))+F(I+M))
      YMS(I)=BX(I)*ANU*(F(I-1)-2.*F(I)+F(I+1))
      TXYM(I)=-AS*EXA*(BET*(F(I-1)-2.*F(I)+F(I+1))+.25*(F(I+M4)-F(I+N1))
     1)
  505 CONTINUE
      BMX(M)=-DX(M)*EXA*(-2.*(AS**2+YMU(M)+BET**2*YMU(M))*WN(M)+(
     1AS**2+BET**2*YMU(M))*WN(M4)+BET*.5*YMU(M)*WN(M9)+YMU(M)*WN(M10))
      BMY(M)=-DY(M)*EXA*(-2.*(1.+BET**2+AS**2*XMU(M))*WN(M)+(BET**2+AS**
     12*XMU(M))*WN(M4)+BET*.5*WN(M9)+WN(M10))
      BMXY(M)=ZETA*CX(M)*(BET*(WN(M4)-2.*WN(M))+.25*WN(M9))
      XMS(M)=BY(M)*EXA*(BET**2*F(M4)-2.*(1.+BET**2)*F(M)+BET*.5*F(M9)+
     1F(M10))
      YMS(M)=BX(M)*ANU*(F(M4)-2.*F(M))
      TXYM(M)=-AS*EXA*(BET*(F(M4)-2.*F(M))+.25*F(M9))
      DO 510 I=N1,K1,M
      BMX(I)=-DX(I)*EXA*(-2.*(AS**2+YMU(I)+BET**2*YMU(I))*WN(I)+(AS**2+
     1BET**2*YMU(I))*WN(I+1)+BET*.5*YMU(I)*(WN(I-M4)-WN(I+N1))+YMU(I)*(
     2WN(I-1)+WN(I+M)))
      BMY(I)=-DY(I)*EXA*(-2.*(1.+BET**2+AS**2*XMU(I))*WN(I)+(BET**2+AS**
     12*XMU(I))*WN(I+1)+BET*.5*(WN(I-M4)-WN(I+N1))+WN(I-M)+WN(I+M))
      BMXY(I)=ZETA*CX(I)*(BET*(-2.*WN(I)+WN(I+1))+.25*(WN(I-M4)-WN(I+N1)
     1))
```

```
      XMS(I)=BY(I)*FXA*(BET**2*F(I+1)-2.*(1.+BET**2)*F(I)+BET*.5*(F(I-MA
     1)-F(I+M4))+F(I-1)+F(I+M))
      YMS(I)=BX(I)*ANU*(-2.*F(I)+F(I+1))
      TXYM(I)=-AS*FXA*(BET*(-2.*F(I)+F(I+1))+.25*(F(I-M4)-F(I+N1)))
  510 CONTINUE
      DO 515 I=2,M4
      DO 515 J=M,ND,M
      JA=I+J
      BMX(JA)=-DX(JA)*FXA*(-2.*(AS**2+YMU(JA)+BET**2*YMU(JA))*WN(JA)+(
     1AS**2+BET**2*YMU(JA))*(WN(JA-1)+WN(JA+1))+BET*.5*YMU(JA)*(WN(JA-M4
     2)-WN(JA-N1)+WN(JA+M4)-WN(JA+N1))+YMU(JA)*(WN(JA-M)+WN(JA+M)))
      BMY(JA)=-DY(JA)*FXA*(-2.*(1.+BET**2+AS**2*XMU(JA))*WN(JA)+(BET**2+
     1AS**2*XMU(JA))*(WN(JA-1)+WN(JA+1))+BET*.5*(WN(JA-M4)-WN(JA-N1)+
     2WN(JA+M4)-WN(JA+N1))+WN(JA-M)+WN(JA+M))
      BMXY(JA)=ZETA*CX(JA)*(BET*(WN(JA-1)-2.*WN(JA)+WN(JA+1))+.25*(WN(J
     1A-M4)-WN(JA-N1)+WN(JA+M4)-WN(JA+N1)))
      XMS(JA)=BY(JA)*FXA*(BET**2*(F(JA-1)+F(JA+1))-2.*(1.+BET**2)*F(JA)+
     1BET*.5*(F(JA-M4)-F(JA-N1)+F(JA+M)-F(JA+N1))+F(JA-M)+F(JA+M))
      YMS(JA)=BX(JA)*ANU*(F(JA-1)-2.*F(JA)+F(JA+1))
      TXYM(JA)=-AS*FXA*(BET*(F(JA-1)-2.*F(JA)+F(JA+1))+.25*(F(JA-M4)-F(
     1JA-N1)+F(JA+M4)-F(JA+N1)))
  515 CONTINUE
      DO 512 I=M10,K11,M
      BMX(I)=-DX(I)*FXA*(-2.*(AS**2+YMU(I)+BET**2*YMU(I))*WN(I)+(AS**2+
     1BET**2*YMU(I))*WN(I-1)+BET*.5*YMU(I)*(-WN(I-N1)+WN(I+M4))+YMU(I)*(
     2WN(I-M)+WN(I+M)))
      BMY(I)=-DY(I)*FXA*(-2.*(1.+BET**2+AS**2*XMU(I))*WN(I)+(BET**2+AS**
     12*XMU(I))*WN(I-1)+BET*.5*(-WN(I-N1)+WN(I+M4))+WN(I-M)+WN(I+M))
      BMXY(I)=ZETA*CX(I)*(BET*(WN(I-1)-2.*WN(I))+.25*(-WN(I-N1)+WN(I+M4)
     1))
      XMS(I)=BY(I)*FXA*(BET**2*F(I-1)-2.*(1.+BET**2)*F(I)+
     1BET*.5*(-F(I-N1)+F(I+M4))+F(I-M)+F(I+M))
      YMS(I)=BX(I)*ANU*(F(I-1)-2.*F(I))
      TXYM(I)=-AS*FXA*(BET*(F(I-1)-2.*F(I))+.25*(-F(I-N1)+F(I+M4)))
  512 CONTINUE
      BMX(K6)=-DX(K6)*FXA*(-2.*(AS**2+YMU(K6)+BET**2*YMU(K6))*WN(K6)
     1+(AS**2+BET**2*YMU(K6))*WN(K7)+BET*.5*YMU(K6)*WN(K17)+YMU(K6)*WN(
     2K16))
      BMY(K6)=-DY(K6)*FXA*(-2.*(1.+BET**2+AS**2*XMU(K6))*WN(K6)+(BET**2+
     1AS**2*XMU(K6))*WN(K7)+BET*.5*WN(K17)+WN(K16))
      BMXY(K6)=ZETA*CX(K6)*(BET*(WN(K7)-2.*WN(K6))+.25*WN(K17))
      XMS(K6)=BY(K6)*FXA*(BET**2*F(K7)-2.*(1.+BET**2)*F(K6)+BET*.5*F(K17
     1)+F(K16))
      YMS(K6)=BX(K6)*ANU*(F(K7)-2.*F(K6))
      TXYM(K6)=-AS*FXA*(BET*(F(K7)-2.*F(K6))+.25*F(K17))
      DO 520 I=K7,K2
      BMX(I)=-DX(I)*FXA*(-2.*(AS**2+YMU(I)+BET**2*YMU(I))*WN(I)+(AS**2+
     1BET**2*YMU(I))*(WN(I+1)+WN(I-1))+BET*.5*YMU(I)*(WN(I-M4)-WN(I-N1))
     2+YMU(I)*WN(I-M))
      BMY(I)=-DY(I)*FXA*(-2.*(1.+BET**2+AS**2*XMU(I))*WN(I)+(BET**2+AS**
     12*XMU(I))*(WN(I+1)+WN(I-1))+BET*.5*(WN(I-M4)-WN(I-N1))+WN(I-M))
      BMXY(I)=ZETA*CX(I)*(BET*(WN(I+1)-2.*WN(I)+WN(I-1))+.25*(WN(I-M4)-
     1WN(I-N1)))
      XMS(I)=BY(I)*FXA*(BET**2*(F(I+1)+F(I-1))-2.*(1.+BET**2)*F(I)+BET*.
     15*(F(I-M4)-F(I-N1))+F(I-M))
      YMS(I)=BX(I)*ANU*(F(I+1)-2.*F(I)+F(I-1))
      TXYM(I)=-AS*FXA*(BET*(F(I+1)-2.*F(I)+F(I-1))
     1+.25*(F(I-M4)-F(I-N1)))
  520 CONTINUE
      BMX(K1)=-DX(K1)*FXA*(-2.*(AS**2+YMU(K1)+BET**2*YMU(K1))*WN(K1)+(
     1AS**2+BET**2*YMU(K1))*WN(K2)+BET*.5*YMU(K1)*(-WN(K12))+YMU(K1)*WN(
     2K11))
      BMY(K1)=-DY(K1)*FXA*(-2.*(1.+BET**2+AS**2*XMU(K1))*WN(K1)+(BET**2+
     1AS**2*XMU(K1))*WN(K2)+BET*.5*(-WN(K12))+WN(K11))
      BMXY(K1)=ZETA*CX(K1)*(BET*(-2.*WN(K1)+WN(K2))+.25*(-WN(K12)))
      XMS(K1)=BY(K1)*FXA*(BET**2*F(K2)-2.*(1.+BET**2)*F(K1)+BET*.5*(-F(
     1K12))+F(K11))
      YMS(K1)=BX(K1)*ANU*(-2.*F(K1)+F(K2))
      TXYM(K1)=-AS*FXA*(BET*(-2.*F(K1)+F(K2))+.25*(-F(K12)))
      DO 503 I=1,K1
      XMSB(I)=BMX(I)*ZBX(I)*AM/XI(I)
      XMST(I)=-XMSB(I)*ZTX(I)/ZBX(I)
      YMSB(I)=BMY(I)*ZBY(I)*AN/YI(I)
      YMST(I)=-YMSB(I)*ZTY(I)/ZBY(I)
      BTXY(I)=-BMXY(I)*ZTX(I)*AM/XI(I)
      TSXB(I)=XMS(I)+XMSB(I)
      TSYB(I)=YMS(I)+YMSB(I)
      TSXT(I)=XMS(I)+XMST(I)
```

```
      TSYT(I)=YMS(I)+YMST(I)
     +TXYT(I)=BTXY(I)+TXYMT(I)
      SIGMA(I)=SQRT(TSXT(I)**2+TSYT(I)**2-TSXT(I)*TSYT(I)+TXYT(I)**2*3.)
      RETURN
      END
```

```
      SUBROUTINE PROP
C     COMPUTATION OF ORTHOTROPIC PLATE RIGIDITIES AND RELATED COEFFICIENTS
C     ASSOCIATED WITH PLATE EQUILIBRIUM AND COMPATIBILITY EQUATIONS
      DIMENSION XI(25),YI(25),YMU(25),BMX(25),BX(25),BMY(25),BY(25),BMXY
     1(25),CX(25),BXY(25),BYX(25),ZTX(25),ZTY(25),SIY(25),SIX(25),GX(25),
     2GY(25),FT(25),FP(25),BXY(25),BYX(25),H(25),D(25),GAM(25),AX(25),
     3XK(25),YK(25),DEL(25),SI(25),AAX(25),AAY(25),TX(25),TY(25),CH(25),
     4BB(25),BA(25),CC(25),B(25,25),C(25),B11(25),B12(25)
      DIMENSION TSXTN(25),TSXBN(25),TSYBN(25),TXYTN(25),TSYTN(25),
     1ZX(25),ZY(25),T(25),XMU(25),ZBX(25),ZBY(25),F(25),W(25),WN(25),W1(
     225),W2(25),ZXN(25),ZYN(25),XMS(25),YMS(25),XBSB(25),YBSB(25),XBST(
     325),YBST(25),BTXY(25),TXYB(25),TXYT(25),SIGMA(25),TSXB(25
     4),TSYT(25),TSXT(25),TSYT(25),TXYT(25),XMSN(25),YMSN(25),G(25)
      DIMENSION CAX(25),CD(25),CGAM(25),A(25,25),D11(25),D12(25),D13(25)
     1,PL(25),L(25),P1(25),IR(25),IC(25),A11(25),A12(25),A13(25),
     2A21(25),A22(25),A23(25),A31(25),A32(25),A33(25),A41(25),A42(25),
     3A43(25),A51(25),A52(25),A53(25),G1(25),G2(25),G3(25),G4(25),G5(25)
     4,GE(25),G7(25),G8(25),A1(25),A2(25),A3(25),A4(25),B1(25),B2(25)
      COMMON/AA/A,F,PL,L,M1,BMX,BMY,BMXY,WN,W1,W2,ZX,ZY,ZBX,
     1ZBY,ZTX,ZTY,XML,YMU,N,NT
      COMMON/BB/AX,DX,H,SI,GAM,D,XK,YK,DEL,BY,BXY,BYX,FT,FP,SIX,SIY,XI,
     1YI,GX,GY,CX,AAX,AAY,TX,TY,CH,BX,BY,CGAM,CD,CAX
      COMMON/CC/XMS,YMS,XBSB,YBSB,XBST,YBST,TSXB,TSYB,TSXT,TSYT,SIGMA,
     1BTXY,TXYB,TXYT
      COMMON/DD/AM,AN,YIELD,FX,FY,FX,FY,G,FI,Z1,Z2,THIC,AL,AB,ZETA,ANU,
     1EXA,AS,BET,ALP,TL,TI,ANG
      COMMON/EE/N1,N2,N3,N4,N5,N7,N8,N9,N11,N12,N13,N14,M2,M3,M4,M5,M7,
     1M8,M9,M10,M12,M13,M14,M15,M17,M18,M19,M20,K1,K2,K3,K4,K6,K7,K8,K9,
     2K11,K12,K13,K14,K16,K17,K18,K19,K21,K22,K23,K24,K26,K27,K28,K29,
     3K31,K32,K33,K34,K35,K37,K38,K39
      DO 601 I=1,K1
      ZBY(I)=(AM*T(I)**(ZY(I)-T(I)/2.)+(ZY(I)-T(I))**2*.5*FY)/(FY*(ZY(I)-
     1T(I))+AM*T(I))
      ZBX(I)=(AM*T(I)*(ZX(I)-T(I)/2.)+(ZX(I)-T(I))**2*.5*FX)/(FX*(ZX(I)-
     1T(I))+AM*T(I))
      ZTY(I)=ZY(I)-ZBY(I)
      ZTX(I)=ZX(I)-ZBX(I)
      YI(I)=FY*((ZY(I)-T(I))**3)/12.+FY*(ZY(I)-T(I))*(((ZY(I)-T(I))/2.-
     1ZBY(I))**2)+AN*T(I)*((ZTY(I)-T(I)/2.)**2)
      XI(I)=FX*((ZX(I)-T(I))**3)/12.+FX*(ZX(I)-T(I))*(((ZX(I)-T(I))/2.-
     1ZBX(I))**2)+AM*(T(I)**3)/12.+AM*T(I)*((ZTX(I)-T(I)/2.)**2)
      SIY(I)=FY*((ZY(I)-T(I))**3)/12.+FY*(ZY(I)-T(I))*(((ZY(I)-T(I))/2.-
     1ZBY(I))**2)
      SIX(I)=FX*((ZX(I)-T(I))**3)/12.+FX*(ZX(I)-T(I))*(((ZX(I)-T(I))/2.-
     1ZBX(I))**2)
      XMU(I)=XMU(I)
      DX(I)=T(I)**3*FX/(12.-12.*XMU(I)*YMU(I))+GX*SIX(I)/AM+(FX*T(I)*((
     1ZTX(I)-T(I)/2.)**2))/(1.-XMU(I)*YMU(I))
      DY(I)=T(I)**3*FY/(12.-12.*XMU(I)*YMU(I))+GY*SIY(I)/AN+(FY*T(I)*((
     1ZTY(I)-T(I)/2.)**2))/(1.-XMU(I)*YMU(I))
      GX(I)=FX*.5/(1.+SQRT(XMU(I)*YMU(I)))
      GY(I)=FY*.5/(1.+SQRT(XMU(I)*YMU(I)))
      FT(I)=AM*.5*(T(I)**3)*.333+FX**3*(ZX(I)-T(I))*.333
      FP(I)=AN*.5*(T(I)**3)*.333+FY**3*(ZY(I)-T(I))*.333
      BXY(I)=GX(I)*FT(I)/AM
      BYX(I)=GY(I)*FP(I)/AN
      CX(I)=(BXY(I)+BYX(I))/4.
      H(I)=(DX(I)*YMU(I)+DY(I)*XMU(I)+4.*CX(I))/2.
      D(I)=2.*H(I)-DX(I)-DY(I)
      GAM(I)=AS**2*(DX(I)-XMU(I)*DY(I))
      AX(I)=AS**2*DX(I)+BET**2*DY(I)
      XK(I)=DX(I)+DY(I)*XMU(I)
      YK(I)=DY(I)+DX(I)*YMU(I)
      DEL(I)=AS**2*XK(I)+BET**2*YK(I)
      SI(I)=AS**2*(2.*H(I)-DX(I)-YMU(I)*DY(I))
      AAX(I)=AM*T(I)+FX*(ZX(I)-T(I))
      AAY(I)=AN*T(I)+FY*(ZY(I)-T(I))
      TX(I)=AAX(I)/AM
      TY(I)=AAY(I)/AN
      BX(I)=T(I)/TY(I)
      BY(I)=T(I)/TX(I)
      CH(I)=1.+SQRT(XMU(I)*YMU(I))-.5*(XMU(I)*BY(I)+YMU(I)*BX(I))
      CAX(I)=AS**2*BX(I)+BET**2*BY(I)
      CD(I)=2.*CH(I)-BX(I)-BY(I)
  601 CGAM(I)=BET**2*BY(I)-AS**2*DX(I)*YMU(I)
      RETURN
      END
```

```
      SUBROUTINE DEFLEC
      GENERATION OF EQUILIBRIUM MATRIX EQUATION
      DIMENSION XI(25),YI(25),XMU(25),BMX(25),BX(25),BMY(25),BY(25),BMXY
     1(25),CX(25),BY(25),BX(25),ZTX(25),ZTY(25),SIY(25),SIX(25),GX(25),
     2GY(25),FT(25),FP(25),BXY(25),BYX(25),H(25),D(25),GAM(25),AX(25),
     3XK(25),YK(25),DEL(25),SI(25),DAX(25),AAY(25),TX(25),TY(25),CH(25),
     4B3(25),B4(25),B5(25),B(25,25),C(25),B11(25),B12(25)
      DIMENSION TSXTN(25),TSXBN(25),TSYBN(25),TXYTN(25),TSYTN(25),
     1ZX(25),ZY(25),T(25),XMU(25),ZBX(25),ZBY(25),F(25),W(25),WN(25),W1(
     225),X2(25),ZXN(25),ZYN(25),XMS(25),YMS(25),XBSB(25),YBSB(25),XBST(
     325),YBST(25),BTXY(25),TXYM(25),SIGMA(25),TSXB(25
     4),TSYB(25),TSXT(25),TSYT(25),TXYT(25),XMSN(25),YMSN(25),C(25)
      DIMENSION CAX(25),CD(25),CGAM(25),A(25,25),B11(25),B12(25),B13(25)
     1,PL(25),L(25),M1(25),M(25),IA(25),IC(25),A11(25),A12(25),A13(25),
     2A21(25),A22(25),A23(25),A31(25),A32(25),A33(25),A41(25),A42(25),
     3A43(25),A51(25),A52(25),A53(25),G1(25),G2(25),G3(25),G4(25),G5(25)
     4,G6(25),G7(25),G8(25),A1(25),A2(25),A3(25),A4(25),B1(25),B2(25)
      COMMON/AA/W,F,PL,L,M1,BMX,BMY,BMXY,WN,W1,W2,ZX,ZY,ZBX,
     1ZBY,ZTX,ZTY,XMU,YMU,M,N,T
      COMMON/BB/AX,DX,H,SI,GAM,D,XK,YK,DEL,DY,BXY,BYX,FT,FP,SIX,SIY,XI,
     1YI,GX,GY,CX,AAX,AAY,TX,TY,CH,BX,BY,CGAM,CD,CAX
      COMMON/CC/XMS,YMS,XBSB,YBSB,XBST,YBST,TSXB,TSYB,TSXT,TSYT,SIGMA,
     1BTXY,TXYM,TXYT
      COMMON/DD/AM,AN,YIELD,FX,FY,EX,EY,G,FI,Z1,Z2,THIC,AL,AB,ZETA,ANU,
     1EXA,AS,BET,ALP,TL,TB,ANG
      COMMON/EE/N1,N2,N3,N4,N5,N7,N8,N9,N11,N12,N13,N14,M2,M3,M4,M5,M7,
     1M8,M9,M10,M12,M13,M14,M15,M17,M18,M19,M20,K1,K2,K3,K4,K6,K7,K8,K9,
     2K11,K12,K13,K14,K15,K17,K18,K19,K21,K22,K23,K24,K26,K27,K28,K29,
     3K31,K32,K33,K34,K36,K37,K38,K39
      DO 100 I=1,K1
      B11(I)=0.
      B12(I)=0.
  100 B13(I)=0.
      DO 149 I=1,K1
      DO 149 J=1,K1
  149 A(I,J)=0.
      NO=-1
      DO 101 JA=1,2
      NO=-NO
      GO TO (105),JA
      I=K1
      GO TO 104
  105 I=1
  104 B11(I)=AS**2*T(I)*(BET**2*F(I+NO)-2.*(1.+BET**2)*F(I)+BET*.5*(-F(
     1I+N1*NO))+F(I+M*NO))
      B12(I)=-AS**2*T(I)*2.*(BET*(-2.*F(I)+F(I+NO))+.25*(-F(I+N1*NO)))
      B13(I)=AS**2*T(I)*(-2.*F(I)+F(I+NO))
      A(I,I)=AX(I)*(5.*ALP+4.)+DY(I)*(5.+4.*ALP+BET**2*.75)+AS**2*D(I)*(
     1BET**2*5.+4.)+BET**2*YK(I)*(GAM(I)-AX(I))/(2.*DEL(I))+2.*(B11(
     2I)+BET*B12(I))+2.*(1.+BET**2)*B13(I)
      A(I,I+NO)=-2.*ALP*(2.*AX(I)+DY(I))-2.*AX(I)-AS**2*2.*D(I)*(BET**2*
     12.+1.)-(B11(I)+BET*B12(I)+BET**2*B13(I))
      A(I,I+2*NO)=ALP*AX(I)+BET**2*(AS**2*D(I)-DY(I)/4.)
      A(I,I+M*NO)=AX(I)*ALP*BET*YK(I)/DEL(I)-BET*.5*(ALP*DY(I)+AX(I))-2.
     1*DY(I)*(2.+ALP)-2.*AX(I)+AS**2*D(I)*(BET**3*YK(I)/DEL(I)-BET/2.-2.
     2)-B13(I)
      A(I,I+N1*NO)=(1.+BET)*(ALP*DY(I)+AX(I)+AS**2*D(I))+2.*BET*DY(I)+
     1B12(I)/4.+BET*.5*B13(I)
      A(I,I+N2*NO)=-BET*.5*(ALP*DY(I)+AX(I)+AS**2*D(I))
      A(I,I+M10*NO)=DY(I)*(1.-BET**2*.75)+BET**2*YK(I)*(GAM(I)-AX(I))/(2
     1.*DEL(I))
      A(I,I+N6*NO)=-BET*DY(I)
  101 A(I,I+N7*NO)=BET**2*DY(I)/4.
      NO=-1
      DO 109 JA=1,2
      NO=-NO
      GO TO (108),JA
      I=K2
      GO TO 107
  108 I=2
  107 B11(I)=AS**2*T(I)*(-BET**2*(F(I-NO)+F(I+NO))-2.*(1.+BET**2)*F(I)+
     1BET*.5*(F(I+M4*NO)-F(I+N1*NO))+F(I+M*NO))
      B12(I)=-AS**2*T(I)*2.*(BET*(F(I-NO)-2.*F(I)+F(I+NO))+.25*(F(I+M4*
     1NO)-F(I+N1*NO)))
      B13(I)=AS**2*T(I)*(F(I-NO)-2.*F(I)+F(I+NO))
      A(I,I-NO)=-2.*ALP*(2.*AX(I)+DY(I))-2.*AX(I)-AS**2*2.*D(I)*(BET**2*
     12.+1.)-B11(I)-(BET*B12(I)-BET**2*B13(I))
      A(I,I)=2.*AX(I)*(5.*ALP+2.)+DY(I)*(5.+4.*ALP+BET**2/2.)+AS**2*2.*
     1A(I,I)=2.*AX(I)*(5.*ALP+2.)+DY(I)*(5.+4.*ALP+BET**2/2.)+AS**2*2.*
```

```
     1D(I)*(BET**2*3.+2.)+2.*(D11(I)+BET*D12(I))+2.*D13(I)*(1.+BET**2)
      A(I,I+N0)=A(I,I-N0)
      A(I,I+2*N0)=ALP*AX(I)+BET**2*(AS**2*D(I)-DY(I)/4.)
      A(I,I+M4*N0)=(1.-BET)*(ALP*DY(I)+AX(I)+AS**2*D(I))-2.*BET*DY(I)-
     1D12(I)/4.-BET*.5*D13(I)
      A(I,I+M*N0)=-2.*DY(I)*(ALP+2.)-2.*(AX(I)+AS**2*D(I))-D13(I)
      A(I,I+N1*N0)=(1.+BET)*(ALP*DY(I)+AX(I)+AS**2*D(I))+2.*BET*DY(I)+
     1D12(I)/4.+BET*.5*D13(I)
      A(I,I+N2*N0)=-BET*.5*(ALP*DY(I)+AX(I)+AS**2*D(I))
      A(I,I+M6*N0)=BET*DY(I)
      A(I,I+M10*N0)=DY(I)*(1.-BET**2/2.)
      A(I,I+N6*N0)=-A(I,I+M6*N0)
  109 A(I,I+N7*N0)=BET**2*DY(I)/4.
      N0=-1
      DO 115 JA=1,2
      N0=-N0
      GO TO (114),JA
      I3=K8
      IM=K3
      GO TO 112
  114 I3=3
      IM=M3
  112 DO 115 I=I3,IM
      D11(I)=AS**2*T(I)*(BET**2*(F(I-N0)+F(I+N0))-2.*(1.+BET**2)*F(I)+
     1BET*.5*(F(I+M4*N0)-F(I+N1*N0))+F(I+M*N0))
      D12(I)=-AS**2*T(I)*2.*(BET*(F(I-N0)-2.*F(I)+F(I+N0))+.25*(F(I+M4*
     1N0)-F(I+N1*N0)))
      D13(I)=AS**2*T(I)*(F(I-N0)-2.*F(I)+F(I+N0))
      A(I,I-2*N0)=ALP*AX(I)+BET**2*(AS**2*D(I)-DY(I)/4.)
      A(I,I-N0)=-2.*ALP*(2.*AX(I)+DY(I))-2.*AX(I)-AS**2*2.*D(I)*(BET**2*
     12.+1.)-D11(I)-BET*D12(I)-BET**2*D13(I)
      A(I,I)=2.*AX(I)*(3.*ALP+2.)+DY(I)*(5.+4.*ALP+BET**2/2.)+AS**2*D(I)
     1*2.*(BET**2*3.+2.)+2.*(D11(I)+BET*D12(I))+2.*D13(I)*(1.+BET**2)
      A(I,I+N0)=A(I,I-N0)
      A(I,I+2*N0)=A(I,I-2*N0)
      A(I,I+M3*N0)=BET*.5*(ALP*DY(I)+AX(I)+AS**2*D(I))
      A(I,I+M4*N0)=(1.-BET)*(ALP*DY(I)+AX(I)+AS**2*D(I))-2.*BET*DY(I)-
     1D12(I)/4.-BET*.5*D13(I)
      A(I,I+M*N0)=-2.*DY(I)*(ALP+2.)-2.*(AX(I)+AS**2*D(I))-D13(I)
      A(I,I+N1*N0)=(1.+BET)*(ALP*DY(I)+AX(I)+AS**2*D(I))+2.*BET*DY(I)+
     1D12(I)/4.+BET*.5*D13(I)
      A(I,I+N2*N0)=-A(I,I+M3*N0)
      A(I,I+M8*N0)=BET**2*DY(I)/4.
      A(I,I+M6*N0)=BET*DY(I)
      A(I,I+M10*N0)=DY(I)*(1.-BET**2/2.)
      A(I,I+N6*N0)=-A(I,I+M6*N0)
  115 A(I,I+N7*N0)=A(I,I+M8*N0)
      N0=-1
      DO 110 JA=1,2
      N0=-N0
      GO TO (117),JA
      I=K7
      GO TO 116
  117 I=M4
  116 D11(I)=AS**2*T(I)*(BET**2*(F(I-N0)+F(I+N0))-2.*(1.+BET**2)*F(I)+
     1BET*.5*(F(I+M4*N0)-F(I+N1*N0))+F(I+M*N0))
      D12(I)=-AS**2*T(I)*2.*(BET*(F(I-N0)-2.*F(I)+F(I+N0))+.25*(F(I+M4*
     1N0)-F(I+N1*N0)))
      D13(I)=AS**2*T(I)*(F(I-N0)-2.*F(I)+F(I+N0))
      A(I,I-2*N0)=ALP*AX(I)+BET**2*(AS**2*D(I)-DY(I)/4.)
      A(I,I-N0)=-2.*ALP*(2.*AX(I)+DY(I))-2.*AX(I)-AS**2*2.*D(I)*(BET**2*
     12.+1.)-D11(I)-BET*D12(I)-BET**2*D13(I)
      A(I,I)=2.*AX(I)*(3.*ALP+2.)+DY(I)*(5.+4.*ALP+BET**2/2.)+AS**2*2.*D
     1(I)*(BET**2*3.+2.)+2.*(D11(I)+BET*D12(I))+2.*D13(I)*(1.+BET**2)
      A(I,I+N0)=A(I,I-N0)
      A(I,I+M3*N0)=BET*.5*(ALP*DY(I)+AX(I)+AS**2*D(I))
      A(I,I+M4*N0)=(1.-BET)*(ALP*DY(I)+AX(I)+AS**2*D(I))-2.*BET*DY(I)
     1-D12(I)/4.-BET*.5*D13(I)
      A(I,I+M*N0)=-2.*DY(I)*(ALP+2.)-2.*(AX(I)+AS**2*D(I))-D13(I)
      A(I,I+N1*N0)=(1.+BET)*(ALP*DY(I)+AX(I)+AS**2*D(I))+2.*BET*DY(I)+
     1D12(I)/4.+BET*.5*D13(I)
      A(I,I+M8*N0)=BET**2*DY(I)/4.
      A(I,I+M6*N0)=BET*DY(I)
      A(I,I+M10*N0)=DY(I)*(1.-BET**2/2.)
  110 A(I,I+N6*N0)=-A(I,I+M6*N0)
      N0=-1
      DO 124 JA=1,2
      N0=-N0
```

```
      GO TO (121),JA
      I=K6
      GO TO 120
  121 I=N
  120 D11(I)=AS**2*T(I)*(BET**2*F(I-NO)-2.*(1.+BET**2)*F(I)+BET*.5*F(
     1I+M6*NO)+F(I+M*NO))
      D12(I)=-AS*2*T(I)*2.*(BET*(F(I-NO)-2.*F(I))+.25*F(I+M4*NO))
      D13(I)=AS**2*T(I)*(F(I-NO)-2.*F(I)+F(I+NO))
      A(I,I-2*NO)=ALP*AX(I)+BET**2*(AS**2*D(I)-DY(I)/4.)
      A(I,I-NO)=-2.*ALP*(2.*AX(I)+DY(I))-2.*AX(I)-AS**2*2.*D(I)*(
     1BET**2*2.+1.)-D11(I)-BET*D12(I)-BET**2*D13(I)
      A(I,I)=AX(I)*(5.*ALP+4.)+DY(I)*(5.+4.*ALP+BET**2*.75)+AS**2*D(I)*
     1(BET**2*6.+4.)+BET**2*YK(I)*(GAM(I)-AX(I))/(2.*DEL(I))+2.*(D11(I)+
     2BET*D12(I))+2.*(1.+BET**2)*D13(I)
      A(I,I+M3*NO)=BET*.5*(ALP*DY(I)+AX(I)+AS**2*D(I))-2.*BET*DY(I)-
      A(I,I+M4*NO)=(1.-BET)*(ALP*DY(I)+AX(I)+AS**2*D(I))-D13(I)
     1D12(I)/4.-BET*.5*D13(I)
      A(I,I+M*NO)=-AX(I)-ALP*BET*YK(I)/DEL(I)+BET*.5*(AX(I)+ALP*DY(I))-
     12.*DY(I)*(ALP+2.)-2.*AX(I)+AS**2*D(I)*(-2.+BET/2.-BET**3*YK(I)/
     1DEL(I))-D13(I)
      A(I,I+M8*NO)=BET**2*DY(I)/4.
      A(I,I+M9*NO)=BET*DY(I)
  124 A(I,I+M10*NO)=DY(I)*(1.-BET**2*.75)-BET**2*YK(I)*(GAM(I)-AX(I))/(
     12.*DEL(I))
      NO=-1
      DO 129 JA=1,2
      NO=-NO
      GO TO (126),JA
      I=K11
      GO TO 125
  127 I=N1
  125 D11(I)=AS**2*T(I)*(BET**2*F(I+NO)-2.*(1.+BET**2)*F(I)+BET*.5*(F(
     1I-M4*NO)-F(I+N1*NO))+F(I-M*NO)+F(I+M*NO))
      D12(I)=-AS**2*T(I)*2.*(BET*(F(I)+F(I+NO))+.25*(F(I-M4*NO)-F(I+
     1N1*NO)))
      D13(I)=AS**2*T(I)*(-2.*F(I)+F(I+NO))
      A(I,I-4*NO)=-DY(I)*(4.+2.*ALP-ALP*BET/2.)+AX(I)*(BET/2.-2.-ALP*BET
     1*YK(I)/DEL(I))+AS**2*D(I)*(BET/2.-2.-BET**3*YK(I)/DEL(I))-D13(I)
      A(I,I-M4*NO)=(1.-BET)*(ALP*DY(I)+AX(I)+AS**2*D(I))-2.*BET*DY(I)-
     1D12(I)/4.-BET*.5*D13(I)
      A(I,I-M3*NO)=BET*.5*(ALP*DY(I)+AX(I)+AS**2*D(I))
      A(I,I)=AX(I)*(5.*ALP+4.)+DY(I)*(4.+4.*ALP+BET**2*1.5)+AS**2*D(I)*
     1(3BET**2*5.+4.)+2.*(D11(I)+BET*D12(I))+2.*D13(I)*(1.+BET**2)
      A(I,I+NO)=-2.*ALP*(2.*AX(I)+DY(I))-2.*AX(I)-AS**2*2.*D(I)*(BET**2*
     12.+1.)-D11(I)-BET*D12(I)-BET**2*D13(I)
      A(I,I+2*NO)=ALP*AX(I)+BET**2*(AS**2*D(I)-DY(I)/2.)
      A(I,I+M*NO)=-DY(I)*(4.+2.*ALP+ALP*BET/2.)+AX(I)*(-BET/2.-2.+ALP*
     1BET*YK(I)/DEL(I))+AS**2*D(I)*(-BET/2.-2.+BET**3*YK(I)/DEL(I))-D13
     2(I)
      A(I,I+N1*NO)=(1.+BET)*(ALP*DY(I)+AX(I)+AS**2*D(I))+2.*BET*DY(I)
     1+D12(I)/4.+BET*.5*D13(I)
      A(I,I+N2*NO)=-A(I,I-M3*NO)
      A(I,I+M10*NO)=DY(I)*(1.-BET**2*.75)
      A(I,I+N6*NO)=-BET*DY(I)
  126 A(I,I+N7*NO)=BET**2*DY(I)/4.
      NO=-1
      DO 134 JA=1,2
      NO=-NO
      GO TO (130),JA
      I=K12
      GO TO 131
  130 I=N2
  131 D11(I)=AS**2*T(I)*(BET**2*(F(I-NO)+F(I+NO))-2.*(1.+BET**2)*F(I)+
     1BET*.5*(F(I-M4*NO)-F(I-N1*NO)+F(I+M4*NO)-F(I+N1*NO))+
     1F(I-M*NO)+F(I+M*NO))
      D12(I)=-AS**2*T(I)*2.*(BET*(F(I-NO)-2.*F(I)+F(I+N1))+.25*(F(I-M4*
     1NO)-F(I-N1*NO)+F(I+M4*NO)-F(I+N1*NO)))
      D13(I)=AS**2*T(I)*(F(I-NO)-2.*F(I)+F(I+NO))
      A(I,I-N1*NO)=(1.+BET)*(ALP*DY(I)+AX(I)+AS**2*D(I))+2.*BET*DY(I)+
     1D12(I)/4.+BET*.5*D13(I)
      A(I,I-M*NO)=-2.*DY(I)*(ALP+2.)-2.*(AX(I)+AS**2*D(I))-D13(I)
      A(I,I-M4*NO)=(1.-BET)*(ALP*DY(I)+AX(I)+AS**2*D(I))-2.*BET*DY(I)-
     1D12(I)/4.-BET*.5*D13(I)
      A(I,I-M3*NO)=BET*.5*(ALP*DY(I)+AX(I)+AS**2*D(I))
      A(I,I-NO)=-2.*ALP*(2.*AX(I)+DY(I))-2.*AX(I)-AS**2*D(I)*2.*(BET**2*
     12.+1.)-D11(I)-BET*D12(I)-BET**2*D13(I)
      A(I,I)=2.*AX(I)*(3.*ALP+2.)+DY(I)*(BET**2+4.*ALP+6.)+AS**2*D(I)*(
     1BET**2*6.+4.)+2.*(D11(I)+BET*D12(I))+2.*D13(I)*(1.+BET**2)
```

```
      A(I,I+N0)=A(I,I-N0)
      A(I,I+2*N0)=ALP*AX(I)+BET**2*(AS**2*D(I)-DY(I)/2.)
      A(I,I+M4*N0)=A(I,I-M4*N0)
      A(I,I+M*N0)=A(I,I-M*N0)
      A(I,I+N1*N0)=A(I,I-N1*N0)
      A(I,I+N2*N0)=-A(I,I-M3*N0)
      A(I,I+M3*N0)=BET*DY(I)
      A(I,I+M10*N0)=DY(I)*(1.-BET**2/2.)
      A(I,I+N5*N0)=-A(I,I+M9*N0)
  134 A(I,I+N7*N0)=BET**2*DY(I)/4.
      NJ=-1
      DO 130 JA=1,2
      N0=-N0
      GO TO (136),JA
      III=K18
      IIM=K13
      GO TO 137
  136 III=N3
      IIM=M8(
  137 DO 139 I=III,IIM
      D11(I)=AS**2*T(I)*(BET**2*(F(I-N0)+F(I+N0))-2.*(1.+BET**2)*F(I)+
     1BET*.5*(F(I-M4*N0)-F(I-N1*N0)+F(I+M4*N0)-F(I+N1*N0))+F(I-M*N0)+
     1F(I+M*N0))
      D12(I)=-AS**2*T(I)*2.*(BET*(F(I-N0)-2.*F(I)+F(I+N0))+.25*(F(I-M4*
     1N0)-F(I-N1*N0)+F(I+M4*N0)-F(I+N1*N0)))
      D13(I)=AS**2*T(I)*(F(I-N0)-2.*F(I)+F(I+N0))
      A(I,I-N2*N0)=-BET*.5*(ALP*DY(I)+AX(I)+AS**2*D(I))
      A(I,I-N1*N0)=(1.+BET)*(ALP*DY(I)+AX(I)+AS**2*D(I))+2.*BET*DY(I)+
     1D12(I)/4.+BET*.5*D13(I)
      A(I,I-M*N0)=-2.*DY(I)*(ALP+2.)-2.*(AX(I)+AS**2*D(I))-D13(I)
      A(I,I-M4*N0)=(1.-BET)*(ALP*DY(I)+AX(I)+AS**2*D(I))-2.*BET*DY(I)-
     1D12(I)/4.-BET*.5*D13(I)
      A(I,I-M3*N0)=-A(I,I-N2*N0)
      A(I,I-2*N0)=ALP*AX(I)+BET**2*(AS**2*D(I)-DY(I)/2.)
      A(I,I-N0)=-2.*ALP*(2.*AX(I)+DY(I))-2.*AX(I)-AS**2*2.*D(I)*(
     1BET**2*2.+1.)-D11(I)-BET*D12(I)-BET**2*D13(I)
      A(I,I)=2.*AX(I)*(3.*ALP+2.)+DY(I)*(BET**2+4.*ALP+6.)+AS**2*D(I)*(
     1BET**2*6.+4.)+2.*(D11(I)+BET*D12(I))+2.*D13(I)*(1.+BET**2)
      A(I,I+N0)=A(I,I-N0)
      A(I,I+2*N0)=A(I,I-2*N0)
      A(I,I+M3*N0)=A(I,I-M3*N0)
      A(I,I+M4*N0)=A(I,I-M4*N0)
      A(I,I+M*N0)=A(I,I-M*N0)
      A(I,I+N1*N0)=A(I,I-N1*N0)
      A(I,I+N2*N0)=A(I,I-N2*N0)
      A(I,I+M8*N0)=BET**2*DY(I)/4.
      A(I,I+M9*N0)=BET*DY(I)
      A(I,I+M10*N0)=DY(I)*(1.-BET**2/2.)
      A(I,I+N6*N0)=-A(I,I+M9*N0)
  139 A(I,I+N7*N0)=A(I,I+M8*N0)
      N0=-1
      DO 145 JA=1,2
      N0=-N0
      GO TO (140),JA
      I=K17
      GO TO 141
  140 I=M9
  141 D11(I)=AS**2*T(I)*(BET**2*(F(I-N0)+F(I+N0))-2.*(1.+BET**2)*F(I)+
     1BET*.5*(F(I-M4*N0)-F(I-N1*N0)+F(I+M4*N0)-F(I+N1*N0))+
     2F(I-M*N0)+F(I+M*N0))
      D12(I)=-AS**2*T(I)*2.*(BET*(F(I-N0)-2.*F(I)+F(I+N0))+.25*(F(I-M4*
     1N0)-F(I-N1*N0)+F(I+M4*N0)-F(I+N1*N0)))
      D13(I)=AS**2*T(I)*(F(I-N0)-2.*F(I)+F(I+N0))
      A(I,I-N2*N0)=-BET*.5*(ALP*DY(I)+AX(I)+AS**2*D(I))
      A(I,I-N1*N0)=(1.+BET)*(ALP*DY(I)+AX(I)+AS**2*D(I))+2.*BET*DY(I)+
     1D12(I)/4.+BET*.5*D13(I)
      A(I,I-M*N0)=-2.*DY(I)*(ALP+2.)-2.*(AX(I)+AS**2*D(I))-D13(I)
      A(I,I-M4*N0)=(1.-BET)*(ALP*DY(I)+AX(I)+AS**2*D(I))-2.*BET*DY(I)-
     1D12(I)/4.-BET*.5*D13(I)
      A(I,I-2*N0)=ALP*AX(I)+BET**2*(AS**2*D(I)-DY(I)/2.)
      A(I,I-N0)=-2.*ALP*(2.*AX(I)+DY(I))-2.*AX(I)-AS**2*2.*D(I)*(BET
     1**2*2.+1.)-D11(I)-BET*D12(I)-BET**2*D13(I)
      A(I,I)=2.*AX(I)*(3.*ALP+2.)+DY(I)*(BET**2+4.*ALP+6.)+AS**2*D(I)*(
     1BET**2*6.+4.)+2.*(D11(I)+BET*D12(I))+2.*D13(I)*(1.+BET**2)
      A(I,I+N0)=A(I,I-N0)
      A(I,I+M3*N0)=-A(I,I-N2*N0)
      A(I,I+M4*N0)=A(I,I-M4*N0)
      A(I,I+M*N0)=A(I,I-M*N0)
```

```
      A(I,I+N1*NO)=A(I,I-N1*NO)
      A(I,I+N4*NO)=BET**2*DY(I)/4.
      A(I,I+M6*NO)=BET*DY(I)
      A(I,I+M10*NO)=DY(I)*(1.-BET**2/2.)
  140 A(I,I+N6*NO)=-A(I,I+M6*NO)
      CALL DEFLF
      RETURN
      END
```

```
      SUBROUTINE DEFLE
      DIMENSION TSXTN(25),TSXBN(25),TSYBN(25),TXYTN(25),TSYTN(25),
     1ZY(25),ZY(25),T(25),XMU(25),ZBX(25),ZBY(25),F(25),W(25),WN(25),W1(
     225),W2(25),ZXN(25),ZYN(25),XMS(25),YMS(25),XBSB(25),YBSB(25),XBST(
     325),YBST(25),BTXY(25),TXYM(25),SIGMA(25),TSXB(25
     4),TSYB(25),TSXT(25),TSYT(25),TXYT(25),XMSN(25),YMSN(25),G(25)
      DIMENSION XI(25),YI(25),YMU(25),BMX(25),DX(25),BMY(25),DY(25),BMXY
     1(25),CX(25),BY(25),BX(25),ZTX(25),ZTY(25),SIY(25),SIX(25),GX(25),
     2GY(25),FT(25),FP(25),BXY(25),BYX(25),P(25),D(25),GAM(25),AX(25),
     3XK(25),YK(25),DEL(25),SI(25),AAX(25),AAY(25),TX(25),TY(25),CH(25),
     4B3(25),B4(25),B5(25),B(25,25),C(25),B11(25),B12(25)
      DIMENSION CAX(25),CD(25),CGAM(25),A(25,25),D11(25),D12(25),D13(25)
     1,PL(25),L(25),M1(25),IA(25),IC(25),A11(25),A12(25),A13(25),
     2A21(25),A22(25),A23(25),A31(25),A32(25),A33(25),A41(25),A42(25),
     3A43(25),A51(25),A52(25),A53(25),G1(25),G2(25),G3(25),G4(25),G5(25)
     4,G6(25),G7(25),G8(25),A1(25),A2(25),A3(25),A4(25),B1(25),B2(25)
      COMMON/AA/W,F,PL,L,M1,BMX,BMY,BMXY,WN,W1,W2,ZX,ZY,ZBX,
     1ZBY,ZTX,ZTY,XMU,YMU,M,N,T
      COMMON/BB/AX,DX,H,SI,GAM,D,XK,YK,DEL,DY,BXY,BYX,FT,FP,SIX,SIY,XI,
     1YI,GX,GY,CX,AAX,AAY,TX,TY,CH,BX,BY,CGAM,CD,CAX
      COMMON/CC/XMS,YMS,XBSB,YBSB,XBST,YBST,TSXB,TSYB,TSXT,TSYT,SIGMA,
     1BTXY,TXYM,TXYT
      COMMON/DD/AM,AN,YIELD,FX,FY,EX,EY,C,FI,Z1,Z2,THIC,AL,AB,ZETA,ANU,
     1BXA,AS,BET,ALP,TL,TB,ANG
      COMMON/EE/N1,N2,N3,N4,N6,N7,N8,N9,N11,N12,N13,N14,M2,M3,M4,M5,M7,
     1M8,M9,M10,M12,M13,M14,M15,M17,M18,M19,M20,K1,K2,K3,K4,K6,K7,K8,K9,
     2K11,K12,K13,K14,K16,K17,K18,K19,K21,K22,K23,K24,K26,K27,K28,K29,
     3K31,K32,K33,K34,K36,K37,K38,K39
      NO=-1
      DO 150 JA=1,2
      NO=-NO
      GO TO (146),JA
      I=K16
      GO TO 144
  146 I=M10
  144 D11(I)=AS**2*T(I)*(BET**2*F(I-NO)-2.*(1.+BET**2)*F(I)+BET*.5*(-F(
     1I-N1*NO)+F(I+M4*NO))+F(I-M*NO)+F(I+M*NO))
      D12(I)=-AS**2*T(I)*2.*(BET*(F(I-NO)-2.*F(I))+.25*(-F(I-N1*NO)+
     1F(I+M4*NO)))
      D13(I)=AS**2*T(I)*(F(I-NO)-2.*F(I))
      A(I,I-N2*NO)=-BET*.5*(ALP*DY(I)+AX(I)+AS**2*D(I))
      A(I,I-N1*NO)=(1.+BET)*(ALP*DY(I)+AX(I)+AS**2*D(I))+2.*BET*DY(I)+
     1D12(I)/4.+BET*.5*D13(I)
      A(I,I-M*NO)=-DY(I)*(4.+2.*ALP+ALP*BET/2.)+AX(I)*(-BET/2.-2.+ALP*
     1BET*YK(I)/DEL(I))+AS**2*D(I)*(-BET/2.-2.+BET**3*YK(I)/DEL(I))-D13(
     2I)
      A(I,I-2*NO)=ALP*AX(I)+BET**2*(AS**2*D(I)-DY(I)/2.)
      A(I,I-NO)=-2.*ALP*(2.*AX(I)+DY(I))-2.*AX(I)-AS**2*D(I)*2.*(BET**2*
     12.+1.)-D11(I)-BET*D12(I)-BET**2*D13(I)
      A(I,I)=AX(I)*(8.*ALP+4.)+DY(I)*(6.+4.*ALP+BET**2*1.5)+AS**2*D(I)*(
     1BET**2*6.+4.)+2.*(D11(I)+BET*D12(I))+2.*D13(I)*(1.+BET**2)
      A(I,I+M3*NO)=-A(I,I-N2*NO)
      A(I,I+M4*NO)=(1.-BET)*(ALP*DY(I)+AX(I)+AS**2*D(I))
     1-2.*BET*DY(I)-D12(I)/4.-BET*.5*D13(I)
      A(I,I+M*NO)=-DY(I)*(4.+2.*ALP-ALP*BET/2.)+AX(I)*(BET/2.-2.-ALP*
     1BET*YK(I)/DEL(I))+AS**2*D(I)*(BET/2.-2.-BET**3*YK(I)/DEL(I))-
     2D13(I)
      A(I,I+M8*NO)=BET**2*DY(I)/4.
      A(I,I+M9*NO)=BET*DY(I)
      A(I,I+M10*NO)=DY(I)*(1.-BET**2*.75)
  150 A(I,I+M13*NO)=-A(I,I-N2*NO)
      DO 180 I=N6,K26,M
      D11(I)=AS**2*T(I)*(BET**2*F(I+1)-2.*(1.+BET**2)*F(I)+BET*.5*(F(
     1I-M4)-F(I+N1))+F(I-M)+F(I+M))
      D12(I)=-AS**2*T(I)*2.*(BET*(-2.*F(I)+F(I+1))+.25*(F(I-M4)-F(I+N1))
     1)
      D13(I)=AS**2*T(I)*(-2.*F(I)+F(I+1))
      A(I,I-M10)=DY(I)*(1.-BET**2*.75)
      A(I,I-M9)=BET*DY(I)
      A(I,I-M8)=BET**2*DY(I)/4.
      A(I,I-M6)=BET**2*DY(I)/4.
      A(I,I-M5)=-DY(I)*(4.+2.*ALP-ALP*BET/2.)+AX(I)*(BET/2.-2.-ALP*BET*Y
     1K(I)/DEL(I))+AS**2*D(I)*(BET/2.-2.-BET**3*YK(I)/DEL(I))-D13(I)
      A(I,I-M4)=(1.-BET)*(ALP*DY(I)+AX(I)+AS**2*D(I))-2.*BET*DY(I)-
     1D12(I)/4.-BET*.5*D13(I)
      A(I,I-M3)=BET*.5*(ALP*DY(I)+AX(I)+AS**2*D(I))
      A(I,I)=AX(I)*(8.*ALP+4.)+DY(I)*(6.+4.*ALP+BET**2*1.5)+AS**2*D(I)*(
     1BET**2*6.+4.)+2.*(D11(I)+BET*D12(I))+2.*D13(I)*(1.+BET**2)
      A(I,I+1)=-2.*ALP*(2.*AX(I)+DY(I))-2.*AX(I)-AS**2*2.*D(I)*(BET**2*
     12.+1.)-D11(I)-BET*D12(I)-BET**2*D13(I)
```

```
      A(I,I+2)=ALP*AX(I)+BET**2*(AS**2*D(I)-DY(I)/2.)
      A(I,I+M)=-DY(I)*(4.+2.*ALP+ALP*BET/2.)+AX(I)*(-BET/2.-2.+ALP*BET*
     1YK(I)/DEL(I))+AS**2*D(I)*(-BET/2.-2.+BET**3*YK(I)/DEL(I))-D13(I)
      A(I,I+N1)=(1.+BET)*(ALP*DY(I)+AX(I)+AS**2*D(I))+2.*BET*DY(I)+
     1D12(I)/4.+BET*.5*D13(I)
      A(I,I+N2)=-A(I,I-M3)
      A(I,I+M10)=A(I,I-M10)
      A(I,I+N6)=-A(I,I-M3)
      A(I,I+N7)=A(I,I-M3)
  180 CONTINUE
      DO 190 I=N7,K27,M
      D11(I)=AS**2*T(I)*(BET**2*(F(I-1)+F(I+1))-2.*(1.+BET**2)*F(I)+
     1BET*.5*(F(I-M4)-F(I-N1)+F(I+M4)-F(I+N1))+F(I-M)+F(I+M))
      D12(I)=-AS**2*T(I)*2.*(BET*(F(I-1)-2.*F(I)+F(I+1))+.25*(F(I-M4)-
     1F(I-N1)+F(I+M4)-F(I+N1)))
      D13(I)=AS**2*T(I)*(F(I-1)-2.*F(I)+F(I+1))
      A(I,I-N6)=-BET*DY(I)
      A(I,I-M10)=DY(I)*(1.-BET**2/2.)
      A(I,I-M9)=-A(I,I-M5)
      A(I,I-M8)=BET**2*DY(I)/4.
      A(I,I-N1)=(1.+BET)*(ALP*DY(I)+AX(I)+AS**2*D(I))+2.*BET*DY(I)+
     1D12(I)/4.+BET*.5*D13(I)
      A(I,I-M)=-2.*DY(I)*(ALP+2.)-2.*(AX(I)+AS**2*D(I))-D13(I)
      A(I,I-M4)=(1.-BET)*(ALP*DY(I)+AX(I)+AS**2*D(I))-2.*BET*DY(I)-
     1D12(I)/4.-BET*.5*D13(I)
      A(I,I-M3)=BET*.5*(ALP*DY(I)+AX(I)+AS**2*D(I))
      A(I,I-1)=-2.*ALP*(3.*AX(I)+DY(I))-2.*AX(I)-AS**2*2.*D(I)*(BET**2*2
     1.+1.)-D11(I)-BET*D12(I)-BET**2*D13(I)
      A(I,I)=2.*AX(I)*(3.*ALP+2.)+DY(I)*(BET**2+4.*ALP+6.)+AS**2*D(I)*(
     1BET**2*6.+4.)+2.*(D11(I)+BET*D12(I))+2.*D13(I)*(1.+BET**2)
      A(I,I+1)=A(I,I-1)
      A(I,I+2)=ALP*AX(I)+BET**2*(AS**2*D(I)-DY(I)/2.)
      A(I,I+M4)=A(I,I-M4)
      A(I,I+M5)=A(I,I-M5)
      A(I,I+N1)=A(I,I-N1)
      A(I,I+N2)=-A(I,I-M7)
      A(I,I+M9)=A(I,I-M9)
      A(I,I+M10)=A(I,I-M10)
      A(I,I+N6)=A(I,I-N6)
      A(I,I+N7)=A(I,I-M8)
  190 CONTINUE
      DO 195 I=3,M3
      DO 195 J=M10,N10,M
      JA=I+J
      D11(JA)=AS**2*T(JA)*(BET**2*(F(JA-1)+F(JA+1))-2.*(1.+BET**2)*F(JA)
     1+BET*.5*(F(JA-M4)-F(JA-N1)+F(JA+M4)-F(JA+N1))+F(JA-M)+F(JA+M))
      D12(JA)=-AS**2*T(JA)*2.*(BET*(F(JA-1)+2.*F(JA)+F(JA+1))+.25*(F(
     1JA-M4)-F(JA-N1)+F(JA+M4)-F(JA+N1)))
      D13(JA)=AS**2*T(JA)*(F(JA-1)-2.*F(JA)+F(JA+1))
      A(JA,JA-N7)=BET*DY(JA)/4.
      A(JA,JA-N6)=-BET*DY(JA)
      A(JA,JA-M10)=DY(JA)*(1.-BET**2/2.)
      A(JA,JA-M9)=-A(JA,JA-N5)
      A(JA,JA-M8)=A(JA,JA-N7)
      A(JA,JA-N2)=-BET*.5*(ALP*DY(JA)+AX(JA)+AS**2*D(JA))+2.*BET*DY(JA)
      A(JA,JA-N1)=(1.+BET)*(ALP*DY(JA)+AX(JA)+AS**2*D(JA))+2.*BET*DY(JA)
     1+D12(JA)/4.+BET*.5*D13(JA)
      A(JA,JA-M)=-2.*DY(JA)*(ALP+2.)-2.*(AX(JA)+AS**2*D(JA))-D13(JA)
      A(JA,JA-M4)=(1.-BET)*(ALP*DY(JA)+AX(JA)+AS**2*D(JA))-2.*BET*DY(JA)
     1-D12(JA)/4.-BET*.5*D13(JA)
      A(JA,JA-M3)=-A(JA,JA-N2)
      A(JA,JA-2)=ALP*AX(JA)+BET**2*(AS**2*D(JA)-DY(JA)/2.)
      A(JA,JA-1)=-2.*ALP*(2.*AX(JA)+DY(JA))-2.*AX(JA)-AS**2*2.*D(JA)*(
     1BET**2*2.+1.)-D11(JA)-BET*D12(JA)-BET**2*D13(JA)
      A(JA,JA)=2.*AX(JA)*(3.*ALP+2.)+DY(JA)*(BET**2+4.*ALP+6.)+AS**2*D
     1(JA)*(BET**2*6.+4.)+2.*(D11(JA)+BET*D12(JA))+2.*D13(JA)*(1.+BET**2
     1)
      A(JA,JA+1)=A(JA,JA-1)
      A(JA,JA+2)=A(JA,JA-2)
      A(JA,JA+M3)=A(JA,JA-M3)
      A(JA,JA+M4)=A(JA,JA-M4)
      A(JA,JA+M)=A(JA,JA-M)
      A(JA,JA+N1)=A(JA,JA-N1)
      A(JA,JA+N2)=A(JA,JA-N2)
      A(JA,JA+M8)=A(JA,JA-M8)
      A(JA,JA+M9)=A(JA,JA-M9)
      A(JA,JA+M10)=A(JA,JA-M10)
      A(JA,JA+N6)=A(JA,JA-N6)
```

```
      A(JA,JA+N7)=A(JA,JA-N7)
  100 CONTINUE
      DO 200 I=M14,K20,M
      D11(I)=AS**2*T(I)*(BET**2*(F(I-1)+F(I+1))-2.*(1.+BET**2)*F(I)+BET*
     1.5*(F(I-M4)-F(I-N1)+F(I+M4)-F(I+N1))+F(I-M)+F(I+M))
      D12(I)=-AS**2*T(I)**2.*(BET*(F(I-1)-2.*F(I)+F(I+1))
     1+.25*(F(I-M4)-F(I-N1)+F(I+M4)-F(I+N1)))
      D13(I)=AS**2*T(I)*(F(I-1)-2.*F(I)+F(I+1))
      A(I,I-N7)=BET**2*DY(I)/4.
      A(I,I-N6)=-BET*DY(I)
      A(I,I-M10)=DY(I)*(1.-BET**2/2.)
      A(I,I-M9)=-A(I,I-N2)
      A(I,I-N2)=-BET*.5*(ALP*DY(I)+AX(I)+AS**2*D(I))
      A(I,I-N1)=(1.+BET)*(ALP*DY(I)+AX(I)+AS**2*D(I))+2.*BET*DY(I)+D12(I
     1)/4.+BET*.5*D13(I)
      A(I,I-M)=-2.*DY(I)*(ALP+2.)-2.*(AX(I)+AS**2*D(I))-D13(I)
      A(I,I-M4)=(1.-BET)*(ALP*DY(I)+AX(I)+AS**2*D(I))-2.*BET*DY(I)-
     1D12(I)/4.-BET*.5*D13(I)
      A(I,I-2)=ALP*AX(I)+BET**2*(AS**2*D(I)-DY(I)/2.)
      A(I,I-1)=-2.*ALP*(2.*AX(I)+DY(I))-2.*AX(I)-AS**2*D(I)*2.*(BET**2*2
     1.+1.)-D11(I)-BET*D12(I)-BET**2*D13(I)
      A(I,I)=2.*AX(I)*(3.*ALP+2.)+DY(I)*(BET**2+4.*ALP+6.)+AS**2*D(I)*(
     1BET**2*6.+4.)+2.*(D11(I)+BET*D12(I))+2.*D13(I)*(1.+BET**2)
      A(I,I+1)=A(I,I-1)
      A(I,I+M3)=-A(I,I-N2)
      A(I,I+M4)=A(I,I-M4)
      A(I,I+M)=A(I,I-M)
      A(I,I+N1)=A(I,I-N1)
      A(I,I+MP)=A(I,I-N7)
      A(I,I+M9)=A(I,I-M9)
      A(I,I+M10)=A(I,I-M10)
      A(I,I+N6)=A(I,I-N6)
  200 CONTINUE
      DO 205 I=M15,K21,M
      D11(I)=AS**2*T(I)*(BET**2*F(I-1)-2.*(1.+BET**2)*F(I)+BET*.5*(-F(I-
     1N1)+F(I+M4))+F(I-M)+F(I+M))
      D12(I)=-AS**2*T(I)*2.*(BET*(F(I-1)-2.*F(I))+.25*(-F(I-N1)+F(I+M4))
     1)
      D13(I)=AS**2*T(I)*(F(I-1)-2.*F(I))
      A(I,I-N7)=BET**2*DY(I)/4.
      A(I,I-N6)=-BET*DY(I)
      A(I,I-M10)=DY(I)*(1.-BET**2*.75)
      A(I,I-M9)=-BET*.5*(ALP*DY(I)+AX(I)+AS**2*D(I))
      A(I,I-N1)=(1.+BET)*(ALP*DY(I)+AX(I)+AS**2*D(I))+2.*BET*DY(I)+D12(I
     1)/4.+BET*.5*D13(I)
      A(I,I-M)=-DY(I)*(4.+2.*ALP+ALP*BET/2.)+AX(I)*(-BET/2.-2.+ALP*BET*
     1YK(I)/DEL(I))+AS**2*D(I)*(-BET/2.-2.+BET**3*YK(I)/DEL(I))-D13(I)
      A(I,I-2)=ALP*AX(I)+BET**2*(AS**2*D(I)-DY(I)/2.)
      A(I,I-1)=-2.*ALP*(2.*AX(I)+DY(I))-2.*AX(I)-AS**2*D(I)*2.*(BET**2*
     12.+1.)-D11(I)-BET*D12(I)-BET**2*D13(I)
      A(I,I)=AX(I)*(6.*ALP+4.)+DY(I)*(6.+4.*ALP+BET**2*1.5)+AS**2*D(I)*(
     1BET**2*3.+4.)+2.*(D11(I)+BET*D12(I))+2.*D13(I)*(1.+BET**2)
      A(I,I+M3)=-A(I,I-N2)
      A(I,I+M4)=(1.-BET)*(ALP*DY(I)+AX(I)+AS**2*D(I))-2.*BET*DY(I)-
     1D12(I)/4.-BET*.5*D13(I)
      A(I,I+M)=-DY(I)*(4.+2.*ALP-ALP*BET/2.)+AX(I)*(3ET/2.-2.-ALP*BET*
     1YK(I)/DEL(I))+AS**2*D(I)*(BET/2.-2.-BET**3*YK(I)/DEL(I))-D13(I)
      A(I,I+MP)=A(I,I-N7)
      A(I,I+M9)=-A(I,I-N6)
      A(I,I+M10)=A(I,I-M10)
  205 CONTINUE
      DO 990 IA=1,K1
      DO 990 JA=1,K1
  990 A(IA,JA)=A(IA,JA)*1.E-4
      CALL MINV(A,25,DS,L,M1)
      DO 703 I=1,K1
      B(I)=AB**4*0
      DO 704 I=1,K1
      WN(I)=0.
      DO 705 J=1,K1
      WN(I)=WN(I)+A(I,J)*BL(J)*1.E-4
  705 CONTINUE
  704 CONTINUE
      PRINT 750
  750 FORMAT (//' NODE                    LOAD 0                    DEFLECTIONS')
      PRINT 751,(I,B(I),WN(I),I=1,K1)
  751 FORMAT (I5,4X,E15.8,4X,E15.8)
      RETURN
```

END

```
      SUBROUTINE MEMBRN
C     GENERATION OF COMPATIBILITY MATRIX EQUATION
      DIMENSION XI(25),YI(25),YMU(25),BMX(25),DX(25),BMY(25),DY(25),BMXY
     1(25),CX(25),AY(25),BX(25),ZTX(25),ZTY(25),SIY(25),SIX(25),GX(25),
     2GY(25),FT(25),FP(25),BXY(25),BYX(25),N(25),D(25),GAM(25),AX(25),
     3XK(25),YK(25),DEL(25),SI(25),AAX(25),AAY(25),TX(25),TY(25),CH(25),
     4B3(25),B4(25),B5(25),B(25,25),C(25),B11(25),B12(25)
      DIMENSION TSXTN(25),TSXBN(25),TSYBN(25),TXYTN(25),TSYTN(25),
     1ZX(25),ZY(25),T(25),XMU(25),ZBX(25),ZBY(25),F(25),W(25),WN(25),W1(
     225),W2(25),ZXN(25),ZYN(25),XMS(25),YMS(25),XBSB(25),YBSB(25),XBST(
     325),YBST(25),BTXY(25),TXYM(25),SIGMA(25),TSXB(25
     4),TSYB(25),TSXT(25),TSYT(25),TXYT(25),XMSN(25),YMSN(25),G(25)
      DIMENSION CAX(25),CD(25),CGAM(25),A(25,25),D11(25),D12(25),D13(25)
     1,PL(25),L(25),M1(25),IP(25),IC(25),A11(25),A12(25),A13(25),
     2A21(25),A22(25),A23(25),A31(25),A32(25),A33(25),A41(25),A42(25),
     3A43(25),A51(25),A52(25),A53(25),G1(25),G2(25),G3(25),G4(25),G5(25)
     4,G6(25),G7(25),G8(25),A1(25),A2(25),A3(25),A4(25),B1(25),B2(25)
      COMMON/AA/W,F,PL,L,M1,BMX,BMY,BMXY,WN,W1,W2,ZX,ZY,ZBX,
     1ZBY,ZTX,ZTY,XMU,YMU,M,N,T
      COMMON/BB/AX,DX,H,SI,GAM,D,XK,YK,DEL,DY,BXY,BYX,FT,FP,SIX,SIY,XI,
     1YI,GX,GY,CX,AAX,AAY,TX,TY,CH,BX,BY,CGAM,CD,CAX
      COMMON/CC/XMS,YMS,XBSB,YBSB,XBST,YBST,TSXB,TSYB,TSXT,TSYT,SIGMA,
     1BTXY,TXYM,TXYT
      COMMON/DD/AM,AN,YIELD,EX,EY,GX,GY,O,FI,Z1,Z2,THIC,AL,AB,ZETA,ANU,
     1EXA,AS,BET,ALP,TL,TB,ANG
      COMMON/EE/N1,N2,N3,N4,N6,N7,N8,N9,N11,N12,N13,N14,M2,M3,M4,M5,M7,
     1M8,M9,M10,M12,M13,M14,M15,M17,M18,M19,M20,K1,K2,K3,K4,K6,K7,K8,K9,
     2K11,K12,K13,K14,K16,K17,K18,K19,K21,K22,K23,K24,K26,K27,K28,K29,
     3K31,K32,K33,K34,K36,K37,K38,K39
      N10=(N-3)*M
      DO 110 I=1,K1
      A11(I)=(1./EX)*(T(I)/TY(I))*((COS(FI))**2-(SIN(FI))**2*YMU(I))
      A12(I)=(1./EX)*(T(I)/TX(I))*((SIN(FI))**2-(COS(FI))**2*XMU(I))
      A13(I)=-SIN(FI)*COS(FI)/GX(I)
      A21(I)=A11(I)+(TAN(FI))**2*A12(I)-A13(I)*TAN(FI)
      A22(I)=2.*A12(I)*TAN(FI)/COS(FI)-A13(I)/COS(FI)
      A23(I)=A12(I)/((COS(FI))**2)
      A31(I)=AS**2*A21(I)
      A32(I)=A22(I)*AS*COS(FI)/4.
      A33(I)=A23(I)*((COS(FI))**2)
      A41(I)=(TAN(FI))**3*T(I)/TX(I)+TAN(FI)
      A42(I)=(TAN(FI))**2*2.*T(I)/(TX(I)*COS(FI))+1./COS(FI)
      A43(I)=TAN(FI)*T(I)/(TX(I)*((COS(FI))**2))
      A51(I)=AS**2*A41(I)
      A52(I)=A42(I)*AS*COS(FI)/4.
      A53(I)=(COS(FI))**2*A43(I)
      G1(I)=BET**2*BY(I)/4.
      G2(I)=G1(I)*A51(I)/A52(I)
      G3(I)=G1(I)*A53(I)/A52(I)
      G4(I)=G2(I)*(-A51(I)*A33(I)+A31(I)*A53(I))/(A32(I)*A51(I)-A31(I)*
     1A52(I))
      G5(I)=ALP*CAX(I)+BET**2*(AS**2)*CD(I)
      G6(I)=G5(I)*(-A33(I)*A52(I)+A32(I)*A53(I))/(A31(I)*A52(I)-A32(I)*
     1A51(I))
      G7(I)=BET*.5*(ALP*BY(I)+CAX(I)+AS**2*CD(I))
      G8(I)=G7(I)*(-A51(I)*A33(I)+A31(I)*A53(I))/(A32(I)*A51(I)-A31(I)*
     1A52(I))
      A1(I)=ALP*CAX(I)+BET**2*(AS**2)*CD(I)-BET**2*BY(I)/4.
      A2(I)=A1(I)*(A33(I)*A52(I)-A32(I)*A53(I))/(A51(I)*A32(I)-A31(I)*
     1A52(I))
      A3(I)=BET*.5*(ALP*BY(I)+CAX(I)+AS**2*CD(I))
      A4(I)=A3(I)*(A33(I)*A51(I)-A53(I)*A31(I))/(A31(I)*A52(I)-
     1A51(I)*A32(I))
      B1(I)=BET**3*BY(I)/(CGAM(I)-BET**2*2.*BY(I))
      B2(I)=BET**2*BY(I)*.25*(A33(I)*A52(I)-A32(I)*A53(I))/(A51(I)*A32(I
     1)-A31(I)*A52(I))
      B2(I)=BET**2*BY(I)*.25*A51(I)/A52(I)
      B4(I)=B3(I)*(A51(I)*A33(I)-A53(I)*A31(I))/(A52(I)*A31(I)-A51(I)*
     1A32(I))
  110 B5(I)=B3(I)/(CGAM(I)-BET**2*BY(I)*2.)
      DO 801 I=1,K1
      DO 801 J=1,K1
      B(I,J)=0.
  801 C(J)=0.
      NO=-1
      DO 101 JA=1,2
      NO=-NO
      GO TO (105),JA
```

```
      I=K1
      GO TO 104
  103 I=1
  104 B11(I)=AS**2*((BET*(-2.*W(I)+W(I+NO))+.25*(-W(I+N1*NO)))**2)
      B12(I)=AS**2*(-2.*W(I)+W(I+NO))*(BET**2*W(I+NO)-2.*(1.+BET**2)*
     1W(I)+BET*.5*(-W(I+N1*NO))+W(I+M*NO))
      C(I)=EX*(B11(I)-B12(I))
      B(I,I)=2.*CAX(I)*(3.*ALP+2.)+BY(I)*(5.+4.*ALP)+AS**2*2.*CD(I)*(
     1BET**2*3.+2.)-A1(I)
      B(I,I+NO)=-2.*CAX(I)*(2.*ALP+1.)-2.*ALP*BY(I)-AS**2*2.*CD(I)*(
     1BET**2*2.+1.)+2.*BY(I)*(B1(I)-B5(I))+BET*BY(I)
      B(I,I+2*NO)=ALP*CAX(I)+BET**2*(AS**2*CD(I)-BY(I)/4.)
      B(I,I+M*NO)=-2.*BY(I)*(ALP+2.)-2.*(CAX(I)+AS**2*CD(I))+A3(I)-2.*B3
     1(I)
      B(I,I+N1*NO)=(1.+BET)*(ALP*BY(I)+CAX(I)+AS**2*CD(I))+2.*BET*BY(I)
      B(I,I+N2*NO)=-BET*.5*(ALP*BY(I)+CAX(I)+AS**2*CD(I))
      B(I,I+M10*NO)=BY(I)*(1.-BET**2/4.)
      B(I,I+N6*NO)=-BET*BY(I)
  101 B(I,I+N7*NO)=BET**2*BY(I)/4.
      NO=-1
      DO 109 JA=1,2
      NO=-NO
      GO TO (108),JA
      I=K2
      GO TO 107
  108 I=2
  107 B11(I)=AS**2*((BET*(W(I-NO)-2.*W(I)+W(I+NO))+.25*(W(I+M4*NO)-
     1W(I+N1*NO)))**2)
      B12(I)=AS**2*(W(I-NO)-2.*W(I)+W(I+NO))*(BET**2*(W(I-NO)+W(I+NO))-
     12.*(1.+BET**2)*W(I)+BET*.5*(W(I+M4*NO)-W(I+N1*NO))+W(I+M*NO))
      C(I)=EX*(B11(I)-B12(I))
      B(I,I-NO)=-2.*CAX(I)*(2.*ALP+1.)-BY(I)*(BET+2.*ALP)-AS**2*2.*CD(I)
     1*(BET**2*2.+1.)
      B(I,I)=2.*CAX(I)*(3.*ALP+2.)+BY(I)*(5.+4.*ALP+BET**2/2.)+AS**2*2.*
     1CD(I)*(BET**2*3.+2.)
      B(I,I+NO)=-2.*CAX(I)*(2.*ALP+1.)+BY(I)*(BET-2.*ALP)-AS**2*2.*CD(I)
     1*(BET**2*2.+1.)
      B(I,I+2*NO)=ALP*CAX(I)+BET**2*(AS**2*CD(I)-BY(I)/4.)
      B(I,I+M4*NO)=(1.-BET)*(ALP*BY(I)+CAX(I)+AS**2*CD(I))-2.*BET*BY(I)
      B(I,I+M*NO)=-2.*BY(I)*(2.+ALP)-2.*(CAX(I)+AS**2*CD(I))
      B(I,I+N1*NO)=(1.+BET)*(ALP*BY(I)+CAX(I)+AS**2*CD(I))+2.*BET*BY(I)
      B(I,I+N2*NO)=-BET*.5*(ALP*BY(I)+CAX(I)+AS**2*CD(I))
      B(I,I+M9*NO)=BET*BY(I)
      B(I,I+M10*NO)=BY(I)*(1.-BET**2/8.)
      B(I,I+N6*NO)=-B(I,I+M9*NO)
  109 B(I,I+N7*NO)=BET**2*BY(I)/4.
      NO=-1
      DO 115 JA=1,2
      NO=-NO
      GO TO (114),JA
      I3=K3
      IM=K3
      GO TO 112
  114 I3=3
      IM=M3
  112 DO 115 I=I3,IM
      B11(I)=AS**2*((BET*(W(I-NO)-2.*W(I)+W(I+NO))+.25*(W(I+M4*NO)-W(I+
     1N1*NO)))**2)
      B12(I)=AS**2*(W(I-NO)-2.*W(I)+W(I+NO))*(BET**2*(W(I-NO)+W(I+NO))-2
     1.*(1.+BET**2)*W(I)+BET*.5*(W(I+M4*NO)-W(I+N1*NO))+W(I+M*NO))
      C(I)=EX*(B11(I)-B12(I))
      B(I,I-2*NO)=ALP*CAX(I)+BET**2*(AS**2*CD(I)-BY(I)/4.)
      B(I,I-NO)=-2.*CAX(I)*(2.*ALP+1.)-BY(I)*(BET+2.*ALP)-AS**2*2.*CD(I)
     1*(BET**2*2.+1.)
      B(I,I)=2.*CAX(I)*(3.*ALP+2.)+BY(I)*(5.+4.*ALP+BET**2/2.)+AS**2*2.*
     1CD(I)*(BET**2*3.+2.)
      B(I,I+NO)=-2.*CAX(I)*(2.*ALP+1.)+BY(I)*(BET-2.*ALP)-AS**2*2.*CD(I)
     1*(BET**2*2.+1.)
      B(I,I+2*NO)=B(I,I-2*NO)
      B(I,I+M3*NO)=BET*.5*(ALP*BY(I)+CAX(I)+AS**2*CD(I))
      B(I,I+M4*NO)=(1.-BET)*(ALP*BY(I)+CAX(I)+AS**2*CD(I))-2.*BET*BY(I)
      B(I,I+M*NO)=-2.*BY(I)*(2.+ALP)-2.*(CAX(I)+AS**2*CD(I))
      B(I,I+N1*NO)=(1.+BET)*(ALP*BY(I)+CAX(I)+AS**2*CD(I))+2.*BET*BY(I)
      B(I,I+N2*NO)=-B(I,I+M3*NO)
      B(I,I+M8*NO)=BET**2*BY(I)/4.
      B(I,I+M9*NO)=BET*BY(I)
      B(I,I+M10*NO)=BY(I)*(1.-BET**2/2.)
      B(I,I+N6*NO)=-B(I,I+M9*NO)
```

```
      B(I,I+N7*NO)=B(I,I+M3*NO)
      NO=-1
      DO 119 JA=1,2
      NO=-NO
      GO TO (117),JA
      I=K7
      GO TO 116
  117 I=M4
  116 B11(I)=AS**2*((BET*(W(I-NO)-2.*W(I)+W(I+NO)))+.25*(W(I+M4*NO)-W(
     1I+N1*NO)))**2)
      B12(I)=AS**2*(W(I-NO)-2.*W(I)+W(I+NO))*(BET**2*(W(I-NO)+W(I+NO))
     1-2.*(1.+BET**2)*W(I)+BET*.5*(W(I+M4*NO)-W(I+N1*NO))+W(I+M*NO))
      C(I)=EX*(B11(I)-B12(I))
      B(I,I-2*NO)=ALP*CAX(I)+BET**2*(AS**2*CD(I)-BY(I)/4.)
      B(I,I-NO)=-2.*CAX(I)*(2.*ALP+1.)-BY(I)*(BET+2.*ALP)-AS**2*2.*CD(I)
     1*(BET**2*2.+1.)
      B(I,I)=2.*CAX(I)*(3.*ALP+2.)+BY(I)*(5.+4.*ALP+BET**2/2.)+
     1AS**2*2.*CD(I)*(BET**2*3.+2.)
      B(I,I+NO)=-2.*CAX(I)*(2.*ALP+1.)+BY(I)*(BET-2.*ALP)-AS**2*2.*CD(I)
     1*(BET**2*2.+1.)
      B(I,I+M3*NO)=BET*.5*(ALP*BY(I)+CAX(I)+AS**2*CD(I))
      B(I,I+M4*NO)=(1.-BET)*(ALP*BY(I)+CAX(I)+AS**2*CD(I))-2.*BET*BY(I)
      B(I,I+M*NO)=-2.*BY(I)*(2.+ALP)-2.*(CAX(I)+AS**2*CD(I))
      B(I,I+N1*NO)=(1.+BET)*(ALP*BY(I)+CAX(I)+AS**2*CD(I))+2.*BET*BY(I)
      B(I,I+M8*NO)=BET**2*BY(I)/4.
      B(I,I+M9*NO)=BET*BY(I)
      B(I,I+M10*NO)=BY(I)*(1.-BET**2/2.)
  119 B(I,I+N6*NO)=-B(I,I+M3*NO)
      NO=-1
      DO 124 JA=1,2
      NO=-NO
      GO TO (121),JA
      I=K6
      GO TO 120
  121 I=M
  120 B11(I)=AS**2*((BET*(W(I-NO)-2.*W(I))+.25*W(I+M4*NO))**2)
      B12(I)=AS**2*(W(I-NO)-2.*W(I))*(BET**2*W(I-NO)-2.*(1.+BET**2)*W(I)
     1+BET*.5*W(I+M4*NO)+W(I+M*NO))
      C(I)=EX*(B11(I)-B12(I))
      B(I,I-2*NO)=ALP*CAX(I)+BET**2*(AS**2*CD(I)-BY(I)/4.)
      B(I,I-NO)=-2.*CAX(I)*(2.*ALP+1.)-2.*ALP*BY(I)-AS**2*2.*CD(I)*(BET
     1**2*2.+1.)-2.*BY(I)*(B1(I)-B5(I))-BET*BY(I)
      B(I,I)=2.*CAX(I)*(3.*ALP+2.)+BY(I)*(5.+4.*ALP)+AS**2*2.*CD(I)*(
     1BET**2*3.+2.)-A1(I)
      B(I,I+M3*NO)=BET*.5*(ALP*BY(I)+CAX(I)+AS**2*CD(I))-2.*BET*BY(I)
      B(I,I+M4*NO)=(1.-BET)*(ALP*BY(I)+CAX(I)+AS**2*CD(I))-A3(I)+2.*B3
     1(I)
      B(I,I+M8*NO)=BET**2*BY(I)/4.
      B(I,I+M9*NO)=BET*BY(I)
  124 B(I,I+M10*NO)=BY(I)*(1.-BET**2/4.)
      NO=-1
      DO 129 JA=1,2
      NO=-NO
      GO TO (126),JA
      I=K11
      GO TO 125
  126 I=N1
  125 B11(I)=AS**2*((BET*(-2.*W(I)+W(I+NO))+.25*(W(I-M4*NO)-W(I+N1*NO)))
     1**2)
      B12(I)=AS**2*(-2.*W(I)+W(I+NO))*(BET**2*W(I+NO)-2.*(1.+BET**2)*W(I
     1)+BET*.5*(W(I-M4*NO)-W(I+N1*NO))+W(I-M*NO)+W(I+M*NO))
      C(I)=EX*(B11(I)-B12(I))
      B(I,I-M*NO)=-4.*BY(I)-2.*(ALP*BY(I)+CAX(I)+AS**2*CD(I))-G7(I)+2.*
     1G2(I)
      B(I,I-M4*NO)=(1.-BET)*(ALP*BY(I)+CAX(I)+AS**2*CD(I))-2.*BET*BY(I)
      B(I,I-M3*NO)=BET*.5*(ALP*BY(I)+CAX(I)+AS**2*CD(I))
      B(I,I)=CAX(I)*(5.*ALP+4.)+BY(I)*(6.+4.*ALP+BET**2)+AS**2*CD(I)*(
     1+.+BET**2*6.)-G5(I)-2.*G1(I)
      B(I,I+NO)=-2.*(CAX(I)+ALP*BY(I))-4.*ALP*CAX(I)-AS**2*CD(I)*(BET**2
     1*4.+2.)
      B(I,I+2*NO)=ALP*CAX(I)+BET**2*(AS**2*CD(I)-BY(I)/2.)
      B(I,I+M*NO)=-4.*BY(I)-2.*(ALP*BY(I)+CAX(I)+AS**2*CD(I))+G7(I)-2.*
     1G2(I)
      B(I,I+N1*NO)=(1.+BET)*(ALP*BY(I)+CAX(I)+AS**2*CD(I))+2.*BET*BY(I)
      B(I,I+N2*NO)=-B(I,I-M3*NO)
      B(I,I+M10*NO)=BY(I)*(1.-BET**2/2.)+G1(I)
      B(I,I+N6*NO)=-BET*BY(I)
```

```
      B(I,I+N7*NO)=BET**2*BY(I)/4.
      NO=-1
      DO 134 JA=1,2
      NO=-NO
      GO TO (130),JA
      I=K12
      GO TO 131
  130 I=N2
  131 B11(I)=AS**2*((BET*(W(I-NO)-2.*W(I)+W(I+NO)))+.25*(W(I-M4*NO)-W(I-
     1N1*NO)+W(I+M4*NO)-W(I+N1*NO)))**2)
      B12(I)=AS**2*(W(I-NO)-2.*W(I)+W(I+NO))*(BET**2*(W(I-NO)+W(I+NO))-2
     1.*(1.+BET**2)*W(I)+BET*.5*(W(I-M4*NO)-W(I-N1*NO)+W(I+M4*NO)-W(I+N1
     2*NO))+B(I-M*NO)+W(I+M*NO))
      C(I)=-X*(B11(I)-B12(I))
      B(I,I-N1*NO)=(1.+BET)*(ALP*BY(I)+CAX(I)+AS**2*CD(I))+2.*BET*BY(I)
      B(I,I-M*NO)=-2.*BY(I)*(ALP+2.)-2.*(CAX(I)+AS**2*CD(I))
      B(I,I-M4*NO)=(1.-BET)*(ALP*BY(I)+CAX(I)+AS**2*CD(I))-2.*BET*BY(I)
      B(I,I-M3*NO)=BET*.5*(ALP*BY(I)+CAX(I)+AS**2*CD(I))
      B(I,I-NO)=-2.*ALP*(2.*CAX(I)+BY(I))-2.*CAX(I)-AS**2*2.*CD(I)*(
     1BET**2*2.+1.)
      B(I,I)=2.*CAX(I)*(3.*ALP+2.)+BY(I)*(BET**2+4.*ALP+6.)+AS**2*CD(I)*
     1(BET**2*6.+4.)
      B(I,I+NO)=B(I,I-NO)
      B(I,I+2*NO)=ALP*CAX(I)+BET**2*(AS**2*CD(I)-BY(I)/2.)
      B(I,I+M4*NO)=B(I,I-M4*NO)
      B(I,I+M*NO)=B(I,I-M*NO)
      B(I,I+N1*NO)=B(I,I-N1*NO)
      B(I,I+N2*NO)=-B(I,I-M3*NO)
      B(I,I+M9*NO)=BET*BY(I)
      B(I,I+M10*NO)=BY(I)*(1.-BET**2/2.)
      B(I,I+N6*NO)=-B(I,I+N)*NO)
  134 B(I,I+N7*NO)=BET**2*BY(I)/4.
      NO=-1
      DO 139 JA=1,2
      NO=-NO
      GO TO (136),JA
      III=K12
      IIM=K13
      GO TO 137
  136 III=N3
      IIM=M8
  137 DO 139 I=III,IIM
      B11(I)=AS**2*((BET*(W(I-NO)-2.*W(I)+W(I+NO)))+.25*(W(I-M4*NO)-
     1W(I-N1*NO)+W(I+M4*NO)-W(I+N1*NO)))**2)
      B12(I)=AS**2*(W(I-NO)-2.*W(I)+W(I+NO))*(BET**2*(W(I-NO)+W(I+NO))-2
     1.*(1.+BET**2)*W(I)+BET*.5*(W(I-M4*NO)-W(I-N1*NO)+W(I+M4*NO)-W(I+N1
     1*NO))+W(I-M*NO)+W(I+M*NO))
      C(I)=-X*(B11(I)+B12(I))
      B(I,I-N2*NO)=-BET*.5*(ALP*BY(I)+CAX(I)+AS**2*CD(I))
      B(I,I-N1*NO)=(1.+BET)*(ALP*BY(I)+CAX(I)+AS**2*CD(I))+2.*BET*BY(I)
      B(I,I-M*NO)=-2.*BY(I)*(ALP+2.)-2.*(CAX(I)+AS**2*CD(I))
      B(I,I-M4*NO)=(1.-BET)*(ALP*BY(I)+CAX(I)+AS**2*CD(I))-2.*BET*BY(I)
      B(I,I-M3*NO)=-B(I,I-N2*NO)
      B(I,I-2*NO)=ALP*CAX(I)+BET**2*(AS**2*CD(I)-BY(I)/2.)
      B(I,I-NO)=-2.*ALP*(2.*CAX(I)+BY(I))-2.*CAX(I)-AS**2*2.*CD(I)*(
     1BET**2*2.+1.)
      B(I,I)=2.*CAX(I)*(3.*ALP+2.)+BY(I)*(BET**2+4.*ALP+6.)+AS**2*CD(I)*
     1(BET**2*6.+4.)
      B(I,I+NO)=B(I,I-NO)
      B(I,I+2*NO)=B(I,I-2*NO)
      B(I,I+M3*NO)=B(I,I-M3*NO)
      B(I,I+M4*NO)=B(I,I-M4*NO)
      B(I,I+M*NO)=B(I,I-M*NO)
      B(I,I+N1*NO)=B(I,I-N1*NO)
      B(I,I+N2*NO)=B(I,I-N2*NO)
      B(I,I+M8*NO)=BET**2*BY(I)/4.
      B(I,I+M9*NO)=BET*BY(I)
      B(I,I+M10*NO)=BY(I)*(1.-BET**2/2.)
      B(I,I+N6*NO)=-B(I,I+M9*NO)
  139 B(I,I+N7*NO)=B(I,I+M8*NO)
      NO=-1
      DO 149 JA=1,2
      NO=-NO
      GO TO (140),JA
      I=K17
      GO TO 141
  140 I=M7
  141 B11(I)=AS**2*((BET*(W(I-NO)-2.*W(I)+W(I+NO)))+.25*(W(I-M4*NO)-W(I-
```

```
     1*N1*NO)) +W(I+M4*NO)-W(I+N1*NO)))**2)
     +12(I)-XS**2*(W(I-NO)+2.*W(I)+W(I+NO))*(BET**2*(W(I-NO)+W(I+NO))-
    - 12.*(1.+BET**2)*W(I)+BET*.5*(W(I-M4*NO)+W(I-N1*NO)+W(I+M4*NO)-
     2W(I+N1*NO))+W(I-M4*NO)+W(I+M4*NO)))
      C(I)=-X*(B11(I)-BY(I))
      B(I,I-N2*NO)=-BET*.5*(ALP*BY(I)+CAX(I)+AS**2*CD(I))
      B(I,I-N1*NO)=(1.+BET)*(ALP*BY(I)+CAX(I)+AS**2*CD(I))+2.*BET*BY(I)
      B(I,I-M*NO)=-2.*BY(I)*(ALP+2.)-2.*(CAX(I)+AS**2*CD(I))-2.*BET*BY(I)
      B(I,I-M4*NO)=(1.-BET)*(ALP*BY(I)+CAX(I)+AS**2*CD(I))-2.*BET*BY(I)
      B(I,I-2*NO)=ALP*CAX(I)+BET**2*(AS**2*CD(I)-BY(I)/2.)
      B(I,I-NO)=-2.*ALP*(2.*CAX(I)+BY(I))-2.*CAX(I)-AS**2*2.*CD(I)*(
     1BET**2*2.+1.)
      B(I,I)=2.*CAX(I)*(3.*ALP+2.)+BY(I)*(BET**2*4.*ALP+6.)+AS**2*CD(I)*
     1(BET**2*6.+4.)
      B(I,I+NO)=B(I,I-NO)
      B(I,I+M3*NO)=-B(I,I-N2*NO)
      B(I,I+M4*NO)=B(I,I-M4*NO)
      B(I,I+M*NO)=B(I,I-M*NO)
      B(I,I+N1*NO)=B(I,I-N1*NO)
      B(I,I+M8*NO)=BET**2*BY(I)/4.
      B(I,I+M9*NO)=BET*BY(I)
      B(I,I+M10*NO)=BY(I)*(1.-BET**2/2.)
  145 B(I,I+N6*NO)=-B(I,I+M9*NO)
      CALL MEMB
      RETURN
      END
```

```
      SUBROUTINE MEMO
      DIMENSION TSXTN(25),TSXBN(25),TSYBN(25),TXYTN(25),TSYTN(25),
     1ZX(25),ZY(25),T(25),XMU(25),ZBX(25),ZBY(25),F(25),W(25),WN(25),WI(
     225),N2(25),ZXN(25),ZYN(25),XMS(25),YMS(25),XBSB(25),YBSB(25),XBST(
     325),YBST(25),TXY(25),TXYM(25),SIGMA(25),TSXB(25
     425),TSYB(25),TSXT(25),TSYT(25),TXYT(25),XMSN(25),YMSN(25),C(25)
      DIMENSION XI(25),YI(25),YBU(25),BMX(25),BX(25),BMY(25),BY(25),BMXY,
     1(25),CX(25),BY(25),BX(25),ZTX(25),ZTY(25),SIY(25),SIX(25),GX(25),
     2GY(25),FT(25),FP(25),BXY(25),BYX(25),AAX(25),AAY(25),TX(25),TY(25),CH(25),
     3XK(25),YK(25),DEL(25),SI(25),GAM(25),D(25),XK(25),YK(25),DL(25),BXY(25),BYX(25),FT(25),FP(25),SIX(25),SIY(25),XI(25),
     4A2(25),B4(25),B5(25),B(25,25),C(25),B11(25),B12(25)
      DIMENSION CAX(25),CD(25),CGAM(25),A(25,25),D11(25),D12(25),D13(25),
     1,DL(25),L(25),M1(25),IP(25),IC(25),A11(25),A12(25),A13(25),A41(25),A42(25),
     2A21(25),A22(25),A23(25),A31(25),A32(25),A33(25),A41(25),A42(25),
     3A43(25),A51(25),A52(25),A53(25),G1(25),G2(25),G3(25),G4(25),G5(25)
     4,G6(25),G7(25),G8(25),A1(25),A2(25),A3(25),A4(25),B1(25),B2(25)
      COMMON/AA/W,F,PL,L,M1,BMX,BMY,BMXY,WN,WI,N2,ZX,ZY,ZBX,
     1ZBY,ZTX,ZTY,XMU,YBU,M,N,T
      COMMON/BB/AX,DX,H,SI,GAM,D,XK,YK,DEL,DY,BXY,BYX,FT,FP,SIX,SIY,XI,
     1YI,GX,GY,CX,AAX,AAY,TX,TY,CH,BX,BY,CGAM,CD,CAX
      COMMON/CC/XMS,YMS,XBSB,YBSB,XBST,YBST,TSXB,TSYB,TSXT,TSYT,SIGMA,
     1BTXY,TXYM,TXYT
      COMMON/DD/AM,AN,YIELD,FX,FY,EX,EY,Q,FI,Z1,Z2,THIC,AL,AB,ZETA,ANU,
     1EXA,AS,BET,ALP,TL,TB,ANG
      COMMON/EE/N1,N2,N3,N4,N5,N6,N7,N8,N9,N11,N12,N13,N14,M2,M3,M4,M5,M7,
     1M8,M9,M10,M12,M13,M14,M15,M17,M18,M19,M20,K1,K2,K3,K4,K6,K7,K8,K9,
     2K11,K12,K13,K14,K16,K17,K19,K10,K21,K22,K23,K24,K26,K27,K28,K29,
     3K31,K32,K33,K34,K36,K37,K38,K39
      NO=-1
      DO 150 JA=1,2
      NO=-NO
      GO TO (146),JA
      I=K16
      GO TO 144
  146 I=M10
  144 B11(I)=AS**2*((BET*(W(I-N1)-2.*W(I))+.25*(-W(I-N1*NO)+W(I+M4*NO)))
     1**2)
      B12(I)=AS**2*(W(I-NO)-2.*W(I))*(BET**2*W(I-NO)-2.*(1.+BET**2)*W(I)
     1+BET*.5*(-W(I-N1*NO)+W(I+M4*NO))+W(I-M*NO)+W(I+M*NO))
      C(I)=EX*(B11(I)-B12(I))
      B(I,I-N2*NO)=-BET*.5*(ALP*BY(I)+CAX(I)+AS**2*CD(I))+2.*BET*BY(I)
      B(I,I-N1*NO)=(1.+BET)*(ALP*BY(I)+CAX(I)+AS**2*CD(I))+G7(I)-2.*
      B(I,I-M*NO)=-4.*BY(I)-2.*(ALP*BY(I)+CAX(I)+AS**2*CD(I))+G7(I)-2.*
     1G2(I)
      B(I,I-2*NO)=ALP*CAX(I)+BET**2*(AS**2*CD(I)-BY(I)/2.)
      B(I,I-NO)=-2.*(CAX(I)+ALP*BY(I))+4.*ALP*CAX(I)-AS**2*CD(I)*(
     1BET**2*4.+2.)
      B(I,I)=CAX(I)*(6.*ALP+4.)+BY(I)*(6.+4.*ALP+BET**2)+AS**2*CD(I)*(
     1+4.+BET**2*6.)-G5(I)-2.*G1(I)
      B(I,I+M3*NO)=-B(I,I-N2*NO)
      B(I,I+M4*NO)=(1.-BET)*(ALP*BY(I)+CAX(I)+AS**2*CD(I))-G7(I)
      B(I,I+M*NO)=-4.*BY(I)-2.*(ALP*BY(I)+CAX(I)+AS**2*CD(I))-G7(I)
     1+2.*G2(I)
      B(I,I+M8*NO)=BET**2*BY(I)/4.
      B(I,I+M9*NO)=BET*BY(I)
  150 B(I,I+M10*NO)=BY(I)*(1.-BET**2/2.)+G1(I)
      DO 815 I=N6,K26,M
      B11(I)=AS**2*((BET*(-2.*W(I)+W(I+1))+.25*(W(I-M4)-W(I+N1)))**2)
      B12(I)=AS**2*(-2.*W(I)+W(I+1))*(BET**2*W(I+1)-2.*(1.+BET**2)*W(I)+
     1BET*.5*(W(I-M4)-W(I+N1))+W(I-M)+W(I+M))
      C(I)=EX*(B11(I)-B12(I))
      B(I,I-M10)=BY(I)*(1.-BET**2/2.)+G1(I)
      B(I,I-M9)=BET*BY(I)
      B(I,I-M8)=BET**2*BY(I)/4.
      B(I,I-M5)=-4.*BY(I)-2.*(ALP*BY(I)+CAX(I)+AS**2*CD(I))-G7(I)+2.*G2(
     1I)
      B(I,I-M4)=(1.-BET)*(ALP*BY(I)+CAX(I)+AS**2*CD(I))-2.*BET*BY(I)
      B(I,I-M3)=BET*.5*(ALP*BY(I)+CAX(I)+AS**2*CD(I))
      B(I,I)=CAX(I)*(6.*ALP+4.)+BY(I)*(6.+4.*ALP+BET**2)+AS**2*CD(I)*(4.
     1+BET**2*6.)-G5(I)-2.*G1(I)
      B(I,I+1)=-2.*(CAX(I)+ALP*BY(I))-4.*ALP*CAX(I)-AS**2*CD(I)*
     1(BET**2*4.+2.)
      B(I,I+2)=ALP*CAX(I)+BET**2*(AS**2*CD(I)-BY(I)/4.)
      B(I,I+M)=-4.*BY(I)-2.*(ALP*BY(I)+CAX(I)+AS**2*CD(I))
     1+G7(I)-2.*G2(I)
      B(I,I+N1)=(1.+BET)*(ALP*BY(I)+CAX(I)+AS**2*CD(I))+2.*BET*BY(I)
      B(I,I+N2)=-B(I,I-M3)
      B(I,I+M10)=B(I,I-M10)
```

```
      B(I,I+N6)=-B(I,I-M9)
      B(I,I+N7)=B(I,I-M8)
  810 CONTINUE
      DO 820 I=17,K27,4
      B11(I)=AS**2*((BET*(W(I-1)-2.*W(I)+W(I+1))+.25*(W(I-M4)-W(I-N1)+
     1W(I+M4)-W(I+N1)))**2)
      B12(I)=AS**2*(W(I-1)-2.*W(I)+W(I+1))*(BET**2*(W(I+1)+W(I-1))-2.*
     1(1.+BET**2)*W(I)+BET*.5*(W(I-M4)-W(I-N1)+W(I+M4)-W(I+N1))+W(I-M)+
     2W(I+M))
      C(I)=CX*(B11(I)-B12(I))
      B(I,I-N6)=-BET*BY(I)
      B(I,I-M10)=BY(I)*(1.-BET**2/2.)
      B(I,I-M9)=-B(I,I-N6)
      B(I,I-M8)=BET**2*BY(I)/4.
      B(I,I-N1)=(1.+BET)*(ALP*BY(I)+CAX(I)+AS**2*CD(I))+2.*BET*BY(I)
      B(I,I-M)=-2.*BY(I)*(ALP+2.)-2.*(CAX(I)+AS**2*CD(I))
      B(I,I-M4)=(1.-BET)*(ALP*BY(I)+CAX(I)+AS**2*CD(I))-2.*BET*BY(I)
      B(I,I-M3)=BET*.5*(ALP*BY(I)+CAX(I)+AS**2*CD(I))
      B(I,I-1)=-2.*ALP*(2.*CAX(I)+BY(I))-2.*CAX(I)-AS**2*2.*CD(I)*(
     1BET**2*2.+1.)
      B(I,I)=2.*CAX(I)*(3.*ALP+2.)+BY(I)*(BET**2+4.*ALP+6.)+AS**2*CD(I)*
     1(BET**2*6.+4.)
      B(I,I+1)=B(I,I-1)
      B(I,I+2)=ALP*CAX(I)+BET**2*(AS**2*CD(I)-BY(I)/2.)
      B(I,I+M4)=B(I,I-M4)
      B(I,I+M)=B(I,I-M)
      B(I,I+N1)=B(I,I-N1)
      B(I,I+N2)=-B(I,I-M3)
      B(I,I+M9)=B(I,I-M9)
      B(I,I+M10)=B(I,I-M10)
      B(I,I+N6)=B(I,I-N6)
      B(I,I+N7)=B(I,I-M8)
  820 CONTINUE
      DO 825 I=3,M3
      DO 825 J=M10,N10,M
      JA=I+J
      B11(JA)=AS**2*((BET*(W(JA-1)-2.*W(JA)+W(JA+1))+.25*(W(JA-M4)-W(JA-
     1N1)+W(JA+M4)-W(JA+N1)))**2)
      B12(JA)=AS**2*(W(JA-1)-2.*W(JA)+W(JA+1))*(BET**2*(W(JA-1)+W(JA+1))
     1-2.*(1.+BET**2)*W(JA)+BET*.5*(W(JA-M4)-W(JA-N1)+W(JA+M4)-W(JA+N1))
     2+W(JA-M)+W(JA+M))
      C(JA)=CX*(B11(JA)-B12(JA))
      B(JA,JA-N7)=BET**2*BY(JA)/4.
      B(JA,JA-N6)=-BET*BY(JA)
      B(JA,JA-M10)=BY(JA)*(1.-BET**2/2.)
      B(JA,JA-M9)=-B(JA,JA-N6)
      B(JA,JA-M8)=B(JA,JA-N7)
      B(JA,JA-N2)=-BET*.5*(ALP*BY(JA)+CAX(JA)+AS**2*CD(JA))
      B(JA,JA-N1)=(1.+BET)*(ALP*BY(JA)+CAX(JA)+AS**2*CD(JA))+2.*BET*BY(
     1JA)
      B(JA,JA-M)=-2.*BY(JA)*(ALP+2.)-2.*(CAX(JA)+AS**2*CD(JA))
      B(JA,JA-M4)=(1.-BET)*(ALP*BY(JA)+CAX(JA)+AS**2*CD(JA))-2.*BET*
     1BY(JA)
      B(JA,JA-N7)=-B(JA,JA-N2)
      B(JA,JA-2)=ALP*CAX(JA)+BET**2*(AS**2*CD(JA)-BY(JA)/2.)
      B(JA,JA-1)=-2.*ALP*(2.*CAX(JA)+BY(JA))-2.*CAX(JA)-AS**2*2.*CD(JA)*
     1(BET**2*2.+1.)
      BY(JA,JA)=2.*CAX(JA)*(3.*ALP+2.)+BY(JA)*(BET**2+4.*ALP+6.)+AS**2*CD
     1(JA)*(BET**2*6.+4.)
      B(JA,JA+1)=B(JA,JA-1)
      B(JA,JA+2)=B(JA,JA-2)
      B(JA,JA+M3)=B(JA,JA-M3)
      B(JA,JA+M4)=B(JA,JA-M4)
      B(JA,JA+M)=B(JA,JA-M)
      B(JA,JA+N1)=B(JA,JA-N1)
      B(JA,JA+N2)=B(JA,JA-N2)
      B(JA,JA+M8)=B(JA,JA-M8)
      B(JA,JA+M9)=B(JA,JA-M9)
      B(JA,JA+M10)=B(JA,JA-M10)
      B(JA,JA+N6)=B(JA,JA-N6)
      B(JA,JA+N7)=B(JA,JA-N7)
  825 CONTINUE
      DO 830 I=M14,K22,4
      B11(I)=AS**2*((BET*(W(I-1)-2.*W(I)+W(I+1))+.25*(W(I-M4)-W(I-N1)+
     1W(I+M4)-W(I+N1)))**2)
      B12(I)=AS**2*(W(I-1)-2.*W(I)+W(I+1))*(BET**2*(W(I-1)+W(I+1))-2.*
     1(1.+BET**2)*W(I)+BET*.5*(W(I-M4)-W(I-N1)+W(I+M4)-W(I+N1))+W(I-M)+
     2W(I+M))
```

```
      C(I)=EX*(B11(I)-B12(I))
      B(I,I-N7)=BET**2*BY(I)/4.
      B(I,I-N6)=-BET*BY(I)
      B(I,I-M10)=BY(I)*(1.-BET**2/2.)
      B(I,I-M9)=-B(I,I-N6)
      B(I,I-N2)=-BET*.5*(ALP*BY(I)+CAX(I)+AS**2*CD(I))+2.*BET*BY(I)
      B(I,I-N1)=(1.+BET)*(ALP*BY(I)+CAX(I)+AS**2*CD(I))
      B(I,I-M)=-4.*BY(I)*(ALP+2.)-2.*(CAX(I)+AS**2*CD(I))
      B(I,I-M4)=(1.-BET)*(ALP*BY(I)+CAX(I)+AS**2*CD(I))-2.*BET*BY(I)
      B(I,I-2)=ALP*CAX(I)+BET**2*(AS**2*CD(I)-BY(I)/2.)
      B(I,I-1)=-2.*ALP*(2.*CAX(I)+BY(I))-2.*CAX(I)-AS**2*2.*CD(I)*(
     1BET**2*2.+1.)
      B(I,I)=2.*CAX(I)*(3.*ALP+2.)+BY(I)*(BET**2+4.*ALP+6.)+AS**2*CD(I)*
     1(BET**2*6.+4.)
      B(I,I+1)=B(I,I-1)
      B(I,I+M3)=-B(I,I-N2)
      B(I,I+M4)=B(I,I-M4)
      B(I,I+M)=B(I,I-M)
      B(I,I+N1)=B(I,I-N1)
      B(I,I+M8)=B(I,I-N7)
      B(I,I+M9)=B(I,I-M9)
      B(I,I+M10)=B(I,I-M10)
      B(I,I+N6)=B(I,I-N6)
  830 CONTINUE
      DO 835 I=M15,K21,M
      B11(I)=AS**2*((BET*(W(I-1)-2.*W(I))+.25*(-W(I-N1)+W(I+M4)))**2)
      B12(I)=AS**2*(W(I-1)-2.*W(I))*(BET**2*W(I-1)-2.*(1.+BET**2)*W(I)+
     1BET*.5*(-W(I-N1)+W(I+M4))+W(I-M)+W(I+M))
      C(I)=EX*(B11(I)-B12(I))
      B(I,I-N7)=BET**2*BY(I)/4.
      B(I,I-N6)=-BET*BY(I)
      B(I,I-M10)=BY(I)*(1.-BET**2/2.)+G1(I)
      B(I,I-N2)=-BET*.5*(ALP*BY(I)+CAX(I)+AS**2*CD(I))+2.*BET*BY(I)
      B(I,I-N1)=(1.+BET)*(ALP*BY(I)+CAX(I)+AS**2*CD(I))+G7(I)-2.*G2(I
     1)
      B(I,I-M)=-4.*BY(I)-2.*(ALP*BY(I)+CAX(I)+AS**2*CD(I))+G7(I)+2.*G2(I
      B(I,I-2)=ALP*CAX(I)+BET**2*(AS**2*CD(I)-BY(I)/2.)
      B(I,I-1)=-2.*(CAX(I)+ALP*BY(I))-4.*ALP*CAX(I)-AS**2*CD(I)*(BET**2
     1*4.+2.)
      B(I,I)=CAX(I)*(6.*ALP+4.)+BY(I)*(6.+4.*ALP+BET**2)+AS**2*CD(I)*(4.
     1+BET**2*6.)-G5(I)-2.*G1(I)
      B(I,I+M3)=-B(I,I-N2)
      B(I,I+M4)=(1.-BET)*(ALP*BY(I)+CAX(I)+AS**2*CD(I))-2.*BET*BY(I)
      B(I,I+M)=-4.*BY(I)-2.*(ALP*BY(I)+CAX(I)+AS**2*CD(I))-G7(I)+2.*G2(I
     1)
      B(I,I+M8)=B(I,I-N7)
      B(I,I+M9)=-B(I,I-N6)
      B(I,I+M10)=B(I,I-M10)
  835 CONTINUE
      CALL MINV(B,25,DF,L,M1)
      DO 804 I=1,K1
      F(I)=0.
      DO 803 J=1,K1
      F(I)=F(I)+B(I,J)*G(J)
  803 CONTINUE
  804 CONTINUE
      RETURN
      END
```

VITA AUCTORIS

1940 Born at Rangamati , Chittagong Hill Tracts, Bangladesh, on January 12.

1957 Completed Secondary School from Rangamati Gov't, H.E. School and received first grade scholarship.

1959 Stood first class second in order of merit in Intermediate Science Examination from Sir A.T. College, Kanungopara, under Dacca University.

1963 Stood first class second in B.Sc. Engg. (Civil) final examination from Bangladesh (formerly East Pakistan) University of Engg. and Technology, Dacca.

1964 Joined the Associated British Consultants Ltd., Chittagong, Bangladesh as an Assistant Engineer.

1965 Appointed as a Resident Engineer in 'The Engineers Ltd.', Dacca, Bangladesh.

1967 Promoted to the post of Senior Engineer (Design) and held this position until left for Canada for higher studies.

1968 Enrolled as a graduate (Teaching and Research) Assistant while pursuing a Master's program at the University of Windsor in September 1968.

1970 In May 1970 graduated from the University of Windsor with a Master's degree in Applied Science with a major in Structural Engineering. In the same year, enrolled as a Ph.D. student in the Department of Civil Engineering.

1973 In May 1973, completed successfully the comprehensive examination in partial fulfillment of the requirement for the Ph.D. degree.

In September 1973, appointed as a Senior Structural Engineer in Harley Ellington-Pierce Yee Associates, Architect Engineers, in Southfield, Michigan, U.S.A.